



Universitat Autònoma de Barcelona

ADVERTIMENT. L'accés als continguts d'aquesta tesi queda condicionat a l'acceptació de les condicions d'ús establertes per la següent llicència Creative Commons:  http://cat.creativecommons.org/?page_id=184

ADVERTENCIA. El acceso a los contenidos de esta tesis queda condicionado a la aceptación de las condiciones de uso establecidas por la siguiente licencia Creative Commons:  <http://es.creativecommons.org/blog/licencias/>

WARNING. The access to the contents of this doctoral thesis it is limited to the acceptance of the use conditions set by the following Creative Commons license:  <https://creativecommons.org/licenses/?lang=en>



**Universitat Autònoma
de Barcelona**

Valorization and reuse of waste modified biomass
**Heavy metal biosorption removal from aqueous
solutions**

Jingjing Zhao

Doctoral Thesis

PhD in Chemistry

Supervisor

Cristina Palet Ballús

Department de Química

Facultat de Ciències

2019



**Universitat Autònoma
de Barcelona**

Dissertation submitted for the degree of doctor

Jingjing zhao

Supervisor

Prof. Cristina Palet Ballús

Full professor of Analytical Chemistry

Group leader in *Grup de Tècniques de Separació en Química (GTS)*, in
Universitat Autònoma de Barcelona (UAB)

Bellaterra (Cerdanyola del Vallès), 5th June 2019

Acknowledgment

First of all, I want to thank my parents and my sister. Your strong support and constant encouragement have given me the opportunity to complete my Ph.D. I want to especially thank my husband Jun Gao, for taking care of me and supporting me. You always accompany me and comfort me whenever I am sad or tired. I very appreciate the days be with you and always feel happy because of you.

I want to express my deepest gratitude to my supervisor Cristina, without your enthusiasm, encouragement, support and continuous optimism this thesis would hardly have been completed. You always have an optimistic attitude towards life and a young mindset. Thanks for encouraging me, supporting me and trusting me whether in life or at work.

Mon, thanks for your kindness and warm heart. Also, help me to analyze the samples and thousands of times help me fix the ICP-MS. I will miss your hug and the time be with you.

Roberto, Eliana, Julio, thank you for your guidance at work. I learned a lot through your rigorous work attitude. Thanks for sharing your work experience with me. Thanks for your hard work on the experiment and papers.

It is also a pleasure to thanks people from lab A team: Maria Angles and Veronica, G office team: Tingting and Lou, biomat team: Albert, Clara, Sandra, Manu, Sergy, Jorge, stone office: Iris. Thanks for the times we spend in the lab, also the wonderful times we shared outside work. In addition, Mari, thanks for your kindness and patience to explain everything to me. I would like to thank all of you. I will miss you and the “croqueta” and coffee times. Thanks for your friendship and support both in life and work.

I also want to thanks people outside my work, Weiqiang, Borja, Elena, Javi, thanks for the time we enjoyed together and the wonderful trips. Nadja, Erica, thanks for your hard work on the experiment. Also, you are a nice person and I hope to meet you again.

Furthermore, I want to express my gratitude to Xinjie, thanks for your support on my work, and make a chance to publish my paper. Also, I very appreciate the trip to Wuhan, thanks very much for you.

I also want to express my gratitude to GTS members, Manuel Valiente, Montserrat López, Gustavo, Nurlin, Maria dolors, Laia, Fa, Víctor. Thanks for the welcomes and fare ware that make me have the chance to meet people and taste different kinds of food from all over the world. Thanks for the wonderful times we shared outside the work.

Finally, I would like to gratefully acknowledge the financial support of Chinese scholarship council (CSC) for granting my personal expenses.



**Universitat Autònoma
de Barcelona**

The work presented in this PhD thesis has been developed under support of the following projects:

- ✓ Spanish research projects (Nos. CTM2015-65414-C2-1-R and AGL2015-70393-R).
- ✓ China Scholarship Council (No. 201509110114).

Moreover, I would like to thank:

- ✓ ALBA Synchrotron facility (Cerdanyola de Valles, Barcelona, Spain) for the XAS analysis at CLAESS beamline.
- ✓ Diamond Light Source facility (London, UK) for beamtime no. SP18561 at B18 beamline.
- ✓ The National Key Research and Development Program of China (No. 2018YFD0200904).
- ✓ The Agricultural Science and Technology Innovation Program of China (No. CAAS-ASTIP-2013-OCRI).
- ✓ UAB Microscopy Service (*Servei de Microscòpia Electrònica* from UAB, Catalunya, Spain) for the SEM analysis.

In addition, the congresses and scientific meeting where the PhD thesis results have been presented are detailed:

Julio Bastos, Zhao Jingjing and Cristina Palet, Simple synthetic routes for the functionalization of nanodiamonds as biocompatible carbon nanoallotropes for future sensing and (bio)targeting applications, **Poster presentation** at NanoBio&Med2015 International Conference (NanoBio&Med2015), November 18-20, 2015, Barcelona (Spain).

Zhao Jingjing, Julio Bastos and Cristina Palet, Simple synthetic routes for the functionalization of nanodiamonds as biocompatible carbon nanoallotropes for future sensing and (bio)targeting applications, **Oral presentation** at 9a Trobada de Joves Investigadors dels Països Catalans, Societat Catalana de Química – Perpinyà, 3-5 February 2016.

Jingjing Zhao, Julio Bastos, Montserrat Resina-Gallego, Raquel Montes, Mireia Baeza and Cristina Palet, Nanoparticle systems for future sensing and (bio)targeting applications, **Oral presentation** at - ISMEC 2016, June 7th – 10th 2016, Barcelona (Spain). Acta of the International Symposia on Metal Complexes – ISMEC Acta.

Cristina Wei Li, Jing Jing ZHAO, Montserrat RESINA, Josep Maria ALCANIZ, Xavier DOMENE, Cristina PALET, Study of the effect of the pyrolysis and post-treatment procedures in the adsorption of heavy metals by biomass application to soil, **Poster presentation** (with 5 minutes Oral defense) at - ISMEC

2016, June 7th – 10th 2016, Barcelona (Spain). Acta of the International Symposia on Metal Complexes – ISMEC Acta.

Raquel Montes, Jingjing Zhao, Julio Bastos, Cristina Palet and Mireia Baeza, Voltammetric (nano)composite sensors based on graphite-epoxy modified with Au@nanodiamonds, **Oral presentation** at 21st edition of Transfrontier Meeting of Sensors and Biosensors (TMSB-2016), September 29th and 30th, 2016, Barcelona, Spain.

Jingjing Zhao, Julio Bastos-Arrieta, Raquel Montes, Mireia Baeza, Cristina Palet.

TiO₂ Modified Biomass and its Application in Removal of Pb²⁺, Cd²⁺, Cu²⁺ and Cr³⁺/Cr⁶⁺ from Aqueous Solution, SESSION: Persistent Inorganic Pollutants, cristina.palet@uab.cat, POSTER PRESENTATION MONDAY, 19th June; Poster Session; ICCE 2017, Oslo, Norway.

Zhao, J., Shen, X., Domene, X., Alcañiz, J.M., Bastos-Arrieta, J., Liao, X., Palet, C.

Biomass/Biochar application in biosorption removal of Pb²⁺, Cd²⁺, Cu²⁺ and Cr³⁺ from aqueous solutions, cristina.palet@uab.cat, ORAL PRESENTATION 16-20th June; ICCE 2019, Thessaloniki, Greece.

Abstract

Polluted water contaminated by heavy metals has received increasing attention due to their high toxicity, persistence in sediment, and biological accumulation of the heavy metals, which lead to a potential threat to animals and human beings even at low concentration. Traditional techniques to remove heavy metal are high cost or making the second pollution that limited large-area applications. Most importantly, traditional techniques cannot apply to such low concentration in water. Therefore, it is emergency to find a low-cost, efficiency and eco-friendly method to deal with this kind of problem. Biosorption can be a promising option in this case due to its high efficiency and eco-friendly, especially the abundant materials in the world such as biomass.

On the other hand, a huge amount of biomass waste in the world will cause an environmental problem if not handled properly. Furthermore, cellulose, hemicellulose and lignin are abundant in biomass wastes that can be employed as cheap adsorbents due to their special physical and chemical properties. The presence of well-known functional groups in these natural components turn them as potential materials for heavy metal interaction and subsequent removal.

Therefore, biomass from agricultural wastes and wood industry have been checked as natural adsorbents to solve two serious environmental problems: firstly the disposal of agriculture wastes, and secondly its use as adsorbents for the removal of heavy metals from wastewaters. With this purpose, many different types of biomass feedstocks and some of their biochars are used to remove Cr(III), Cd(II), Cu(II) and Pb(II) ions from a mixture of multiple heavy metals. Furthermore, TiO₂ nanoparticles are also a good adsorbent for removing heavy metals. Pine and pyrolyzed pine loaded with TiO₂ (Pine/TiO₂) have been used as sorbent for the removal of heavy metal ions from aqueous solution. Single and multi-element systems are used for the heavy metals removal. In addition, Cr(III) and Cr(VI) speciation has been checked for pine biomass/biochar systems.

In all cases, different parameters of the biosorption processes are optimized in batch systems (pH of the solution, the initial concentration and the contact time), and kinetics and isotherm modelling have been performed to elucidate the possible biosorption mechanisms. Surface morphology of the adsorbents are analyzed using scanning electron microscopy (SEM) and Fourier transform infrared spectroscopy (FTIR). Moreover, X-ray absorption spectroscopy (XAS) is performed to study the biosorption mechanism at the molecular level.

The adsorption capacity of biomass is ranked as follows: FO (from industry sludge waste) > ZO (from agriculture corn biomass waste) >> CO (from wood poplar biomass waste). Complexation and cation exchange have been found to be the two main adsorption mechanisms in systems containing multiple heavy metals, with cation exchange being the most significant. As a summary of the chromium speciation study by pine biomass/biochar systems, the adsorption of Cr(III) is mainly through ion exchange with the mineral components present on the biomaterials surfaces. Pyrolysis process can increase the concentration of such

minerals to increase the adsorption capacity. For Pine/TiO₂, together with the ion exchange also complexation with catechol can help Cr(VI) adsorption. From XAS measurements it can be concluded that the ion exchange process with carboxylic site groups is the main biosorption step, followed by the chromium reduction.

Finally, utilization of biosorbent loaded with heavy metal as brick materials is a promising way to solve disposal problem. These biosorbents are promising materials that can be applied in large scale to deal with the polluted water in the world.

Resum

Les aigües contaminades per metalls pesants han rebut una atenció creixent a causa de la seva alta toxicitat, persistència en els sediments i acumulació biològica dels metalls pesants, sent una amenaça potencial per als sers vius, fins i tot a baixa concentració. Les tècniques tradicionals per eliminar metalls pesants són processos contaminants i de cost elevat, fet que limita les seves aplicacions. Així, és urgent trobar un mètode de baix cost, de bona eficiència i *eco-friendly* per fer front a aquest tipus de problemes. La biosorció pot ser una opció prometedora en aquest cas gràcies a mostrar bones eficiències i ser un material respectuós amb el medi ambient, emprant biomassa.

D'altra banda, hi ha gran quantitat de residus de biomassa al món els quals poden causar un problema ambiental si no es gestionen correctament. D'altra banda, la cel·lulosa, la hemicelulosa i la lignina són abundants en residus de biomassa. La presència de grups funcionals ben coneguts en aquests components naturals els converteixen en materials potencials per a la biosorció de metalls pesants.

Així, la biomassa s'ha emprat com adsorbent natural permetent resoldre dos problemes ambientals: en primer lloc, l'eliminació de residus agrícoles (de biomassa agrícola) i, en segon lloc, la seva utilització com a adsorbents per a l'eliminació de metalls pesants procedents de les aigües residuals.

Amb aquest propòsit, s'utilitzen tipus diferents de biomassa i alguns dels seus biochars per eliminar els ions Cr(III), Cd(II), Cu(II) i Pb(II) a partir d'una barreja d'aquests. D'altra banda, les partícules de TiO₂ també són un bon adsorbent per eliminar metalls pesants. El pi i el pi pirolitzat carregat amb TiO₂ (Pine/TiO₂) s'empen com a adsorbents per eliminar els metalls pesants de les aigües. S'ha comprovat l'especiació de Cr(III) i Cr(VI) emprant els sistemes de biomassa/biochar del pi.

En tots els casos, s'optimitzen diferents paràmetres dels processos de biosorció en experiments en discontinu (el pH de la solució, la concentració inicial i el temps de contacte), i s'han ajustat tan models cinètics com d'isotermes per aclarir els possibles mecanismes d'adsorció. La morfologia superficial dels adsorbents s'analitza mitjançant microscòpia electrònica de rastreig (SEM) i espectroscòpia infraroja de transformada de Fourier (FTIR). A més, es realitza espectroscòpia d'absorció de raigs X (XAS) per estudiar el mecanisme de biosorció a nivell molecular.

La capacitat de biosorció de les biomasses avaluades es classifica de la manera següent: FO (residus de fangs de la indústria) > ZO (de l'agricultura, residus de biomassa de blat de moro) >> CO (residus de biomassa de fusta de pollancre). S'ha trobat que la complexació i l'intercanvi de cations són els dos principals mecanismes d'adsorció en sistemes que contenen mescla de metalls pesants, sent l'intercanvi de cations el més significatiu. Com a resum de l'estudi de l'especiació de crom realitzat per sistemes de biomassa/biochar de pi, els resultats mostren que l'adsorció de Cr(III) es fa principalment a través d'un intercanvi iònic amb els components minerals presents a les superfícies dels biomaterials. El procés de piròlisi pot augmentar la concentració d'aquests minerals per augmentar la capacitat d'adsorció. Per al Pi/TiO₂, juntament amb l'intercanvi iònic també la complexació amb el catecol pot ajudar la biosorció Cr(VI). Des de mesures XAS es pot concloure que el procés d'intercanvi iònic amb grups carboxílics és el principal pas de biosorció, seguit de la reducció del crom.

Finalment, la utilització de biosorbents contenint metalls pesants com a materials de maó és una manera prometedora de resoldre el problema d'eliminació. Aquests biosorbents són materials prometedors que es poden aplicar a gran escala per tractar l'aigua contaminada del món.

List of Symbols

O	Raw biomass
R	Fast pyrolysis
L	Slow pyrolysis
G	Gasification pyrolysis
ATR-FTIR	Attenuated total reflectance Fourier transform infrared spectroscopy
SEM	Scanning electron microscopy
ICP-MS	Inductively coupled plasma mass spectrometry
XRD	X-ray diffraction
BET	Brunauere Emmette-Teller technique
XAS	X-ray absorption spectroscopy
XANES	X-ray absorption near-edge spectroscopy
EXAFS	X-ray absorption fine-structure spectroscopy
q_e	The amount of heavy metal adsorbed at equilibrium per gram of the adsorbent
V	volume of solution (L)
C_0, C_e	The initial and the equilibrium heavy metal concentrations in solution (mmol /L)
m	Dried mass of adsorbent (g)
ΔG^0	The Gibbs free energy
R	Universal gas constant
K	The absolute temperature
k_1	First-order rate constant (min^{-1})
k_2	Second-order rate constant ($\text{g mmol}^{-1} \text{min}^{-1}$)
α	The initial rate constant (mg/g min)
β	Desorption constant (mg/g)
K_F	Freundlich isotherm constant
n	Freundlich isotherm constant
K_L	Langmuir isotherm constant
n	Langmuir isotherm constant
K_L	Langmuir equilibrium constant ($\text{L}/\mu\text{mol}$)
R^2	Correlation coefficient
T	Solution temperature ($^{\circ}\text{C}$)
DTA-TGA	Thermal gravimetric analysis

Index

Introduction	5
1.1 Heavy metals pollution problem in the world	5
1.1.1 Chemical properties of selected heavy metals	8
1.1.2 Wastewater treatment methods	10
1.2 Biosorption (with biomasses)	15
1.2.1 Components of biomass	16
1.2.2 Potential capacity of biomass for heavy metal removal.....	18
1.3 Biosorption of heavy metals using biomass waste	20
1.3.1 Biosorbent from biochar	20
1.3.2 Biomass/biochar modification with particles	22
1.4 Biosorption mechanism study of heavy metals	24
1.4.1 Analytical techniques	24
1.4.2 X-ray Absorption Spectroscopy (XAS)	25
1.4.3 Main functional groups on biosorption systems	29
1.4.4 Biosorption mechanisms	32
1.4.5 Advance in biosorption mechanism by XAS	34
1.5 Recycling biosorbents	37
1.6 Objectives.....	38
References.....	39
Methodology.....	59
2.1 Chemicals	59
2.2 Adsorbents	59
2.2.1 Biomass and biochar	59
2.2.2 Chemical pretreatment of adsorbents.....	61
2.2.3 TiO ₂ loaded on the pine biochar	62
2.2.4 SPION loaded on the biomass.....	62
2.3 Characterization	63
2.3.1 Fourier transform infrared spectroscopy (ATR-FTIR)	63
2.3.2 Scanning electron microscopy (SEM).....	63
2.3.3 Inductively coupled plasma mass spectrometry (ICP-MS)	64
2.3.4 X-ray diffraction (XRD).....	64
2.3.5 Brunauere Emmette-Teller technique (BET).....	65
2.3.6 Zeta potential	66
2.3.7 X-ray absorption spectroscopy (XAS)	66

2.4 Procedures	67
2.4.1 Batch biosorption experiments.....	67
2.4.2 Parameters influencing on heavy metal biosorption.....	68
2.4.3 Biosorption kinetics modelling	68
2.4.4 Biosorption isotherm modelling.....	72
References.....	77
3 Result and discussion	83
3.1 Biosorption of heavy metals by agriculture and industry wood wastes.....	84
3.1.1 Biosorption comparison by different biomass systems.....	85
3.1.2 Characterization of biomass systems.....	86
3.1.3 Influence of the contact time for biomass systems.....	90
3.1.4 Biosorption kinetics modeling for banana peel (BO), canola (LO) and rice (RO)	93
3.1.5 Influence of the initial heavy metal concentration on biomass systems: rice (RO) and canola (LO)	97
3.1.6 Biosorption isotherm modeling for rice (RO) and canola (LO)	98
3.1.7 Influence of the aqueous solution pH for rice (RO), canola (LO) and banana peel (BO)	101
3.1.8 Influence of the temperature with BO	102
3.1.9 Thermodynamic parameters for rice (RO) and canola (LO).....	103
3.1.10 Summary	105
3.2 Biosorption of heavy metals by biochar systems.....	107
3.2.1 Comparison biosorption percentage of poplar, corn and sludge system	108
3.2.2 Characterization of poplar (CO/CL/CR), corn (ZO/ZL) and sewage sludge (FO/FL)	110
3.2.3 The influence of the contact time.....	115
3.2.4 Kinetic modelling for biomass/biochar systems: poplar (CO/CL), corn (ZO/ ZL), and sewage sludge (FO/FL)	117
3.2.5 Comparison of pine wood systems: biomass (PO) and biochars (PL, PR and PG).....	118
3.2.6 Comparison of biosorption capacity for all biosorbents	118
3.2.7 Summary	121
3.3 Biosorption of heavy metals by particles loaded biochar.....	123
3.3.1 Biosorption characteristics for TiO ₂ modified biomass: sugar cane (SO, SO/TiO ₂), corn (ZO, ZO/TiO ₂), and pine (PO, Pine/TiO ₂)	124
3.3.2 Summary	134

3.4 Biosorption mechanism of heavy metals by XAS.....	135
3.4.1 Chromium speciation: biosorption mechanism elucidation by XAS.	135
3.4.2 Mechanism study for Cr(III) and Pb(II) by XAS	145
3.4.3 Summary	149
3.5 Future trends: Disposal of biosorbents-heavy metals mixture	150
References.....	154
Conclusions	163
Annex I	169
Annex II	190
Annex III	208
Annex IV	226

Chapter 1

Introduction

Chapter 1

Introduction	5
1.1 Heavy metals pollution problem in the world	5
1.1.1 Chemical properties of selected heavy metals	8
1.1.2 Wastewater treatment methods	10
1.2 Biosorption (with biomasses)	15
1.2.1 Components of biomass	16
1.2.2 Potential capacity of biomass for heavy metal removal	18
1.3 Biosorption of heavy metals using biomass waste	20
1.3.1 Biosorbent from biochar	20
1.3.2 Biomass/biochar modification with particles	22
1.4 Biosorption mechanism study of heavy metals	24
1.4.1 Analytical techniques	24
1.4.2 X-ray Absorption Spectroscopy (XAS)	25
1.4.3 Main functional groups on biosorption systems	29
1.4.4 Biosorption mechanisms.....	32
1.4.5 Advance in biosorption mechanism by XAS.....	34
1.5 Recycling biosorbents	37
1.6 Objectives.....	38
References.....	39

Introduction

1.1 Heavy metals pollution problem in the world

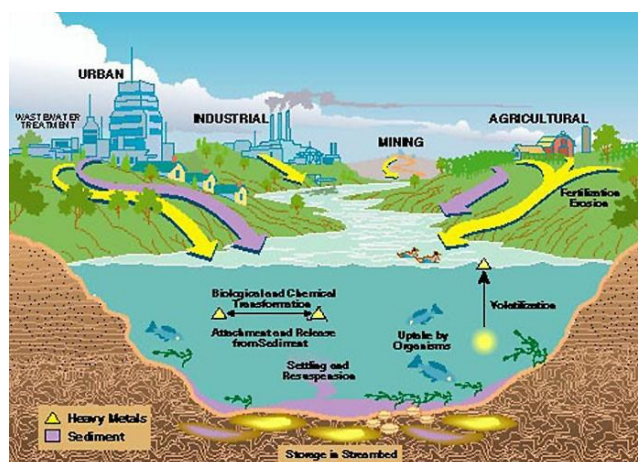


Figure 1.1. Sources of heavy metals in water¹.

Polluted water contaminated by heavy metals has received increasing attention due to their high toxicity, persistence in sediment, and biological accumulation of the heavy metals, which lead to a potential threat to animals and human beings even at low concentration^{2,3}. As shown in Table 1.1, is the main heavy metal pollutants and their main sources, including fertilizer leaching, sewage discharge, industrial wastewater, and urban construction over the last decades⁴⁻⁶. Normally heavy metals are transported as either dissolved species in water or as an integral part of suspended sediments. They also may be volatilized to the atmosphere or stored in river bed sediments. Once organisms take up toxic heavy metals, the metals dissolved in fluids have the greatest potential of causing the most deleterious effects (shown in Figure 1.1).

Table 1.1 Sources of heavy metal contamination in nature⁷.

Sources	Heavy metals	Severity
Industrial waste: Mining, pharmaceutical, textile, petrochemical and oil spills and E-waste	Zn, Ni, Cu, Cr, Pb, Cd, Mn	High
Airborne sources: Stack, vehicular and fugitive emissions	As, Cd, Pb	Wide area distribution Severe
Fertilizers	Co, Cu, Fe, Mn,	Average
Pesticides	Cu, Hg, Mn, Pb, and Zn	Low
Sewage Sludge	As, Cd, Cr, Cu, Pb, Hg, Ni, Se, Mo, Zn, Tl and Sb	Low to average

In general, rivers are the main source of life because they provide fresh water, which is critical for the survival of both flora and fauna. However, the releases of toxic heavy metals from different sources have contaminated the rivers resulting in serious water problems such as the lack of clean drinking water. Most heavy metal polluted rivers around the world in 2019 are also listed in Table 1.2. Although the concentration of heavy metals in water is usually employed as a pollution indicator, sediments is also an important indicator. Many researches have been published with these indicators to describe the conditions of heavy metal pollution in rivers.

As shown in Table 1.2, arsenic (As), cadmium (Cd), chromium (Cr), copper (Cu), cobalt (Co), iron (Fe), mercury (Hg), manganese (Mn), nickel (Ni), lead (Pb) and zinc (Zn) are the widespread heavy metals pollutants in rivers. In the case of Cu, Zn, Fe, Mn, Ni, and Co, they are essential for life but can be toxic if taken in excess⁸. And for As, Cd, Cr, Hg and Pb have high toxicity either at modest concentration levels.

Table 1.2. Literatures related to heavy metal pollutants in rivers around the world.

Rivers	Location	Heavy metals in water or sediments	References
Ganges River	India	As, Cd Cr, Cu, Co, Fe, Hg, Mn, Ni, Pb, Zn	(Dipak Paul, 2017) ⁹
Citarum River	Indonesia	Cu	(Indah et al., 2008) ¹⁰
Yangtze River	China	As, Cd, Cr, Cu, Hg, Ni, Pb, Zn	(Fu et al., 2013) ¹¹
Sarno River	Italy	Cr, Sn, Pb, Hg, Zn, Cd, Sb	(Domenico et al., 2013) ¹²
Buringanga River	Bangladesh	Pb, Cr, Mn, Co, Ni, Cu, Zn, As, and Cd	(Indah et al., 2015) ¹³
Mississippi River	North American	Pb, Cd	(B. J. PresleyJ. et al., 1980) ¹⁴
Jordan River	West Asia	Cd, Zn	(Ibrahim et al., 2018) ¹⁵
Mantaza Riachuelo River	Argentina	Cr, Pb, Cu, Zn, Ni, Cd	(Castro et al., 2018) ¹⁶

Rivers are the main source of drinking water, so the effects of heavy metals in rivers also have been extensively studied. It is worth noting that Mantaza Riachuelo River and Sarno River are heavily polluted by Cr due to the waste solutions from tanneries industries nearby. While Cr(VI) has been identified as a top-priority hazardous pollutant with low modest concentration¹⁷. Table 1.3 listed some main heavy metals, and their damage to human being. Hence, the removal of these heavy metals toxicity from rivers has been attracted attention for a long time.

In conclusion, rivers are polluted by heavy metals, and emergency to find a suitable way to clear it to protect environmental, animals and human health.

Table 1.3. limitation of heavy metal, sources and potential damage in drinking water according to U.S. Environmental Protection Agency¹⁸.

Contaminant	Limitation mg/L	Potential Health Effects from Long-Term Exposure	Sources
Cadmium	0.005	Kidney damage	Corrosion of galvanized pipes; erosion of natural deposits; discharge from metal refineries; runoff from waste batteries and paints
Chromium (total)	0.1	Allergic dermatitis	Discharge from steel and pulp mills; erosion of natural deposits
Copper	1.3	Liver or kidney damage	Corrosion of household plumbing systems; erosion of natural deposits
Lead	0	Kidney problems; high blood pressure. Slight deficits in attention span and learning abilities for children.	Corrosion of household plumbing systems; erosion of natural deposits
Arsenic	0	Skin damage or problems with circulatory systems, and may have increased risk of getting cancer	Erosion of natural deposits; runoff from orchards, runoff from glass and electronics production wastes

1.1.1 Chemical properties of selected heavy metals

Lead, cadmium, copper and chromium are studied here for their removal from aqueous solution since they are widely used in industrially. Moreover, cadmium and chromium are highly toxic even at low concentration level. Therefore, efficiency techniques are needed to remove these toxic heavy metals from wastewaters.

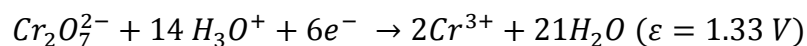
Lead is a chemical element with symbol Pb and atomic number 82. Pb has two main oxidation states: Pb(II) and Pb(IV). It can be accumulated in the environment due to its no biodegradable nature and concentrated in organisms leading to damaging effects on human, plants and animals. For example, lead intake in humans causes disruption of the biosynthesis of hemoglobin, the rise in blood pressure, kidney damage, miscarriages and abortions, brain damage and diminished learning abilities in children¹⁹.

Copper is a chemical element with symbol Cu and atomic number 29. It is essential for the human being and involved in the life process in the form of enzymes. However, higher concentrations (>5 mg/l) in the body can cause kidney damage, high fever, hemolysis and vomiting. Excessive copper in the marine system has been found to damage marine life leading to the damage of gills, liver, kidneys, the nervous system and changing sexual life of fishes²⁰.

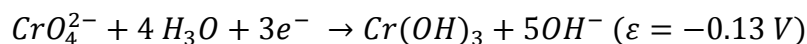
Cadmium is a chemical element with symbol Cd and atomic number 48. It demonstrates oxidation +2 in most of its compounds. It is one of the most toxic heavy metals in wastewater, which can accumulate in living organisms and pass through the food chain into human organs (such as skeletal, urinary, reproductive, cardiovascular, central and peripheral nervous, and respiratory systems), causing serious toxicity with the modest concentration of 0.001- 0.1 mg/L²¹.

Chromium is a chemical element with symbol Cr and atomic number 24. Cr has six oxidation states including Cr(0), Cr(I), Cr(II), Cr(III), Cr(IV) and Cr(VI), while Cr(III) and Cr(VI) are the most common states in the world. Chromium(VI) has two forms Chromate anions (CrO_4^{2-}) and dichromate ($\text{Cr}_2\text{O}_7^{2-}$) anions, which have a five hundred times toxicity than Cr(III). Cr(VI) is considered to be one of the most toxicity metals, causing severe physiological or neurological damage on a human being with modest concentration²².

In addition, Cr(VI) anions are strong oxidizing reagents at low pH:



They are, however, only moderately oxidizing at high pH:



The Pourbaix diagram is a map of the most stable species in a solution. It depends on temperature, pressure and most importantly, the total relative concentration of the element present. It is great for discussing the corrosion behavior of different metals. In our case, it is great for discussing the most stable form of metal in water solution at different pH. As shown the Pourbaix diagram of Cr in figure 1.2, the region between the green lines are places where stable Cr species can exist in pure water.

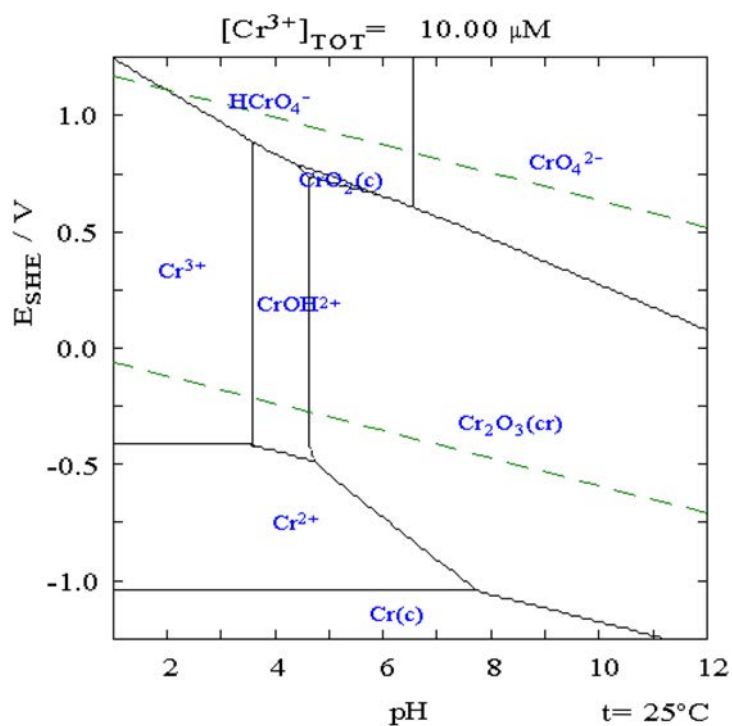


Figure 1.2. The Pourbaix diagram of Cr

1.1.2 Wastewater treatment methods

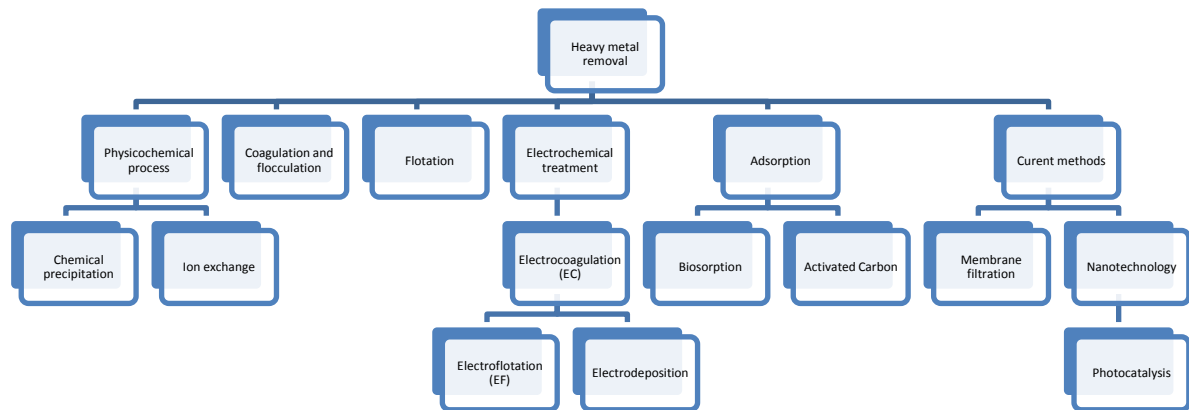


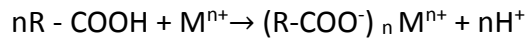
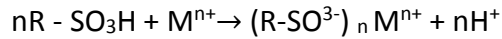
Figure 1.3. Diagram for wastewater treatment methods²³.

In recent years, various methods for heavy metal removal from wastewater have been extensively studied. These technologies mainly include chemical process, adsorption, membrane filtration, adsorption, electrochemical and nanotechnology methods. Diagram for wastewater treatment methods has been shown in Figure 1.3.

Chemical precipitation is effective and by far the most widely used process in the industry includes hydroxide and sulfide precipitation. In precipitation processes, chemicals react with heavy metal ions to form insoluble precipitates. The forming precipitates can be separated from the water by sedimentation or filtration. And the treated water is then decanted and appropriately discharged or reused²⁴. *Chen et.al* showed that fly ash-lime-carbonation treatment can increase the particle size of the precipitate and significantly improved sedimentation of sludge and the efficiency of heavy metal removal. The residual concentrations of chromium, copper, lead and zinc in effluents can be reduced from 100 mg/L to 0.08, 0.14, 0.03 and 0.45 mg/L, respectively²⁵.

Ion exchange treatment is based on a reversible interchange of ions between the solid (resin) and liquid phases (wastewater). Cation exchangers are strongly acidic resins normally interact with sulfonic acid groups ($-\text{SO}_3\text{H}$), or weakly acid resins with carboxylic acid groups ($-\text{COOH}$). Hydrogen of a sulfonic group or carboxylic group of

the resin can exchange with metal cations. When the solution of heavy metal passes through the cationic column, metal ions can exchange with hydrogen on the resin by following the ion-exchange process:



Bilge et al. performed down HCR S/S cation exchange resin for removal of nickel and zinc from aqueous solutions. It was observed that more than 98% removal efficiency was achieved under optimal conditions for nickel and zinc²⁶. *Dąbrowski et al.* selective removal of heavy metals from wastewaters by ion-exchange method, and the method is confirmed technologically simple and high efficiency for the removal of Pb(II), Hg(II), Cd(II), Ni(II), V(IV,V), Cr(III,VI), Cu(II) and Zn(II)²⁷. *Zhao et al.* reported the results of a new anion exchanger, referred to as polymeric ligand exchanger or PLE, which shows very high chromate affinity under otherwise identical conditions²⁸.

Membrane filtration technologies are a pressure-driven separation process that employs a membrane for both mechanical and chemical sieving of particles and macromolecules. Based on the pore size of the membranes, it can be classified as microfiltration, ultrafiltration, nanofiltration, and reverse osmosis (shown in Figure 1.4). The membranes techniques have been widely used for heavy metal removal from aqueous solution. *Bessbousse et al.* used a novel complexing membrane for the removal of Pb, Cd and Cu from aqueous solution. The filtration of solutions of each metal ion with membrane modified systems showed large elimination ratios (96–99.5%) for each metal²⁹. *Resina et al.* reported the application of hybrid membranes for metal separation³⁰. Similar researches can be found in many reviews papers^{31,32}. Furthermore, membrane filtration can remove some bacteria from water, which have been used in drinking water treatment³³.

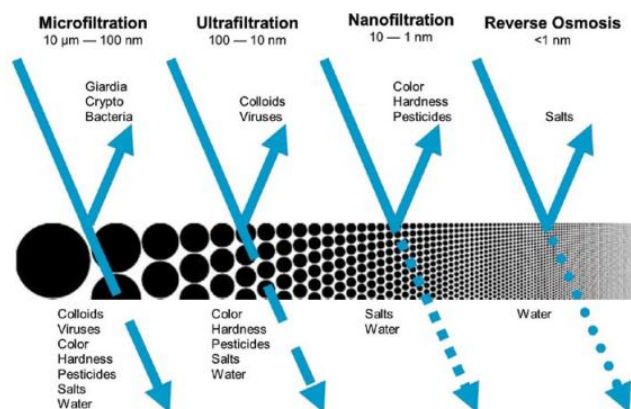


Figure 1.4. Type of membrane based on the size of membrane.

Coagulation and flocculation involve combining insoluble particles and dissolved organic matter into larger aggregates that can be removed in subsequent sedimentation and filtration stages. Alum (aluminum sulfate), lime $[\text{Ca}(\text{OH})_2]$ and ferric salts $[\text{FeCl}_3$ or $\text{Fe}_2(\text{SO}_4)_2]$ are the most widely used coagulant agents. Coagulants destabilize suspended and colloidal particles in wastewater by forming microflocs. These are aggregated by flocculation, which consists of a stirring procedure that encourages particles to clump allowing their removal in subsequent treatment stages³⁴.

Fong et.al combined hydroxide precipitation and coagulation-flocculation methods to remove heavy metals from aqueous solution. The jar test showed that up to 99% of Pb was removed from solution³⁴.

Flotation is based on imparting the ionic metal species in waste waters hydrophobic by use of surface-active agents (surfactants) and subsequent removal of these hydrophobic species by air bubbles. *Polat et.al* used flotation method to remove Cu, Zn, Cr and Ag from waste water. The result shows that 74% of metals were removed under optimum conditions at low pH and reached up to 90% at basic pH³⁵.

Electrochemical methods can remove or recover heavy metals based on the principle that metals become precipitated in their elemental form on the solid electrodes when the potential or electricity is applied on the electrode. The basic reaction occurring is the reduction of metals in different oxidation states into a zero oxidation state (elemental state of metal) at the cathode when there is a flow of electrons through the circuit from the anode³⁶. This technique includes electrocoagulation (EC), electroflotation (EF) and electrodeposition. By using this method, *Basha et.al* showed that Cu, As, Cd and Zn were reduced from 164 to 1.96 mg/L, 1979 to 103 mg/L, 76 to 39 mg/L and 455 to 166 mg/L, respectively³⁷.

Adsorption is the adhesion of atoms, ions or molecules from a gas, liquid or dissolved solid to a surface. The adsorption mechanism is based on weak bonds such as the *Van der Waal's* forces and electrostatic and hydrophobic interactions between the adsorbate and matrix³⁸. Adsorbents sources are varied, they can be derived from agricultural waste, industrial by-products and natural materials. This method has been widely used to remove pollutants due to its low cost, eco-friendly and easy handling^{39,40}. Adsorption will be the main topic of this thesis so it will be developed in depth later.

Advantages and disadvantages of techniques

Although all the heavy metal wastewater treatment techniques can be employed to remove heavy metals, they have advantages and limitations as well.

Heavy metals removal from aqueous solutions has been traditionally carried out by **chemical precipitation** for its simplicity process and inexpensive capital cost. However, chemical precipitation is usually adapted to treat high concentration wastewater containing heavy metal ions and it is ineffective when the metal ion concentration is low. And chemical precipitation is not economical and can produce a large amount of sludge to be treated with great difficulties²³.

Ion exchange has been widely applied for the removal of heavy metal from wastewater. However, ion exchange resins must be regenerated by chemical reagents when they are exhausted, and the regeneration can cause serious secondary pollution. And it is expensive, especially when treating a large amount of wastewater containing heavy metal in low concentration, so they cannot be used at a large scale²⁴.

Membrane filtration technology can remove heavy metal ions with high efficiency, but its problems such as quite high cost, process complexity, membrane fouling and low permeate flux have limited their use in heavy metal removal²³.

Electrochemical heavy metal wastewater treatment techniques are regarded as rapid and well controlled that require fewer chemicals, provide good reduction yields and produce less sludge. However, electrochemical technologies involving high initial capital investment and the expensive electricity supply, this restricts its development²⁴.

Using **coagulation-flocculation and electrocoagulation** heavy metal wastewater treatment technique, the produced sludge has good sludge settling and dewatering characteristics. But this method involves high chemical consumption and increased sludge volume generation²⁴.

Flotation offers several advantages over the more conventional methods, such as high metal selectivity, high removal efficiency, high overflow rates, low detention periods, low operating cost and production of more concentrated sludge. But the disadvantages involve high initial capital cost, high maintenance costs^{24,35}.

Adsorption is a recognized method for the removal of heavy metals from low concentration wastewaters. Many varieties of low-cost adsorbents have been developed and tested to remove heavy metal ions. However, the adsorption efficiency depends on the type of sorbents, mainly biomass systems. Biosorption of heavy metals from aqueous solutions is a relatively new process that has proven very promising for the removal of heavy metal from wastewater^{39,40}. However, disadvantages also cannot be negligible such as few studies at the pilot and industrial scale, the complexity of the adsorption process, and the disposal problem of biosorbent after biosorption of heavy metal.

1.2 Biosorption (with biomasses)

As we discussed above, most of the techniques are high cost or making the second pollution that limited large-area applications. Most importantly, the removal of heavy metals from the polluted rivers, making it below the strict standard concentration is difficult. As shown in Table 1.4, is the standard concentration of heavy metal in water or sediments, it clears to show a very low concentration of heavy metals in water according to U.S. Environmental Protection Agency (EPA)⁴¹. Especially cadmium (Cd) and lead (Pb) will cause huge damage with little concentration in drinking water (5 ppb and 0 ppb, respectively). While 6 ppm of Cd and 60 ppm of Pb is a heavily polluted water in sediments form.

However, most of the traditional techniques such as precipitation cannot apply to such low concentration in water. Therefore, it is emergency to find a low-cost, efficiency and eco-friendly method to deal with this kind of problem.

Table 1.4. Maximum permitted levels for heavy metals in nature, according to U.S. Environmental Protection Agency¹.

	Cadmium	Chromium	Copper	Lead
Drinking water, in mg/L ¹⁸	0.0050	0.10	1.3	0
Water supporting aquatic life, in mg /L	0.12	0.10	0.020	0.1
Nature sediments, nonpolluted, in mg /g	--	<0.025	<0.025	<0.04
Nature sediments, moderately polluted, in mg /g	--	0.025 to 0.075	0.025 to 0.050	0.04 to 0.06
Nature sediments, heavily polluted, in mg /g	>0.0060	>0.075	>0.050	>0.06

Biosorption can be an promising option in this case due to its high efficiency and eco-friendly, especially the abundant materials in the world such as biomass. Biomass is an organic matter that can be converted into energy, which are widely used around the world⁴². Common examples of biomass have been used as energy source include wood, crops, seaweed, and animal wastes⁴³. Furthermore, the amount of biomass waste in the world is huge and the sources are varied.

Biomass from agriculture wastes, such as rice, wheat, cotton, maize, sugarcane, soybean, coffee and cotton are the most cultivated plants all over the world, but the parts of shell or stalk are useless. The field burning of agriculture waste is a common

method to dispose of waste after harvesting seasons. However, burning in an open field is forbidden in most countries due to the emission of CO₂ that leads to global warming⁴⁴.

In addition, one case in China is rice (*Oryza sativa L*) and canola (*Brassica napus L.*). It is well known that China is the most producers and consumers of rice and canola in the world. Meanwhile, canola is suitable rotational crop with rice, while canola is grown in winter and rice in summer⁴⁵. Mass cultivation of rice and canola were grown on a large scale in China, and harvested area reached 30 million ha in 2010 and 6.5 ha in 2014 for rice and canola, respectively^{46,47}.

Similar, Brazil also has the disposal problem of sugarcane and coffee shell. Brazil has an average yield of ~80 Mg ha⁻¹ of sugarcane, and around 14 Mg ha⁻¹ of dry biomass is disposal on the earth after each harvest⁴⁸. Meanwhile, Brazil is the largest producer of Coffee arabica, and is also the major coffee exporter with an annual production of 28 billion bags⁴⁹.

Banana, a tropical fruit, its world production is about 81.3 Mt per year. Considering that banana peel (the peel of banana) represents the 25%–30% of the total dry matter, about 5 Mt of peels is produced every year⁵⁰. On another hand, Colombia is the world's fifth largest banana exporter and the area cultivated were 49,146 hectares in 2017⁵¹.

Wood biomass waste (such as pine, poplar) from pulp industry will be biologically broken down to release CO₂ gases. Moreover, wood biomass waste such as sawdust, a solid waste produced in large quantities at sawmills and timber industry each year. These wood biomass are no market values at all and disposal in the world.

Therefore, biomass wastes have been considered a significant disposal problem and will cause an environmental problem if not handled properly. However, some components from these waste biomass can be used as biosorbent to remove heavy metals.

1.2.1 Components of biomass

Cellulose, Hemicellulose and Lignin are the three main components of biomass, general account for 40-60, 20-40, and 10-25 wt.% of dried biomass, respectively⁵². The percentage of these three components in biomass are varies depending on the

mother biomass. These components working together in the cell wall of plant and giving the plant rigidity (show in Figure 1.5).

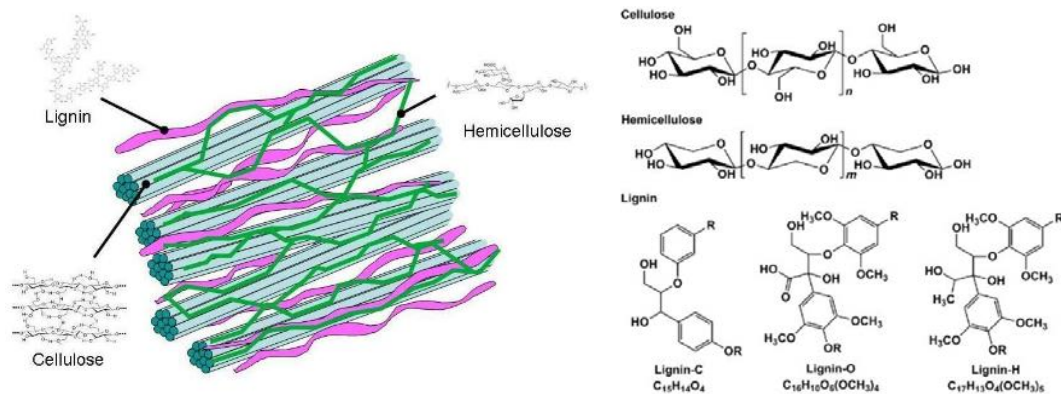


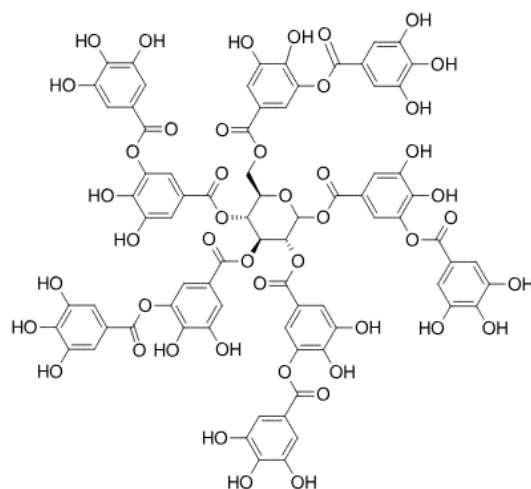
Figure 1.5. Structures of cellulose, hemicellulose, and lignin.

Cellulose is argued to be the most abundant polymer in nature and constitutes the main component of plant fibers, giving the plant rigidity. It can be derived from a variety of sources, such as woods, annual plants, microbes, and animals and including various functional groups, such as carboxylic, hydroxyl, methoxy, and phenolic groups that are potentially active in metals binding⁵³.

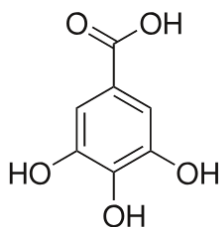
Close to cellulose, lignin is the most abundant plant-derived polymer in the world. It is an amorphous and complex aromatic polymer providing structural rigidity to the cell walls of many plant species. Along with cellulose is hemicellulose (also known as polyose), is one of a number of heteropolymer (matrix polysaccharides). While cellulose is crystalline, strong, and resistant to hydrolysis, hemicelluloses have a random, amorphous structure with little strength.

Tannins are polyphenolic compounds that have become widely present in woody plants⁵⁴. They play a role in protection from predation (including as pesticides) and could help in regulating plant growth⁵⁵. Tannic acid is a specific form of tannin and it has three main forms, namely, gallic, digallic, or ellagic acid (shown in Figure 6). As can be seen, tannins contain multiple adjacent hydroxyl groups that can form chelates with metal ions. This characteristic allows tannins to be used in water treatment when present in biomass systems. Especially, tannins are found mostly in the bark of pine, the wattle of mimosa and hemlock and in the wood of certain trees such as quebracho and sumach trees⁵⁶.

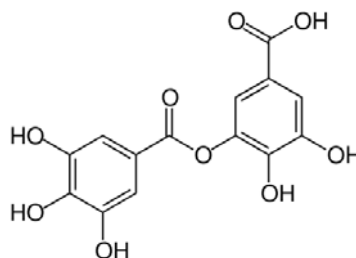
(a) Tannic acid



(b) Gallic acid



(c) Digallic acid



(d) Ellagic acid

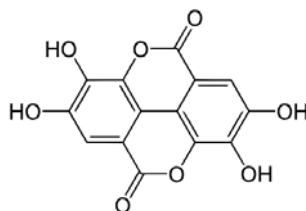


Figure 1.6. Tannic acid and its three forms; (a) Tannic acid, (b) Gallic acid, (c) Digallic acid, and (d) Ellagic acid.

1.2.2 Potential capacity of biomass for heavy metal removal

Cellulose, hemicellulose and lignin are abundant in the world and they can be employed as cheap adsorbents due to their special physical and chemical properties. The functional groups in these natural materials can potentially interact with heavy metals for their removal. *Sanna et.al* reviewed that modified cellulose can improve adsorption capacity⁵³. Also, *Nontipa et.al* reviewed that the pretention of lignin-derived activated carbons can be used as adsorbents for heavy metals removal (such as Cu, Zn, Pb and Cd), or for the recovery of noble metals (e.g., Pd, Au and Pt)⁵⁷.

Moreover, sugarcane has been widely used to remove heavy metal since it is rich in components of cellulose, lignin and hemicellulose. *Want et.al* reported that modified cellulose derived from sugarcane can be used to remove heavy metal from aqueous solution⁵⁸. Biochar of sugarcane was used as biosorbent for the removal of Cr(III) by *Yang et.al*⁵⁹. *Umesh K. Garg* successfully removes Cr(VI) by using sugarcane⁶⁰. *Basso et.al* reported that lignocellulosic in sugarcane was potential biosorbent for Ni and Cd removal⁶¹. Therefore, cellulose and lignin are considering being the low-cost and eco-friendly adsorbents to remove heavy metals from wastewaters.

The ability of tannins to chelate metal ions has been shown in several studies due to the presence of –OH groups, which can be applied as biosorbents for heavy metal removal in waters. Especially, tannins have a special binding process with Cr and Cu. *Boris et.al* studied the heavy metal binding by tannic acid. Their results show that the tannic acid can interact with heavy metal and the affinity increases in the order Cd(II)<Zn(II)<Pb(II), while Cu(II) seems to form an inner complex with tannic acid⁶².

Hirohumi et.al extracted tannin from withered oak leaves, and they found that tannin can reduce Cr(VI) to Cr(III). Two forms tannins (gallic acid and catechin) were found in oak leaves and later they confirmed gallic acid is involved in the reduction process⁶³. In addition, catechol, which is a component of tannin molecules, was assumed to be the responsible of the surface reduction of Cr(VI) by first binding chromate and later reducing it to Cr(III), which can be adsorbed by ion exchange with the functional groups of the tannin⁶⁴.

1.3 Biosorption of heavy metals using biomass waste

Biosorption is a physical-chemical process, simply defined as the removal of substances from solution by biological materials such as biomass waste. The sources of materials include both living and dead organisms (and their components). It has been considered as promising biotechnology because of its simplicity, the analogous operation to conventional ion-exchange technology, apparent efficiency and availability of biomass and waste bio-products⁶⁵. Various living biomaterials, such as micro-organisms, bacteria, fungi, yeast and algae have been reported for the removal of heavy metal from aqueous solutions^{24–26}, which is not the main purpose of the present thesis (even the influence of microorganisms will be discussed briefly).

As discussed above, agriculture waste and wood biomass can be applied as biosorbents to remove heavy metal due to their low-cost, high efficiency and eco-friendly. In addition, modified biomass waste were also studied since its higher capacity after pretreatment compared with original materials, especially the case performed in multiple systems.

This is possible due to the presence of some polar functional groups such as alcohols, aldehydes, ketones, carboxylic, phenolic and ether groups present in the agriculture and woody biomass wastes, in their structure of cellulose, hemicellulose and lignin (as mentioned)⁵⁸. These groups can ion exchange with heavy metals from water and also can bind heavy metals by donation of an electron pair from these groups to form complexes with the heavy metal in solution⁴⁰.

During the past decades, numerals articles were published reporting the successful use of different kinds of agricultural wastes in the removal of heavy metal from aqueous solution such as Cr, Cu, Ni, Pb, Cd, As and Hg etc^{23,24,40,69}. Biosorption of Cr by agriculture waste is quite high and varies from 50 to 100%, while high biosorption efficiency was found at pH 2, in which Cr(III) is the main form present in solution⁶⁸. Besides, rice straw and rice husk are the most used adsorbents and they show high-efficiency adsorption for Pb and Cd⁶⁸. Similarly reviews papers can be found everywhere⁷⁰.

1.3.1 Biosorbent from biochar

To increase the biosorption capacity, chemical activating agents can be used to modify the adsorbents in order to increase the large surface. However, modification processes usually consume high energy and labor cost, so they do not bring high

economic and efficient process⁷¹.

In this sense, biochar can be produced by pyrolysing biomass systems at different range temperatures and times. Biochar has a high pore structure with large surface area, and it is obtained without an expensive process. Biochar is an emerging biosorption material which can be an economical substitute of the activated carbon to remove different kinds of pollutants.

Biochar, a low-cost carbonaceous material, is a byproduct of pyrolysis or gasification pyrolysis processes, both at high temperature (300–900°C), and in absence or presence of O₂ limiting conditions, respectively⁷². Its sources are vary, while agriculture waste, algal biomass, forest residues, manures, activated sludge, energy crops, digestate, etc. have been used to produce biochar^{73–75}. Similarly, biochar has been widely used to remove heavy metals from wastewaters⁷⁶. Furthermore, The heavy metal adsorption efficiency of biochars can vary widely depending on the types of feedstocks and the pyrolysis temperature^{77,78}

The most commonly used feedstock to produce biochar is from agricultural wastes, such as corn, rice, fruit peels, coconut, peanut, olive, coffee shell, sugar cane and wood from forests⁷⁹. In addition, biochar derived from other kind of original materials, such as daily manure, wastewater sludges and micro algae, has also been studied in the last decade^{80–82}. Hence, a large body of literature focuses on the use of biochar to remove heavy metals, such as Pb, Cu, Cr, Cd, Ni and Zn, which are the most studied heavy metals present in wastewaters^{83,84}.

Rice biochar produced at different temperature were studied by *Shen* for Pb removal and those produced at higher temperatures increase the pH biomaterial values and increase the surface areas, resulting in higher metal removal capacities and faster uptake of Pb.⁸⁵

Crop residues such as wheat straw, rice straw, corn stover, rape stalk and cotton stalk were checked to study the yield of biochar at different temperatures by *He et.al*. In general, biochar yields decreased and the gas yields increased from 300°C to 600°C. Therefore, pyrolysis temperature and time can affect the biosorption capacity.

Functional groups from the original biomass will decreased with the increase of the pyrolysis temperature, which caused an increase pH of biochar since the loss of

negative functional groups compared with raw biomass. Meanwhile, mineral concentration will increase as they were present in plant and released from biomass through pyrolysis process⁷⁴.

1.3.2 Biomass/biochar modification with particles

As seen biomass contains functional groups that help bind to heavy metals in solution and have a good biosorption capacity, which decreases in multiple systems due to the metal competition. On the other hand, biochar, pyrolysis product of biomass will increase biosorption capacity, but with loss of much functional groups during the pyrolysis process.

To overcome this lost, nanoparticles such as Iron, titanium were introduced to biomass/biochar system to enrich either the functional groups in biomass, as well as to expand the surface⁸⁶. Numerals studies successfully increased adsorption capacity after introducing nanoparticles⁸⁷⁻⁹². *Liang, J. et al.* reported that MnO₂ modified biochar showed superior adsorption performance (maximum capacity for Pb 268 mg/g and Cd 45.8 mg/g) to original biochar (Pb 128 and Cd 14.4 mg/g)⁸⁷. *Yan, L. et al.* successfully synthesised magnetic biochar/ZnS which showed a high maximum adsorption capacity for Pb (II) up to 368 mg/g, which was 10 times higher than that of reported by biochar/magnetic⁸⁸.

TiO₂ nanoparticles were also studied since its photocatalyst under UV/visible light. *Shi, M. et al.* synthesis TiO₂ on biomass can successfully remove organic pollutants by photodegradation.⁸⁹ *Wang et. al* performed adsorption of Cr(VI) by UV/TiO₂ as photocatalyst system, and 94% of Cr(VI) was photoreduced within 1h at pH 3⁹³. The challenge for applying such particles is how to develop highly photocatalysts to accelerate the reactions. Particles size is a key point to affect the photocatalyst because the smaller size and smaller thickness of particles can accelerate reactions. However, nanoparticles (between 1-100nm) are easier to aggregate which largely hindering the photocatalyst process. Synthesis particles on a supporter is an effective way to solve the aggregate problem. CoO_x loaded TiO₂-based nanosheets showed excellent photocatalytic activity for the removal of Cr(VI) under visible light⁹⁴. Carbon nanotubes were also used as a supporter for the removal of Cr(VI) by *Wang et.al*⁹⁵. Supporter such as carbon nanotube, nanofibers, nanosheet and nanoflower were also studied, however, these supports are really expensive. So, low-cost nanosupports can become a potential way to remove heavy metals. *Ragupathy et.al* loaded TiO₂ on cashew nut shell under sunlight radiation for the removal of organic

dyes⁹⁶. Similar, *Jihyun et.al* using a biochar-supported TiO₂ photocatalyst for the degradation of sulfamethoxazole⁹⁷.

On the other hand, iron oxide nanoparticles are widely used for water treatment due to its specific properties of nanoparticle and easy magnetic separation of sorbent from water after adsorption. Different kinds of sorbents combined with iron oxide nanoparticles were successfully used for the removal of heavy metals from water. *Kiomars et.al* used this salicylhydrazide modified magnetic nanoparticles to remove heavy metals (Pb, Cd, Cu, Zn and Co) from industrial wastes. The maximum adsorption capacities of Pb, Cd, Cu, Zn and Co were found to be 189, 108, 76.9, 51.3, and 27.7 mg/g, respectively⁹⁸. Activated carbon combined with iron oxide was successfully used for the removal of Cr(VI), Cu and Cd by *Jain et.al*⁹⁹.

In summary, many researchers have been studied on the biosorption of heavy metal in a single(mono) and multiple systems. As it is known, the biosorption behaviour varies depending on the species of co-metals ions and the concentration of each metal in solution¹⁰⁰. It also reported that the properties of biosorbents, such as surface area, mineral components and functional groups, participate in the biosorption process¹⁰¹. Moreover, the biosorption capacity decreased since the competition of metal ions. Therefore, it is also important to study biosorption in multiple systems to understand the biosorption mechanism. Moreover, multiple systems are closer to the real system and will provide beneficial information for heavy metal removal in the future.

The biosorption mechanism study in multiple system also can be found in the literature. *Xu et.al* used dairy manure and derived biochars as sorbents for simultaneously removing Pb, Cu, Zn, and Cd from aqueous solutions. The stronger competition of heavy metals in solution was mainly from complexation with phenolic-O and hydroxyl-O groups, and precipitation of metals with PO_4^{3-} and/or CO_3^{2-} .¹⁰¹ Crop milling waste was used to remove Pb, Cd, Cu, Ni and Zn by *Asma Saeed et.al* showed that biosorption of heavy metals with the selectivity order: Pb> Cd> Zn> Cu> Ni¹⁰². Marine Alga was used to remove Pb, Cd and Cu by *Sheng et.al* indicated that biosorption of heavy metals with the selectivity order: Pb> Cu > Cd in multiple system¹⁰³. Ion-exchange was proved the main mechanism in biosorption of Cd, Ni, Zn, Cu, Cr and Pb by macrophytes, while in this biosorption process heavy metals can be exchanged with Na⁺ and K⁺¹⁰⁴. Although many types of research have been studied on this part, deeply mechanism should be further developed.

1.4 Biosorption mechanism study of heavy metals

1.4.1 Analytical techniques

Many techniques have been used to measure and characterize the adsorbents. It is because characterization such as the morphological structure and surface chemistry of biomass that are essential for understanding the metal binding mechanism on the biomass surface. Depending on the nature of the biomass and surface characterization, the biosorption mechanisms can be elucidated using different techniques, including potentiometric titrations, Fourier transform infrared spectroscopy (ATR-FTIR), scanning electron microscopy (SEM), transmission electron microscopy (TEM), energy-dispersive X-ray microanalysis (EDXMA), X-ray diffraction (XRD), X-ray photoelectron spectroscopy (XPS), etc.¹⁰⁵.

However, use of any one of these techniques could not help in complete understanding of the mechanisms involved in biosorption. Hence, a combination of these techniques is used to discover the description of the structure, morphology, metal binding groups, and the composition of biomass, which can optimize and explore the biosorption mechanisms^{106,107}.

Measuring concentration of heavy metal in aqueous solution, can use ICP-mass spectrometry (ICP-MS)¹⁰⁰, atomic absorption spectrophotometry (AAS)¹⁰⁸, ion selective electrodes (ISE)¹⁰⁹ and UV-Vis spectrophotometry¹¹⁰ as main analytical techniques used for this purpose.

X-ray diffraction (XRD) was used to identify changes in the amorphous or crystallographic structure, and also to elucidate the chemical composition of the native and metal-loaded on biosorbents¹¹¹.

Visualization of the inner morphology of control and metal-laden biosorbents is checked by using scanning or transmission electron microscopy coupled with energy dispersive X-ray spectroscopy (SEM/TEM-EDX)¹¹².

Qualitative determination of surface binding sites present on the biosorbent or concentrations of the acidic and basic sites of the biosorbent were checked by potentiometric titration.¹¹³ Also, identification of surface functional groups and the nature of bond between functional groups of biomass can be determined by infrared spectroscopy or Fourier-transform infrared spectroscopy (IR or FTIR)¹¹⁴, electron spin resonance spectroscopy (ESR) and nuclear magnetic resonance (NMR),¹¹⁵ thermal

stability analysis by thermogravimetric analysis (TGA) and differential scanning calorimetry (DSC).¹¹⁶

X-ray absorption spectroscopy (XAS) can be used for the evaluation of the elemental oxidation state of control and metal-laden biosorbents, as well as the coordination environment of metal ions in the biological systems, at the meanwhile, confirmation of participation of functional groups along with existence of covalent and ionic interactions in the biosorption mechanism¹¹⁷. X-ray photoelectron spectroscopy (XPS) for comparison of the surface chemistry and elemental characterization of control and metal-laden biosorbents¹¹⁸.

In this study, ICP-MS, SEM/EDX, FTIR, XRD, zeta potential, BET and XAS have been used to study the biosorption mechanism of heavy metals.

1.4.2 X-ray Absorption Spectroscopy (XAS)

X-ray absorption spectroscopy (XAS) is a widely used technique for investigating atomic local structure as well as electronic states. The electrons that are excited are typically from the 1s or 2p shell and the energies are on the order of thousands of electron volts. Therefore, the experiment is usually performed at synchrotron radiation facilities due to the requirement of high-energy X-ray excitation. Moreover, XAS is particularly convenient because it is a non-destructive method to examine samples directly. Structures can be determined from samples that are both heterogeneous and amorphous. The species of samples also can be in the form of gas-phase, solution, or as solids.

Theory

The process of XAS can be simply described that the photon can be absorbed by the sample after the irradiation and the electrons can be excited to higher energy unoccupied state. When the incident X-ray energy reaches the binding energies that the core electron can be excited, those are called edges. Edge is labeled by the core electron shell, such as shell K = 1s, L1 = 2s (illustrate graphs shown in Figure 1.7).

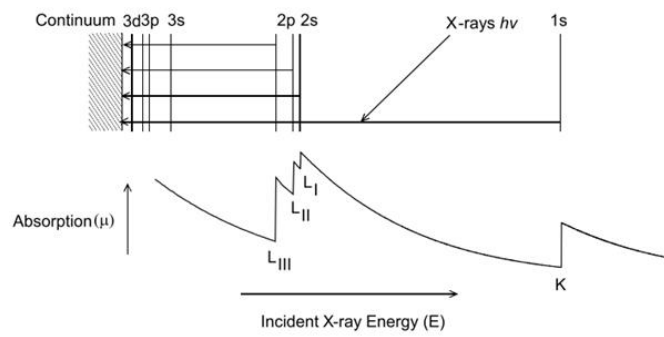
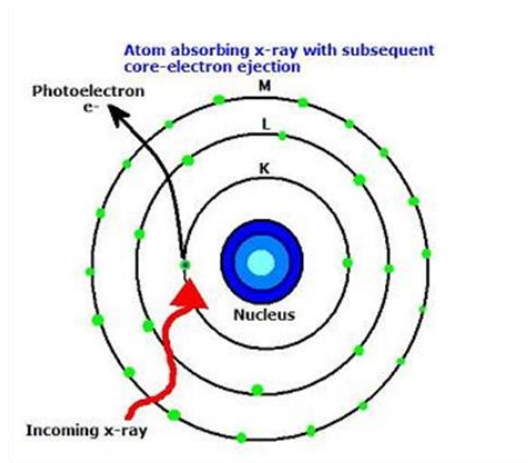


Figure 1.7. Illustrate graphs of XAS process.

Detection of X-ray Absorption Spectra

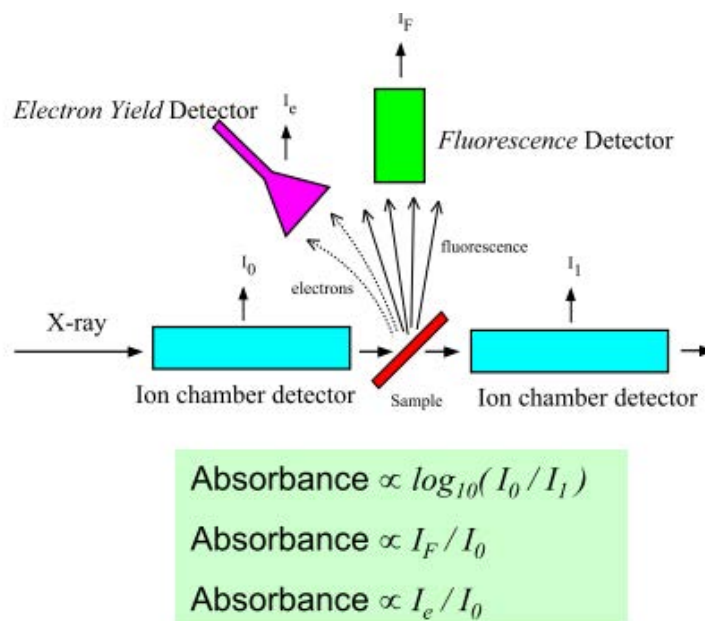


Figure 1.8. Typical experimental apparatus for XAS measurements.

In the simplest case, the measurement of an X-ray absorption spectrum involves the only measurement of the incident and the transmitted X-ray flux. Incident and transmitted intensities are typically measured using an ion chamber and a variety of detectors can be used to measure X-ray fluorescence intensity for dilute samples (shown in Figure 1.8).¹¹⁹

An XAS spectrum can be obtained after the measurement of signal, including two main parts: X-ray absorption near-edge spectroscopy (XANES) and extended X-ray absorption fine-structure (EXAFS). These spectra can provide us the bond distance between heavy metals and biosorbent (shown in the Figure 1.9).

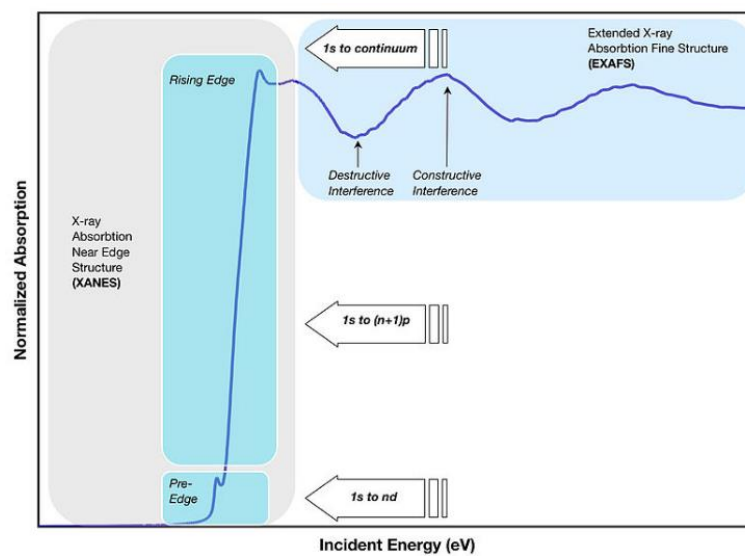


Figure 1.9. Spectra of XAS is composed of two parts: XANES and EXAFS spectra.

XANES spectra

X-ray absorption near-edge spectroscopy (XANES) is the region of the spectra that includes the pre-edge, the edge and a post-edge of 50-100 eV after the edge. XANES is sensitive to electronic structure and they can be used to “fingerprint” the chemical species present, chemical form and coordination chemistry of absorption atom (shown in Figure 1.10). Complex mixtures also can be analyzed by fitting to a linear combination of model spectra (shown in Figure 1.10).

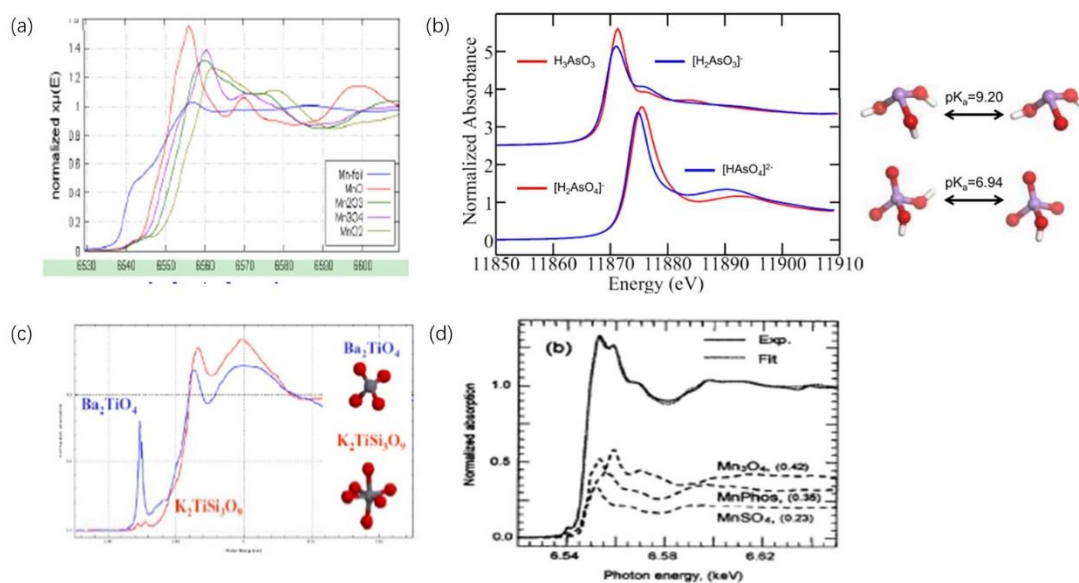


Figure 1.10. Four main information from XANES spectra, “fingerprint” the chemical species (Figure 10a), chemical form (Figure 10b), coordination chemistry of absorption atom (Figure 10c) and complex mixtures (Figure 10d).

EXAFS spectra

Extended X-ray absorption fine-structure spectroscopy (EXAFS) in the post-edge region above 100 eV. In fact, the X-ray excited photoelectron can be scattered from different neighboring atoms. The observed oscillations are extracted into wave function, which is a combination of the interactions of the wave functions from the scattering of each individual neighbor. It provides information about bond distance, coordination numbers, and static and dynamic disorder.

EXAFS spectra normally plotted into two forms, one is plotted as a function of the wavevector k , and typically k^3 weighted in order to increase the signal. Where χ is the oscillatory part of the absorption coefficient (shown in Figure 1.9). Besides, Fourier transform can be used to decompose a k -space signal into its different constituent frequencies and it is a more convenient form for visualizing the information content of an EXAFS spectrum (shown in Figure 1.11). whereas the peaks in the transform correspond to atomic distances¹¹⁹.

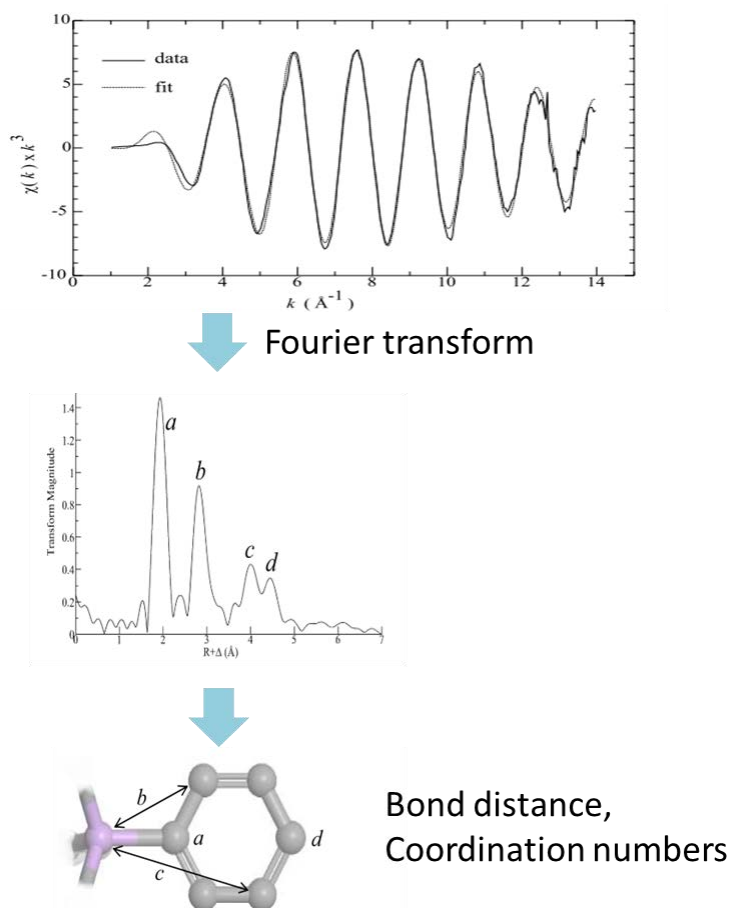


Figure 1.11. Main information extract from EXAFS spectra.

1.4.3 Main functional groups on biosorption systems

Biosorption is mainly depending on functional groups, including carboxylic acid, hydroxyl, amine, sulfhydryl and amide groups. To better understand the interaction between biomass and heavy metals, these functional groups; pK_a and related information are listed in Table 1.5. Depending on the pH, different functional groups can be involved in heavy metal binding, for example, in pH 2–5 carboxyl, in the pH range of 5–9 carboxyl and phosphate, and in the pH range of 9–12 carboxyl (ketone), phosphate, hydroxyl, and amine (shown in Table 5).

Protonation and deprotonation are fundamental chemical speciation that will affect heavy metal biosorption. Both species (with or without protons) are pH depending, while the functional groups with lower pK_a are easily deprotonated to effectively attract cationic metal ions; similarly, functional groups with higher pK_a are easily protonated so to attract anionic species, also of metal ions, if is the case.^{120,121} In addition, carboxylic acid and carbonyl group are the widely used functional groups that could cation exchange mainly, and some complex with heavy metals in solution can be formed¹²². These functional groups can be confirmed by FTIR and their

relevant wavenumbers are shown in Table 1.6.

Table 1.5. Main functional groups are responsible of the heavy metal biosorption.

Functional group	pK _a	Formula
Hydroxyl	9.5-13	-OH
Carboxyl	1.7-4.7	-COOH
Sulfhydryl	8.3-10.8	-SH
Phosphate	6.1-6.8	PO ₄ ³⁻
Amine	8-12	-NH ₂
Secondary amine	12.1-13	>NH
Carbonyl (ketone)	9.5-13	>C=O
Amide	-	$\begin{array}{c} \text{-C=O} \\ \\ \text{NH}_2 \end{array}$

Table 1.6. Functional groups found in biosorbents by FTIR technique from literature.

Biosorbent	Functional groups	Wavenumber(cm ⁻¹)	Reference
Cellulose, lignin and hemicellulose (Finger print region 1830-730 cm ⁻¹)	-OH stretching	3600-3300	52
	C-H stretching	2860-2970	
	C=O stretching	1510-1560	
	C=C Benzene	1632	
	C=C Aromatic skeletal	1613,1450	
	O-CH ₃ Methoxyl	1470-1430	
	OH bending	1440	
	CH bending	1402	
	C-O-C stretching	1232	
	C-O stretching	1215	
	C-O-C stretching vibrations	1170, 1082	
	OH association	1108	
	C-O stretching and C-O deformation	1060	
	C-H Aromatic	700-900	
	Aromatic C-C stretching	700-400	
Cotton cellulose (biomass)	-OH stretching	3400	123
	C=O stretching	1630	
	C-O-C	1160	

Lignin	aromatic and aliphatic OH C-H stretching Carboxyl and carbonyl Aromatic skeletal vibration Aromatic methyl group C-O stretching Syringyl units	3412 2925, 2849 1703, 1648 1600,1514,1425 1463 1329, 1217 1114, 827	124
Lignin (Lignocellulosic biomasses)	-OH group C-O, C-C and C-OH bonds	3600-3000 1000-1300	125
Sour orange residue (Agriculture waster)	-OH group CH stretching C=O band C-O Carboxyl band	3423 2925 1631 1257-1244	126
Dried activated sludge (biochar)	-OH, -NH stretching -CH asymmetric vibration C-O stretching -CN stretching -OH, -C-O stretching -COO- stretching -C-O-C, -OH	3224 2925 1651 1532 1424 1396 1027	127
Peanut shell (biochar)	-OH C=C, C=O of aromatic or ester C-O, -OH -CH of aromatic	3420 1620 1315, 1385 876,781	122
Fe ₃ O ₄ (Nanoparticles)	Fe-O	567	128
Leaf (Biochar/Fe ₂ O ₃)	-OH stretching C=O stretching C=C stretching C-N stretching Fe-O	3448 1616 1425 1020 580	129
TiO ₂ (Nanoparticles)	TiO-O-TiO	550-653	130
cellulose acetate/TiO ₂	-OH CH stretching	3490 2900	131

	CH stretching of aromatic	890	
	Broad peak of TiO-O-TiO	600-800	
Crude wintermelon (Biomass/TiO ₂)	-OH, C-H, C=O in COOH	3450, 2890, 1692	89
	Aromatic C=C	1631	
	Carboxyl C-O	1442	
	C-O of epoxy and alkoxy	1224	
	Broad peak of TiO-O-TiO	500-800	

1.4.4 Biosorption mechanisms

The removal of heavy metals from aqueous solutions using agricultural and wood materials is based upon metal biosorption. The process of biosorption involves a solid phase (sorber) and a liquid phase (solvent) containing a dissolved species to be sorbed⁶⁹. Due to high affinity of the sorber for the heavy metal species, the latter is attracted and bound by rather complex process affected by several mechanisms (shown in Figure 1.12)⁴⁰. Among these mechanisms, chemisorption, complexation, ion exchange and chelation are the most described for heavy metal removal from wastewater⁶⁸.

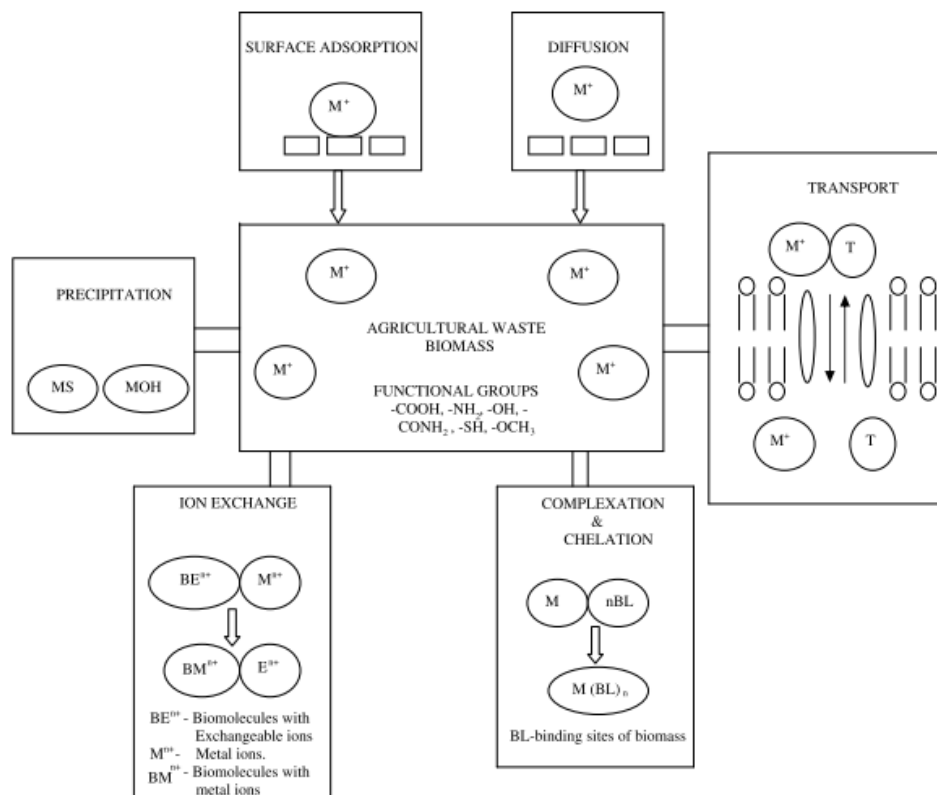


Figure 1.12. Biosorption mechanism of agricultural waste biomass⁶⁸.

The Figure 1.13 summarizes heavy metal biosorption mechanisms of **biochar**. Five mechanisms have been proposed to govern heavy metal biosorption by biochar from aqueous solutions, such as complexation, cation exchange, precipitation, electrostatic interactions, and chemical reduction. However, the role of each mechanism plays for each heavy metal varies considerably depending on target metals.

Moreover, solution pH significantly influences heavy metal capacity due to the change of surface charge of biochar. It is well known that functional groups such as carboxyl, hydroxyl, and amino are negative charge⁶⁸. An increase in pH makes these negative functional groups such as carboxyl group deprotonated to effectively attract positively charged metals. Such as corncob biomass/biochar are found more negatively charged at higher pH¹³².

On the other hand, biochar properties vary considerably, mainly depending on pyrolysis temperature and feedstock¹³³. As pyrolysis temperature increased, ash content, pH, electrical conductivity, basic functional groups, carbon stability, and total content of C, N, P, K, Ca, and Mg increased while biochar yield, and total content of O, H and S, unstable form of organic C and acidic functional groups decreased¹³³⁻¹³⁶.

However, temperature could have opposite effects on biochar properties, leading to opposite effects on metal sorption. For example, high pyrolysis temperature leads to a higher surface area, providing more sites for metal sorption. However, it reduces the amounts of functional groups, which may lead to lower metal sorption via complexation between heavy metals and functional groups⁶³. In addition, the mechanisms are varied with biochar properties and species of heavy metal.

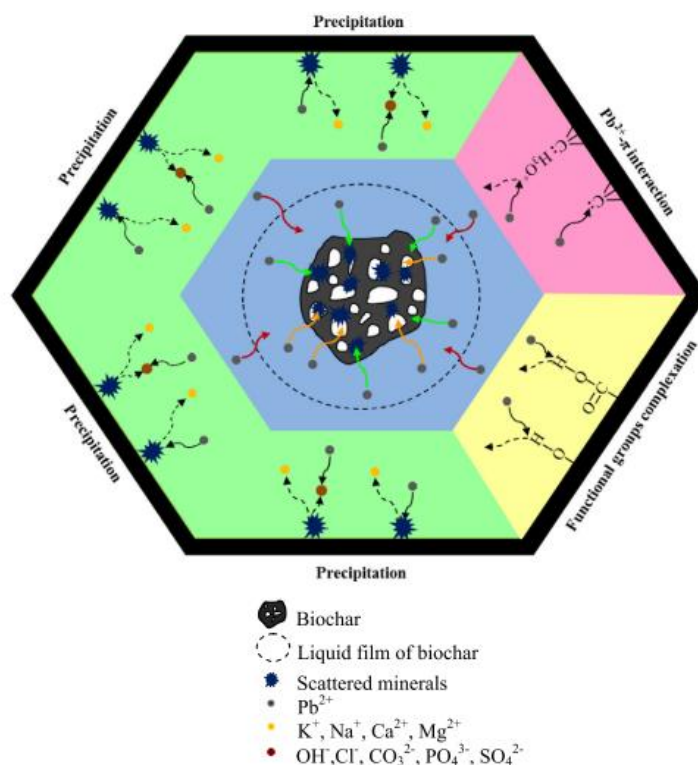


Figure 1.13. Graph illustration of heavy metal sorption mechanisms on biochar¹²².

1.4.5 Advance in biosorption mechanism by XAS

Thus far, the overall metal binding mechanism is complicated and not fully understood. Main mechanisms include adsorption, ionic exchange (displacement of a proton or bound metal cation), electrostatic interaction, complexation, chelation (covalent or ionic interaction), coordination, van der Waals forces, precipitation and reduction by reducing functional groups, etc. However, the competitive sorption and selectivity order of heavy metals are not clear. The XAS technique utilizes X-rays to probe the physical and chemical structures of a material at an atomic scale that can help us to understand the biosorption mechanism in molecular level^{117,138}.

Using this technique, several studies have performed to study the adsorption of biomass/biochar^{139,140}. However, a limited number of studies have used this technique to analyse biosorption of heavy metals since limited beamtime in synchrotron facilities. A limited heavy metal has been studied of biosorption from aqueous solution. The most studied heavy metal is Cr, few of Cu, Pb, Ni and Zn.

Cr as we mentioned before, Cr(III) and Cr(VI) are the two major valence states and the latter is five hundred times more poisonous than the former that has been identified as a top-priority hazardous pollutant¹⁷. It is of great significance to develop

a cost-effective and eco-friendly technique to removal Cr(VI) from industrial wastewater before being disposed into the aqueous system.

Cr(VI) primarily exists in the form of chromate (CrO_4^{2-} and HCrO_4^-) and dichromate ($\text{Cr}_2\text{O}_7^{2-}$), which are highly toxic and water soluble¹⁴¹. The traditional way to removal Cr(VI) by adsorption include two steps: first reduction the Cr(VI) to Cr(III), and then adsorb Cr(III) onto the surface of sorbents. In this sense, Iron as a reducing agent was widely applied to reduce Cr(III), such as synthesis iron nanoparticles on adsorbents or combined with iron particles in different ways to reduce Cr(VI)^{118,142,143}.

Another way was taking advantage of positive groups on adsorbents surface, such as ammonium and pyrrolic groups both could attractive HCrO_4^- anions to the surface of sorbent by electrostatic interaction^{144–146}. They also can provide the electron to Cr(VI) and reduce it to Cr(III). In this process, these positive groups act as a role of electron donor and electrons shuttle¹⁴⁵. Similarly, Cr(VI) adsorbed on the surface of TiO_2 particles can be photoreduced to Cr(III) almost completely under UV/ TiO_2 reduction process^{147–149}.

Furthermore, adsorption of heavy metals by biomass as a biosorbent have been attracted attention recently due to its low cost and eco-friendly, especially its ability to reduce much toxicity of Cr(VI) to a less toxicity form of Cr(III) without additional chemical pre-treatment^{139,150}.

One popular explanation for the reduction of Cr(VI) by biomass/biochar is that the hydroxyl groups of biomass/biochar can be protonated, and the surface was positively charged, which would electrostatically attract the negatively charged chromate ions^{74,75,151,152}. While biochar had better adsorption capability due to its abundant carboxyl and hydroxyl groups that can provide more positive adsorption sites for Cr(VI). However, until now, the adsorption-reduction mechanisms of hexavalent chromium on biomass/biochar is not clear.

Moreover, *Li et.al* reported that surface functional groups are protonated and positively charged in the form of $-\text{OH}_2^+$, $-\text{COOH}_2^+$ in acid medium, and can electrostatic attract for HCrO_4^- and CrO_4^{2-} since the affluence of pH value. Depending on the pH, Cr(VI) exists mainly as H_2CrO_4 (pH < 1), CrO_4^{2-} (pH > 6) and HCrO_4^- (pH 1~6). They also assumed that catechol (a component of tannin from the woody plant) can adsorb chromate through esterification between catechol and CrO_4^- .⁶⁴

In addition, biochar, a pyrolysis product obtained from biomass highly increased the adsorption of heavy metals due to its large surface, pore structure and higher concentrated mineral after pyrolyzing compared with original biomass. Biochar also can reduce Cr(VI) to Cr(III) probably due to the activated carbon¹⁵³.

By using XAS technique *Anushka* found that Cr(VI) species were reduced to Cr(III) at the biochar surface following Cr(VI) adsorption¹³⁹. *Wenjun* reported that the functional groups of humic acid is responsible for the reduction of Cr(VI) to Cr(III) by XAS¹⁴⁰. In addition, biochar can be served as electron shuttle to increase the electron donating capacity of lactate (2-Hydroxypropanoic acid) and transform electron to reduce Cr(VI), which has been proved by Xu et.al¹⁵⁴. Co-pyrolysis of cellulose biomass and Cr(VI), by-product of cellulose such as the volatile fraction (VF) of cellulose (gas and tar) was responsible for Cr(VI) reduction¹⁵⁵. All the XAS studies above show that the key point for Cr(VI) reduction needs a reduction media that can provide electron and an electron shuttle for transport to complete the whole reduction process of Cr(VI).

Biomass/biochar can reduce Cr(VI) as it has been proved by XAS technique, but the adsorption mechanism has not solved in the above cases. Who provides the electron and how it transformed to Cr(VI) is still unclear.

Also, combined with XAS technique to study the biosorption mechanism of heavy metal from aqueous solution are very few. *Fei et.al* applied ICP-MS and XAS to study the mechanisms of competitive adsorption of Pb, Cu, and Cd on peat in single and multiple systems¹⁵⁶. The XAS results revealed that both Pb and Cu were predominantly bind to carboxylic functional group, next is hydroxyl group. *Samrat Alam et.al* have similar results of biochar, results of XAS along with FT-IR analyses suggest that Ni(II) and Zn(II) adsorption occurred primarily through proton-active carboxyl and hydroxyl functional groups on the biochar surface¹⁵⁷.

Maather F. et.al show that carboxyl and phenolic groups play a major role in the binding of the Cr(III) resulting from the abiotic reduction of Cr(VI) by the biomass¹⁵⁸.

As we discussed above, the real system includes multiple heavy metals and the competition between metal ions will influence the biosorption process even decrease the biosorption capacity. Therefore, it is a key point to study the competition mechanism and guide the application of disposal biomass in a real system.

1.5 Recycling biosorbents

All the biosorbents loaded with heavy metals can release the immobilized heavy metals as secondary pollutants, especially under acidic conditions¹⁵⁹. Recycling of waste materials containing heavy metals is an important and challenging task.

Biochar loaded with heavy metals can be washed with a strong acid (HNO₃, HCl and H₂SO₄) or strong alkali (NaOH), then can be recycled for further using¹⁶⁰. Considering that there is a huge amount of biomass waste disposal in the world, this method is expensive so it can be not the best option.

Pyrolysis biomass loaded with heavy metals is another way to solve the toxicity materials. In this pyrolysis process, heavy metal on biomass can be served as a catalyst to enhance the conversion of tar and convert high-valence metals to a low-valence^{155,161,162}. *Shen et. al* synthesized rice husk biochar modified with Ni-Fe catalysts, showing that the tar yield and CO₂ concentration obviously decreased after the addition of the Ni-Fe catalysts¹⁶¹. Result from *S´wierczyn´ski et. al* also showed that Ni-based catalysts are extremely effective for biomass gasification tar removal and syngas conditioning¹⁶². In addition, *Zhang et.al* reported that co-pyrolysis of cellulose biomass with Cr(VI), the volatile fraction (VF) of cellulose (gas and tar) can reduce Cr(VI) to Cr(III), in which biosorbents severed as catalyst was found to be both cost effective and environmentally friendly¹⁵⁵.

Moreover, utilization of biosorbent loaded with heavy metal as brick materials is a promising way to solve disposal problem^{163,164}. *Weng et.al* reported that bricks contain 20% sludge met relevant standards, most importantly, the metal leaching level is low that can be used in building¹⁶⁵. Not only sludge, *Luisa et.al* successful made bricks by using agriculture waste¹⁶⁶. Sludge and rice husk were used by *Chiang et.al* to make lightweight bricks¹⁶⁷.

1.6 Objectives

The aim of this thesis is to investigate low-cost and efficiency biomass as biosorbent to remove heavy metals from wastewaters. In order to increase the biosorption capacity in multiple system (simulated to real wastewater), modified biomasses are also studied to study their biosorption process efficiency. Experimental conditions including contact time, the pH, initial concentration and temperature are optimized. Characterization by using SEM, TEM, XRD, ATR-FTIR, and XAS have also been checked to investigate the morphology surface, functional groups, and species of neighbors of the absorbing atom. All of this information will provide suitability of biomass waste, which can be applied to wastewater treatment and provide remediation methodologies for the environment.

The specific objectives of this study are:

- ✓ Evaluation of biomasses capacity to adsorb heavy metals from multiple heavy metal system composed of Cr(III), Cd(II), Cu(II) and Pb(II).
- ✓ Preparation and characterization of different biomass system modifications, in order to find new features and efficiencies in the biosorption processes.
- ✓ Comparison of the adsorption efficiency of such different biomass and modified biomasses.
- ✓ Investigation of the selectivity to Cr(III) and Cr(VI) by Pine and pyrolyzed Pine.
- ✓ The study of the mechanism for Pine biomass and pyrolyzed Pine loaded with TiO₂ to chromium (Cr(III) and Cr(VI)) biosorption from aqueous solutions.
- ✓ Recycling of waste materials containing heavy metals.

References

- (1) John R. Garbarino, Heidi C. Hayes, David A. Roth, R. C. A.; Terry I. Brinton, and H. E. T. *Heavy Metals in the Mississippi River*; 1995.
- (2) Azimi, A.; Azari, A.; Rezakazemi, M.; Ansarpour, M. Removal of Heavy Metals from Industrial Wastewaters: A Review. *ChemBioEng Rev.* **2017**, *4* (1), 37–59. <https://doi.org/10.1002/cben.201600010>.
- (3) Şen, A.; Pereira, H.; Olivella, M. A.; Villaescusa, I. Heavy Metals Removal in Aqueous Environments Using Bark as a Biosorbent. *Int. J. Environ. Sci. Technol.* **2015**, *12* (1), 391–404. <https://doi.org/10.1007/s13762-014-0525-z>.
- (4) Luo, S.; Cai, T.; Liu, C.; Zhang, Y.; Liu, Y.; Ma, J.; Wei, Y.; Ali, O.; Zhang, S. Fast Adsorption of Heavy Metal Ions by Waste Cotton Fabrics Based Double Network Hydrogel and Influencing Factors Insight. *J. Hazard. Mater.* **2017**, *344*, 1034–1042. <https://doi.org/10.1016/j.jhazmat.2017.11.041>.
- (5) Nguyen, T. A. H.; Ngo, H. H.; Guo, W. S.; Zhang, J.; Liang, S.; Yue, Q. Y.; Li, Q.; Nguyen, T. V. Bioresource Technology Applicability of Agricultural Waste and By-Products for Adsorptive Removal of Heavy Metals from Wastewater. **2013**, *148*, 574–585.
- (6) Abdel-Ghani, N.; El-Chaghaby, G. Biosorption for Metal Ions Removal From Aqueous Solutions: A Review of Recent Studies. *Mnkjournals.Com* **2014**, *3* (1), 24–42.
- (7) Kadirvelu, K.; Pugazhendhi, A.; Kumar, S. S.; Prabakar, D.; Karthik, C.; Saratale, R. G.; Jacob, J. M. Biological Approaches to Tackle Heavy Metal Pollution: A Survey of Literature. *J. Environ. Manage.* **2018**, *217*, 56–70. <https://doi.org/10.1016/j.jenvman.2018.03.077>.
- (8) Z. Rengel. Heavy Metals as Essential Nutrients. *Heavy Met. Stress Plants* **1999**, 231–251.
- (9) Paul, D. Research on Heavy Metal Pollution of River Ganga: A Review. *Ann. Agrar. Sci.* **2017**, *15* (2), 278–286. <https://doi.org/10.1016/j.aasci.2017.04.001>.
- (10) Salami, I. R. S.; Rahmawati, S.; Sutarto, R. I. H.; Jaya, P. M. Accumulation of Heavy Metals in Freshwater Fish in Cage Aquaculture at Cirata Reservoir, West Java, Indonesia. *Ann. N. Y. Acad. Sci.* **2008**, *1140*, 290–296. <https://doi.org/10.1196/annals.1454.037>.
- (11) Fu, J.; Hu, X.; Tao, X.; Yu, H.; Zhang, X. Risk and Toxicity Assessments of Heavy Metals in Sediments and Fishes from the Yangtze River and Taihu Lake, China. *Chemosphere* **2013**, *93* (9), 1887–1895. <https://doi.org/10.1016/j.chemosphere.2013.06.061>.
- (12) Albanese, S.; Giaccio, L.; Civitillo, D.; De Vivo, B.; Lima, A.; Cicchella, D.; Cosenza, A. Assessment of the Topsoil Heavy Metals Pollution in the Sarno River Basin, South Italy. *Environ. Earth Sci.* **2013**, 5129–5143. <https://doi.org/10.1007/s12665-013-2916-8>.
- (13) Bhuiyan, M. A. H.; Dampare, S. B.; Islam, M. A.; Suzuki, S. Source Apportionment and Pollution Evaluation of Heavy Metals in Water and Sediments of Buriganga River, Bangladesh, Using Multivariate Analysis and Pollution Evaluation Indices. *Environ. Monit. Assess.* **2015**, *187* (1). <https://doi.org/10.1007/s10661-014-4075-0>.

-
- (14) B. J. Presley, J. H. Trefry, R. F. Shokes. Heavy Metal Inputs to Mississippi Delta Sediments. *Water, Air, Soil Pollut.* **1980**, *13* (4), 481–494.
- (15) Al-arab, U. W.; Ahmad, I.; Bany, A. Assessment of the Heavy Metal Pollution in the Surface Sediments along Assessment of the Heavy Metal Pollution in the Surface Sediments along Upstream at Wadi Al-Arab, Jordan. **2018**, No. December 2016.
- (16) Castro, L. N.; Rendina, A. E.; Orgeira, M. J. Assessment of Toxic Metal Contamination Using a Regional Lithogenic Geochemical Background, Pampean Area River Basin, Argentina. *Sci. Total Environ.* **2018**, *627*, 125–133.
<https://doi.org/10.1016/j.scitotenv.2018.01.219>.
- (17) Pellerin, C.; Booker, S. Reflections on Hexavalent Chromium: Health Hazards of an Industrial Heavyweight. *Env. Heal. Perspect* **2000**, *108* (9), A402-7.
- (18) EPA. National Primary Drinking Water Regulations
<https://www.epa.gov/ground-water-and-drinking-water/national-primary-drinking-water-regulations>.
- (19) Ofomaja, A. E.; Naidoo, E. B.; Modise, S. J. Biosorption of Copper(II) and Lead(II) onto Potassium Hydroxide Treated Pine Cone Powder. *J. Environ. Manage.* **2010**, *91* (8), 1674–1685. <https://doi.org/10.1016/j.jenvman.2010.03.005>.
- (20) Hossain, M. A.; Ngo, H. H.; Guo, W. S.; Setiadi, T. Adsorption and Desorption of Copper(II) Ions onto Garden Grass. *Bioresour. Technol.* **2012**, *121*, 386–395.
<https://doi.org/10.1016/j.biortech.2012.06.119>.
- (21) Cai, K.-Z.; Huang, G.-F.; Gao, L.-Y.; Liu, Y.; Deng, J.-H.; Li, K.; Huang, F. Relative Distribution of Cd²⁺ Adsorption Mechanisms on Biochars Derived from Rice Straw and Sewage Sludge. *Bioresour. Technol.* **2018**, *272* (August 2018), 114–122.
<https://doi.org/10.1016/j.biortech.2018.09.138>.
- (22) Liang, S.; Xiao, K.; Shi, S.; Li, M.; Yang, J.; Hu, J.; Gan, Q. Enhanced Cr(VI) Removal from Acidic Solutions Using Biochar Modified by Fe₃O₄@SiO₂-NH₂ Particles. *Sci. Total Environ.* **2018**, *628–629*, 499–508. <https://doi.org/10.1016/j.scitotenv.2018.02.091>.
- (23) Fu, F.; Wang, Q. Removal of Heavy Metal Ions from Wastewaters: A Review. *J. Environ. Manage.* **2011**, *92* (3), 407–418. <https://doi.org/10.1016/j.jenvman.2010.11.011>.
- (24) Fu, F.; Wang, Q. Removal of Heavy Metal Ions from Wastewaters: A Review. *J. Environ. Manage.* **2011**, *92* (3), 407–418. <https://doi.org/10.1016/j.jenvman.2010.11.011>.
- (25) Chen Q, Luo Z, Hills C, Xue G, T. M. Precipitation of Heavy Metals from Wastewater Using Simulated Flue Gas: Sequent Additions of Fly Ash, Lime and Carbon Dioxide. *Water Res.* **2009**, *43* (10), 2605–2614.
- (26) Bilge Alyüz, S. V. Kinetics and Equilibrium Studies for the Removal of Nickel and Zinc from Aqueous Solutions by Ion Exchange Resins. *J. Hazard. Mater.* **2009**, *167* (1–3), 482–488.
- (27) Dąbrowski, A.; Hubicki, Z.; Podkościelny, P.; Robens, E. Selective Removal of the Heavy

- Metal Ions from Waters and Industrial Wastewaters by Ion-Exchange Method. *Chemosphere* **2004**, *56* (2), 91–106. <https://doi.org/10.1016/j.chemosphere.2004.03.006>.
- (28) Zhao, D.; SenGupta, A. K.; Stewart, L. Selective Removal of Cr(VI) Oxyanions with a New Anion Exchanger. *Ind. Eng. Chem. Res.* **1998**, *37* (11), 4383–4387. <https://doi.org/10.1021/ie980227r>.
- (29) H.BessbousseabT.RhlaloubJ.-F.VerchèreaL.Lebrun. Removal of Heavy Metal Ions from Aqueous Solutions by Filtration with a Novel Complexing Membrane Containing Poly(Ethyleneimine) in a Poly(Vinyl Alcohol) Matrix. *J. Memb. Sci.* **2008**, *307* (2), 249–259.
- (30) Resina, M.; Macanás, J.; de Gyves, J.; Muñoz, M. Development and Characterization of Hybrid Membranes Based on an Organic Matrix Modified with Silanes for Metal Separation. *J. Memb. Sci.* **2007**, *289* (1–2), 150–158. <https://doi.org/10.1016/j.memsci.2006.11.049>.
- (31) Adhikari, S.; Fernando, S. Hydrogen Membrane Separation Techniques. *Ind. Eng. Chem. Res.* **2006**, *45* (3), 875–881. <https://doi.org/10.1021/ie050644l>.
- (32) Li, Y.; Yang, W. Microwave Synthesis of Zeolite Membranes: A Review. *J. Memb. Sci.* **2008**, *316* (1–2), 3–17. <https://doi.org/10.1016/j.memsci.2007.08.054>.
- (33) Radjenović, J.; Petrović, M.; Ventura, F.; Barceló, D. Rejection of Pharmaceuticals in Nanofiltration and Reverse Osmosis Membrane Drinking Water Treatment. *Water Res.* **2008**, *42* (14), 3601–3610. <https://doi.org/10.1016/j.watres.2008.05.020>.
- (34) Hargreaves, A. J.; Vale, P.; Whelan, J.; Alibardi, L.; Constantino, C.; Dotro, G.; Cartmell, E.; Campo, P. Coagulation – Flocculation Process with Metal Salts , Synthetic Polymers and Biopolymers for the Removal of Trace Metals (Cu , Pb , Ni , Zn) from Municipal Wastewater. *Clean Technol. Environ. Policy* **2018**, *20* (2), 393–402. <https://doi.org/10.1007/s10098-017-1481-3>.
- (35) Polat, H.; Erdogan, D. Heavy Metal Removal from Waste Waters by Ion Flotation. **2007**, *148*, 267–273. <https://doi.org/10.1016/j.jhazmat.2007.02.013>.
- (36) Y.V.Nancharaiah,S.Venkata Mohanc, P. N. L. L. Metals Removal and Recovery in Bioelectrochemical Systems: A Review. *Bioresour. Technol.* **2015**, *195*, 102–114.
- (37) Basha, C. A.; Bhadrinarayana, N. S.; Anantharaman, N.; Sheriffa, K. M. M. Heavy Metal Removal from Copper Smelting Effluent Using Electrochemical Cylindrical Flow Reactor. **2008**, *152*, 71–78. <https://doi.org/10.1016/j.jhazmat.2007.06.069>.
- (38) Adsorption <https://www.sciencedirect.com/topics/earth-and-planetary-sciences/adsorption>.
- (39) Correia, P.; Vilar, V. J. P.; Botelho, C. M. S.; Pintor, A. M. A.; Boaventura, R. A. R.; Ferreira, C. I. A.; Silva, S. P.; Pereira, J. C. Use of Cork Powder and Granules for the Adsorption of Pollutants: A Review. *Water Res.* **2012**, *46* (10), 3152–3166. <https://doi.org/10.1016/j.watres.2012.03.048>.

-
- (40) Demirbas, A. Heavy Metal Adsorption onto Agro-Based Waste Materials: A Review. *J. Hazard. Mater.* **2008**, *157* (2–3), 220–229.
<https://doi.org/10.1016/j.jhazmat.2008.01.024>.
- (41) Environmental Protection Agency (EPA) <https://www.epa.gov/>.
- (42) Cristina del Pozo Carvajal, Jordi Bartroli, Neus Puy, E. F. Separation of Value-Added Chemical Groups from Bio-Oil of Olive Mill Waste. *Industrial Crops and Products. Ind. Crops Prod.* **2018**, *125*, 160–167.
- (43) Biomass—renewable energy from plants and animals
https://www.eia.gov/energyexplained/?page=biomass_home.
- (44) Sun, J.; Peng, H.; Chen, J.; Wang, X.; Wei, M.; Li, W.; Yang, L.; Zhang, Q.; Wang, W.; Mellouki, A. An Estimation of CO₂ Emission via Agricultural Crop Residue Open Field Burning in China from 1996 to 2013. *J. Clean. Prod.* **2016**, *112*, 2625–2631.
<https://doi.org/10.1016/j.jclepro.2015.09.112>.
- (45) OECD. *China in the Global Economy Environment, Water Resources and Agricultural Policies Lessons from China and OECD Countries*; 2006.
- (46) Wang, H.; Hijmans, R. J.; Res, E. Climate Change and Geographic Shifts in Rice Production in China Climate Change and Geographic Shifts in Rice Production in China. **2019**.
- (47) Liang CHAI, Haojie LI, Benchuan ZHENG, Jinfang ZHANG, Cheng CUI, Jun JIANG, Bi ZHANG, liangcai JIANG, Lintao WU, J. K. Recent Advance, Problems and Outlooks in Rapeseed (*Brassica Napus L.*) Breeding in China. *Agric. Sci. Technol.* **2017**, *18* (12), 2612–2616.
- (48) Carvalho, J. L. N.; de Figueiredo, E. B.; de Oliveira, B. G.; La Scala, N.; Bordonal, R. de O.; Lal, R. Sustainability of Sugarcane Production in Brazil. A Review. *Agron. Sustain. Dev.* **2018**, *38* (2). <https://doi.org/10.1007/s13593-018-0490-x>.
- (49) Siqueira, J. O.; Saggin-Júnior, O. J.; Flores-Aylas, W. W.; Guimarães, P. T. G. Arbuscular Mycorrhizal Inoculation and Superphosphate Application Influence Plant Development and Yield of Coffee in Brazil. *Mycorrhiza* **1998**, *7* (6), 293–300.
<https://doi.org/10.1007/s005720050195>.
- (50) Vilardi, G.; Palma, L. Di; Verdone, N. Heavy Metals Adsorption by Banana Peels Micro-Powder . Equilibrium Modeling by Non-Linear Models Chinese Journal of Chemical Engineering Heavy Metals Adsorption by Banana Peels Micro-Powder : Equilibrium Modeling by Non-Linear Models. *Chinese J. Chem. Eng.* **2017**, *26* (3), 455–464.
<https://doi.org/10.1016/j.cjche.2017.06.026>.
- (51) Colombia: Banana production grew by 4.7% in 2017
<https://www.freshplaza.com/article/2190036/colombia-banana-production-grew-by-4-7-in-2017/>.
- (52) Yang, H.; Yan, R.; Chen, H.; Lee, D. H.; Zheng, C. Characteristics of Hemicellulose, Cellulose

- and Lignin Pyrolysis. *Fuel* **2007**, *86* (12–13), 1781–1788.
<https://doi.org/10.1016/j.fuel.2006.12.013>.
- (53) Hokkanen, S.; Bhatnagar, A.; Sillanpää, M. A Review on Modification Methods to Cellulose-Based Adsorbents to Improve Adsorption Capacity. *Water Res.* **2016**, *91*, 156–173. <https://doi.org/10.1016/j.watres.2016.01.008>.
- (54) M.P. GONZALEZ-HERNANDEZ, J. K. A. E. E. S. Research Observation: Hydrolyzable and Condensed Tannins in Plants of Northwest Spain Forests. *J. Range Manag.* **2003**, *56*, 461–465.
- (55) Gode, F.; Atalay, E. D.; Pehlivan, E. Removal of Cr(VI) from Aqueous Solutions Using Modified Red Pine Sawdust. *J. Hazard. Mater.* **2008**, *152* (3), 1201–1207.
<https://doi.org/10.1016/j.jhazmat.2007.07.104>.
- (56) Alessandro Gandini. Polymers From Renewable Resources. *Compr. Polym. Sci. Suppl.* **1989**, 527–573.
- (57) Tsang, D. C. W.; Knijnenburg, J. T. N.; Hunt, A. J.; Supanchaiyamat, N.; Jetsrisuparb, K. Lignin Materials for Adsorption: Current Trend, Perspectives and Opportunities. *Bioresour. Technol.* **2018**, *272* (June 2018), 570–581.
<https://doi.org/10.1016/j.biortech.2018.09.139>.
- (58) Wang, F.; Pan, Y.; Cai, P.; Guo, T.; Xiao, H. Single and Binary Adsorption of Heavy Metal Ions from Aqueous Solutions Using Sugarcane Cellulose-Based Adsorbent. *Bioresour. Technol.* **2017**, *241*, 482–490. <https://doi.org/10.1016/j.biortech.2017.05.162>.
- (59) Yang, Z. H.; Xiong, S.; Wang, B.; Li, Q.; Yang, W. C. Cr(III) Adsorption by Sugarcane Pulp Residue and Biochar. *J. Cent. South Univ.* **2013**, *20* (5), 1319–1325.
<https://doi.org/10.1007/s11771-013-1618-4>.
- (60) Garg, U. K.; Kaur, M. P.; Garg, V. K.; Sud, D. Removal of Hexavalent Chromium from Aqueous Solution by Agricultural Waste Biomass. *J. Hazard. Mater.* **2007**, *140* (1–2), 60–68. <https://doi.org/10.1016/j.jhazmat.2006.06.056>.
- (61) Basso, M. C.; Cerrella, E. G.; Cukierman, A. L. Lignocellulosic Materials as Potential Biosorbents of Trace Toxic Metals from Wastewater. *Ind. Eng. Chem. Res.* **2002**, *41* (15), 3580–3585. <https://doi.org/10.1021/ie020023h>.
- (62) Cruz, B. H.; Díaz-Cruz, J. M.; Ariño, C.; Esteban, M. Heavy Metal Binding by Tannic Acid: A Voltammetric Study. *Electroanalysis* **2000**, *12* (14), 1130–1137.
[https://doi.org/10.1002/1521-4109\(200010\)12:14<1130::AID-ELAN1130>3.0.CO;2-7](https://doi.org/10.1002/1521-4109(200010)12:14<1130::AID-ELAN1130>3.0.CO;2-7).
- (63) Hirohumi ARAKAWA; Masato TSUSHIMA; Masami KISHI; Norimoto WATANABE. Reduction of Chromium(VI) by Water-Extracts from Withered Oak Leaves. **1993**, 2113–2116.
- (64) Li, W.; Gong, X.; Li, X.; Zhang, D.; Gong, H. Removal of Cr(VI) from Low-Temperature Micro-Polluted Surface Water by Tannic Acid Immobilized Powdered Activated Carbon.

- Bioresour. Technol.* **2012**, *113*, 106–113. <https://doi.org/10.1016/j.biortech.2011.12.037>.
- (65) Kaur, R.; Singh, J.; Khare, R.; Ali, A. Biosorption the Possible Alternative to Existing Conventional Technologies for Sequestering Heavy Metal Ions from Aqueous Streams : A Review. *Univers. J. Environ. Res. Technol.* **2012**, *2* (4), 325–335.
- (66) Rangabhashiyam, S.; Suganya, E.; Selvaraju, N.; Varghese, L. A. Significance of Exploiting Non-Living Biomaterials for the Biosorption of Wastewater Pollutants. *World J. Microbiol. Biotechnol.* **2014**, *30* (6), 1669–1689. <https://doi.org/10.1007/s11274-014-1599-y>.
- (67) Park, D.; Yun, Y. S.; Park, J. M. The Past, Present, and Future Trends of Biosorption. *Biotechnol. Bioprocess Eng.* **2010**, *15* (1), 86–102. <https://doi.org/10.1007/s12257-009-0199-4>.
- (68) Sud, D.; Mahajan, G.; Kaur, M. P. Agricultural Waste Material as Potential Adsorbent for Sequestering Heavy Metal Ions from Aqueous Solutions - A Review. *Bioresour. Technol.* **2008**, *99* (14), 6017–6027. <https://doi.org/10.1016/j.biortech.2007.11.064>.
- (69) Kratochvil, D.; Volesky, B. Advances in the Biosorption of Heavy Metals. *Trends Biotechnol.* **1998**, *16* (7), 291–300. [https://doi.org/10.1016/S0167-7799\(98\)01218-9](https://doi.org/10.1016/S0167-7799(98)01218-9).
- (70) Rafatullah, M.; Sulaiman, O.; Hashim, R.; Ahmad, A. Adsorption of Methylene Blue on Low-Cost Adsorbents: A Review. *J. Hazard. Mater.* **2010**, *177* (1–3), 70–80. <https://doi.org/10.1016/j.jhazmat.2009.12.047>.
- (71) Almeida, M. F.; Dias, J. M.; Sánchez-Polo, M.; Alvim-Ferraz, M. C. M.; Rivera-Utrilla, J. Waste Materials for Activated Carbon Preparation and Its Use in Aqueous-Phase Treatment: A Review. *J. Environ. Manage.* **2007**, *85* (4), 833–846. <https://doi.org/10.1016/j.jenvman.2007.07.031>.
- (72) Qambrani, N. A.; Rahman, M. M.; Won, S.; Shim, S.; Ra, C. Biochar Properties and Eco-Friendly Applications for Climate Change Mitigation, Waste Management, and Wastewater Treatment: A Review. *Renew. Sustain. Energy Rev.* **2017**, *79* (May), 255–273. <https://doi.org/10.1016/j.rser.2017.05.057>.
- (73) Oliveira, F. R.; Patel, A. K.; Jaisi, D. P.; Adhikari, S.; Lu, H.; Khanal, S. K. Environmental Application of Biochar: Current Status and Perspectives. *Bioresour. Technol.* **2017**, *246* (July), 110–122. <https://doi.org/10.1016/j.biortech.2017.08.122>.
- (74) Li, H.; Dong, X.; da Silva, E. B.; de Oliveira, L. M.; Chen, Y.; Ma, L. Q. Mechanisms of Metal Sorption by Biochars: Biochar Characteristics and Modifications. *Chemosphere* **2017**, *178*, 466–478. <https://doi.org/10.1016/j.chemosphere.2017.03.072>.
- (75) Tan, X.; Liu, Y.; Zeng, G.; Wang, X.; Hu, X.; Gu, Y.; Yang, Z. Application of Biochar for the Removal of Pollutants from Aqueous Solutions. *Chemosphere* **2015**, *125*, 70–85. <https://doi.org/10.1016/j.chemosphere.2014.12.058>.
- (76) Cha, J. S.; Park, S. H.; Jung, S. C.; Ryu, C.; Jeon, J. K.; Shin, M. C.; Park, Y. K. Production and Utilization of Biochar: A Review. *J. Ind. Eng. Chem.* **2016**, *40*, 1–15.

- <https://doi.org/10.1016/j.jiec.2016.06.002>.
- (77) Zhao, S. X.; Ta, N.; Wang, X. D. Effect of Temperature on the Structural and Physicochemical Properties of Biochar with Apple Tree Branches as Feedstock Material. *Energies* **2017**, *10* (9). <https://doi.org/10.3390/en10091293>.
- (78) Sun, Y.; Gao, B.; Yao, Y.; Fang, J.; Zhang, M.; Zhou, Y.; Chen, H.; Yang, L. Effects of Feedstock Type, Production Method, and Pyrolysis Temperature on Biochar and Hydrochar Properties. *Chem. Eng. J.* **2014**, *240*, 574–578. <https://doi.org/10.1016/j.cej.2013.10.081>.
- (79) Mohan, D.; Sarswat, A.; Ok, Y. S.; Pittman, C. U. Organic and Inorganic Contaminants Removal from Water with Biochar, a Renewable, Low Cost and Sustainable Adsorbent - A Critical Review. *Bioresour. Technol.* **2014**, *160*, 191–202. <https://doi.org/10.1016/j.biortech.2014.01.120>.
- (80) Agrafioti, E.; Kalderis, D.; Diamadopoulos, E. Arsenic and Chromium Removal from Water Using Biochars Derived from Rice Husk, Organic Solid Wastes and Sewage Sludge. *J. Environ. Manage.* **2014**, *133*, 309–314. <https://doi.org/10.1016/j.jenvman.2013.12.007>.
- (81) Son, E. B.; Poo, K. M.; Chang, J. S.; Chae, K. J. Heavy Metal Removal from Aqueous Solutions Using Engineered Magnetic Biochars Derived from Waste Marine Macro-Algal Biomass. *Sci. Total Environ.* **2018**, *615*, 161–168. <https://doi.org/10.1016/j.scitotenv.2017.09.171>.
- (82) Kizito, S.; Wu, S.; Kipkemoi Kirui, W.; Lei, M.; Lu, Q.; Bah, H.; Dong, R. Evaluation of Slow Pyrolyzed Wood and Rice Husks Biochar for Adsorption of Ammonium Nitrogen from Piggery Manure Anaerobic Digestate Slurry. *Sci. Total Environ.* **2015**, *505*, 102–112. <https://doi.org/10.1016/j.scitotenv.2014.09.096>.
- (83) Donat, R.; Akdogan, A.; Erdem, E.; Cetisli, H. Thermodynamics of Pb²⁺ and Ni²⁺ adsorption onto Natural Bentonite from Aqueous Solutions. *J. Colloid Interface Sci.* **2005**, *286* (1), 43–52. <https://doi.org/10.1016/j.jcis.2005.01.045>.
- (84) Kenawy, I. M.; Hafez, M. A. H.; Ismail, M. A.; Hashem, M. A. Adsorption of Cu(II), Cd(II), Hg(II), Pb(II) and Zn(II) from Aqueous Single Metal Solutions by Guanyl-Modified Cellulose. *Int. J. Biol. Macromol.* **2018**, *107*, 1538–1549. <https://doi.org/10.1016/j.ijbiomac.2017.10.017>.
- (85) Shen, Z.; Hou, D.; Jin, F.; Shi, J.; Fan, X.; Tsang, D. C. W.; Alessi, D. S. Effect of Production Temperature on Lead Removal Mechanisms by Rice Straw Biochars. *Sci. Total Environ.* **2019**, *655*, 751–758. <https://doi.org/10.1016/j.scitotenv.2018.11.282>.
- (86) Li, J.; Gu, Y.; Liu, S.; Liu, Y.; Zeng, G.; Liu, S.; Hu, X.; Wang, X.; Tan, X.; Xu, Y. Biochar-Based Nano-Composites for the Decontamination of Wastewater: A Review. *Bioresour. Technol.* **2016**, *212*, 318–333. <https://doi.org/10.1016/j.biortech.2016.04.093>.
- (87) Liang, J.; Li, X.; Yu, Z.; Zeng, G.; Luo, Y.; Jiang, L.; Yang, Z.; Qian, Y.; Wu, H. Amorphous

- MnO₂ Modified Biochar Derived from Aerobically Composted Swine Manure for Adsorption of Pb(II) and Cd(II). *ACS Sustain. Chem. Eng.* **2017**, *5* (6), 5049–5058. <https://doi.org/10.1021/acssuschemeng.7b00434>.
- (88) Yan, L.; Kong, L.; Qu, Z.; Li, L.; Shen, G. Magnetic Biochar Decorated with ZnS Nanocrystals for Pb (II) Removal. *ACS Sustain. Chem. Eng.* **2015**, *3* (1), 125–132. <https://doi.org/10.1021/sc500619r>.
- (89) Shi, M.; Wei, W.; Jiang, Z.; Han, H.; Gao, J.; Xie, J. Biomass-Derived Multifunctional TiO₂ /Carbonaceous Aerogel Composite as a Highly Efficient Photocatalyst. *RSC Adv.* **2016**, *6* (30), 25255–25266. <https://doi.org/10.1039/C5RA28116D>.
- (90) Wang, H.; Gao, B.; Wang, S.; Fang, J.; Xue, Y.; Yang, K. Removal of Pb(II), Cu(II), and Cd(II) from Aqueous Solutions by Biochar Derived from KMnO₄ Treated Hickory Wood. *Bioresour. Technol.* **2015**, *197*, 356–362. <https://doi.org/10.1016/j.biortech.2015.08.132>.
- (91) Jiang, Y.-Q.; An, Q.; Jiang, J.-N.; Nan, H.-Y.; Yu, Y. Unraveling Sorption of Nickel from Aqueous Solution by KMnO₄ and KOH-Modified Peanut Shell Biochar: Implicit Mechanism. *Chemosphere* **2018**, *214*, 846–854. <https://doi.org/10.1016/j.chemosphere.2018.10.007>.
- (92) Li, B.; Yang, L.; Wang, C. quan; Zhang, Q. pei; Liu, Q. cheng; Li, Y. ding; Xiao, R. Adsorption of Cd(II) from Aqueous Solutions by Rape Straw Biochar Derived from Different Modification Processes. *Chemosphere* **2017**, *175*, 332–340. <https://doi.org/10.1016/j.chemosphere.2017.02.061>.
- (93) Wang, X.; Pehkonen, S. O.; Ray, A. K. Removal of Aqueous Cr(VI) by a Combination of Photocatalytic Reduction and Coprecipitation. *Ind. Eng. Chem. Res.* **2007**, *43* (7), 1665–1672. <https://doi.org/10.1021/ie030580j>.
- (94) Lu, D.; Chai, W.; Yang, M.; Fang, P.; Wu, W.; Zhao, B.; Xiong, R.; Wang, H. Visible Light Induced Photocatalytic Removal of Cr(VI) over TiO₂-Based Nanosheets Loaded with Surface-Enriched CoOx Nanoparticles and Its Synergism with Phenol Oxidation. *Appl. Catal. B Environ.* **2016**, *190*, 44–65. <https://doi.org/10.1016/j.apcatb.2016.03.003>.
- (95) Wang, S.; Ji, L. J.; Wu, B.; Gong, Q.; Zhu, Y.; Liang, J. Influence of Surface Treatment on Preparing Nanosized TiO₂ Supported on Carbon Nanotubes. *Appl. Surf. Sci.* **2008**, *255* (5 PART 2), 3263–3266. <https://doi.org/10.1016/j.apsusc.2008.09.031>.
- (96) Ragupathy, S.; Raghu, K.; Prabu, P. Synthesis and Characterization of TiO₂ Loaded Cashew Nut Shell Activated Carbon and Photocatalytic Activity on BG and MB Dyes under Sunlight Radiation. *Spectrochim. Acta - Part A Mol. Biomol. Spectrosc.* **2015**, *138*, 314–320. <https://doi.org/10.1016/j.saa.2014.11.087>.
- (97) Kim, J. R.; Kan, E. Heterogeneous Photocatalytic Degradation of Sulfamethoxazole in Water Using a Biochar-Supported TiO₂ Photocatalyst. *J. Environ. Manage.* **2016**, *180*, 94–101. <https://doi.org/10.1016/j.jenvman.2016.05.016>.
- (98) Zargoosh, K.; Abedini, H.; Abdolmaleki, A.; Molavian, M. R. Effective Removal of Heavy

- Metal Ions from Industrial Wastes Using Thiosalicylhydrazide-Modified Magnetic Nanoparticles. *Ind. Eng. Chem. Res.* **2013**, *52* (42), 14944–14954.
<https://doi.org/10.1021/ie401971w>.
- (99) Jain, M.; Yadav, M.; Kohout, T.; Lahtinen, M.; Garg, V. K.; Sillanpää, M. Development of Iron Oxide/Activated Carbon Nanoparticle Composite for the Removal of Cr(VI), Cu(II) and Cd(II) Ions from Aqueous Solution. *Water Resour. Ind.* **2018**, *20* (October), 54–74.
<https://doi.org/10.1016/j.wri.2018.10.001>.
- (100) Clemente, J. S.; Beauchemin, S.; MacKinnon, T.; Martin, J.; Johnston, C. T.; Joern, B. Initial Biochar Properties Related to the Removal of As, Se, Pb, Cd, Cu, Ni, and Zn from an Acidic Suspension. *Chemosphere* **2017**, *170*, 216–224.
<https://doi.org/10.1016/j.chemosphere.2016.11.154>.
- (101) Xu, X.; Cao, X.; Zhao, L. Comparison of Rice Husk- and Dairy Manure-Derived Biochars for Simultaneously Removing Heavy Metals from Aqueous Solutions: Role of Mineral Components in Biochars. *Chemosphere* **2013**, *92* (8), 955–961.
<https://doi.org/10.1016/j.chemosphere.2013.03.009>.
- (102) Saeed, A.; Iqbal, M.; Akhtar, M. W. Removal and Recovery of Lead(II) from Single and Multimetal (Cd, Cu, Ni, Zn) Solutions by Crop Milling Waste (Black Gram Husk). *J. Hazard. Mater.* **2005**, *117* (1), 65–73. <https://doi.org/10.1016/j.jhazmat.2004.09.008>.
- (103) Sheng, P.; Ting, Y.; Chen, J. Biosorption of Heavy Metal Ions (Pb, Cu, and Cd) from Aqueous Solutions by the Marine Alga *Sargassum* Sp. in Single- and Multiple-Metal Systems. *Ind. Eng. Chem.* ... **2007**, 2438–2444.
- (104) Verma, V. K.; Tewari, S.; Rai, J. P. N. Ion Exchange during Heavy Metal Bio-Sorption from Aqueous Solution by Dried Biomass of Macrophytes. *Bioresour. Technol.* **2008**, *99* (6), 1932–1938. <https://doi.org/10.1016/j.biortech.2007.03.042>.
- (105) Fomina, M.; Gadd, G. M. Biosorption: Current Perspectives on Concept, Definition and Application. *Bioresour. Technol.* **2014**, *160*, 3–14.
<https://doi.org/10.1016/j.biortech.2013.12.102>.
- (106) Yang, S.; Ren, X.; Zhao, G.; Shi, W.; Montavon, G.; Grambow, B.; Wang, X. Competitive Sorption and Selective Sequence of Cu(II) and Ni(II) on Montmorillonite: Batch, Modeling, EPR and XAS Studies. *Geochim. Cosmochim. Acta* **2015**, *166*, 129–145.
<https://doi.org/10.1016/j.gca.2015.06.020>.
- (107) Liu, H.; Zhu, Y.; Xu, B.; Li, P.; Sun, Y.; Chen, T. Mechanical Investigation of U(VI) on Pyrrhotite by Batch, EXAFS and Modeling Techniques. *J. Hazard. Mater.* **2017**, *322*, 488–498. <https://doi.org/10.1016/j.jhazmat.2016.10.015>.
- (108) Shaikh, R. B.; Saifullah, B.; ur Rehman, F.; Shaikh, R. I. Greener Method for the Removal of Toxic Metal Ions from the Wastewater by Application of Agricultural Waste as an Adsorbent. *Water (Switzerland)* **2018**, *10* (10). <https://doi.org/10.3390/w10101316>.

- (109) Wang, M.; Xu, J.; Koopal, L. K.; Fang, L.; Xiong, J.; Tan, W. Copper Binding to Soil Fulvic and Humic Acids: NICA-Donnan Modeling and Conditional Affinity Spectra. *J. Colloid Interface Sci.* **2016**, *473*, 141–151. <https://doi.org/10.1016/j.jcis.2016.03.066>.
- (110) Sorolla, M. G.; Dalida, M. L.; Khemthong, P.; Grisdanurak, N. Photocatalytic Degradation of Paraquat Using Nano-Sized Cu-TiO₂/SBA-15 under UV and Visible Light. *J. Environ. Sci. (China)* **2012**, *24* (6), 1125–1132. [https://doi.org/10.1016/S1001-0742\(11\)60874-7](https://doi.org/10.1016/S1001-0742(11)60874-7).
- (111) Shen, X.; Wang, Q.; Chen, W.; Pang, Y. One-Step Synthesis of Water-Dispersible Cysteine Functionalized Magnetic Fe₃O₄ Nanoparticles for Mercury(II) Removal from Aqueous Solutions. *Appl. Surf. Sci.* **2014**, *317*, 1028–1034. <https://doi.org/10.1016/j.apsusc.2014.09.033>.
- (112) Morillo, D.; Uheida, A.; Pérez, G.; Muhammed, M.; Valiente, M. Arsenate Removal with 3-Mercaptopropanoic Acid-Coated Superparamagnetic Iron Oxide Nanoparticles. *J. Colloid Interface Sci.* **2015**, *438*, 227–234. <https://doi.org/10.1016/j.jcis.2014.10.005>.
- (113) Alam, M. S.; Alessi, D. S. *Modeling the Surface Chemistry of Biochars*; Elsevier Inc., 2018. <https://doi.org/10.1016/b978-0-12-811729-3.00004-2>.
- (114) Obinaju, B. E.; Martin, F. L. ATR-FTIR Spectroscopy Reveals Polycyclic Aromatic Hydrocarbon Contamination despite Relatively Pristine Site Characteristics: Results of a Field Study in the Niger Delta. *Environ. Int.* **2016**, *89–90*, 93–101. <https://doi.org/10.1016/j.envint.2016.01.012>.
- (115) Uchimiya, M.; Lima, I. M.; Thomas Klasson, K.; Chang, S.; Wartelle, L. H.; Rodgers, J. E. Immobilization of Heavy Metal Ions (CuII, CdII, NiII, and PbII) by Broiler Litter-Derived Biochars in Water and Soil. *J. Agric. Food Chem.* **2010**, *58* (9), 5538–5544. <https://doi.org/10.1021/jf9044217>.
- (116) Huang, M.; Mishra, S. B.; Liu, S. Waste Glass Fiber Fabric as a Support for Facile Synthesis of Microporous Carbon to Adsorb Cr(VI) from Wastewater. *ACS Sustain. Chem. Eng.* **2017**, *5* (9), 8127–8136. <https://doi.org/10.1021/acssuschemeng.7b01762>.
- (117) Whaley-Martin, K. J.; Koch, I.; Reimer, K. J. Determination of Arsenic Species in Edible Periwinkles (*Littorina Littorea*) by HPLC-ICPMS and XAS along a Contamination Gradient. *Sci. Total Environ.* **2013**, *456–457*, 148–153. <https://doi.org/10.1016/j.scitotenv.2013.03.066>.
- (118) Hu, J.; Chen, G.; Lo, I. M. C. Removal and Recovery of Cr(VI) from Wastewater by Maghemite Nanoparticles. *Water Res.* **2005**, *39* (18), 4528–4536. <https://doi.org/10.1016/j.watres.2005.05.051>.
- (119) Gates, W. P. X-Ray Absorption Spectroscopy. **2006**, *1* (05). [https://doi.org/10.1016/S1572-4352\(05\)01029-9](https://doi.org/10.1016/S1572-4352(05)01029-9).
- (120) Yuan, J. H.; Xu, R. K.; Zhang, H. The Forms of Alkalis in the Biochar Produced from Crop Residues at Different Temperatures. *Bioresour. Technol.* **2011**, *102* (3), 3488–3497.

- <https://doi.org/10.1016/j.biortech.2010.11.018>.
- (121) Alam, M. S.; Gorman-Lewis, D.; Chen, N.; Flynn, S. L.; Ok, Y. S.; Konhauser, K. O.; Alessi, D. S. Thermodynamic Analysis of Nickel(II) and Zinc(II) Adsorption to Biochar. *Environ. Sci. Technol.* **2018**, *52* (11), 6246–6255. <https://doi.org/10.1021/acs.est.7b06261>.
- (122) Wang, Z.; Liu, G.; Zheng, H.; Li, F.; Ngo, H. H.; Guo, W.; Liu, C.; Chen, L.; Xing, B. Investigating the Mechanisms of Biochar's Removal of Lead from Solution. *Bioresour. Technol.* **2015**, *177*, 308–317. <https://doi.org/10.1016/j.biortech.2014.11.077>.
- (123) Liu, R.; Ma, W.; Jia, C. ying; Wang, L.; Li, H. Y. Effect of PH on Biosorption of Boron onto Cotton Cellulose. *Desalination* **2007**, *207* (1–3), 257–267. <https://doi.org/10.1016/j.desal.2006.07.012>.
- (124) Guo, X.; Zhang, S.; Shan, X. Adsorption of Metal Ions on Lignin. **2008**, *151*, 134–142. <https://doi.org/10.1016/j.jhazmat.2007.05.065>.
- (125) Lea, A.; Programa, C.; Investigación, D.; Fuentes, D. De; Materias, A. De. Metal Ion Biosorption Potential of Lignocellulosic Biomasses and Marine Algae for Wastewater Treatment †. **2006**, 227–244. <https://doi.org/10.1260/026361707782398182>.
- (126) Khormaei, M.; Nasernejad, B.; Edrisi, M.; Eslamzadeh, T. Copper Biosorption from Aqueous Solutions by Sour Orange Residue. **2007**, *149* (424), 269–274. <https://doi.org/10.1016/j.jhazmat.2007.03.074>.
- (127) Si-qingl, X. I. A.; Ling, C.; Jian-fbl, Z.; Jean-marc, C.; Jaffi-ezic-renault, N. Biosorption of Cadmium(I1) and Lead(I1) Ions from Aqueous Solutions onto Dried Activated Sludge. **2006**, No. 20050247016.
- (128) Ahangaran, F.; Hassanzadeh, A.; Nouri, S. Surface Modification of Fe₃O₄@SiO₂ Microsphere by Silane Coupling Agent. **2013**, 3–7.
- (129) Wang, C.; Wang, H. Pb(II) Sorption from Aqueous Solution by Novel Biochar Loaded with Nano-Particles. *Chemosphere* **2018**, *192*, 1–4. <https://doi.org/10.1016/j.chemosphere.2017.10.125>.
- (130) Jin, Z.; Gao, H.; Hu, L. Removal of Pb(II) by Nano-Titanium Oxide Investigated by Batch, XPS and Model Techniques. *RSC Adv.* **2015**, *5* (107), 88520–88528. <https://doi.org/10.1039/c5ra14004h>.
- (131) Gebru, K. A.; Das, C. Removal of Pb (II) and Cu (II) Ions from Wastewater Using Composite Electrospun Cellulose Acetate/Titanium Oxide (TiO₂) Adsorbent. *J. Water Process Eng.* **2017**, *16*, 1–13. <https://doi.org/10.1016/j.jwpe.2016.11.008>.
- (132) Lin, H.; Han, S.; Dong, Y.; He, Y. The Surface Characteristics of Hyperbranched Polyamide Modified Corncob and Its Adsorption Property for Cr(VI). *Appl. Surf. Sci.* **2017**, *412*, 152–159. <https://doi.org/10.1016/j.apsusc.2017.03.061>.
- (133) Mohammad, A.-W.; Abdulrasoul, A.; Ahmed H., E.-N.; Mahmoud E.A., N.; Adel R. A., U. Pyrolysis Temperature Induced Changes in Characteristics and Chemical Composition of

- Biochar Produced from Conocarpus Wastes. *Bioresour. Technol.* **2013**, *131*, 374–379.
<https://doi.org/10.1016/j.biortech.2012.12.165>.
- (134) He, X.; Liu, Z.; Niu, W.; Yang, L.; Zhou, T.; Qin, D.; Niu, Z.; Yuan, Q. Effects of Pyrolysis Temperature on the Physicochemical Properties of Gas and Biochar Obtained from Pyrolysis of Crop Residues. *Energy* **2018**, *143*, 746–756.
<https://doi.org/10.1016/j.energy.2017.11.062>.
- (135) Viglašová, E.; Galamboš, M.; Danková, Z.; Krivosudský, L.; Lengauer, C. L.; Hood-Nowotny, R.; Soja, G.; Rompel, A.; Matík, M.; Briančin, J. Production, Characterization and Adsorption Studies of Bamboo-Based Biochar/Montmorillonite Composite for Nitrate Removal. *Waste Manag.* **2018**, *79*, 385–394.
<https://doi.org/10.1016/j.wasman.2018.08.005>.
- (136) Song, X. D.; Xue, X. Y.; Chen, D. Z.; He, P. J.; Dai, X. H. Application of Biochar from Sewage Sludge to Plant Cultivation: Influence of Pyrolysis Temperature and Biochar-to-Soil Ratio on Yield and Heavy Metal Accumulation. *Chemosphere* **2014**, *109*, 213–220.
<https://doi.org/10.1016/j.chemosphere.2014.01.070>.
- (137) Park, J. H.; Ok, Y. S.; Kim, S. H.; Kang, S. W.; Cho, J. S.; Heo, J. S.; Delaune, R. D.; Seo, D. C. Characteristics of Biochars Derived from Fruit Tree Pruning Wastes and Their Effects on Lead Adsorption. *J. Korean Soc. Appl. Biol. Chem.* **2015**, *58* (5), 751–760.
<https://doi.org/10.1007/s13765-015-0103-1>.
- (138) Cui, L.; Noerpel, M. R.; Scheckel, K. G.; Ippolito, J. A. Wheat Straw Biochar Reduces Environmental Cadmium Bioavailability. *Environ. Int.* **2019**, *126* (January), 69–75.
<https://doi.org/10.1016/j.envint.2019.02.022>.
- (139) Rajapaksha, A. U.; Alam, M. S.; Chen, N.; Alessi, D. S.; Igalavithana, A. D.; Tsang, D. C. W.; Ok, Y. S. Removal of Hexavalent Chromium in Aqueous Solutions Using Biochar: Chemical and Spectroscopic Investigations. *Sci. Total Environ.* **2018**, *625*, 1567–1573.
<https://doi.org/10.1016/j.scitotenv.2017.12.195>.
- (140) Jiang, W.; Cai, Q.; Xu, W.; Yang, M.; Cai, Y.; Dionysiou, D. D.; O’Shea, K. E. Cr(VI) Adsorption and Reduction by Humic Acid Coated on Magnetite. *Environ. Sci. Technol.* **2014**, *48* (14), 8078–8085. <https://doi.org/10.1021/es405804m>.
- (141) Papaevangelou, V. A.; Gikas, G. D.; Tsihrintzis, V. A. Chromium Removal from Wastewater Using HSF and VF Pilot-Scale Constructed Wetlands: Overall Performance, and Fate and Distribution of This Element within the Wetland Environment. *Chemosphere* **2017**, *168*, 716–730. <https://doi.org/10.1016/j.chemosphere.2016.11.002>.
- (142) Entezari, M. H.; Dionysiou, D. D.; O’Shea, K.; Pelaez, M.; Jiang, W.; Tsoutsou, D. Chromium(VI) Removal by Maghemite Nanoparticles. *Chem. Eng. J.* **2013**, *222*, 527–533.
<https://doi.org/10.1016/j.cej.2013.02.049>.
- (143) Gao, W.; Yan, J.; Qian, L.; Han, L.; Chen, M. Surface Catalyzing Action of Hematite

- (α -Fe₂O₃) on Reduction of Cr(VI) to Cr(III) by Citrate. *Environ. Technol. Innov.* **2018**, *9* (71), 82–90. <https://doi.org/10.1016/j.eti.2017.11.007>.
- (144) Peshkur, T. A.; Gibson, L. T.; Idris, S. A.; Alotaibi, K.; Anderson, P. Preconcentration and Selective Extraction of Chromium Species in Water Samples Using Amino Modified Mesoporous Silica. *J. Colloid Interface Sci.* **2012**, *386* (1), 344–349. <https://doi.org/10.1016/j.jcis.2012.07.040>.
- (145) Marchetti, S. G.; Martin, P. P.; Bengoa, J. F.; Fellenz, N.; Rojas, S.; García-Fierro, J. L.; Perez-Alonso, F. J. Chromium (VI) Removal from Water by Means of Adsorption-Reduction at the Surface of Amino-Functionalized MCM-41 Sorbents. *Microporous Mesoporous Mater.* **2016**, *239*, 138–146. <https://doi.org/10.1016/j.micromeso.2016.10.012>.
- (146) Ko, Y. J.; Choi, K.; Lee, S.; Jung, K. W.; Hong, S.; Mizuseki, H.; Choi, J. W.; Lee, W. S. Strong Chromate-Adsorbent Based on Pyrrolic Nitrogen Structure: An Experimental and Theoretical Study on the Adsorption Mechanism. *Water Res.* **2018**, *145*, 287–296. <https://doi.org/10.1016/j.watres.2018.08.033>.
- (147) Chen, G.; Feng, J.; Wang, W.; Yin, Y.; Liu, H. Photocatalytic Removal of Hexavalent Chromium by Newly Designed and Highly Reductive TiO₂nanocrystals. *Water Res.* **2017**, *108*, 383–390. <https://doi.org/10.1016/j.watres.2016.11.013>.
- (148) Liu, W.; Chen, H.; Borthwick, A. G. L.; Han, Y.; Ni, J. Mutual Promotion Mechanism for Adsorption of Coexisting Cr(III) and Cr(VI) onto Titanate Nanotubes. *Chem. Eng. J.* **2013**, *232*, 228–236. <https://doi.org/10.1016/j.cej.2013.07.100>.
- (149) Liu, W.; Ni, J.; Yin, X. Synergy of Photocatalysis and Adsorption for Simultaneous Removal of Cr(VI) and Cr(III) with TiO₂ and Titanate Nanotubes. *Water Res.* **2014**, *53* (Iii), 12–25. <https://doi.org/10.1016/j.watres.2013.12.043>.
- (150) Zhao, N.; Yin, Z.; Liu, F.; Zhang, M.; Lv, Y.; Hao, Z.; Pan, G.; Zhang, J. Environmentally Persistent Free Radicals Mediated Removal of Cr(VI) from Highly Saline Water by Corn Straw Biochars. *Bioresour. Technol.* **2018**, *260* (March), 294–301. <https://doi.org/10.1016/j.biortech.2018.03.116>.
- (151) Zhu, N.; Yan, T.; Qiao, J.; Cao, H. Adsorption of Arsenic, Phosphorus and Chromium by Bismuth Impregnated Biochar: Adsorption Mechanism and Depleted Adsorbent Utilization. *Chemosphere* **2016**, *164*, 32–40. <https://doi.org/10.1016/j.chemosphere.2016.08.036>.
- (152) Cho, J.-S.; Park, J.-H.; Ok, Y. S.; Seo, D.-C.; Delaune, R. D.; Kim, S.-H.; Heo, J.-S. Competitive Adsorption of Heavy Metals onto Sesame Straw Biochar in Aqueous Solutions. *Chemosphere* **2015**, *142*, 77–83. <https://doi.org/10.1016/j.chemosphere.2015.05.093>.
- (153) Módenes, A. N.; Espinoza-Quiñones, F. R.; Palácio, S. M.; Kroumov, A. D.; Stutz, G.; Tirao, G.; Camera, A. S. Cr(VI) Reduction by Activated Carbon and Non-Living Macrophytes

- Roots as Assessed by K β Spectroscopy. *Chem. Eng. J.* **2010**, *162* (1), 266–272.
<https://doi.org/10.1016/j.cej.2010.05.045>.
- (154) Xu, X.; Huang, H.; Zhang, Y.; Xu, Z.; Cao, X. Biochar as Both Electron Donor and Electron Shuttle for the Reduction Transformation of Cr(VI) during Its Sorption. *Environ. Pollut.* **2019**, *244*, 423–430. <https://doi.org/10.1016/j.envpol.2018.10.068>.
- (155) Zhang, D. L.; Zhang, M. Y.; Zhang, C. H.; Sun, Y. J.; Sun, X.; Yuan, X. Z. Pyrolysis Treatment of Chromite Ore Processing Residue by Biomass: Cellulose Pyrolysis and Cr(VI) Reduction Behavior. *Environ. Sci. Technol.* **2016**, *50* (6), 3111–3118.
<https://doi.org/10.1021/acs.est.5b05707>.
- (156) Qin, F.; Wen, B.; Shan, X. Q.; Xie, Y. N.; Liu, T.; Zhang, S. Z.; Khan, S. U. Mechanisms of Competitive Adsorption of Pb, Cu, and Cd on Peat. *Environ. Pollut.* **2006**, *144* (2), 669–680.
<https://doi.org/10.1016/j.envpol.2005.12.036>.
- (157) Alam, M. S.; Gorman-Lewis, D.; Chen, N.; Flynn, S. L.; Ok, Y. S.; Konhauser, K. O.; Alessi, D. S. Thermodynamic Analysis of Nickel(II) and Zinc(II) Adsorption to Biochar. *Environ. Sci. Technol.* **2018**, *52* (11), 6246–6255. <https://doi.org/10.1021/acs.est.7b06261>.
- (158) Park, D.; Yun, Y. S.; Park, J. M. XAS and XPS Studies on Chromium-Binding Groups of Biomaterial during Cr(VI) Biosorption. *J. Colloid Interface Sci.* **2008**, *317* (1), 54–61.
<https://doi.org/10.1016/j.jcis.2007.09.049>.
- (159) Wang, L.; Wang, Y.; Ma, F.; Tankpa, V.; Bai, S.; Guo, X.; Wang, X. Mechanisms and Reutilization of Modified Biochar Used for Removal of Heavy Metals from Wastewater: A Review. *Sci. Total Environ.* **2019**, *668*, 1298–1309.
<https://doi.org/10.1016/j.scitotenv.2019.03.011>.
- (160) Naiya, T. K.; Bhattacharya, A. K.; Das, S. K. Adsorption of Cd(II) and Pb(II) from Aqueous Solutions on Activated Alumina. *J. Colloid Interface Sci.* **2009**, *333* (1), 14–26.
<https://doi.org/10.1016/j.jcis.2009.01.003>.
- (161) Shen, Y.; Zhao, P.; Shao, Q.; Ma, D.; Takahashi, F.; Yoshikawa, K. In-Situ Catalytic Conversion of Tar Using Rice Husk Char-Supported Nickel-Iron Catalysts for Biomass Pyrolysis/Gasification. *Appl. Catal. B Environ.* **2014**, *152–153* (1), 140–151.
<https://doi.org/10.1016/j.apcatb.2014.01.032>.
- (162) Świerczyński, D.; Libs, S.; Courson, C.; Kiennemann, A. Steam Reforming of Tar from a Biomass Gasification Process over Ni/Olivine Catalyst Using Toluene as a Model Compound. *Appl. Catal. B Environ.* **2007**, *74* (3–4), 211–222.
<https://doi.org/10.1016/j.apcatb.2007.01.017>.
- (163) Benlalla, A.; Elmoussaouiti, M.; Dahhou, M.; Assafi, M. Utilization of Water Treatment Plant Sludge in Structural Ceramics Bricks. *Appl. Clay Sci.* **2015**, *118*, 171–177.
<https://doi.org/10.1016/j.clay.2015.09.012>.
- (164) Muñoz V., P.; Morales O., M. P.; Letelier G., V.; Mendivil G., M. A. Fired Clay Bricks Made

-
- by Adding Wastes: Assessment of the Impact on Physical, Mechanical and Thermal Properties. *Constr. Build. Mater.* **2016**, *125*, 241–252.
<https://doi.org/10.1016/j.conbuildmat.2016.08.024>.
- (165) Weng, C. H.; Lin, D. F.; Chiang, P. C. Utilization of Sludge as Brick Materials. *Adv. Environ. Res.* **2003**, *7* (3), 679–685. [https://doi.org/10.1016/S1093-0191\(02\)00037-0](https://doi.org/10.1016/S1093-0191(02)00037-0).
- (166) Barbieri, L.; Andreola, F.; Lancellotti, I.; Taurino, R. Management of Agricultural Biomass Wastes: Preliminary Study on Characterization and Valorisation in Clay Matrix Bricks. *Waste Manag.* **2013**, *33* (11), 2307–2315.
<https://doi.org/10.1016/j.wasman.2013.03.014>.
- (167) Chiang, K. Y.; Chou, P. H.; Hua, C. R.; Chien, K. L.; Cheeseman, C. Lightweight Bricks Manufactured from Water Treatment Sludge and Rice Husks. *J. Hazard. Mater.* **2009**, *171* (1–3), 76–82 <https://doi.org/10.1016/j.jhazmat.2009.05.144>.

Chapter 2

Methodology

Chapter 2

Methodology.....	59
2.1 Chemicals	59
2.2 Adsorbents	59
2.2.1 Biomass and biochar	59
2.2.2 Chemical pretreatment of adsorbents.....	61
2.2.3 TiO ₂ loaded on the pine biochar	62
2.2.4 SPION loaded on the biomass.....	62
2.3 Characterization	63
2.3.1 Fourier transform infrared spectroscopy (ATR-FTIR)	63
2.3.2 Scanning electron microscopy (SEM).....	63
2.3.3 Inductively coupled plasma mass spectrometry (ICP-MS)	64
2.3.4 X-ray diffraction (XRD)	64
2.3.5 Brunauere Emmette-Teller technique (BET)	65
2.3.6 Zeta potential	66
2.3.7 X-ray absorption spectroscopy (XAS)	66
2.4 Procedures	67
2.4.1 Batch biosorption experiments.....	67
2.4.2 Parameters influencing on heavy metal biosorption.....	68
2.4.3 Biosorption kinetics modelling	68
2.4.4 Biosorption isotherm modelling	72
References.....	77

Methodology

2.1 Chemicals

A 1000 mg/L stock solution of single element system was prepared by dissolving the required amounts of $\text{Pb}(\text{NO}_3)_2$, $\text{Cd}(\text{NO}_3)_2 \cdot 4\text{H}_2\text{O}$, $\text{Cu}(\text{NO}_3)_2 \cdot 3\text{H}_2\text{O}$ and $\text{Cr}(\text{NO}_3)_3 \cdot 9\text{H}_2\text{O}$ (all 99% from Panreac, Barcelona, Spain). All the chemicals used were of analytical grade. The ethanol ($\text{C}_2\text{H}_6\text{O}$, 97%), nitric acid (HNO_3 , 72%) and hydrochloric acid (HCl , 37% v/v), sodium hydroxide (NaOH , 98%) were purchased from Panreac (Barcelona, Spain). Titanium (IV) butoxide ($\text{C}_{16}\text{H}_{36}\text{O}_4\text{Ti}$, 97% v/v) was from Sigma-Aldrich (MO, USA). Sodium hydroxide (NaOH , 98%) and nitric acid (HNO_3 , 72%) were used to adjust the solution pH.

2.2 Adsorbents











2.2.1 Biomass and biochar

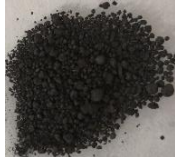






All the adsorbents are grinded and dried before using, which were kindly supplied by CREAM Institute (at Autonomous University of Barcelona, UAB, Barcelona, Spain). Biochar products are derived from different types of pyrolysis processes that are showed in Table 2.1. Supplementary detailed information of biomass and biochars is listed in Table 2.2.

Table 2.1 Biochars derived from different Pyrolysis processes

Pyrolysis proceses	Temperature °C	Time	Particle size (mm)
Fast (R)	Pine: 440-480 Poplar: 430-510	2s	<6
Slow(L)	500-550	15 min	≤65
Gasification(G)	600-900	75 min	≤50

Table 2.2 Biosorbents studied in this work.

Type	Abbreviation	Image	location
Poplar	CO		Spain
Poplar Slow pyrolysis	CL		Spain
Poplar Fast pyrolysis	CR		Spain
Corn	ZO		Spain
Corn Slow pyrolysis	ZL		Spain
Pine (Pinus radiata)	PO		Spain
Pine Slow pyrolysis	PL		Spain
Pine Fast pyrolysis	PR		Spain
Pine Gasification pyrolysis	PG		Spain
Sludge (urban sewage sludge)	FO		Spain

Sludge Slow pyrolysis	FL		Spain
Banana peel	BO		Colombia
Sugar cane	SO		Brazil
Coffee shell	EO		Brazil
Canola	LO		China
Rice	RO		China
TiO ₂ loaded on pine	Pine/TiO ₂		Spain

2.2.2 Chemical pretreatment of adsorbents

Biomass and biochar are chemically pretreated in order to increase the adsorption efficiency and capacity by improving the properties of adsorbents. So, CO, CL CR, ZO, ZL, FO, FL are treated with both 0.1 M of HNO₃ solution and deionized water, for 24 hours to compare the adsorption capacity of both options. Then samples are washed with deionized water three times in the first case before drying in the oven at 75°C for 24 hours.

2.2.3 TiO₂ loaded on the pine biochar

The sample of pine, previously acid-treated, washed with deionized water and dried before using. So, 5 g of this acid-treated biomass were suspended in nitric acid at pH 3.0 for 4 days as a conditioning procedure. After a step of filtration from the acidic media, the biomass is washed with deionized water three times until neutral pH of the washing water. Then, the material is dried in the oven at 75°C for 24 hours.

TiO₂ loaded on the pine biochar (Pine/TiO₂) is prepared using the sol-gel method reported by Wang¹. 5 g of the obtained material are dispersed in 120 mL of ethanol followed by addition of 40 mL of Titanium (IV) butoxide solution (97%) that is the TiO₂ precursor. The mixture is stirred at ambient temperature for 1 hour before adding a solution containing 16 mL of HCl 37% (v/v) and 40 mL of ethanol (97%) with constant stirring (for 1 hour more). The solution is filtered, and then is washed with ethanol before drying at 70°C for 24 hours. The dried sample is milled and pyrolyzed at 300 °C for 1 hour in a muffle to yield the Pine/TiO₂.

2.2.4 SPION loaded on the biomass

SPION loaded on the biomass (Fe₃O₄-Biomass) is prepared by the methods reported by Morillo². Heating 100 mL deionized water to 40 °C under stirring at the speed of 300 rpm/min. Deoxygenate the solution for a half an hour. Weight 0.40 g of biomass, 0.26 g of FeCl₂·4H₂O and 0.70 g of FeCl₃·6H₂O, and put them to the water stirring continuously (we call this as “mix” solution). In this process, the concentration rate of the iron species FeCl₂·4H₂O (Fe(II)) and FeCl₃·6H₂O (Fe(III)) is 1:2. Prepare a 125mL solution of NaOH (0.5M) and deoxygenated under stirring for 1h. Add this NaOH solution to the mix solution drop by drop and stirring for another 1 hour. The solution will be turn into black after adding the NaOH solution. Wash the sample with deionized water before drying at 50°C for 24 hours.


2.3 Characterization

The morphology is analyzed by scanning electron microscopy (SEM) coupled with energy dispersive X-ray (EDX). The X-ray diffraction (XRD) patterns are collected to identify any crystallographic structures for the samples by using a powder X-ray Diffractometer with Cu K α radiation (XRD, D8 ADVANCE, Bruker). Attenuated total reflectance Fourier transform infrared spectroscopy (ATR-FTIR) spectra were recorded on a Nicolet IS10 spectrometer with a spectral range from 600 to 4000 cm⁻¹. XAS data include X-ray absorption near-edge structures (XANES) and extended X-ray absorption fine structure (EXAFS) spectroscopy that are performed at ALBA Synchrotron (Barcelona, Spain) and Diamond Synchrotron (London, England).

2.3.1 Fourier transform infrared spectroscopy (ATR-FTIR)

Attenuated total reflectance Fourier transform infrared spectroscopy (ATR-FTIR) is widely used either to identify compounds or to evaluate the purity of a material. In this study, an ATR-FTIR (Tensor 27, Bruker, Germany from *Servei d'Anàlisi Química*, UAB, Barcelona, Spain) is used to analyze the structural changes of adsorbents samples. The spectrum ranged from 400 to 4000 cm⁻¹ with 16 scans and with a resolution of 4 cm⁻¹. The equipment description is specified in Table 2.3.

Table 2.3 Equipment description of Attenuated total reflectance Fourier transform infrared spectrometer (FTIR)


Equipment	ATR-FTIR
Model	Tensor 27
Company and Country	Bruker, Germany
Laboratory of analysis	<i>Servei d'Anàlisi Química</i> (SAQ, UAB, Barcelona, Spain)
Image	

2.3.2 Scanning electron microscopy (SEM)

Scanning electron microscopy (SEM) images are used to reveal the surface topography of the different adsorbents samples. The scanning electron microscopy (SEM ZEISS EVO® MA 10, Oberkochen, Germany) is a powerful tool to analyze the morphological structure of the adsorbents materials. The preparation of samples is simple, and the sputter-coating arrangement of adsorbents is relatively stable in the

penetrating electron beam. Detailed description of the equipment is showed in Table 2.4.


Table 2.4 Equipment description of Scanning electron microscopy (SEM)

Equipment	SEM
Model	ZEISS EVO MA 10
Company and Country	Carl Zeiss, Germany
Laboratory of analysis	<i>Servei de Microscòpia Electrònica (UAB, Barcelona, Spain)</i>
Image	

2.3.3 Inductively coupled plasma mass spectrometry (ICP-MS)

Inductively coupled plasma mass spectrometry (ICP-MS) is a powerful technique that has been widely used in trace elemental analysis, mainly in aqueous solution. ICP-MS is the most sensitive technique for trace elements in solution and the detection limits are around 0.01-1 $\mu\text{g/L}$ (ppb) in solution. Detailed information of the ICP-MS equipment used in this work to measure the heavy metal concentration in the solutions, before and after the adsorption experiments, is listed in Table 2.5.

Table 2.5 Equipment description of ICP-MS


Equipment	ICP-MS
Model	VG Plasma Quad ExCell and XSeries 2
Company and Country	Thermo Scientifics, USA
Laboratory of analysis	Group of Separation Techniques in Chemistry, GTS (UAB, Barcelona, Spain)
Image	

2.3.4 X-ray diffraction (XRD)

X-ray diffraction (XRD) is one of the most important non-destructive tools to analyze all kinds of matter ranging from fluids, to powders and crystals. From research to production and engineering, XRD is an indispensable method for materials

characterization and quality control. In this study, XRD is used to identify any crystallographic structures of nanoparticles loaded on adsorbents. Detailed information of the XRD equipment used is listed in Table 2.6.


Table 2.6 Equipment description of X-ray diffraction (XRD)

Equipment	XRD
Model	D8 ADVANCE
Company and Country	Bruker, USA
Laboratory of analysis	<i>Serveis Científicotècnics</i> (UAB, Barcelona, Spain)
Image	

2.3.5 Brunauere Emmette-Teller technique (BET)

BET is widely used to measure the surface area, pore volume, and pore diameter. In this study, surface area determination is done by measurement of N₂ adsorption, applying Brunauere Emmette-Teller technique (BET) and Autosorb iQinstrument (Quantachrome, USA). Cumulative pore volume for mesoporous is calculated using BarreteJoynere Halenda method. The Dubinine Radushkevich test was applied to get micropore volume. Detailed information of the used equipment is listed in Table 2.7.


Table 2.7 Equipment description of Autosorb iQinstrument.

Equipment	Surface Area and Porosity Instrument
Model	TriStar II 3020
Company and Country	Micromeritics, USA
Laboratory of analysis	Oil Crops Research Institute of Chinese Academy of Agricultural Sciences
Image	

2.3.6 Zeta potential

Zeta potential is used to determine the surface charge of the adsorbent. It helps us to understand the biosorption process, especially the influence of functional groups that present on the surface. Equipment information is listed in Table 2.8.



Table 2.8 Equipment description of Autosorb iQinstrument.

Equipment	Zetasizer Nano
Model	Zen 3600
Company and Country	Malvern,
Laboratory of analysis	Oil Crops Research Institute of Chinese Academy of Agricultural Sciences
Image	

2.3.7 X-ray absorption spectroscopy (XAS)

XAS is a technique that allows the study of the local structure around a selected element at an atomic and molecular scale. The theory of this technique is described in chapter 1.4.2. In the next Table 2.9, a brief presentation of both facilities used are presented (Diamond and ALBA):

Table 2.9 The Synchrotron faculties where present work were performed.

Synchrotron Faculty	Diamond	ALBA
Country	London, England	Barcelona, Spain
Beamline	B18	CLAESS
Energy range	2.05 – 35 keV	6.4 – 12.5 keV
Optics	Si(111) and Si(311)	Si(111) and Si(311)
Image		

2.4 Procedures

2.4.1 Batch biosorption experiments

Biosorption experiments are carried out at room temperature ($25 \pm 1^\circ\text{C}$). Individual heavy metal solutions (single systems) and a mixed heavy metal solution (multiple system) are checked. Metal concentration, for both different systems, is ranged from 0.05 to 4 mmol/L. Batch experiments are performed by adding 25 mg of biomass in a 5 mL tubes, and then filled with 2.5 mL of the corresponding heavy metal aqueous solutions. The tubes are then placed on a rotary mixer (CE 2000 ABT-4, SBS Instruments SA, Barcelona, Spain) to be properly shaken at 25 rpm for 24 hours. Thus, after the heavy metal biosorption experiment, the two aqueous and solid phases are separated by decantation and the aqueous solution is filtered through 0.22 μm Millipore filters (Barcelona, Spain). The concentration of the heavy metals in the supernatant phases is determined by the inductively coupled plasma mass spectrometry equipment, ICP-MS.

The uptake of the heavy metal by adsorbents is evaluated as the percentage of biosorption that is calculated following the Equation [1]. Moreover, the capacity of the material is expressed as the amount of adsorbate per gram of adsorbent at the equilibrium, following the Equation [2].

$$\% \text{ Removal} = \frac{(C_0 - C_e)}{C_0} \times 100 \quad [1]$$

$$q_e = \frac{(C_0 - C_e) \times V}{m} \quad [2]$$

Where q_e (mmol/g) is the amount of heavy metal adsorbed at equilibrium per gram of the adsorbent; V (L) is the volume of solution; C_0 (mmol /L) and C_e (mmol /L) are the initial and the equilibrium heavy metal concentrations in solution, respectively; and m (g) is the dried mass of adsorbent. All results were expressed as the mean value of the replicates.

2.4.2 Parameters influencing on heavy metal biosorption

The influence of the aqueous pH

The influence of the initial aqueous pH on the adsorbent uptake of metal ions is investigated in the pH range from 2 to 6 in the multiple system. In this set of experiments, higher pH values are not evaluated to avoid possible metal hydrolysis and precipitation. The pH of the aqueous multiple heavy metal solution is adjusted by using NaOH and HNO₃ solutions. The initial concentration of heavy metals is 0.18 mM. 25 mg of adsorbents are mixed with 2.5 mL metals solution and stirred for 24 hours to reach the adsorption equilibrium. The temperature of the experiments is 25±1°C.

The influence of the contact time

In order to evaluate the effect of the contact time onto the biosorption efficiency, biosorption experiments were run at different times. 25 mg of biomass are added to 2.5 mL solutions of 0.18 mM of the heavy metals in a multiple system, adjusted at pH 4. Different tubes with adsorbent and the multiple system solution are prepared and each one is shaken at 25 rpm at different times, for 5, 10, 20, 30, 45, 60, 120, 240, 480, 1440 min. The temperature of the experiments is 25±1°C.

The influence of the temperature

To study the effect of temperature on the biosorption process, experiments are performed at four different temperatures (25, 40, 55 and 70°C) as explained above. So, 25 mg of biomass are added to 2.5 mL solutions of 0.18 mM multiple system and adjusted at pH 4.0. Samples are shaken at 25 rpm for 24 h at each controlled temperature.

The influence of the initial metal concentration

The initial heavy metal concentration is ranged from 0.05 to 4 mmol/L for the four metals under study (Pb²⁺, Cd²⁺, Cu²⁺ and Cr³⁺) in the multiple system. Following the same procedure as mentioned above, the concentration of all the heavy metals is varied as 0.05, 0.1, 0.2, 0.5, 1, 2, 4 mmol/L for 24 hours under stirring (at 25 rpm). All the solutions are adjusted to pH 4 and the temperature is 25±1°C.

2.4.3 Biosorption kinetics modelling

Following the batch experiments mentioned above, when checking the influence of the contact time, experimental data obtained can be used to adjust different kinetic models. This modelling can help to better understand the biosorption mechanisms

with the different adsorbents and adsorbates. All these kinetic models are explained in the next part.

To further understand the biosorption process and identify the biosorption mechanisms of the heavy metals adsorption onto the different biomass and biochar systems under study, the biosorption kinetics curves are analyzed. These kinetic models included the pseudo-first order (PFO), the pseudo-second order (PSO), the Elovich and the Intra-particle Diffusion models. Following these models are properly presented.

The pseudo-first-order model (PFO)

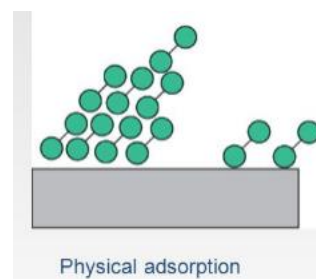


Figure 2.1 Schematic biosorption process for PFO model.

The pseudo-first-order model (PFO) for solid/liquid systems of adsorption states that the rate is proportional to the number of unoccupied sites, which is controlled by physic process (as shown in Figure 2.1)³. A simple kinetic analysis of the biosorption process can be followed by using the equation in the corresponding form [3]:

$$\frac{dq_t}{dt} = k_1(q_e - q_t) \quad [3]$$

where k_1 (min^{-1}) is the rate constant of the PFO adsorption model, q_e (mmol/g of dry weight) is the amount of metal ion sorbed at the equilibrium, and q_t (mmol/g of dry weight) is the amount of metal ion on the surface of the sorbent at any time t (min). By applying the boundary conditions $q_t = 0$ at $t = 0$ in the Equation 3, and linearizing Equation 3, Equation [4] follows.

$$\log(q_e - q_t) = \log(q_e) - \frac{k_1}{2.303} t \quad [4]$$

Where q_t and q_e are the biosorption amount at time t and at equilibrium, respectively; and k_1 is the first-order rate constant (min^{-1}). According to the literature, in most cases, the PFO equation is linear only over approximately the first 30 min, so it is appropriate for the initial contact time, not for the whole range⁴.

The pseudo-second-order model

The pseudo-second-order model (PSO) assumes that the rate of adsorption is proportional to the square of the number of unoccupied sites, that the chemical sorption process controls the rate of the biosorption, including valence forces sharing or exchange of electrons between adsorbent and adsorbate (shown in Figure 2.2)⁵.

The corresponding PSO kinetic rate equation is:

$$\frac{dq_t}{dt} = k_2(q_e - q_t)^2 \quad [5]$$

where k_2 ($\text{g mmol}^{-1} \text{min}^{-1}$) is the rate constant of pseudo second-order adsorption. From Equation 6 by applying the boundary conditions $t = 0$ to $t = t$ and $q_0 = 0$ to $q_t = q_t$, the Equation [5], which corresponds to the integrated rate law for a second-order reaction, is obtained:

$$\frac{1}{q_e - q_t} = \frac{1}{q_e} + k_2 t \quad [6]$$

Equation [6] can be rearranged to obtain Equation 7, as follows:

$$\frac{t}{q_t} = \frac{1}{k_2 q_e^2} + \frac{t}{q_e} \quad [7]$$

Here, the following abbreviations apply: q_t and q_e are the biosorption amount at any time t and at equilibrium, respectively; and k_2 represents the second-order rate constant (min^{-1}).

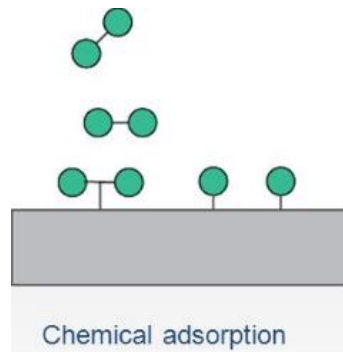


Figure 2.2 Schematic biosorption process for PSO model.

Elovich model

The Elovich equation is often used to describe the kinetics of chemisorption on highly heterogeneous adsorbents, which means a multilayer adsorption if adsorption sites are increase exponentially with adsorption^{4,6}. The equation of the Elovich model is formulated as:

$$\frac{dq_t}{dt} = \alpha \exp(-\beta q_t) \quad [8]$$

where q_e and q_t are the amounts of adsorbate uptake per mass of adsorbent at equilibrium and at any time t (min), respectively; α (mg/g min) is the initial rate

constant, β (mg/g) is the desorption constant during any one experiment. The integrated form of Equation [8] is as follows:

$$q_t = \frac{\ln(\alpha\beta)}{\beta} + \frac{\ln t}{\beta} \quad [9]$$

Thus the constants can be obtained from the slope and intercept of the linear plot of q_t versus $\ln t$.

Intra-particle Diffusion model

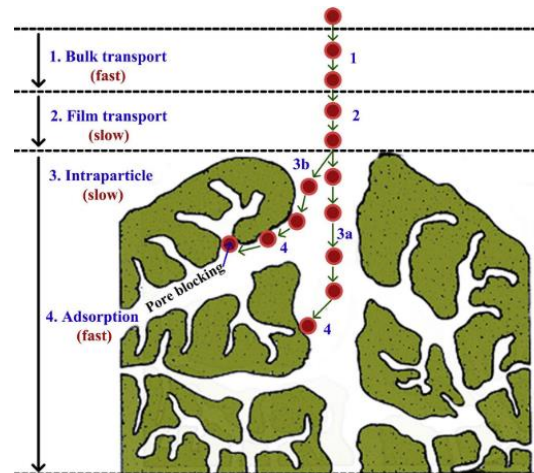


Figure 2.3 Schematic biosorption process for Intra-particle diffusion model⁴.

The intra-particle diffusion model is schematically shown in Figure 2.3. The Weber-Morris (1963) intra-particle diffusion model parameters are calculated to determine whether film diffusion or intraparticle diffusion is the rate limiting step⁴. The model suggested that if the sorption mechanism is via intraparticle diffusion then a plot of q_t versus $t_{1/2}$ will be linear; and intraparticle diffusion is the sole rate-limiting step when such a plot passes through the origin. When the sorption process is controlled by more than one mechanism, then a plot of q_t versus $t_{1/2}$ will be multi-linear⁷. The equation is expressed as:

$$q_t = k_i(t_{1/2}) + C \quad [10]$$

Which can be linearized as:

$$\log q_t = \log k_i + 0.5 \log t \quad [11]$$

Where q_t is the amount of metals adsorbed on the adsorbent at a time t , and k_i is the rate parameter of the intra-particle diffusion control stage. C values indicate the thickness of the boundary layer.

In Table 2.10 is a summary list of the equations of all the kinetics models here presented and used in this work.

Table 2.10 Summary of the biosorption kinetic model equations

Isotherm	Equation	Linear form	plots	Parameters
pseudo-first-order	$\frac{dq_t}{dt} = k_1(q_e - q_t)$	$\log(q_e - q_t) = \log(q_e) - \frac{k_1}{2.303}t$	$\log(q_e - q_t)$ versus t	q_e, k_1
pseudo-second-order	$\frac{dq_t}{dt} = k_2(q_e - q_t)^2$	$\frac{t}{q_t} = \frac{1}{k_2q_e^2} + \frac{t}{q_e}$	$\frac{t}{q_t}$ versus t	q_e, k_2
Elovich	$\frac{dq_t}{dt} = \alpha \exp(-\beta q_t)$	$q_t = \beta \ln(\alpha\beta) + \beta \text{Int}$	q_t versus Int	α, β
Intra-particle Diffusion	$q_t = k_i(t_{1/2}) + C$	$\log q_t = \log k_i + 0.5 \log t$	q_t versus $t_{1/2}$	k_i, C

2.4.4 Biosorption isotherm modelling

Biosorption isotherm studies are carried out carrying batch experiments as mentioned above. Now, 10 mg of adsorbents are mixed with 1.0 mL of a solution containing different heavy metal concentrations (ranging from 0.05 up to 4 mmol/L) in both individual and multiple systems, stirring at 25 rpm for 24 hours to reach the adsorption equilibrium state. All the solutions are adjusted to pH 4 and the temperature was $25 \pm 1^\circ\text{C}$.

A biosorption isotherm is an expression that shows the relation between the amount of biosorbate adsorbed per unit weight of biosorbent (q_e , mmol/g) with the concentration of biosorbate in the bulk solution under equilibrium conditions (C_e , mmol/L) and at a given temperature⁸. At this stage, the equilibrium concentrations in both phases are constant. The equilibrium biosorption isotherms are very useful in giving information on biosorption mechanisms, surface properties and affinity of a biosorbent towards some biosorbates, such as heavy metal ions⁹.

Different isotherm models, like those of Freundlich, Langmuir and Redlich-Peterson(R-P), have been used to describe the equilibrium characteristics of the biosorption process for individual system. Extended and modified adsorption isotherm equations have also been proposed to represent the binary and multiple elemental system adsorption equilibria.

It is important to establish the most appropriate correlation for the equilibrium curves. Freundlich, Langmuir and Temkin have been widely used in this case. A

summary list of the equations of the isotherm models are showed in Table 2.14.

The Freundlich isotherm

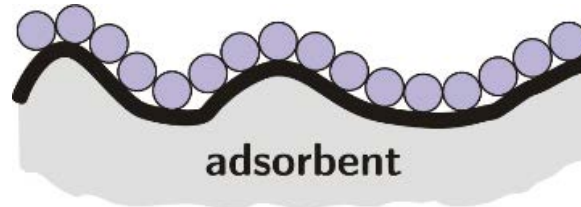


Figure 2.4 Schematic biosorption process explained by the Freundlich model

The Freundlich isotherm model follows an empirical equation and is employed to describe the equilibrium process on an heterogeneous surface. The adsorption equilibrium constant is determined by the adsorbent non-homogeneous surface¹⁰. The linear and non-linear expressions of Freundlich isotherm model can be expressed as equations [12] and [13], respectively:

$$\ln q_e = \ln K_F + \frac{1}{n} \ln C_e \quad [12]$$

$$q_e = K_F C_e^{1/n} \quad [13]$$

Where K_F ($\mu\text{mol/g}/(\mu\text{mol/L})^n$) and n (dimensionless) are the Freundlich isotherm constants, which indicate the biosorption capacity and the heterogeneity factor, respectively⁴. The slope of $1/n$ ranging between 0 and 1 is a measure of the surface heterogeneity, becoming more heterogeneous as its value gets closer to zero¹¹. The value of $1/n$ below one indicates a normal Freundlich isotherm while $1/n$ above one is indicative of cooperative adsorption. The plot of $\ln q_e$ versus $\ln C_e$ gave a straight line with an slope of $1/n$ and an intercept of $\ln K_F$.

The magnitude of the exponent n gives an indication on the favorability of adsorption. It is generally stated the signification of the values of n (shown in Table 2.11).

Table 2.11 Favorability of adsorption.

Value of n	Type of isotherm
$0 < \frac{1}{n} < 1$	more heterogeneous as its value gets closer to zero
$\frac{1}{n} < 1$	normal Freundlich isotherm
$0 < \frac{1}{n}$	cooperative adsorption

or

Value of n	Type of isotherm
$2 < n < 10$	good
$1 < n < 2$	moderately difficult
$n < 1$	poor adsorption characteristics

Langmuir isotherm

Langmuir isotherm model is an empirical model assuming that adsorption can only occur at a finite number of definite localized sites and occurs on homogeneous surface by a monolayer deposition¹². The generalized Langmuir isotherm can be represented by linear and non-linear equations [14] and [15] as follow:

$$\frac{C_e}{q_e} = \frac{C_e}{q_{max}} + \frac{1}{K_L q_{max}} \quad [14]$$

$$q_e = \frac{Q_{max} K_L C_e}{1 + K_L C_e} \quad [15]$$

Where C_e is the equilibrium concentration of metal ions in the solution ($\mu\text{mol/L}$), q_{max} is the amount of metal ion required to form a monolayer (in this case is $\mu\text{mol/g}$) and $K_L(\text{L}/\mu\text{mol})$ is the equilibrium constant related to the energy of adsorption.

The essential characteristics of Langmuir isotherm can be expressed by a dimensionless constant called separation factor or equilibrium parameter, R_L , defined by Weber and Chakkravorti as¹²:

$$R_L = \frac{1}{1 + K_L C_0} \quad [16]$$

The parameter R_L indicates the kind of reaction process, as follows:

Table 2.12 Favorability of adsorption.

Value of R_L	Type of isotherm
$R_L = 0$	irreversible
$0 < R_L < 1$	favorable
$R_L = 1$	linear
$R_L > 1$	unfavorable

Furthermore, K_L can be calculated as following:

$$K_L = Q_0 b \quad [17]$$

The Langmuir equation can be reorganized properly and described as:

$$\frac{C_e}{q_e} = \frac{b}{K_L} C_e + \frac{1}{K_L} \quad [18]$$

Where K_L and b are the Langmuir isotherm constants, which indicate the biosorption capacity and the affinity factor, respectively. Low value of b presents high affinity onto the adsorbents.

The term b (the Langmuir constant) can also be used to calculate the standard Gibbs's free energy (ΔG^0) of the biosorption process following Equation 19:

$$\Delta G^0 = -RT \ln b \quad [19]$$

Where R is the universal gas constant (8.314 J/mol K) and T is the absolute temperature (295 K).

The Gibbs free energy is used to describe the degree of spontaneity of the biosorption process, so as higher negative Gibbs energy value more energetically favorable biosorption process related. The negative values of ΔG^0 suggested that the biosorption of these metal ions onto the biosorbent is a spontaneous processes and thermodynamically favorable under the experimental conditions checked. In addition, The values of Gibbs energy, ΔG^0 , correlates with the different kind of possible biosorption process, as follows:

Table 2.13 Different kind of possible biosorption process as a function of the Gibbs energy, ΔG^0 .

Value of ΔG^0	Type of process
$-20 < \Delta G^0 < 0$	physisorption
$-400 < \Delta G^0 < -80$	chemisorption

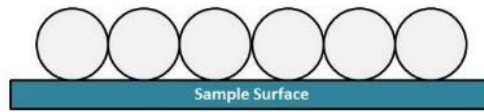


Figure 2.5 Schematic biosorption process explained by the Langmuir model.

Temkin isotherm

Temkin and Pyzhev considered the effects of some indirect adsorbate interactions on adsorption isotherms and suggested that because of these interactions the heat of adsorption of all the molecules in the layer would decrease linearly with coverage¹⁵. The Temkin isotherm has been used in this work in the following forms:

$$q_e = \frac{RT}{b} \ln A + \frac{RT}{b} \ln C_e \quad [20]$$

$$q_e = \frac{RT}{b} (\ln AC_e) \quad [21]$$

Where $B = \frac{RT}{b}$ (J/mol) is the Temkin constant related to heat of sorption, whereas A (L/g) is the equilibrium binding constant corresponding to the maximum binding energy. R (8.314 J/mol K) is the universal gas constant and T (K) is the absolute solution temperature.

In Table 2.14 there is a summary list of the equations of all the isotherm models here presented and used in this work.

Table 2.14 Summary of the equations for biosorption isotherm models.

Isotherm	Equation	Linear form	Plots	Parameter	Ref.
Langmuir	$q_e = \frac{Q_{max}K_L C_e}{1 + K_L C_e}$	$\frac{C_e}{q_e} = \frac{C_e}{q_{max}} + \frac{1}{K_L q_{max}}$	$\frac{C_e}{q_e}$ versus C_e	Q_{max}, K_L	16,17
Freundlich	$q_e = K_F C_e^n$	$\ln q_e = \ln K_f + \ln C_e$	$\ln q_e$ versus $\ln C_e$	K_F, n	18–20
Temkin	$q_e = \frac{RT}{b} (\ln AC_e)$	$q_e = \frac{RT}{b} \ln A + \frac{RT}{b} \ln C_e$ where $B = \frac{RT}{b}$	$\ln C_e$ versus q_e	A, B	21

References

- (1) Wang, S.; Ji, L. J.; Wu, B.; Gong, Q.; Zhu, Y.; Liang, J. Influence of Surface Treatment on Preparing Nanosized TiO₂ Supported on Carbon Nanotubes. *Appl. Surf. Sci.* **2008**, *255* (5 PART 2), 3263–3266. <https://doi.org/10.1016/j.apsusc.2008.09.031>.
- (2) Morillo, D.; Pérez, G.; Valiente, M. Efficient Arsenic(V) and Arsenic(III) Removal from Acidic Solutions with Novel Forager Sponge-Loaded Superparamagnetic Iron Oxide Nanoparticles. *J. Colloid Interface Sci.* **2015**, *453*, 132–141. <https://doi.org/10.1016/j.jcis.2015.04.048>.
- (3) Wang, C.; Wang, H. Pb(II) Sorption from Aqueous Solution by Novel Biochar Loaded with Nano-Particles. *Chemosphere* **2018**, *192*, 1–4. <https://doi.org/10.1016/j.chemosphere.2017.10.125>.
- (4) Nguyen, H.; You, S.; Hosseini-bandegharaei, A. Mistakes and Inconsistencies Regarding Adsorption of Contaminants from Aqueous Solutions : A Critical Review. *Water Res.* **2017**, *120*, 88–116. <https://doi.org/10.1016/j.watres.2017.04.014>.
- (5) Tan, X.; Liu, Y.; Zeng, G.; Wang, X.; Hu, X.; Gu, Y.; Yang, Z. Application of Biochar for the Removal of Pollutants from Aqueous Solutions. *Chemosphere* **2015**, *125*, 70–85. <https://doi.org/10.1016/j.chemosphere.2014.12.058>.
- (6) Cheung, C. W.; Porter, J. F.; McKay, G. Elovich Equation and Modified Second-Order Equation for Sorption of Cadmium Ions onto Bone Char. *J. Chem. Technol. Biotechnol.* **2000**, *75* (11), 963–970.
- (7) Chaudhry, S. A.; Zaidi, Z.; Siddiqui, S. I. Isotherm, Kinetic and Thermodynamics of Arsenic Adsorption onto Iron-Zirconium Binary Oxide-Coated Sand (IZBOCS): Modelling and Process Optimization. *J. Mol. Liq.* **2017**, *229*, 230–240. <https://doi.org/10.1016/j.molliq.2016.12.048>.
- (8) Rahman, M. S.; Islam, M. R. Effects of PH on Isotherms Modeling for Cu(II) Ions Adsorption Using Maple Wood Sawdust. *Chem. Eng. J.* **2009**, *149* (1–3), 273–280. <https://doi.org/10.1016/j.cej.2008.11.029>.
- (9) Syafiuddin, A.; Salmiati, S.; Jonbi, J.; Fulazzaky, M. A. Application of the Kinetic and Isotherm Models for Better Understanding of the Behaviors of Silver Nanoparticles Adsorption onto Different Adsorbents. *J. Environ. Manage.* **2018**, *218* (20), 59–70.
- (10) Allen, S. J.; McKay, G.; Porter, J. F. Adsorption Isotherm Models for Basic Dye Adsorption by Peat in Single and Binary Component Systems. *J. Colloid Interface Sci.* **2004**, *280* (2), 322–333. <https://doi.org/10.1016/j.jcis.2004.08.078>.
- (11) Foo, K. Y.; Hameed, B. H. Insights into the Modeling of Adsorption Isotherm Systems. *Chem. Eng. J.* **2010**, *156* (1), 2–10. <https://doi.org/10.1016/j.cej.2009.09.013>.
- (12) Ayawei, N.; Ebelegi, A. N.; Wankasi, D. Modelling and Interpretation of Adsorption Isotherms. *J. Chem.* **2017**, *2017*, 1–11. <https://doi.org/10.1155/2017/3039817>.

-
- (13) Srivastava, V. C.; Mall, I. D.; Mishra, I. M. Equilibrium Modelling of Single and Binary Adsorption of Cadmium and Nickel onto Bagasse Fly Ash. *Chem. Eng. J.* **2006**, *117* (1), 79–91. <https://doi.org/10.1016/j.cej.2005.11.021>.
- (14) Wu, F. C.; Liu, B. L.; Wu, K. T.; Tseng, R. L. A New Linear Form Analysis of Redlich-Peterson Isotherm Equation for the Adsorptions of Dyes. *Chem. Eng. J.* **2010**, *162* (1), 21–27. <https://doi.org/10.1016/j.cej.2010.03.006>.
- (15) Fierro, V.; Torné-Fernández, V.; Montané, D.; Celzard, A. Adsorption of Phenol onto Activated Carbons Having Different Textural and Surface Properties. *Microporous Mesoporous Mater.* **2008**, *111* (1–3), 276–284. <https://doi.org/10.1016/j.micromeso.2007.08.002>.
- (16) Kim, W.-H.; Chung, H.-K.; Park, J.; Park, P.-K.; Cho, J.; Jeong, T.-Y. Application of Langmuir and Freundlich Isotherms to Predict Adsorbate Removal Efficiency or Required Amount of Adsorbent. *J. Ind. Eng. Chem.* **2015**, *28*, 241–246. <https://doi.org/10.1016/j.jiec.2015.02.021>.
- (17) Basso, M. C.; Cerrella, E. G.; Cukierman, A. L. Lignocellulosic Materials as Potential Biosorbents of Trace Toxic Metals from Wastewater. *Ind. Eng. Chem. Res.* **2002**, *41* (15), 3580–3585. <https://doi.org/10.1021/ie020023h>.
- (18) Yuvaraja, G.; Krishnaiah, N.; Subbaiah, M. V.; Krishnaiah, A. Biosorption of Pb(II) from Aqueous Solution by Solanum Melongena Leaf Powder as a Low-Cost Biosorbent Prepared from Agricultural Waste. *Colloids Surfaces B Biointerfaces* **2014**, *114*, 75–81. <https://doi.org/10.1016/j.colsurfb.2013.09.039>.
- (19) Lee, S. Y.; Choi, H. J. Persimmon Leaf Bio-Waste for Adsorptive Removal of Heavy Metals from Aqueous Solution. *J. Environ. Manage.* **2018**, *209*, 382–392. <https://doi.org/10.1016/j.jenvman.2017.12.080>.
- (20) Yu, F.; Zhou, Y.; Gao, B.; Qiao, H.; Li, Y.; Wang, E.; Pang, L.; Bao, C. Effective Removal of Ionic Liquid Using Modified Biochar and Its Biological Effects. *J. Taiwan Inst. Chem. Eng.* **2016**, *67*, 318–324. <https://doi.org/10.1016/j.jtice.2016.07.038>.
- (21) Mupa, M.; Mautsi, M. P.; Gwizangwe, I. Adsorption of a Cationic Dye by Marula (*Sclerocarya Birrea*) Fruit Seed Shell Based Biosorbent: Equilibrium and Kinetic Studies. *African J. Biotechnol.* **2017**, *16* (40), 1969–1976. <https://doi.org/10.5897/ajb2016.15830>.
- (22) Ho, Y. S.; McKay, G. Application of Kinetic Models to the Sorption of Copper(II) on to Peat. *Adsorpt. Sci. Technol.* **2003**, *20* (8), 797–815. <https://doi.org/10.1260/026361702321104282>.
- (23) Choy, K. K. H.; Porter, J. F.; McKay, G. Langmuir Isotherm Models Applied to the Multicomponent Sorption of Acid Dyes from Effluent onto Activated Carbon. *J. Chem. Eng. Data* **2000**, *45* (4), 575–584. <https://doi.org/10.1021/je9902894>.

Chapter 3

Results and discussion

Chapter 3

3 Result and discussion	83
3.1 Biosorption of heavy metals by agriculture and industry wood wastes.....	84
3.1.1 Biosorption comparison by different biomass systems	85
3.1.2 Characterization of biomass systems.....	86
3.1.3 Influence of the contact time for biomass systems	90
3.1.4 Biosorption kinetics modeling for banana peel (BO), canola (LO) and rice (RO)	93
3.1.5 Influence of the initial heavy metal concentration on biomass systems: rice (RO) and canola (LO)	97
3.1.6 Biosorption isotherm modeling for rice (RO) and canola (LO)	98
3.1.7 Influence of the aqueous solution pH for rice (RO), canola (LO) and banana peel (BO)	101
3.1.8 Influence of the temperature with BO	102
3.1.9 Thermodynamic parameters for rice (RO) and canola (LO).....	103
3.1.10 Summary	105
3.2 Biosorption of heavy metals by biochar systems.....	107
3.2.1 Comparison biosorption percentage of poplar, corn and sludge system	108
3.2.2 Characterization of poplar (CO/CL/CR), corn (ZO/ZL) and sewage sludge (FO/FL)	110
3.2.3 The influence of the contact time.....	115
3.2.4 Kinetic modelling for biomass/biochar systems: poplar (CO/CL), corn (ZO/ ZL), and sewage sludge (FO/FL)	117
3.2.5 Comparison of pine wood systems: biomass (PO) and biochars (PL, PR and PG).....	118
3.2.6 Comparison of biosorption capacity for all biosorbents	118
3.2.7 Summary	121
3.3 Biosorption of heavy metals by particles loaded biochar.....	123
3.3.1 Biosorption characteristics for TiO ₂ modified biomass: sugar cane (SO, SO/TiO ₂) corn (ZO, ZO/TiO ₂), and pine (PO, Pine/TiO ₂)	124
3.3.2 Summary	134
3.4 Biosorption mechanism of heavy metals by XAS.....	135
3.4.1 Chromium speciation: biosorption mechanism elucidation by XAS.	135
3.4.2 Mechanism study for Cr(III) and Pb(II) by XAS.....	145

3.4.3 Summary	149
3.5 Future trends: Disposal of biosorbents-heavy metals mixture	150
References.....	154

3 Result and discussion

As mentioned in the introduction part, polluted waters in the world are mainly due to the human activities and drain from industrial wastewater over the last decades. Development of low-cost techniques for removing toxic heavy metals from the environment is one of the most important goals in environmental science. In this sense, biosorption methods are considered the most advantageous due to their high efficiency, low cost and ease handling.

Therefore, biomasses as adsorbents to remove heavy metals have emerged as novel candidates for developing economic and eco-friendly wastewater treatments. The most important is that two big environmental problems can be solved at the same time: re-use of the huge amount of biomass wastes and removal of contaminants from waters by using biomass as biosorbents. Although many researches have been carried out on biosorption for heavy metals removal, there is still very little scientific understanding of comparison of different biosorbents in multiple systems and the related biosorption mechanisms.

According to this idea, Chapter 3 of this thesis is composed of four themed parts. The first part is devoted to the study the biosorption process of heavy metals by agriculture and wood industry waste biomass systems. The second part is focused on the biosorption characterization of modified biomass systems, mainly biochars that are product of the biomass pyrolysis process. The third part focuses on another type of modified biomass systems that are modified by particles. The purpose of this modification is to increase the efficiency of heavy metals removal comparing with the original biomass. The last part is dedicated to find out the mechanism of biosorption of the heavy metals here selected by XAS techniques.

In each part, the characterization of all the biosorbents checked (by using such as FT-IR, XRD, SEM/TEM) is performed to elucidate their structure, morphology, metal binding groups, and also their composition. Later, kinetics and isotherm are performed to better understand the biosorption process in each biosorbent/heavy metals case. Kinetics modeling including the pseudo-first order, the pseudo-second order, the Elovich model and the Intraparticle diffusion model are analyzed to fit the experimental data. Isotherms modeling including Langmuir Freundlich and Temkin models are also analyzed to fit the experimental data. In addition, different parameters of biosorption processes are optimized in batch systems (the pH of the solution, the

initial concentration and the contact time).

3.1 Biosorption of heavy metals by agriculture and industry wood wastes

In this part, rice (RO, *Oryza sativa* L), canola (LO, *Brassica napus* L.), sugarcane (SO), coffee shell (EO), banana peel (BO), and corn (ZO) as agricultural wastes, poplar wood (CO) and pine (PO) from wood industry wastes, and waste sludge (FO) are studied.

While mass cultivation of rice and canola grown on a large scale in China, and harvested area reached 30 million ha in 2010 and 6.5 ha in 2014 for rice and canola, respectively^{1,2}. The amount of canola waste is not high like rice, even we have collaboration with people from Oil Crops Research Institute of Chinese Academy of Agricultural Sciences (Wuhan, China) for both wastes. The aim of the collaboration is to help them to solve the disposal problem of both rice and canola.

Sugarcane is chosen from Brazil since it has an average yield of $\sim 80 \text{ Mg ha}^{-1}$ and around 14 Mg ha^{-1} of dry biomass after each harvest³. Coffee is grown on a large scale in Brazil around 2.4 million hectares and coffee production at 59.3 million bags (60 kilograms per bag) in 2019⁴. This part (sugarcane and coffee) is in collaboration with Eliane C de Resende from *Federal Institute of Minas Gerais* (Brazil).

While banana is chosen from Colombia because about 81.3 Mt of banana are produced per year in there. Considering that banana peel represents the 25%–30% of the total dry matter, about 5 Mt of peels are produced every year in Colombia⁵. On another hand, Colombia, is the world's fifth largest banana exporter and the area cultivated were 49,146 hectares in 2017⁶. This collaboration is with Candelaria Tejada Tovar and Angel Villabona Ortíz from the *Universidad de Cartagena* (Colombia).

Moreover, pine and poplar wood biomass wastes are collected from Spain as they can be produced in large quantities at sawmills. Waste sludge is a different case from among the others here presented. Last three cases, pine, poplar and sludge wastes have been checked in collaboration of Josep Maria Alcañiz and Xavier Domene from CREAM-UAB research center on ecology and forestry (*Centre de Recerca Ecològica i Aplicacions Forestals*), under a national Spanish research project number AGL2015-70393-R.

3.1.1 Biosorption comparison by different biomass systems

LO, RO, EO, BO, ZO, CO, PO and FO are evaluated as biosorbents for the removal of heavy metals from a multiple-metal aqueous solution composed of four metal ions Cr(III), Cu(II), Cd(II), and Pb(II). The results are shown in Figure 3.1. These biosorbents show different biosorption capacities for the different metal ions. In general, biosorbents from agricultures wastes (LO, RO and ZO) show better biosorption than those from wood biomass wastes (PO and CO). In particular, EO (from coffee shell), PO and CO (from wood) show the lowest biosorption for Cd(II).

It is worth noting that LO exhibit higher biosorption capacities for all metal ions, especially for Cd(II), comparing with the others agricultural biomass wastes. FO from sludge wastes shows the highest biosorption capacities for all metal ions, probably due to the more negative charge on its surface that can interact with the cationic heavy metals form. The Zeta potential measurements of FO is checked later (see Section 3.2) that confirmed our hypothesis.

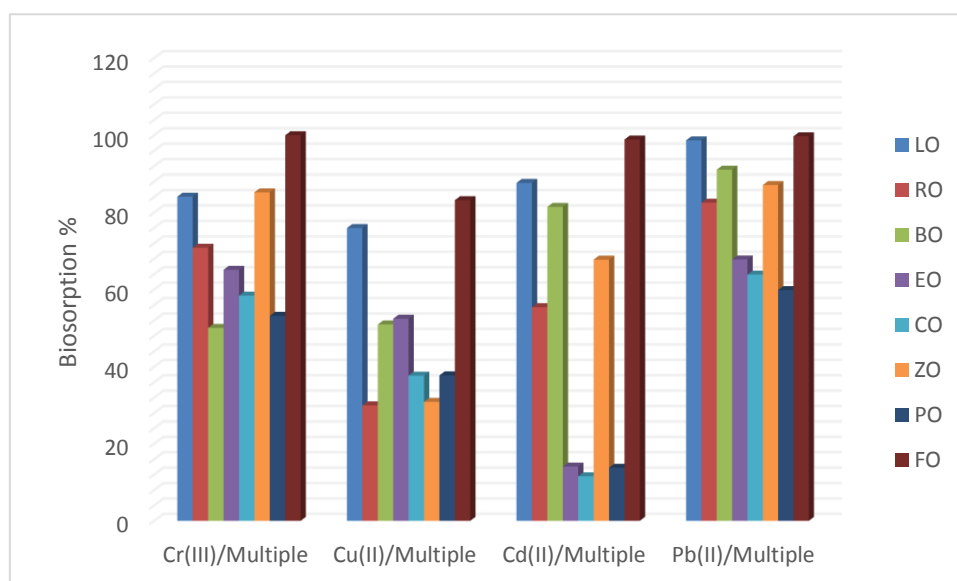


Figure 3.1 Biosorption of metal ions from multiple system composed of Cr(III), Cu(II), Cd(II) and Pb(II) by different biosorbents. Initial 2.5 mL of aqueous solutions concentration are 0.18 mmol/L for each element, pH =4.0, same amount of 25 mg of biosorbents is used, at T=25.0°C, and stirring for 24 h.

This behavior probably can be related to the composition of the biomass wastes that mainly is cellulose, hemicellulos and lignin. These have a chemical composition that can help the interaction with heavy metals. For example, carboxylic and hydroxyl groups are probably present on the surface and they can interact with our analytes by ion exchange. Therefore, it is interesting to accomplish with the proper

characterization of their composition (FTIR analysis is shown later in Section 3.1.2). Furthermore, mineral composition can be also considered, depending on each type of biomass waste residue, which is further discussed later in Section 3.2 (biochar results part).

3.1.2 Characterization of biomass systems

SEM characterization

SEM was used to study the morphological structure of the biomass. The images of the original biomasses and their SEM images are shown in Figure 3.2. In general, the morphological structures shown in SEM images are different depending on biomass residues.

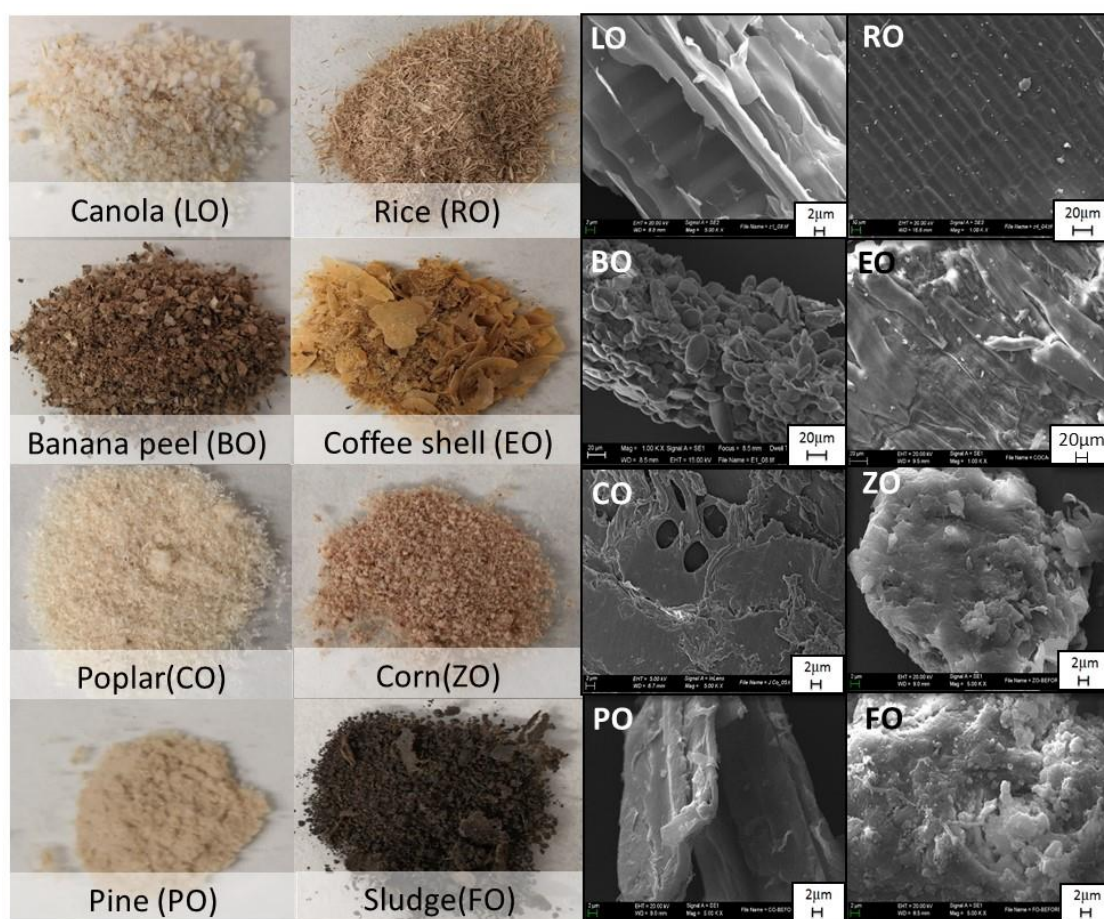


Figure 3.2 Images of the original biomasses and their SEM images.

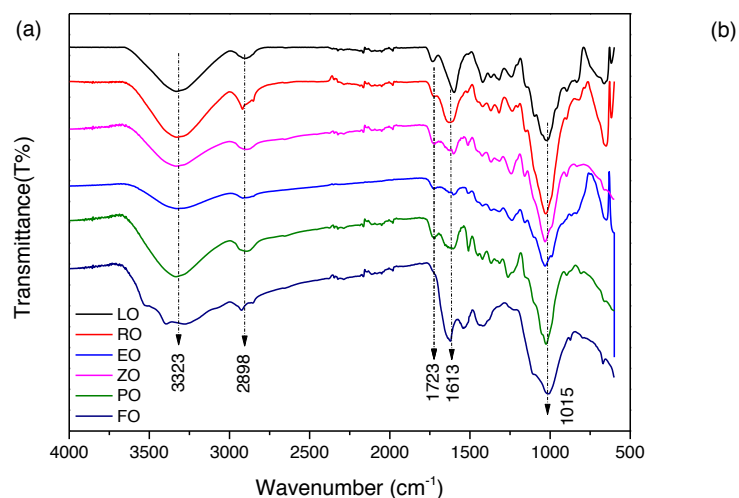
It is well known that lignin provides structural rigidity to the cell walls of many plant species and accounts for a 15–40% of the dried biomasses, for wood and agricultural residues, together with cellulose and hemicelluloses⁷. Furthermore, lignin has been proved a potential adsorbent to remove heavy metals due to its unique polyphenol

structure and physicochemical properties^{8,9}. In particular, RO present a typical structure of lignin. LO is also show a bigger mesopore diameter, which probably is a key factor that can influence the sorption of heavy metals onto biomass, as *Bagreev et al* reported similar results^{10–12}.

ATR-FTIR analysis

ATR-FTIR analysis was carried out to identify the functional groups present in the biosorbents that might be involved in the biosorption process. In Figure 3.3 (a) ATR-FTIR of some biomasses are collected. As shown, all biosorbents have similar ATR-FTIR spectra except for FO. These differences can be explained by the compositions of LO, RO, EO, CO, ZO and PO, which are cellulose and lignin-based biomasses that contain carboxyl groups. However, FO is from industry sewage sludge, and its composition, probably a mix of organic and inorganic compounds containing carbon, hydrogen and oxygen and also nitrogen, respectively¹³.

In addition, cellulose, hemicellulose and lignin are the main components of agriculture and wood biomass and their well-known functional groups can be found in their ATR-FTIR spectra¹⁴. The range of 800–1800 cm^{-1} is the “fingerprint” region, where stretching vibrations of different groups of cellulose and lignin components can be assigned. In this “fingerprint” region, the peaks at 1620, 1599, 1421, 1236 and 1228 cm^{-1} correspond to C=C, C-O stretching or bending vibrations of the different chemical groups present in lignin (such as aromatic rings). The peaks at 1723 and 1737 cm^{-1} are due to C=O, C-H, C-O-C, C-O deformation or stretching vibrations of different groups in carbohydrates compounds of those biomass materials.



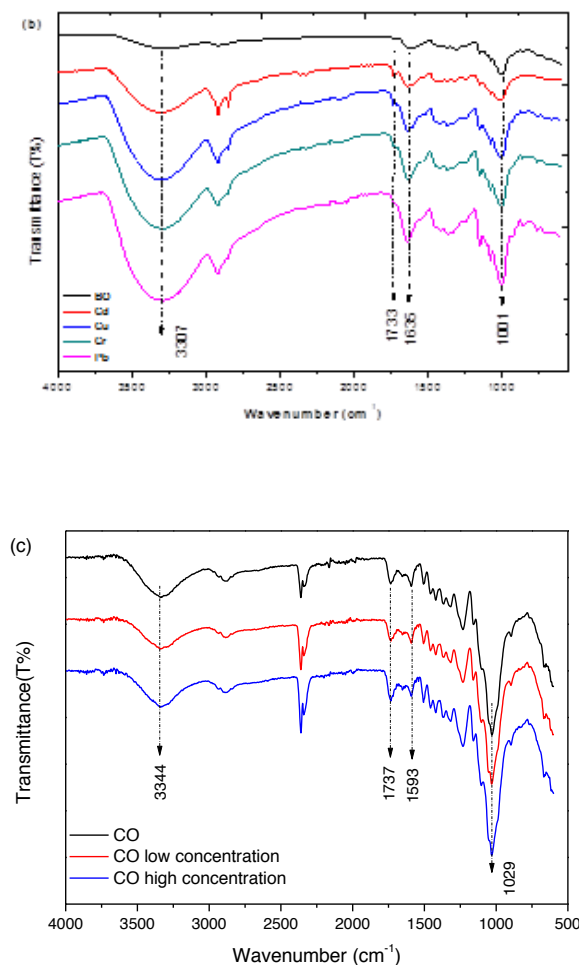


Figure 3.3 ATR-FTIR spectra of different biosorbents: (a) the spectra of LO, RO, EO, ZO, PO and FO; (b) ATR-FTIR spectra of BO before and after biosorption experiments with different heavy metal individual solutions; (c) ATR-FTIR spectra of CO before and after biosorption experiments with different concentration levels of heavy metals multiple solution system. In both latter cases, b and c, the initial aqueous concentration of heavy metals was kept at 0.18 mmol/L, at pH 4.0 and 25.0 °C, and stirring for 24h.

Some main peaks related to biosorption have been marked by line present in Figure 3.3. It can be observed that there are strong broad peaks, one around 3400 cm⁻¹ which is assigned to different O-H stretching and another around 2920 cm⁻¹ related to asymmetric and symmetric methyl and methylene stretching groups, which can be also found in the spectra of cellulose¹⁵. While according to the literatures, the peaks at 3200-3270 cm⁻¹ and 1780-1710 cm⁻¹ correspond to the O-H and C=O stretching vibrations, respectively, which confirms the presence of carboxyl groups (-COOH) on the adsorbents. The additional peaks at 1029 and 1022 cm⁻¹ are characteristic of C-H, C-O deformation, bending, or stretching vibrations of many groups in lignin and carbohydrates. In addition, carboxyl groups are expected to be the responsible for the

heavy metals biosorption onto biomasses and they have been found in all ATR-FTIR cases. This confirms their role in the biosorption process.

Moreover, the effect on the ATR-FTIR of biomass before and after 24 h biosorption of heavy metals is also considered. *Blázquez et al.* reported that biosorption could be taking place through an ion-exchange process rather than through complexation due to small changes in wavenumber (in most cases, less than 10 cm^{-1}).¹⁶ Shifting of bands to lower frequencies indicates bond weakening while a shift to higher frequencies indicates an increase in bond strength¹⁷. To distinguish the small differences, BO was chosen to compare the differences before and after biosorption of a mixed solution containing Cr(III), Cu(II), Cd(II) and Pb(II) as show in Figure 3.3(b). In the case of BO, the changes in wavenumbers are slightly shifted to higher wavenumbers in our study. So, ion-exchange process of heavy metals onto the biomass surface can be here explained.

The concentration of heavy metals is considered in order to try to check their interaction with the functional groups of biomass surface (as indicated, the main responsible of the heavy metal removal), as shown in Figure 3.3(c). CO is chosen for comparison and two different concentration levels of heavy metal are assayed, 0.18 and 20 mmol/L of Cr(III). The ATR-FTIR spectra of CO in both cases are exactly the same. Thus, no relevant information can be taken from this experiment to confirm the ion-exchange interaction in the biosorption process for CO. ATR-FTIR wavenumbers of BO, LO and RO are shown in Table 3.1, while the rest of biomasses will appear later as compared with other systems.

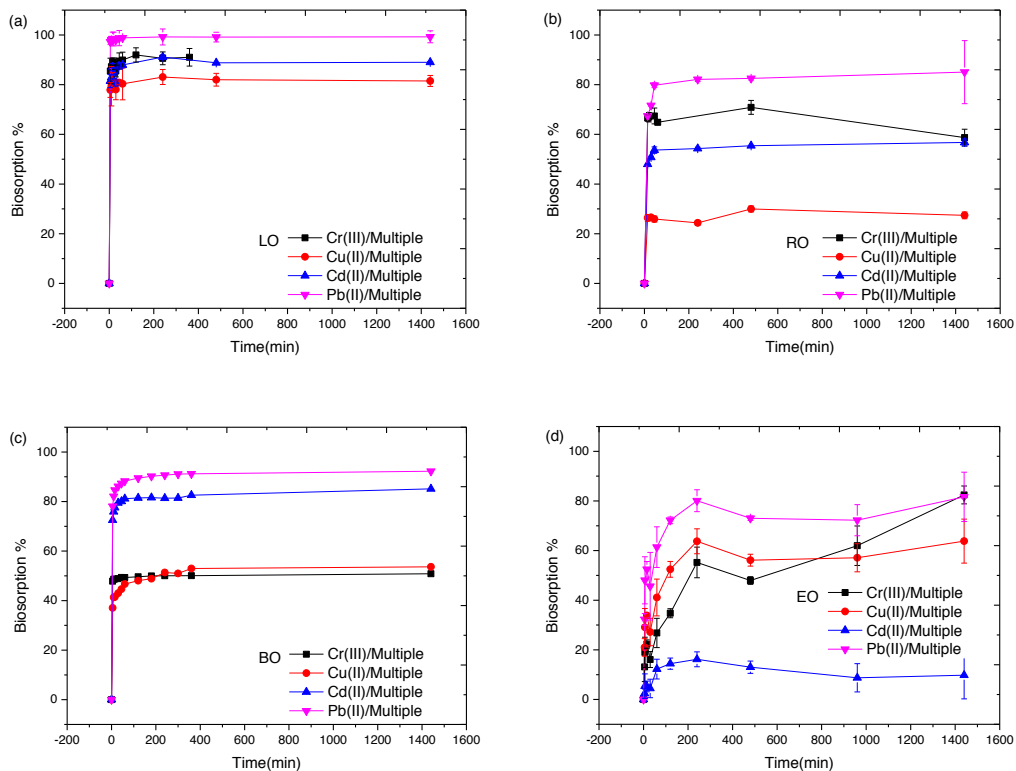
Table 3.1 ATR-FTIR spectral bands assignments for banana peel (BO), rice (RO) and canola (LO) before use.

Wave Number (cm^{-1})	Assignments	Compounds	Band positions (cm^{-1})		
			BO	RO	LO
3200-3700	O-H stretching	Acid, methanol	3323	3323	3323
2700-3000	C-H _n stretching	Alkyl, aliphatic	2890	2898	2898
1700-1730	C=O stretching	Carboxyl, Carbonyl	1733	1723	1723
1450-1600	C=O stretching	Ketone, carbonyl	1635	1613	1613
1000-1200	C=O stretching C-O-C stretching/bending C-N,R-O-C/R-O-CH ₃	Ketone, ether, phenol, chain anhydride	1001	1015	1015

3.1.3 Influence of the contact time for biomass systems

The effect of the contact time between biosorbents (RO, LO, BO, EO, PO, CO, ZO and FO) and heavy metals in single and multiple-metal systems (Cr(III), Cu(II), Cd(II), Pb(II)) are studied. For that purpose, biosorption experiments are performed (as indicated in the experimental section) at different times (from 5 to 1440 minutes) for each biosorbent (results show in Figures 3.4 and 3.5).

In multiple system (shown in Figure 3.4), in general, LO and FO are more effective than other biomasses, and CO and PO are the less effective ones. Biosorption equilibrium is reached at different times for each biomass. FO is really effective for the biosorption and reaches the equilibrium in 5 minutes for all metal ions. In contrast, EO reaches equilibrium for all metal ions within 24 hours. In the case of CO, the equilibrium time differs as a function of the heavy metal, so biosorption equilibrium is reached in 5 minutes for Pb(II) and Cd(II), in 1 h for Cu(II), and in 24 h for Cr(III). Additionally, RO, BO, ZO and PO reach equilibrium requiring approximately 6 h for all heavy metal ions. Thus, 24 h is chosen as the optimal contact time for further biosorption experiments, to assure a complete sorption process in all cases (for all biomasses and heavy metals here selected).



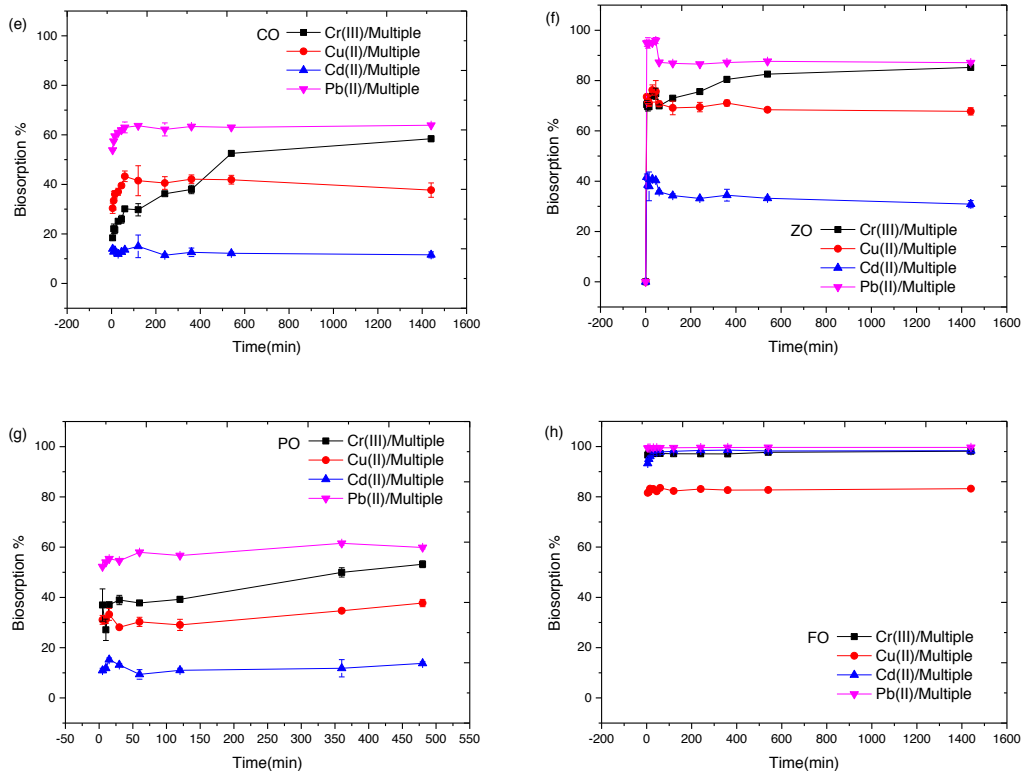
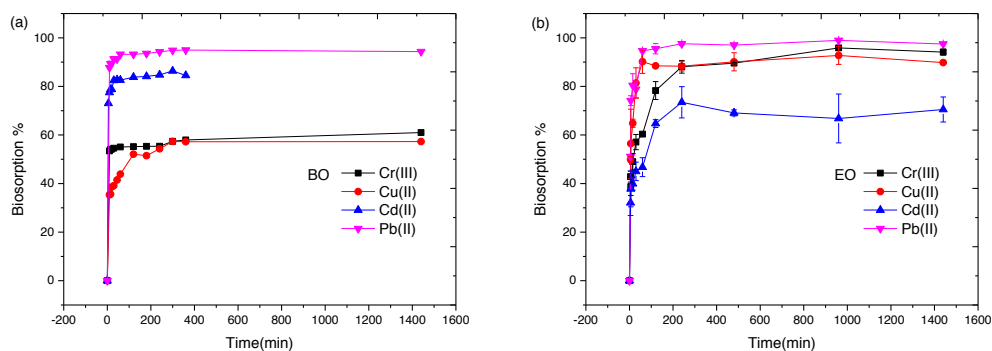


Figure 3.4 Biosorption of heavy metals in multiple system by different biosorbents against time: (a) Canola, (b) Rice, (c) Banana peel, (d) Coffee shell, (e) Poplar, (f) Corn, (g) Pine, and (h) Sludge. Initial 2.5 mL of aqueous solutions concentration are 0.18 mmol/L for each element, pH =4.0, same amount of 25 mg of biosorbents used, at T=25.0 °C.

In single systems (shown in Figure 3.5), only BO, EO, CO, ZO and FO are checked to analyse the effect of contact time, as examples. In general, BO, CO, ZO and FO have been shown to be more effective in single systems comparing their behaviour in multiple system. This can be explained due to a less competition between heavy metals for occupying biosorption sites on the surface of biosorbents. On the other hand, biosorption equilibrium is reached within 6 hours for all metal ions in all systems.



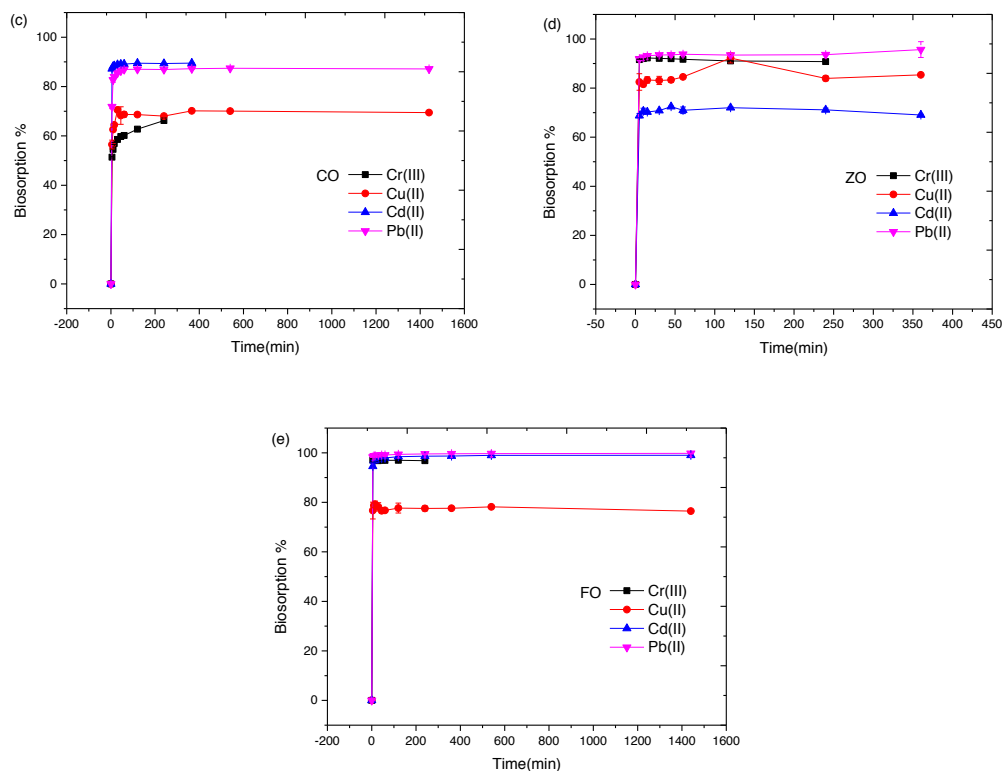


Figure 3.5 Biosorption of heavy metals in single systems by different biosorbents against time: (a) Banana peel, (b) Coffee shell, (c) Poplar, (d) Corn, and (e) Sludge. Initial 2.5 mL of aqueous solutions concentration are 0.18 mmol/L for each element, pH =4.0, same amount of 25 mg of biosorbents used, at $T=25.0^{\circ}\text{C}$.

In addition, as can be deduced from Figures 3.4 and 3.5, EO, CO, ZO, and PO show some selectivity to these four heavy metals, and the biosorption sequence follows as: $\text{Pb(II)} > \text{Cr(III)} > \text{Cd(II)} > \text{Cu(II)}$. In particular, LO, RO and BO show high selectivity of Cd(II) compared with other biosorbents. The biosorption capacity (see Equation [2] in Chapter 2, Section 2.4.1) in multiple heavy metal systems is compared in Table 3.1 for the biomasses here studied, including other previous works of our research group (cork and coffee grounds), and working under the same biosorption experimental conditions. As show in Table 3.1, BO, LO and RO have better biosorption capacities for heavy metal ions than the other biomasses. It is worth noting that BO, LO and RO adsorbents show higher adsorption capacity of Cd, with $14.3 \mu\text{mol/g}$, 10.5 mmol/g and 6.7 mmol/g , respectively. Our study show lower removal percentage in most biomass residues, which limited the application of these materials in multiple wastewater systems. The better selectivity for Cd in our study indicates that these three biomass residues (BO, RO, LO) are potential biosorbents for heavy metals removal from multiple systems.

Table 3.2 Adsorption capacities of metal ions with different biosorbents from the same initial heavy metal concentration (0.18mmol/L).

adsorbents	Cr(III) q×10 ³ (mmol/g)	Cu(II) q×10 ³ (mmol/g)	Cd(II) q×10 ³ (mmol/g)	Pb(II) q×10 ³ (mmol/g)
LO	9.81	9.75	10.5	8.92
RO	7.24	3.78	6.76	8.92
BO	8.67	8.65	14.3	16.1
PO	7.35	4.02	1.48	9.09
CO	9.41	7.04	1.93	7.04
ZO	11.8	10.1	4.87	1.78
EO	2.48	4.61	0.75	20.1
SO	2.46	3.41	0.515	9.59
cork	7.98	5.92	2.53	11.5
coffee grounds	3.48	7.10	0.143	10.8

To understand the different biosorption behaviour in multiple systems, kinetic analysis is performed. Kinetics modelling can help to explain the obtained results and to obtain information about the mechanisms of heavy metal biosorption onto biomass.

In the following sections, from kinetics to isotherm modelling, only data from banana peel (BO, Brazil collaboration) and from canola and rice (RO and LO, respectively, China collaboration) can be found. About the information related to the rest of biomasses, such as poplar (CO), corn (ZO), pine (PO), or waste sludge (FO), they will be presented in another section when comparing original biomass biosorption behaviour with the corresponding of their biochar materials (obtained by pyrolysis of the original biomasses).

3.1.4 Biosorption kinetics modeling for banana peel (BO), canola (LO) and rice (RO)

As mentioned, kinetics modelling is presented in biomass groups, as checked separately (as belong to different collaborations, as indicated previously). So, in this section kinetics modelling of BO, LO and RO can be found.

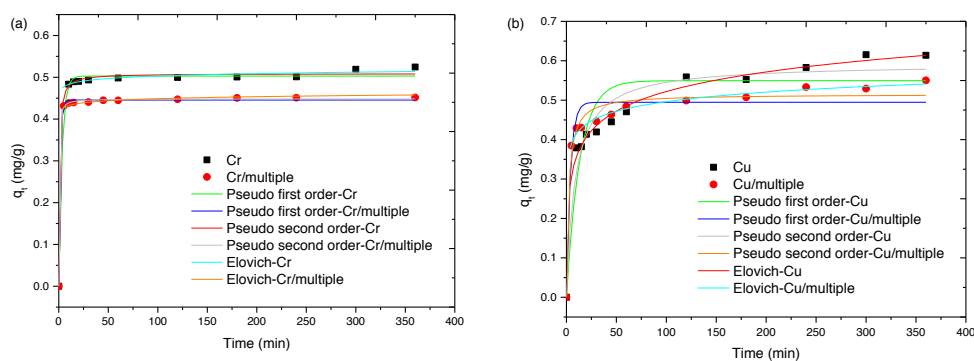
For the kinetics study, the corresponding experimental data are fitted by the pseudo-first-order (PFO), pseudo-second-order (PSO) and Elovich models, which are typically used to describe the adsorption process. The PFO and PSO models assume that the rate of metals adsorbed on the surface of sorbents is proportional to the number of unoccupied sites. PFO model describes a biosorption system controlled by a physical process, whereas PSO describes by a chemical one. The Elovich model often describes

the kinetics of chemisorption as the rate-controlling step, mainly on highly heterogeneous adsorbents, and assuming that the heavy metal adsorption increase exponentially with the adsorption sites, following a multilayer biosorption process. The PFO, PSO and Elovich mathematic model expressions are given in Equations (6), (7) and (8) in the methodology chapter (Chapter 2).

Kinetics modeling of banana peel (BO)

Kinetic models are followed to thoroughly check the rate of the biosorption process and also to propose a potential rate-controlling step for the biosorption of heavy metals by banana peel (BO).

The plots of q_t versus t of each metal (in single and multiple systems) are show in Figure 3.6 and the corresponding constant values are shown in Table 3.2, for all the models checked (PFO, PSO and Elovich). From the data collected in Table 3.2 some information can be highlighted. The correlation coefficients (R^2) values are very low suggesting that the biosorption does not follow the modeling. Both PSO and Elovich models fit well with the experimental data for all metal ions with high correlation coefficients (being $R^2 > 0.950$ and $R^2 > 0.999$, respectively). PFO fit the experimental data well except for the case of Cu in single system with a low correlation coefficient ($R^2 = 0.872$). Therefore, biosorption process of BO is rate-controlled by both physiosorption and chemisorption, and it is followed by a multilayer biosorption due to the heterogeneous surface. SEM images have confirmed the heterogeneous surface that has been shown in BO SEM image (in Figure 3.2). Furthermore, the equilibrium biosorption capacities calculated for Cr(III), Cu(II), Cd(II) and Pb(II) are 9.80, 9.30, 14.3 and 16.2 $\mu\text{mol/g}$ in single system, respectively, and 8.60, 8.10, 13.3 and 15.8 $\mu\text{mol/g}$ in multiple system, respectively (data are from isotherm result of BO).



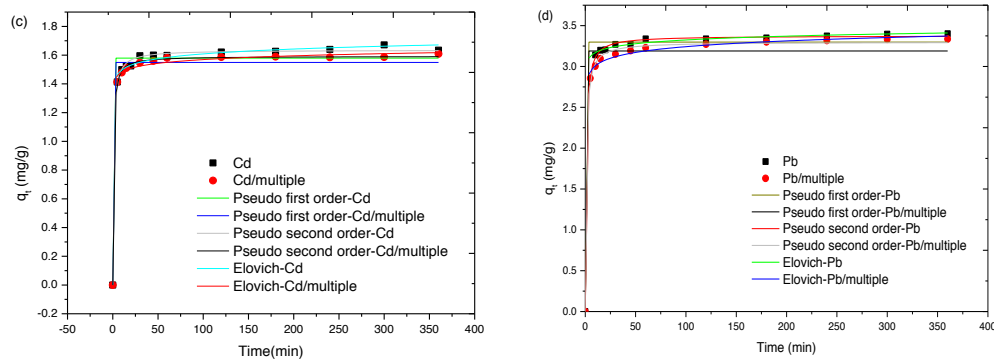


Figure 3.6 Biosorption kinetics modeling of BO for (a) Cr, (b) Cu, (c) Cd, and (d) Pb, all in both single and multiple systems, as a function of biomass capacity (q_t) versus time. Initial 2.5 mL of aqueous solutions concentration are 0.18 mmol/L for each element, pH =4.0, same amount of 25 mg of biosorbents used, at T=25.0°C.

Table 3.3 Biosorption kinetic constant values for the Cr(III), Cu(II), Cd(II) and Pb(II) by BO, all in both single and multiple systems.

BO	Experim	PFO				PSO			Elovich		
	ental										
	$q_{exp} \times 10^3$	k_1	$q_1 \times 10^3$	R^2	$k_2 \times 10^3$	$q_2 \times 10^3$	R^2	α	β	R^2	
	(mmol/g)	(min^{-1})	(mmol/g)		(g/mmol min)	(mmol/g)					
Cr(III)	10.6	0.307	9.67	0.995	4.17	9.79	0.997	3.5×10^{21}	117	0.998	
Cr(III)/Mult	8.85	0.684	8.56	0.999	7.77	8.62	0.999	3.8×10^{23}	142	0.999	
Cu(II)	9.65	0.0750	8.59	0.873	0.37	9.27	0.952	1.0	13.9	0.992	
Cu(II)/Multi	8.75	0.256	7.73	0.936	1.00	8.05	0.974	488	28.5	0.997	
Cd(II)	15.2	66600	13.9	0.972	43.5	14.4	0.998	11	20.6	0.997	
Cd(II)/Multi	14.7	2130	13.6	0.983	51.5	13.3	0.999	43	26.5	0.998	
Pb(II)	16.3	11.8	15.9	0.992	218	16.3	0.999	2.5	14.9	1.000	
Pb(II)/Multi	16.3	13.1	15.3	0.973	198	15.9	0.998	7.0×10^{18}	9.80	0.998	

Kinetics modeling of rice (RO) and canola (LO)

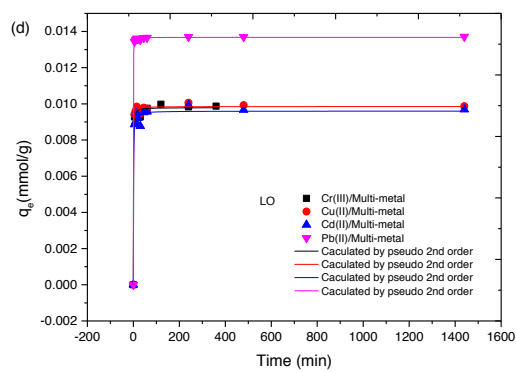
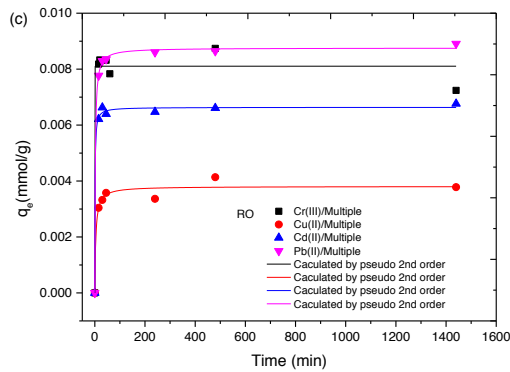
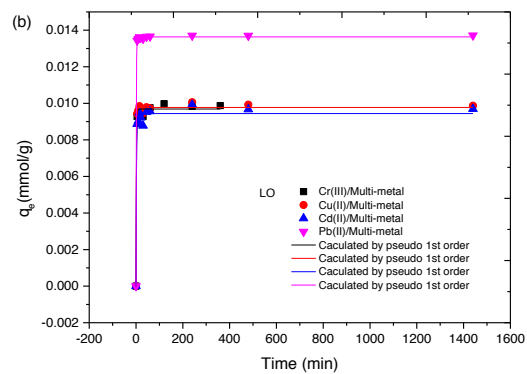
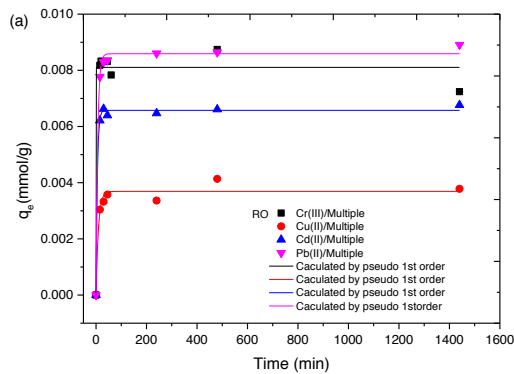
Here, for rice (RO) and canola (LO) biomass, also the same three kinetic models are followed to describe the mechanism of the heavy metals biosorption process. Experimental data for RO and LO are adjusted to the models as it is shown in Figure 3.7, The RO and LO constants values from the kinetic models, such as k_i , q_i , α and the calculated q_e , (experimental adsorption capacity) are listed in Table 3.3, together with the correlation fits of each model (R^2).

The results of RO and LO indicate that PFO, PSO and Elovich equations all fitted well with experimental data for all metal ions with high correlation coefficients ($R^2 > 0.960$). The equilibrium biosorption capacities for Cr(III), Cu(II), Cd(II) and Pb(II) in multiple

system are 8.70, 3.80, 6.70 and 8.90 $\mu\text{mol/g}$ for RO, and 9.90, 9.90, 9.70 and 14.0 $\mu\text{mol/g}$ for LO.

Table 3.4. Biosorption kinetic constant values for Cr(III), Cu(II), Cd(II) and Pb(II) by LO and RO in multiple system.

		Experim ental	PFO			PSO			Elovich		
		$q_{\text{exp}} \times 10^3$ (mmol/g)	k_1 (min^{-1})	$q_1 \times 10^3$ (mmol/ g)	R^2	k_2 (g/mmol min)	$q_2 \times 10^3$ (mmol/g)	R^2	a	b	R^2
Cr(III)	LO	9.90	0.624	9.70	0.995	322	9.80	0.997	7152	3.1×10^{24}	0.998
	RO	8.70	160	8.10	0.972	67.6	3.80	0.972	6063	2787	0.965
Cu(II)	LO	9.90	0.662	9.70	0.997	418	9.80	0.998	11970	7.0×10^{44}	0.998
	RO	3.80	0.107	3.70	0.961	67.6	3.80	0.971	6063	2787	0.968
Cd(II)	LO	9.70	0.543	9.40	0.986	206	9.60	0.991	6306	1.4×10^{20}	0.992
	RO	6.70	0.194	6.60	0.997	168	6.60	0.997	12110	1.2×10^{28}	0.997
Pb(II)	LO	14.0	0.845	14.0	0.999	746	14.0	0.999	8526	5.6×10^{44}	0.999
	RO	8.90	0.153	8.60	0.996	60.2	8.80	0.999	4870	1.1×10^{12}	0.998



Model
Equation
Residual
Chi-Sqr
Adj. R-Square

mix cr
mix cu
mix cd
mix pb

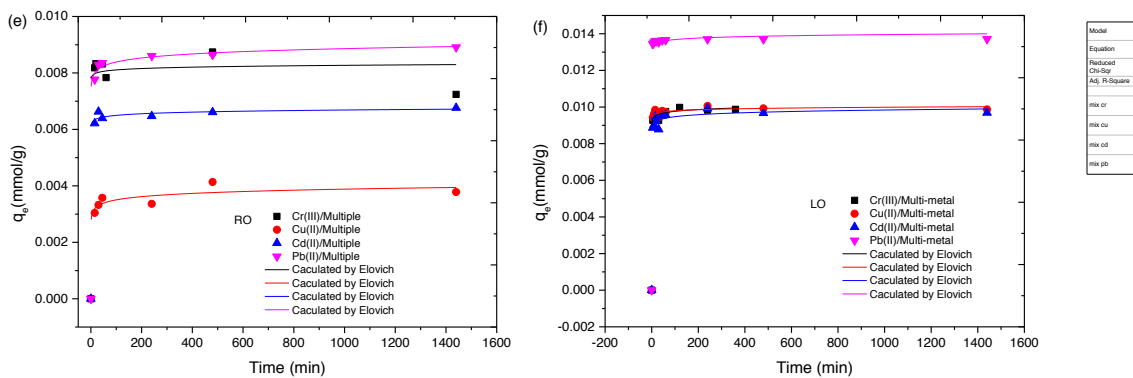


Figure 3.7 Kinetics modeling for Cr(III), Cu(II), Cd(II) and Pb(II) in multiple system by using (a), (c) and (e) RO and (b), (d) and (f) LO, both fitted by PFO, PSO, and Elovich, respectively. Initial 2.5 mL of aqueous solutions concentration are 0.18 mmol/L for each element, pH =4.0, same amount of 25 mg of biosorbents used, at T=25.0°C.

In summary, biosorption process of rice (RO) and canola (LO) are rate-controlled by physisorption and chemisorption, and they follow a multilayer biosorption process, as in the banana peel (BO) case. In addition, a mention should be done to the intraparticle diffusion model that does not fit well for any case. So, all those results mean that the biosorption of heavy metals on the surface of the biosorbent is mainly due to a combination of the physics and chemical interaction between both. Furthermore, it is a multilayer biosorption process.

3.1.5 Influence of the initial heavy metal concentration on biomass systems: rice (RO) and canola (LO)

The effect of the amount of initial concentration onto RO and LO for heavy metals removal in single and multiple systems are checked by varying initial concentration from 0.05 up to 3 mmol/L of each metal ion. From the results shown in Figure 3.8, it can be seen that the adsorption capacity of RO and LO for the heavy metals under study (Pb, Cd, Cu and Cr) increases with the increase of the metal ion initial concentration until reaching a maximum level in both, individual and multiple systems (except for Pb in single system that the maximum capacity of the materials have not been achieved). In multiple systems in general, RO and LO both reach the adsorption maximum capacity for all heavy metals probably due to the competition between them caused by limited adsorption sites on surface of adsorbents. In single systems, LO show potential adsorption ability for Cr, Cu and Pb, and RO only for Pb. Cu and Cr adsorption by RO reaches a maximum adsorption rate, probably related to their lower affinity to the RO site groups. Basically, this result can be explained by the availability

of the adsorption sites on the surface of RO and LO. At low initial concentration, the ratio of surface adsorption sites and heavy metal ion amount is high, hence the metal ions could interact with the adsorbent to occupy the adsorption sites, so they can be removed from the solution. But with the increase in adsorbate concentration of all the heavy metals in the multiple system, there is a competition of occupying adsorption sites, and the number of adsorption sites is not enough to adsorb all heavy metals, which is in agreement with previous works found in the literature^{18,19}.

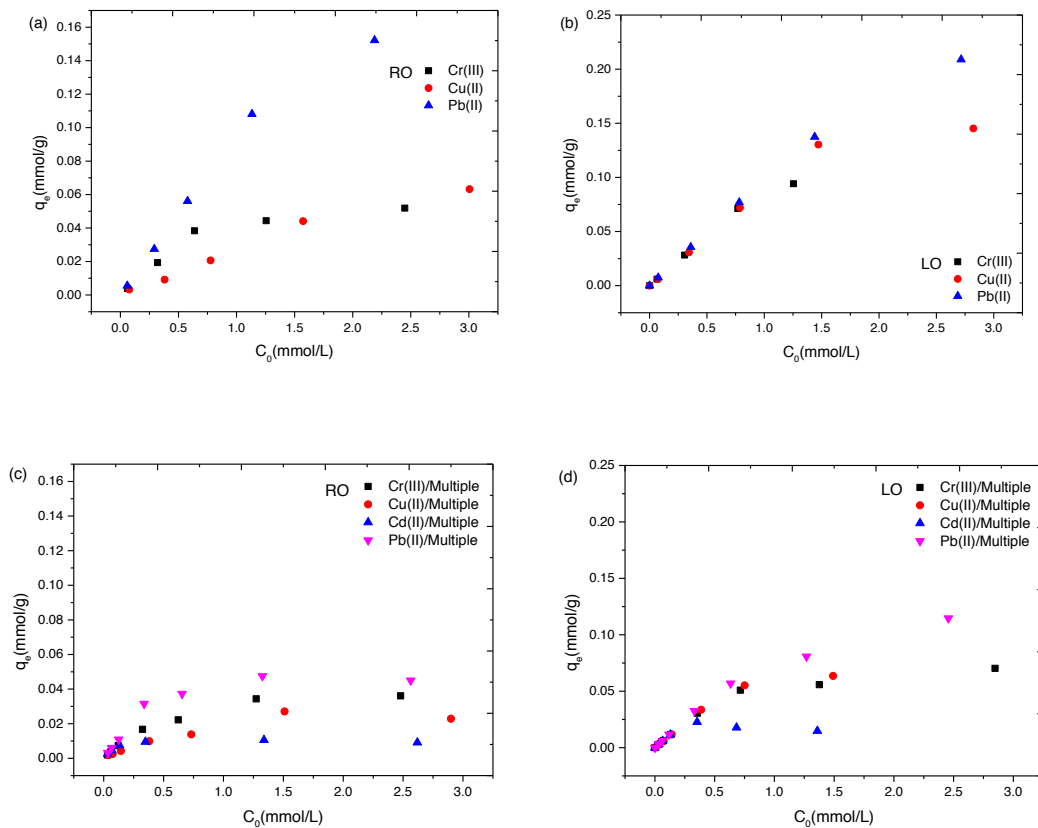


Figure 3.8 Influence of the initial concentration of heavy metals on their adsorption by (a) CO, (b) CL, (c) ZO, (d) ZL, (e) FO and (f) FL in multiple-metal systems. Experimental conditions were $T=25\pm 1^\circ\text{C}$, $\text{pH } 4.0$, 25 mg of adsorbent, 2.5 mL of metals solution and stirring for 24 hours.

3.1.6 Biosorption isotherm modeling for rice (RO) and canola (LO)

To evaluate the maximum biosorption capacity of biosorbents RO and LO, Langmuir and Freundlich isotherm models are here used. The Langmuir and Freundlich isotherm model expressions are given in Equation (6), (7) and (8) in Chapter 2. While the Freundlich is used for modeling the biosorption of metal ions on heterogeneous surfaces and Langmuir is used for modelling the monolayer biosorption process in

homogeneous cases.

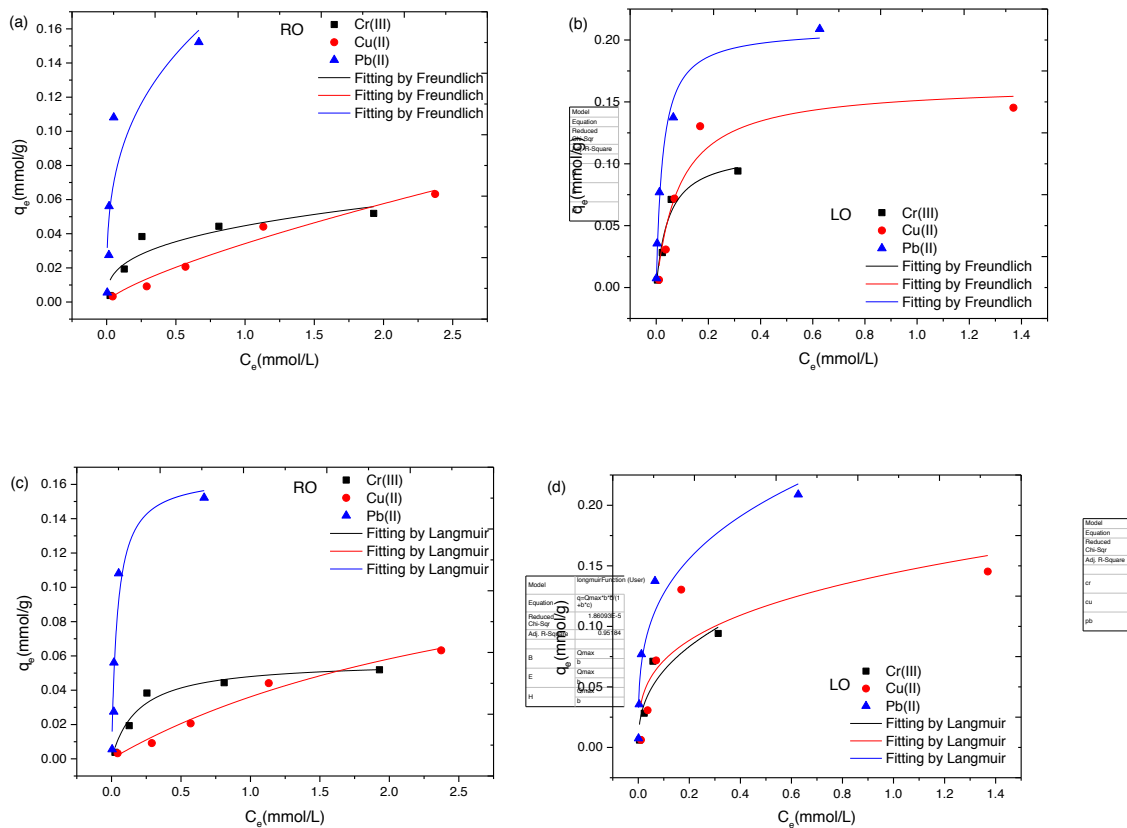


Figure 3.9 Biosorption isotherms of heavy metals in individual-element systems by RO (a) (c) and LO (b) (d) by Freundlich and Langmuir models, respectively. Biosorption conditions are: initial 2.5 mL of aqueous solutions, pH 4.0, and same amount of 25 mg of biosorbents used, at $T=25.0^{\circ}\text{C}$ and stirring for 24h.

The plots of q_t (adsorption capacity) versus C_e (concentration at the equilibrium state) of each metal in individual systems are shown in Figure 3.9, and in the multiple system are presented in Figure 3.10. The corresponding constant values are shown in Table 3.3. The correlation coefficients (R^2) values are very low suggesting that the biosorption does not follow the modeling. R_L is calculated by the Langmuir constant (b) that suggesting a biosorption is favorable or unfavorable. It must lie within 0–1, where $R_L > 1$, $R_L = 1$ and $R_L < 0$ indicate the unfavorable, linear and irreversible biosorption, respectively.

In this study, the Langmuir equation fits the experimental data better than the Freundlich equation in both biosorbent systems (RO and LO). The Freundlich model cannot fit all the experimental data properly, as R^2 values are generally lower than

Langmuir (shown in Table 3.4 and as represented in Figures 3.9 and 3.10). Moreover, Langmuir does not fit well for Cd in multiple system by LO probably due to the competition between all the metal ions (Cd was together with Pb, Cu and Cr), as can be seen in Figure 3.10. In addition, the R_L values are between 0 and 1 for all metal ions in all systems indicates that the biosorption of all the metal ions onto LO and RO are favorable (either in single and multiple systems by LO and RO).

Furthermore, the maximum biosorption capacities for Cr(III), Cu(II) and Pb(II) in single systems by LO are 112, 165 and 210 $\mu\text{mol/g}$, respectively, while by RO are 57.2, 150 and 166 $\mu\text{mol/g}$, respectively. In the case of the multiple system for Cr(III), Cu(II), Cd(II) and Pb(II) those values by LO are 67.2, 72.3, 15.7 and 102 $\mu\text{mol/g}$, respectively, while by RO are 40.9, 30.9, 10.5 and 45.5 $\mu\text{mol/g}$, respectively. All these data is properly collected in Table 3.4. So, as expected from the previous results, RO shows less adsorption maximum capacities than LO for all heavy metals either in single and multiple systems.

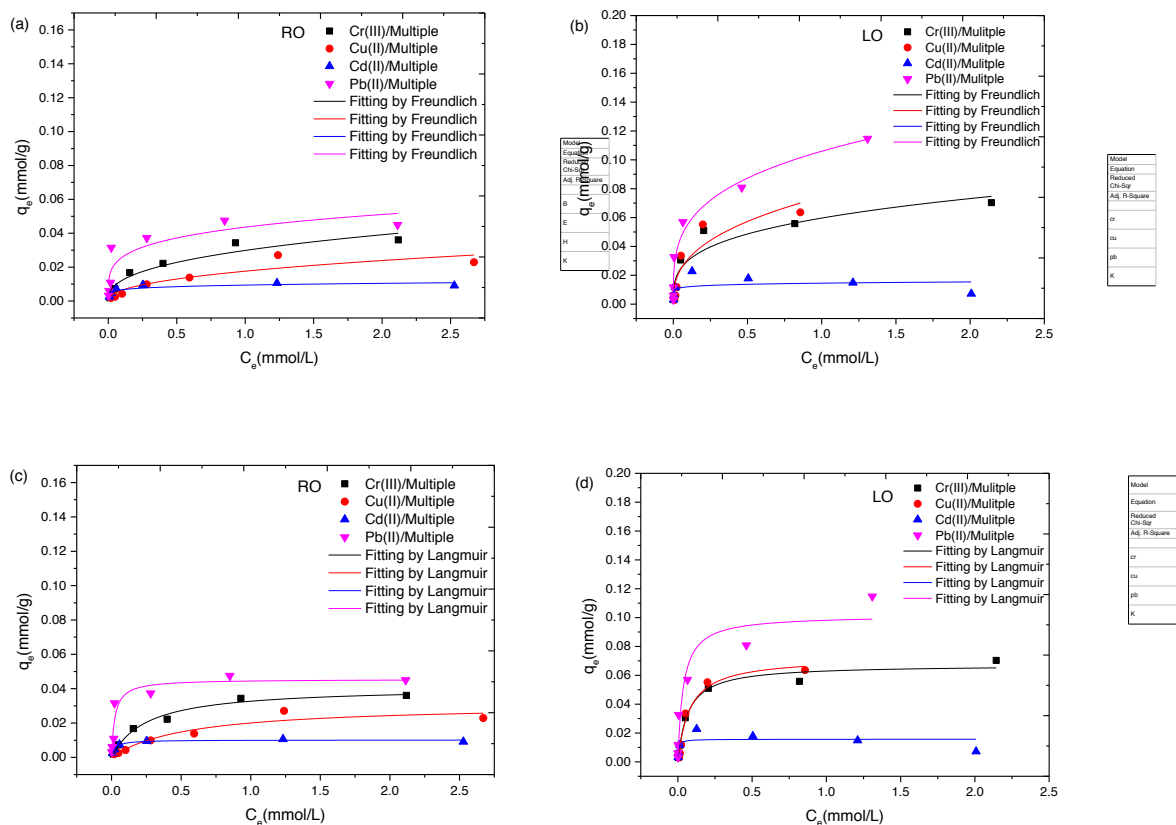


Figure 3.10 Biosorption isotherms of heavy metals in multiple system by RO (a) (c) and LO (b) (d) by Freundlich and Langmuir models, respectively. Biosorption conditions are 25 mg of biosorbent in each case at $T=25.0^{\circ}\text{C}$ and aqueous solution at $\text{pH } 4.0$ and stirring for 24 hours.

Table 3.5 Langmuir and Freundlich isotherm parameters for the biosorption onto LO and RO of Pb, Cu and Cr ions in both individual and multiple systems, and Cd only in multiple system.

		Freundlich			Langmuir			
		K_f (mmol/g)	n	R^2	q_{max} (mmol/g)	b (L/mol)	R^2	R_L
Cr(III)	LO	0.157	0.392	0.796	0.112	21	0.939	0.04
	RO	0.0447	0.339	0.813	0.0572	5.1	0.950	0.07
Cu(II)	LO	0.144	0.303	0.657	0.165	11	0.907	0.03
	RO	0.0342	0.751	0.963	0.150	0.31	0.979	0.5
Pb(II)	LO	0.249	0.292	0.921	0.210	40	0.979	0.02
	RO	0.181	0.321	0.752	0.166	24	0.924	0.02
Cr(III)/Multiple	LO	0.0596	0.295	0.888	0.0672	14	0.963	0.02
	RO	0.0298	0.389	0.923	0.0409	3.9	0.985	0.09
Cu(II)/Multiple	LO	0.0743	0.375	0.801	0.0723	12	0.963	0.2
	RO	0.0176	0.440	0.824	0.0309	1.8	0.909	0.2
Cd(II)/Multiple	LO	0.0145	0.082	0.040	0.0157	202	0.441	0.002
	RO	0.00940	0.150	0.651	0.0105	42	0.960	0.009
Pb(II)/Multiple	LO	0.106	0.280	0.968	0.102	28	0.886	0.001
	RO	0.0436	0.228	0.764	0.0455	42	0.894	0.01

3.1.7 Influence of the aqueous solution pH for rice (RO), canola (LO) and banana peel (BO)

As can be seen, Figure 3.11 shows the influence of pH onto RO, LO and BO, where it can be seen that LO has better adsorption capacity compared with RO and BO. The adsorption of metal ions increases with the pH increase, up to pH 5.0 (higher pH is not checked to avoid the well-known hydrolysis of the heavy metal ions)²⁰. When pH lower than 3.0, hydronium ion (H_3O^+) concentration increases in the biomass sites (surface ligands). Heavy metal ions are in their predominant cation form at this pH level, so H_3O^+ limits the metal ions interaction and sorption due to their competitiveness and repulsive force²¹. When increasing the pH over pH 3.0, a competition between heavy metals is also found in all biomasses in the multiple system, as shown in Figure 3.11.

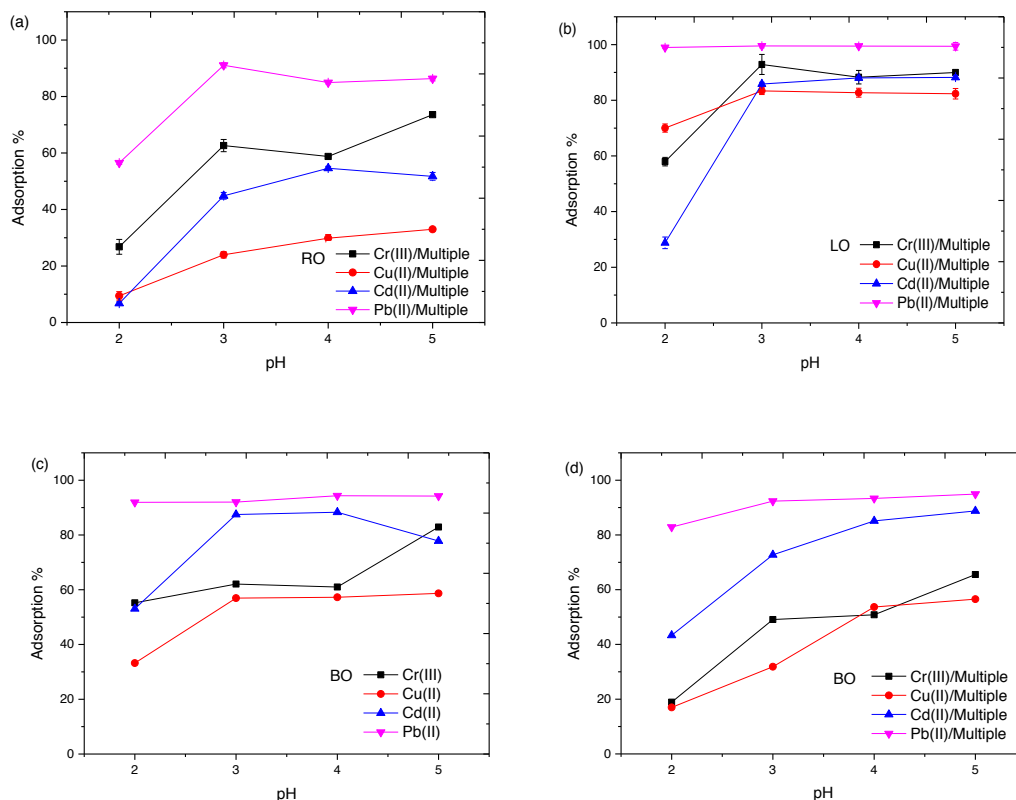


Figure 3.11 Influence of the solution pH on the biosorption for individual heavy metal ion systems by BO, and for multiple system (containing Cr(III), Cu(II), Cd(II) and Pb(II)) by BO, RO and LO. Biosorption conditions are at $T=25.0^{\circ}\text{C}$, 25 mg of adsorbent, initial concentration of 2.5 mL solution is 0.18 mmol/L, and stirring during 24h.

So, the adsorption sequence by all, BO, RO and LO at pH over 3.0 is ranked as follows: Pb(II) > Cr(III) > Cd(II) > Cu(II). We can consider that many real waters have a pH value over 5.0, even the heavy metal cations start to probably hydrolyze and precipitate in real systems. So, to totally avoid this hydrolysis and to be able to characterize the biosorption systems under study, pH 4.0 is chosen as the optimized value in the following biosorption experiments.

3.1.8 Influence of the temperature with BO

To study the influence of the temperature, biosorption experiments by using BO as the adsorbent are performed at four different temperatures (25, 40, 55 and 70°C). The experimental results in both single and multiple systems are presented in Figure 3.12.

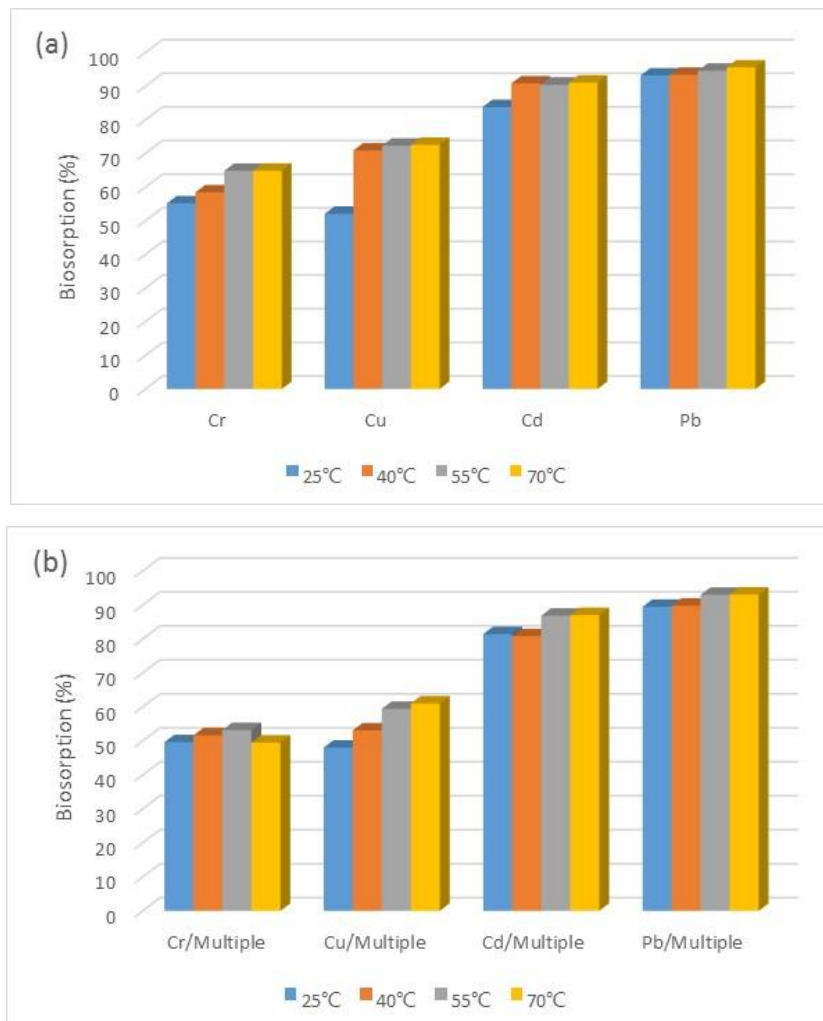


Figure 3.12 Influence of the temperature on the biosorption by BO in both (a) single system, and (b) multiple system. Biosorption conditions were 25 mg of biosorbent, pH 4.0, initial concentration of 2.5 mL solution is 0.18 mmol/L, and stirring for 24h.

As seen, the heavy metal biosorption percentage of BO does not change much with the increase of the temperature. Only for the single system of Cu there is a significant difference with the temperature from 25 to 40°C. This indicates that the biosorption of metal ions onto BO is not endothermic in nature. Similarly it is found in the literature²². Therefore, the same behaviour is expected for the other biomasses under study.

3.1.9 Thermodynamic parameters for rice (RO) and canola (LO)

The Gibbs free energy is used to describe the degree of spontaneity of the biosorption process. It is assumed that a more energetically favorable biosorption deals with a higher negative Gibbs free energy value. It can be evaluated using Langmuir constants calculated by Equation (9) (as presented in Chapter 2, Section 2.3.4).

The standard Gibb's free energy (G_0) values for RO and LO of each heavy metal in the

multiple metal system are listed in Table 3.5. The negative values ΔG^0 suggested that the biosorption of these metal ions onto RO and LO are spontaneous processes and thermodynamically favorable under the experimental conditions.

Table 3.6 the Gibbs free energy of LO and RO in multiple system.

Biosorbent	Metal ion	b	ΔG^0 J/mol
LO	Cr(III)/Multiple	14.9	-6695
	Cu(II)/Multiple	12.6	-6279
	Cd(II)/Multiple	202	-13160
	Pb(II)/Multiple	28.0	-8254
RO	Cr(III)/Multiple	3.97	-3414
	Cu(II)/Multiple	1.80	-1493
	Cd(II)/Multiple	42.3	-9279
	Pb(II)/Multiple	42.1	-9264

3.1.10 Summary

This part sets out to apply waste biomass as biosorbent for heavy metal removal from single and multiple systems. Eight biomasses have been chosen to compare the biosorption efficiency, namely, rice, canola, corn, coffee shell, banana peel (from agriculture waste), poplar, pine (from wood biomass) and sludge (from industry sludge waste).

Characterization of the biosorbents including SEM and ATR-FTIR were performed for all biomasses to study their morphology and metal binding groups. The morphological structures are different depending on the groups of biomass residues. RO present a typical structure of lignin. It is also clearly shown that LO has a bigger mesoporous diameter, which probably is a key factor that can influence its high sorption capacity for the heavy metals onto this biomass. The surfaces of BO and EO are not flat and many grooves are present on them, which probably is a key factor that can influence the sorption of heavy metals onto those biomass. The ATR-FTIR result show that carboxyl group present in all biomasses which is assigned to be the main responsible for heavy metals biosorption, as reported elsewhere^{23,24}. In addition, the concentration of metals loaded onto biomasses does not affect the ATR-FTIR spectra of the functional groups for the biomass of poplar (CO). The same behaviour is expected for the rest of biomasses.

BO, RO and LO have better biosorption of metal ions than other biomasses. It is worth noting that BO, RO and LO adsorbents show higher adsorption capacity for Cd, which is the one with lower biosorption capacities in the rest of the checked biomasses. This better selectivity for Cd in our study indicates that these three biomass wastes are potential biosorbents for heavy metals removal in multiple systems.

So, different parameters of biosorption processes for these three biomass systems (BO, RO and LO) are optimized in batch systems, including the pH of the solution, the initial concentration, the contact time and the temperature. BO, RO and LO show better biosorption capacity efficiency in single systems than multiple one that can be related to the metal ions competition in solution for the biomasses surface site groups. Biosorption equilibrium is reached within 5-6 hours for all metal ions in both systems. Then 24 h is chosen as a proper time for the rest of the biomass systems.

The biosorption capacity of biomasses increases with the pH increase, and the lowest metal biosorption is found at pH 2. At lower pH, hydronium ions (H_3O^+) on surface site

groups (ligands) limit cations sorption due to their repulsive force and competition. At pH over 4, possible hydrolysis of heavy metal cations is expected followed by their precipitation. Therefore, pH 4 is chosen as the optimized value in the following studies.

The experimental results with the influence of the temperature show that the biosorption percentage of BO do not increases with the increase of temperature. This indicates that the biosorption of metal ions onto BO is not endothermic in nature. So the same behaviour is expected for the other biomasses under study.

Kinetics modelling is performed to better understand the biosorption process, including the pseudo-first order, the pseudo-second order, the Elovich model and intraparticle diffusion models to fit the experimental data. The kinetics modelling results show that BO, RO and LO are rate-controlled by physisorption and chemisorption mechanisms, and also that in the three cases is a multilayer biosorption process.

Isotherm modeling, including Langmuir and Freundlich models, is also checked. The Langmuir model fits the experimental data better than the Freundlich one in both systems for RO and LO. R_L values show that biosorption of metals onto RO and LO are favorable.

Furthermore, the equilibrium biosorption capacities for Cr(III), Cu(II) and Pb(II) in single systems by RO are 57.2, 150 and 166 $\mu\text{mol/g}$, respectively, while by LO are 112, 165 and 210 $\mu\text{mol/g}$, respectively as show in isotherm curves (Figure 3.9). In the case of the multiple system for Cr(III), Cu(II), Cd(II) and Pb(II) those values by RO are 40.9, 30.9, 10.5 and 45.5 $\mu\text{mol/g}$, respectively, while by LO are 67.2, 72.3, 15.7 and 102 $\mu\text{mol/g}$, respectively (Figure 3.10). So, as expected from the previous results, RO shows less adsorption maximum capacities than LO for all heavy metals either in single and multiple systems. as show in isotherm curves curves (show in Figure 3.9 and Fugure 3.10).

3.2 Biosorption of heavy metals by biochar systems

In the previous section, different biomass residues have been checked in both single and multiple systems. Different biosorption capacities have been found depending on the group type of biomasses (agricultural wastes, wood industry wastes, sludge industry waste). Besides, biosorption efficiency decreased in a multiple system due to the metal ions competition for biosorption sites.

Biochar has proven to be effective in the removal of heavy metal contaminants from wastewaters due to its specific properties, such as a large surface area, a porous structure, surface-enriched functional groups and the presence of some mineral components^{25,26}. So, biochar is regarded as a promising material due to its characteristics that can improve the biosorption capacity of the original biomass, even in multiple heavy metal systems.

In this part, Pine (PO), Corn (ZO), Poplar (CO) and sludge (FO) wastes will be here properly characterized (as done for the previous cases BO, RO and LO). As there is an interest in this part of the study on biochar systems, those biomasses will be properly pyrolyzed to obtain their biochars products, such as PL (from pine), ZL (from corn), CL and CR (both from poplar) and FL (from sludge). Different pyrolysis procedures are followed at different temperatures and times for each case. In Chapter 2, Section 2.2.1, the pyrolysis conditions and the biochar obtained are collected in Table 1 and Table 2, respectively.

Both biomasses and their corresponding biochar systems are here checked for single and multiple heavy metal removal from waste waters.

As previously followed for biomasses, characterization of biochars by ATR-FTIR and SEM analysis are performed to study their structures, morphology, metal binding groups, and compositions, and compared with the information previously obtained for related biomasses (results presented in Section 3.3). The kinetics modelling is also performed for biomasses and biochars to better understand the biosorption process in each biomaterial case. Kinetics modeling including the pseudo-first order, the pseudo-second order, the Elovich model and the intraparticle diffusion model are also analyzed to fit the experimental data. Biosorption capacity are compared in multiple system of 100 ppm, which is composed by Cr(III), Cu(II), Cd(II) and Pb(II).

3.2.1 Comparison biosorption percentage of poplar, corn and sludge system

Firstly, CO, CL, CR, ZO, ZL, FO and FL are evaluated as biosorbents for the removal of heavy metals from a multiple metal aqueous solution systems composed of the previous selected four metal ions Cr(III), Cu(II), Cd(II), and Pb(II). The results are shown in Figure 3.13. These biosorbents show different biosorption efficiency for the different metal ions.

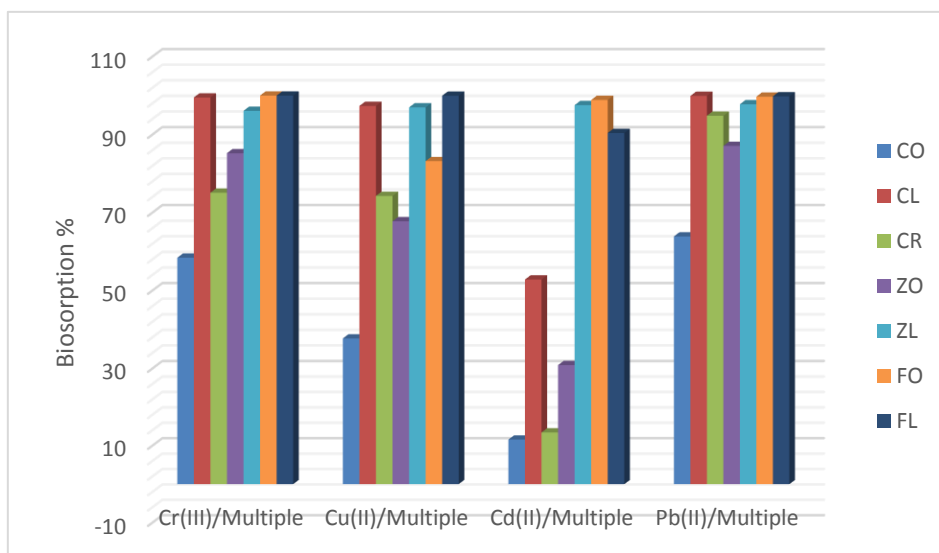


Figure 3.13 Biosorption of metal ions from multiple system containing Cr(III), Cu(II), Cd(II) and Pb(II) by different biosorbents. Initial 2.5 mL of aqueous solutions concentration are 0.18 mmol/L for each element, pH =4.0, same amount of 25 mg of biosorbents used, at T=25.0°C, and stirring for 24h.

In general, for all metals, biochars have better sorption capacities than the original biomass, which can be explained by surface changes during the pyrolysis process, such as changes in porosity, functional groups and mineral content. Based on the literature, high pyrolysis temperatures lead to increased porosity and surface area compared with the original biomaterial. High porosity and large surface areas can increase the adsorption of metals²⁷. High temperature of pyrolysis also increases the concentration of minerals (K, Ca, Mg and P) on the surface of sorbents that can be used for ion exchange with heavy metals²⁷⁻²⁹. Minerals from biomass are not burned, so the pyrolysis process acts as a mineral pre-concentration step (as can be seen from mineral content information collected in Table 3.7).

Table 3.7 Physicochemical properties of CL, ZL and FL.

	CL wood	ZL corn	FL sewage sludge
Components	Cellulose (50%), Hemicellulose (25-35%) Lignin (15-25%),	Cellulose/glucan (37%), Xylan (21%) Lignin (18%)	Carbon (50-70 %), Hydrogen (6-7.3 %), Oxygen (21-24 %), Nitrogen (15-18 %),
Temperature	500-550 °C	400-500 °C	500-550 °C
pH	8.2	10	8.7 (FO 7.9)
H/C*	0.026	0.29 (ZO 1.7)	0.054 (FO 0.17)
O/C*	0.15	0.090 (ZO 0.74)	0.22 (FO 2.5)
K g/kg	6.6	23 (ZO 9.4)	9.1 (FO 4.1)
Ca g/kg	9.6	2.6 (ZO 0.22)	89 (FO 41)
Mg g/kg	1.3	1.2 (ZO 0.15)	12 (FO 5.5)
P g/kg	2.0	1.8 (ZO 0.20)	51 (FO 24)

*H/C and O/C values are the molar ratio.

The adsorption percentages according to the type of feedstock are ranked as follows: sewage sludge (FO) >> agriculture waste biomass (ZO) >> wood biomass (CO). This ranking can be explained by the different mineral compositions and by the functional groups present in the biomaterials surfaces, which is confirmed by the measured adsorption capacity (see Figure 3.13 and Figure 3.21). Concentration of minerals on ZO and FO are all increased after pyrolysis process, with 23 g/kg of K, 2.6 g/kg of Ca, 1.2 g/kg of Mg and 1.8 g/kg of P for ZL, which is much higher than ZO (with 9.4g/kg of K, 0.22 g/kg of Ca, 0.15 g/kg of Mg and 0.20 g/kg of P). Whereas FL only increases the mineral content about two or three times than FO, probably due to the difference type of biomass, in which less organic components are present comparing with plant biomass (FO being a mixed material of inorganic and organic content, as mentioned previously).

Furthermore, the higher mineral content in ZL and FL can provide more opportunities to adsorb heavy metals from wastewaters than original biomass systems (ZO and FO, respectively), which can explain the biosorption results (ZL>ZO), as shown in Figure 3.13. Therefore, this behaviour illustrates the importance of mineral composition in the biosorption process.

3.2.2 Characterization of poplar (CO/CL/CR), corn (ZO/ZL) and sewage sludge (FO/FL)

3.2.2.1 SEM characterization

Biosorbents from poplar system (CO/CL/CR)

SEM is used to study the morphological structure of the CO biomass and its biochars (CL, CR). As shown in Figure 3.14, biochars CL and CR show more porous structures than CO. Thus, this information together with poplar biosorption data collected in Figure 3.14 demonstrates that pore structure is a key factor that can influence the biosorption of heavy metals onto biomass/biochar. Additionally, biochar yield decreases as pyrolysis temperature increases (from 100 to 500°C), however the decrease diminished at temperatures from 500 to 700°C, due to the loss of the volatile components that had been removed at lower temperatures³⁰. The content of H, N, and O in biochars all decreased with increasing pyrolysis temperature due to the loss of the volatile component and dehydration of organic compounds. Correspondingly, H/C and O/C of the CL decreased with increasing production temperature (Table 3.7), suggesting the surface of CL is more aromatic and less hydrophilic³¹.

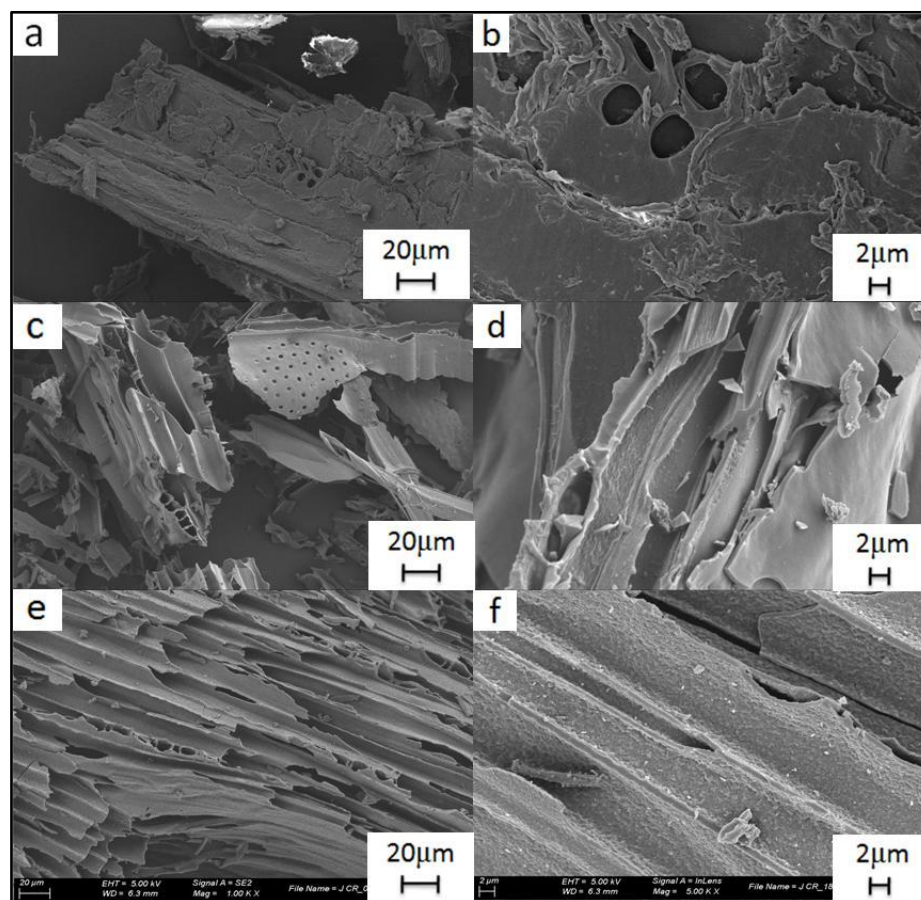


Figure 3.14 SEM images of the biosorbents: (a) and (b) correspond to the CO, (c) and (d) correspond to CL, (e) and (f) correspond to CR, all in two different magnifications.

Biosorbents from corn (ZO/ZL) and sewage sludge (FO/FL)

The most commonly used feedstock to produce biochar is agricultural waste, such as corn, rice, fruit peels, and wood from forests (as poplar presented in section 3.2.1). In addition, biochar derived from original materials, such as daily manure, wastewaters sludge and micro algae, has also been studied in the last decade^{32–34}.

The SEM image analysis of corn (ZO), sewage sludge (FO) and their biochars (ZL and FL, respectively) is shown in Figure 3.15. As can be seen, ZL shows more pore structure than ZO. In contrast, FL do not have much changes in porosity compared with the original biomass FO. As it has been discussed in a previous section (Section 3.2.1), the higher porosity and the larger pore size of biochars is a key point will positively affect the biosorption capacity. In the case of FL, it can be found that porosity does not play an important role in biosorption process, not different at the original biomass (FO).

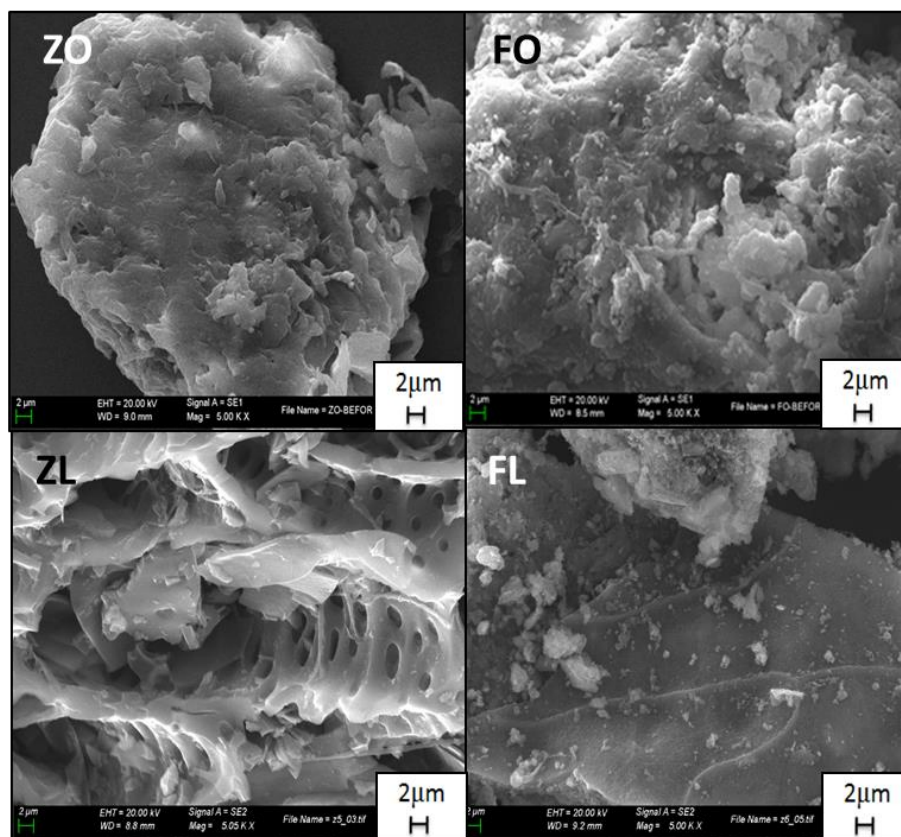


Figure 3.15 SEM images of ZO and FO biomasses, and their biochar products ZL and FL.

3.2.2.2 ATR-FTIR characterization

Biosorbents from poplar (CO/CL/CR)

The ATR-FTIR spectra of the adsorbents are shown in Figure 3.16. As we mentioned before, carboxyl and hydroxyl groups are involved for heavy metal removal. Furthermore, the peak at 1575 cm^{-1} that appears in each ATR-FTIR spectrum of CO, CL and CR, representing aromatic carbon. The peaks at 1025 cm^{-1} are attributable to the stretching of C-O bonds. A fingerprint region between $800\text{--}1800\text{ cm}^{-1}$ is observed for CO, which are mainly from the cellulose, hemicellulose and lignin. Additionally, CO when is decomposed at the higher temperature pyrolysis program (see Chapter 2, Section 2.2.1, Table 2.1), a more active aromatic structure is formed producing CL biochar, resulting in the disappearance of the peaks between 800 and 1800 cm^{-1} and the appearance of peaks representing aromatic C-C stretching peak at 816 cm^{-1} for CL. There is not aromatic peak in CR probably due to the difference of pyrolysis time as CR cannot fully pyrolyse CO in 2 seconds. All the wavenumbers are summarized in Table 3.7.

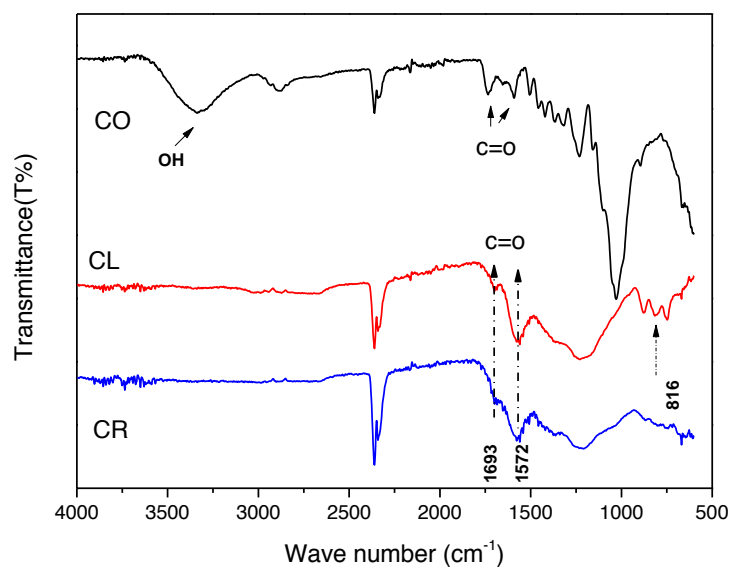


Figure.3.16 ATR-FTIR spectra of CO, CL, and CR.

Table 3.8 ATR-FTIR spectra bands assignments for CO, CL and CR before use.

Wave Number (cm ⁻¹)	Assignments	Compounds	Band positions (cm ⁻¹)		
			CO	CL	CR
3200-3700	O-H stretching	Acid, methanol	3323	-	-
2700-3000	C-H _n stretching	Alkyl, aliphatic	2886		
1700-1730	C=O stretching	Carboxyl, carbonyl	1730	1693	1693
1450-1600	C=O stretching	Ketone, carbonyl	1684	1572	1572
1000-1200	C=O stretching C-O-C stretching/bending C-N,R-O-C/R-O-CH ₃	Ketone, ether, phenol, chain anhydride	1025		
800		aromatic C-C stretching		816	

Biosorbents from corn (ZO/ZL) and sewage sludge (FO/FL)

ATR-FTIR spectra of ZO, ZL, FO and FL are shown in Figure 3.17. The peaks at 3200-3270 cm⁻¹ and 1780-1600 cm⁻¹ correspond to the O-H and C=O stretching vibrations, respectively, which confirms the presence of carboxyl groups on the original biomass adsorbents (ZO and ZL)³⁵.

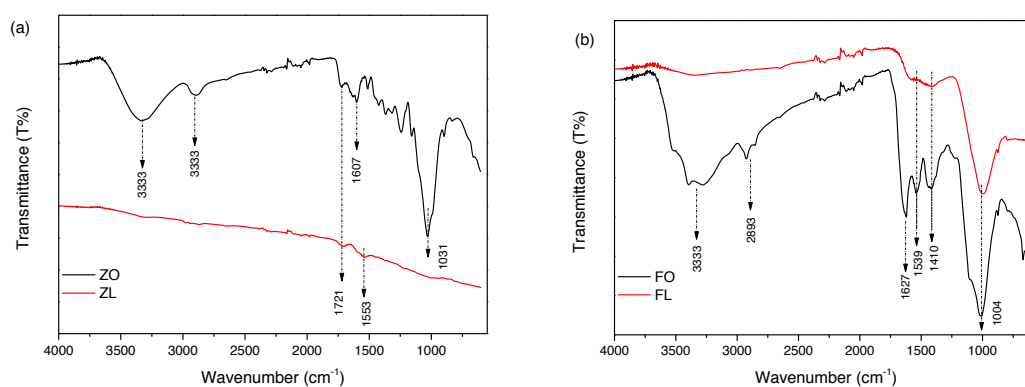


Figure.3.17 ATR-FTIR spectra of a) ZO and ZL, and b) FO and FL.

Carboxyl acid groups are very useful for the adsorption of heavy metal ions and can be found in most of the adsorbents studied here (ZO, ZL), except for FO (sewage sludge) and the corresponding biochar FL (see Figure 3.17b). These differences can be explained by the compositions of ZO, which is cellulose and lignin-based biomass that contain carboxyl groups. However, FO and FL are from industry sewage sludge and their main composition is probably a mix of inorganic and organic content, which show the difference with ZO. Furthermore, a decrease in the intensity of the peaks

corresponding to carboxyl (-COOH) and hydroxyl (-OH) groups is observed in the ATR-FTIR spectra after pyrolysis, probably due to the loss of functional groups in the lignocellulosic materials with increasing temperature. The decrease in the H/C and O/C atomic ratios for biochars (Table 3.7) confirms this hypothesis.

3.2.2.3 Zeta potential

Zeta potential is used to determine the surface charge of the adsorbent. It helps us to understand the biosorption process, especially the influence of functional groups that are present on the biomass and biochar surfaces.

The pH_{zpc} (pH at point of zero charge) of all adsorbents are showed in Figure 3.18. It can be seen that the zeta potential values of biomass (CO, ZO) are more close to the pH_{zpc} value than biochar (CL, ZL), which means less negatively charged than biochar. So the higher negative charge on the surface of biochar is leading to more chance for electrostatic interactions with heavy metal cations. The negative charge values at pH 4 ranked as: ZL > FO > CL > FL > CO > ZO. Therefore, the surface charge increased after the pyrolysis process except the case of FL. So, zeta potential results show (Figure 3.18) that FO has more negative charge than FL that can attract more cation metals, which is corresponding to the biosorption capacities results (shown in Table 3.11). Furthermore, with the rise of solution pH in biochar systems, the dissociation of remaining functional groups increased and thus the ability to form complexes with cation metal ions also increases.

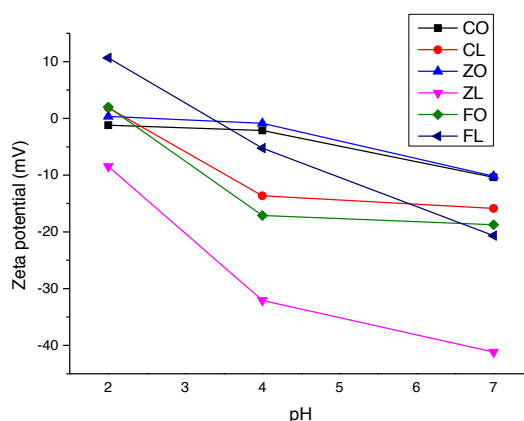


Figure 3.18. Zeta potential values of all adsorbents. For each situation triplicate measurements are performed and each sample is measured 3 times to determine the zeta potential values.

3.2.3 The influence of the contact time

Biosorbents from poplar (CO/CL/CR)

The influence of the contact time between biosorbents (CO, CL, CR) and heavy metal aqueous solution in multiple-metal systems (Cr(III), Cu(II), Cd(II), Pb(II)) are studied. For that purpose, adsorption experiments are performed (as indicated in the experimental section) for different times (from 5 to 1440 minutes) for each biosorbent (Figure 3.19). Biosorption equilibrium is reached at different times for each biosorbents (CO, CL, CR). In the case of CO, the equilibrium time differed as a function of the heavy metal, so the biosorption equilibrium is reached in 5 minutes for Pb(II) and Cd(II), in 1 h for Cu(II), and in 24 h for Cr(III). Additionally, CL reached the equilibrium slowly compared with CO, requiring approximately 8 h for Cr(III), Cu(II) and Pb(II) and at least 24 h for Cd(II). CR is the slowest one to reach the adsorption equilibrium, requiring at least 8 h for all metal ions.

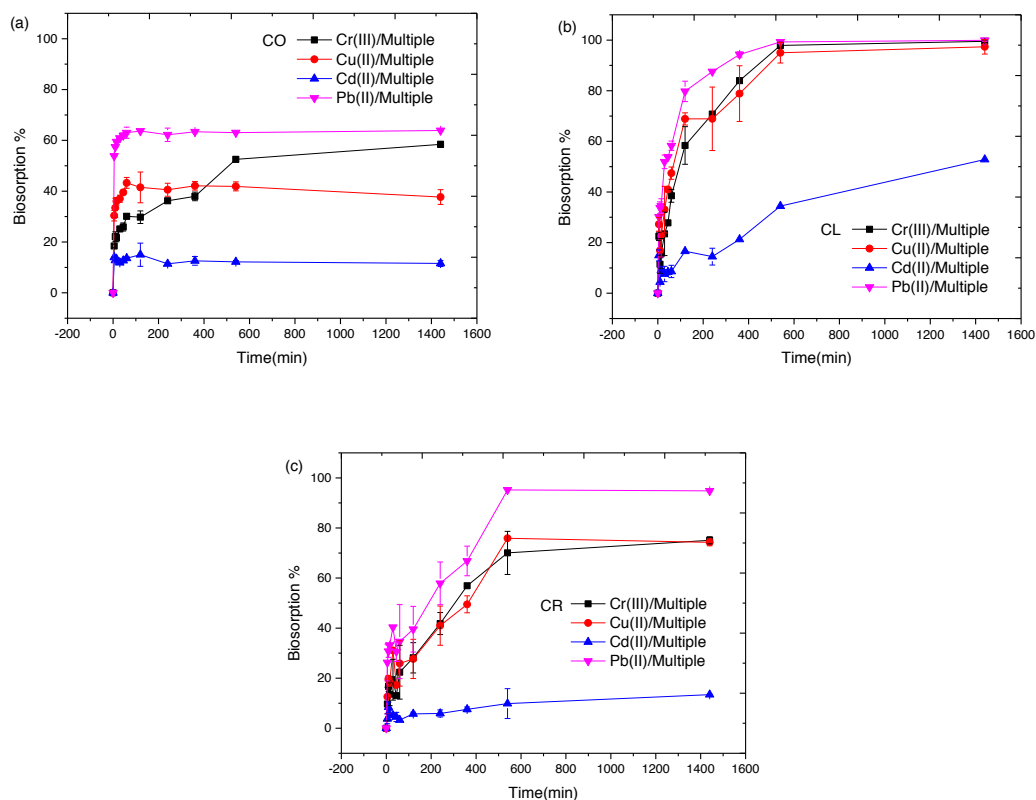


Figure 3.19 Biosorption of heavy metals in multiple system by poplar biomass/biochar system over time: (a) biomass CO, (b) biochar CL, and (c) biochar CR. Initial 2.5 mL of aqueous solutions concentration are 0.18 mmol/L for each element, pH =4.0, same amount of 25 mg of biosorbents used, at T=25.0°C.

Biosorbents from corn (ZO/ZL) and sewage sludge (FO/FL)

The influence of the contact time between biosorbents (ZO, ZL, FO, FL) and heavy metal aqueous solution in multiple-metal systems (Cr(III), Cu(II), Cd(II), Pb(II)) are studied. For that purpose, adsorption experiments are performed as indicated previously (from 5 to 1440 minutes) for each biosorbent (Figure 3.20).

ZO and ZL have both fast biosorption profiles for all metal ions and reached equilibrium in 5 minutes, being ZL more effective than ZO with lower biosorption rates at the equilibrium. On the other hand, biochar from sewage sludge (FL) is less effective than FO (especially for Cd(II)). FL also needed a longer time than FO to reach adsorption equilibrium (approximately 6 h), while FO adsorption of all metals took only 5 minutes (as corn biomass/biochar case). Thus, to ensure the biosorption of all the heavy metals either in multiple system, 24 h is chosen as the optimal contact time for further adsorption experiments.

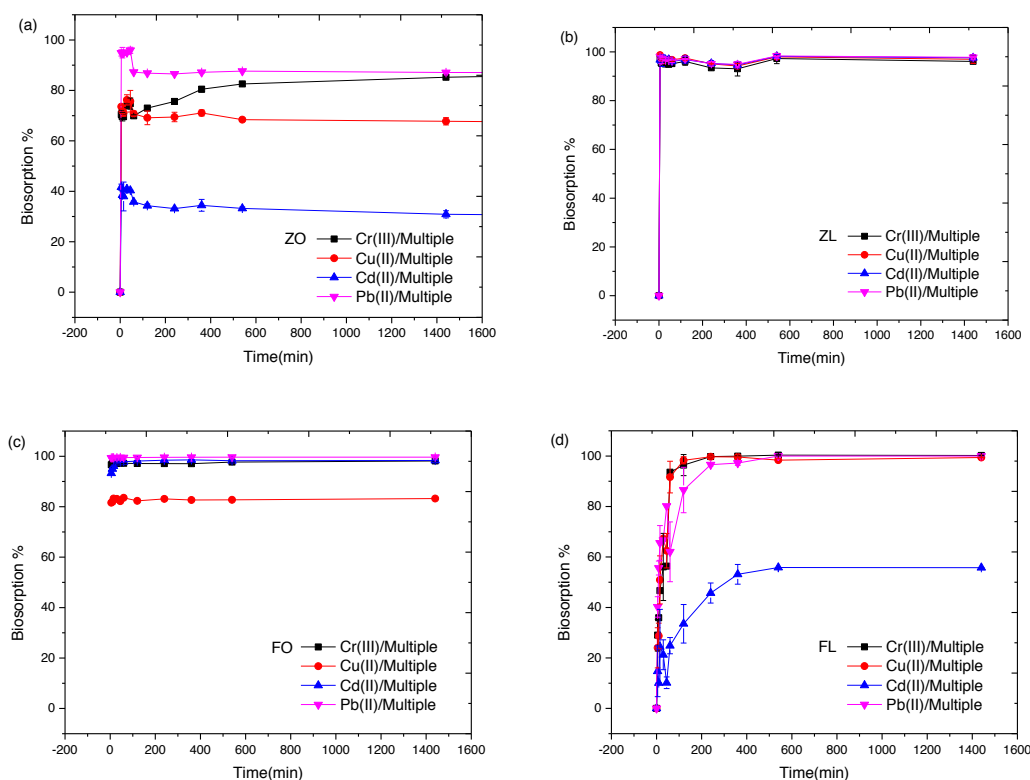


Figure 3.20 Biosorption of heavy metals in multiple system by different biomasses/biochars against time: (a) biomass ZO, (b) biochar ZL, (c) biomass FO and (d) biochar FL. Initial 2.5 mL of aqueous solutions concentration are 0.18 mmol/L for each element, pH =4.0, same amount of 25 mg of biosorbents used, at T=25.0°C.

3.2.4 Kinetic modelling for biomass/biochar systems: poplar (CO/CL), corn (ZO/ZL), and sewage sludge (FO/FL)

To understand the different adsorption behaviour of different biomass/biochar systems for multiple-heavy-metal biosorption, kinetic analysis is performed to find a model that explains the obtained results and to obtain information about the mechanisms of heavy metal adsorption onto biomass and biochar systems.

Two different kinetic models, the pseudo-first-order (PFO) and pseudo-second-order (PSO) models are used to fit the experiment data. In most cases, the PFO equation is linear only approximately the first 30 minutes; therefore, it is appropriate for the initial contact time but not for the whole range³⁶.

Kinetics modelling analysis showed that the biosorption process do not fit well with the PFO model but fit well with the PSO model for all the biosorbents. This result means that the biosorption of heavy metals on the surface of the biosorbents is a rate-controlled system by chemisorption process, such as valence forces sharing or exchanging electrons between the adsorbent and adsorbate. The relative constants found by applying the pseudo-second order model are listed in Table 3.9 only for Pb in the multiple-metal system. Quite high capacities of Pb(II) have been found except in the case of CO, when comparing with other biomaterials checked in this thesis.

Table 3.9 Biosorption kinetic constants of the pseudo-second order model for Pb(II) by CO, CL, ZO, ZL, FO and FL CR in the multiple-metal system.

Pb(II)/Multi-metal	Pseudo-second-order model		
	k_2 (g/mmol min)	q_2 ($\mu\text{mol/g}$)	R^2
CO	0.98	9.20	1.000
CL	0.26	14.7	0.998
ZO	12	12.7	1.000
ZL	0.26	16.7	0.999
FO	5.7	16.7	0.999
FL	0.66	16.5	0.999

3.2.5 Comparison of pine wood systems: biomass (PO) and biochars (PL, PR and PG)

Previous research articles have reported the successful use of different kinds of wood biomass for removal of metal ions from aqueous solution, such as *pine cone* for Cd(II) and Pb(II) with the maximum biosorption capacity of 285.7 and 140.1 $\mu\text{mol/g}$, respectively³⁷. *Pine cone powder* for the removal of Cu(II) and Pb(II) with maximum capacity of 411.1 and 155.8 $\mu\text{mol/g}$, respectively³⁸. Pb(II), Cu(II), and Cd(II) with maximum sorption capacities of 739.6, 534.4, and 250.9 $\mu\text{mol/g}$ by *hickory wood*, respectively³⁹.

Although all of these biomasses show high biosorption capacity, it is important to remark that they are applied in single-element system. It is known that biosorption in multi-element system is decreased due to the competition of heavy metals.

Therefore, it is necessary to find an effective approach for heavy metal removal in multi-element system. Pine wood could be highlighted as a potential material, once among the wood biomass, pine is abundantly grown in the world and the waste is of no market value. Also in the literature, biosorption capacity of pine wood biomass can be increased by using pyrolyzed biomass comparing with the original one.

With this purpose, pine(PO) and three different biochars obtained via different pyrolysis processes (PL, PR, and PG) are used as biosorbents to remove heavy metal from aqueous solution. SEM and ATR-FTIR are carried out to study the morphological structure and the functional groups of biosorbent, which are responsible for the biosorption process. Similar to the previous study, The kinetics and isotherm are checked in both single and multiple heavy metal systems, the initial concentration is also checked. However, the results of PL and PG are not present here due to their low capacity than the original pine wood. About the information related to Pine and PG will be presented in another section when comparing with other biosorbents.

3.2.6 Comparison of biosorption capacity for all biosorbents

In order to compare the adsorption ability, all biomasses and biochars have been checked at the same experiment conditions (Table 3.10). The multiple system is composed by Cr(III), Cu(II), Cd(II) and Pb(II) as usual, and the initial concentration of all is 100 ppm (shown in Figure 3.21). In general, the biochars produced from wood and agriculture waste have higher adsorption capacities than the initial biomasses do.

Moreover, biochar obtained from slow pyrolysis process showed better biosorption behavior than a fast one except for the case of pine biochars (PL and PR). Gasification pyrolysis of pine wood show the highest biosorption capacities, while biochar obtained through slow or fast pyrolysis showed lower biosorption than pine probably due to the loss of functional groups during the pyrolysis process.

The case of sewage sludge (FO) showed that pyrolysis (FL) cannot improve the biosorption capacity probably due to the different biosorption mechanism. As we discussed above, the biosorption mechanism of sewage sludge is through ion exchange. There is an increase in porosity and a pre-concentration of mineral components when during the pyrolysis process, even a lost of volatile compounds reduce the FL efficiency. Therefore, the sludge can be used directly to remove heavy metals without pyrolysis pretreatment, which is a most sustainable application saving the required energy for the pyrolysis process, and lets to cheapest and more eco-friendly system for the removal of heavy metals by biosorption process.

Furthermore, complexation and cation exchange are the two main adsorption mechanisms in multiple-heavy-metal systems, and these mechanisms are influenced by the kind of biomass feedstock and its mineral composition and by the pyrolysis treatment, being more effective the pyrolysis process for agriculture waste than for wood biomass.

Table 3.10 Biosorption capacity of biomass and its biochars in multiple system (100 ppm of each metal ions).

Biosorbent	Cr(III) (mg/g)	Cu(II) (mg/g)	Cd(II) (mg/g)	Pb(II) (mg/g)
CO	1.2	0.90	0.30	1.4
CL	2.5	2.5	0.30	4.2
CR	1.0	1.0	0.60	2.2
ZO	1.9	1.3	0.60	1.7
ZL	5.1	6.5	2.4	7.3
FO	5.9	7.6	6.2	8.8
FL	5.1	6.3	1.2	7.1
PO	0.90	0.7	0.60	0.7
PL	0.50	NA	NA	1.7
PR	NA	NA	NA	1.0
PG	9.3	13	3.4	11

NA means no data

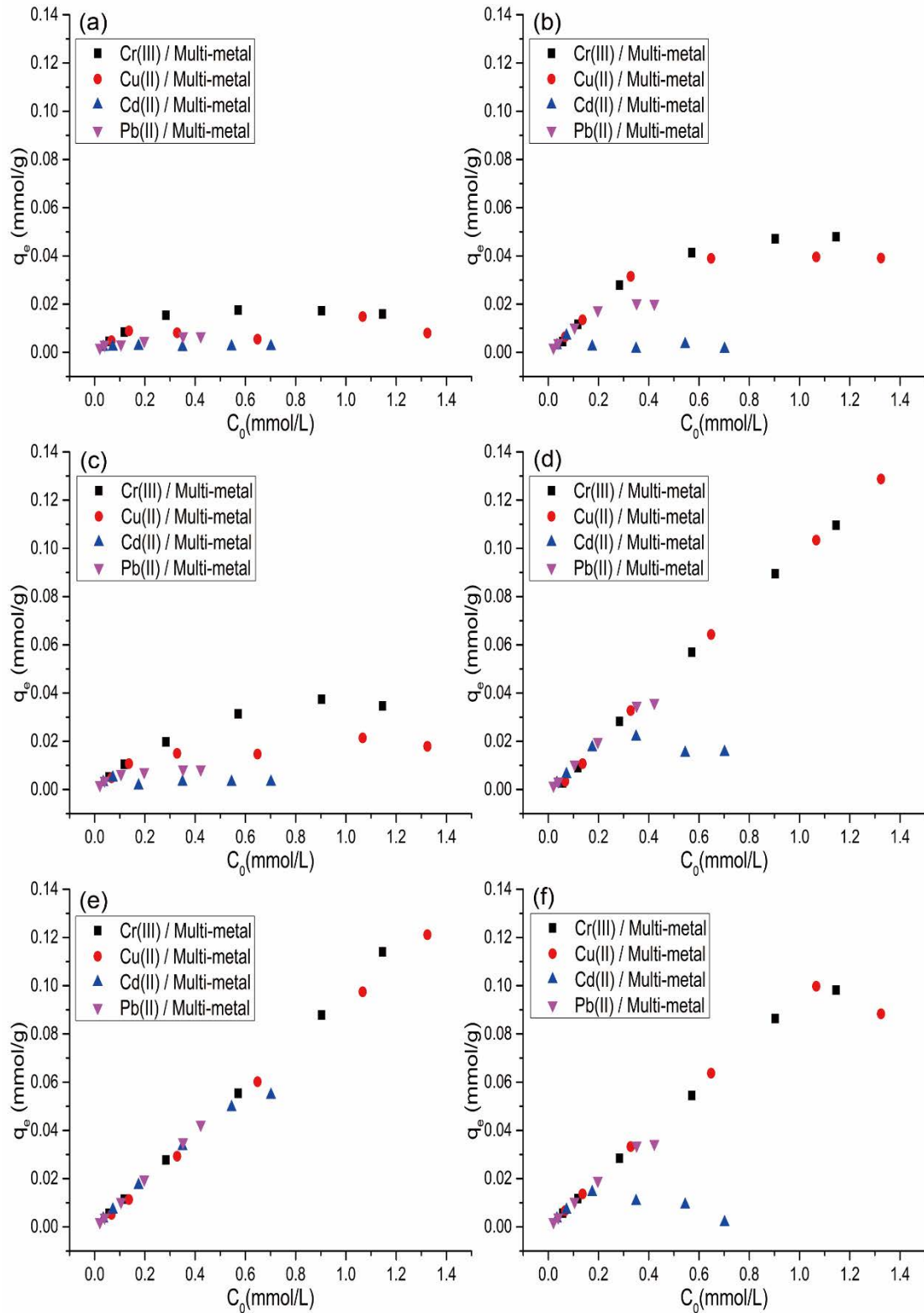


Figure 3.21 Influence of the initial concentration of heavy metals on their adsorption by (a) CO, (b) CL, (c) ZO, (d) ZL, (e) FO and (f) FL in multiple-metal systems. Experimental conditions were $T=25\pm 1^\circ\text{C}$, pH 4.0, 25 mg of adsorbent, 2.5 mL of metals solution and stirring for 24 hours.

3.2.7 Summary

In this part, biomasses such as pine (PO) and poplar (CO) as wood wastes, from agricultural waste corn is here selected (ZO) and sewage sludge (FO) and their biochars obtained by pyrolysis different processes (at different temperatures and times) have been checked and compared for the removal of heavy metals from a multiple metal aqueous solution composed of four metal ions Cr(III), Cu(II), Cd(II), and Pb(II).

In general, biochars products have better sorption capacity than the original biomass for almost all metals, which can be explained by surface changes during the pyrolysis process, such as changes in porosity, functional groups and mineral content.

The biosorption percentages according to the type of feedstock were ranked as follows: sewage sludge (FO) >> agriculture waste biomass (ZO) >> wood biomass (CO). This ranking can be explained by the different mineral compositions and functional site groups present, related analysis confirm by the obtained biosorption capacity. For example, it can be said that the mineral composition in the biosorption process play an important role for biochar behaviour.

Biochars show more porous structures than original biomass. Additionally, biochar yield decreases as production temperature increases, however the decreases diminished at high temperatures (from 500 to 700 °C) due to the loss of the volatile components that had been removed at lower temperatures. The H, N, and O contents in the biochars all decrease with increasing production temperature due to the loss of the volatile component and dehydration of organic compounds. The ATR-FTIR result show that carboxyl group present in all biochars which is responsible for heavy metals biosorption except the case of FL. All biochars show better biosorption capacity efficiency in single system than multiple system due to the metal ions competition in solution. Biosorption equilibrium is reached within 8 hours for all metal ions in both systems. Then 24 h was chosen for the optimize time for all cases.

Kinetics modelling analysis show that the biosorption process do not fit well with the PFO model but fit well with the PSO model for CL, ZL and FL. It is suggested a chemical adsorption process, such as valence forces sharing or exchanging electrons between the adsorbent and adsorbate.

The biosorption capacity of four heavy metals increases while increasing metal initial concentration until reaching the equilibrium in both systems. Biochar reaches

biosorption equilibrium in multiple system due to the biosorption competition caused by limited adsorption sites on the surface of adsorbents.

As a main conclusion, complexation and cation exchange are the two main adsorption mechanisms in multiple-heavy-metal systems, and these mechanisms are influenced by the kind of feedstock and its mineral composition and by the pyrolysis treatment, being more effective for agriculture waste than for wood biomass.

3.3 Biosorption of heavy metals by particles loaded biochar

TiO₂ nanoparticles are a good adsorbent for removing heavy metals due to its large surface and photocatalyst ability under UV condition, but TiO₂ nanoparticles easily aggregate which limited their application. However, once biomass as a holder, the aggregation of TiO₂ could be avoided. In this study, combined wood biomass and TiO₂, a new pretreatment of pine is carried out, by adding Titanium dioxide (TiO₂) before the pyrolysis procedure. It is possible to obtain less aggregation of TiO₂ (less than 1 μm) on the biomass surface.

As indicated, TiO₂ can be used for the removal of heavy metals from waters. Furthermore, lignin composites are now becoming a promising alternative to conventional adsorbents for the removal of heavy metal ions. So, as a combination of both, *Klapiszewska et al* developed the TiO₂/lignin material for the adsorption of Pb(II)⁴⁰. Lignin is the main component in biomass, in this sense, a new pretreatment of biomass combined with TiO₂ and temperature is here performed to check the biosorption ability.

In this part, pine wood (PO), corn (ZO) and sugar cane (SO) agricultural wastes biomass, and their biochars loaded with TiO₂ (Pine/TiO₂, ZO/TiO₂ and SO/TiO₂) have been used as sorbents for the removal of heavy metal ions from aqueous solution. So, TiO₂ nanoparticles are synthesized on this three different biomasses followed the sol-gel method to compare the biosorption capacity with the original biomasses.

A multi-element system composed by a mixture of Cr(III), Cd(II), Cu(II) and Pb(II) ions is used. Biosorption capacity of all those biosorbents (biomass/biochars with TiO₂) is also checked to exploit their potential for heavy metal removal. The corresponding batch experiments are performed in room temperature (25.0 °C) for 24 h, by using a 2.5 mL aqueous solution with the initial heavy metal concentration of 0.18 mmol/L for each element in the multiple system, and with 25 mg of biosorbents. Surface morphology of the biosorbents are also analyzed using scanning electron microscopy (SEM) and chemical functional groups are checked by attenuated reflectance Fourier transform infrared spectroscopy (ATR-FTIR).

3.3.1 Biosorption characteristics for TiO₂ modified biomass: sugar cane (SO, SO/TiO₂), corn (ZO, ZO/TiO₂), and pine (PO, Pine/TiO₂)

First, related results to the systems of sugar cane (SO), corn (ZO) and pine (PO) are here reported. So, the evaluation of the prepared SO/TiO₂, ZO/TiO₂ and Pine/TiO₂ follows.

3.3.1.1 SEM characterization

Sugar cane (SO, SO/TiO₂) and corn (ZO, ZO/TiO₂)

The SEM images from the TiO₂ modified and pyrolyzed biomasses (SO/TiO₂ and ZO/TiO₂) are collected in Figure 3.22. Differences in the morphology of all materials can be seen. Furthermore, the diameter of TiO₂ nanoparticles is able to be checked and found to be in the range of 25 and 70 nm in all cases. TiO₂ aggregate can be found in different sizes, but most of the aggregates are less than 1 μm. The spectra of EDS, corresponding to a semi-quantitative analysis, shows a strong peak of Ti, which confirms the presence of TiO₂ onto the pyrolyzed materials surface.

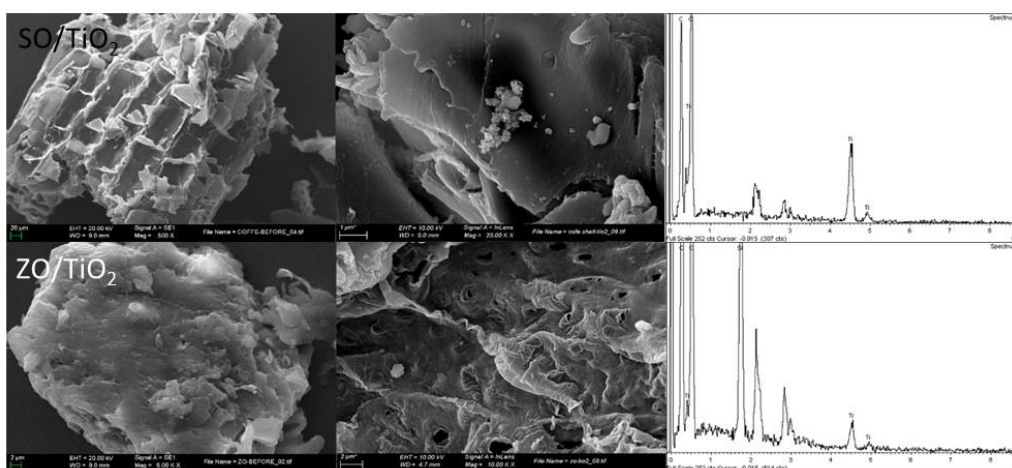


Figure 3.22 SEM images of SO/TiO₂ and ZO/TiO₂.

Pine (PO, Pine/TiO₂)

The SEM images of pine and Pine/TiO₂ show differences in the morphology of both materials. As it can be seen in Figure 3.23 panels (a) and (b), Pine/TiO₂ shows more developed pore structure than bare Pine. The images Figure 3.23 panel (c) exhibits TiO₂ synthesized on the surface of Pine. The pore volume and surface area are ranked as Pine/TiO₂ > pine (shown in Table 3.15 from BET analysis).

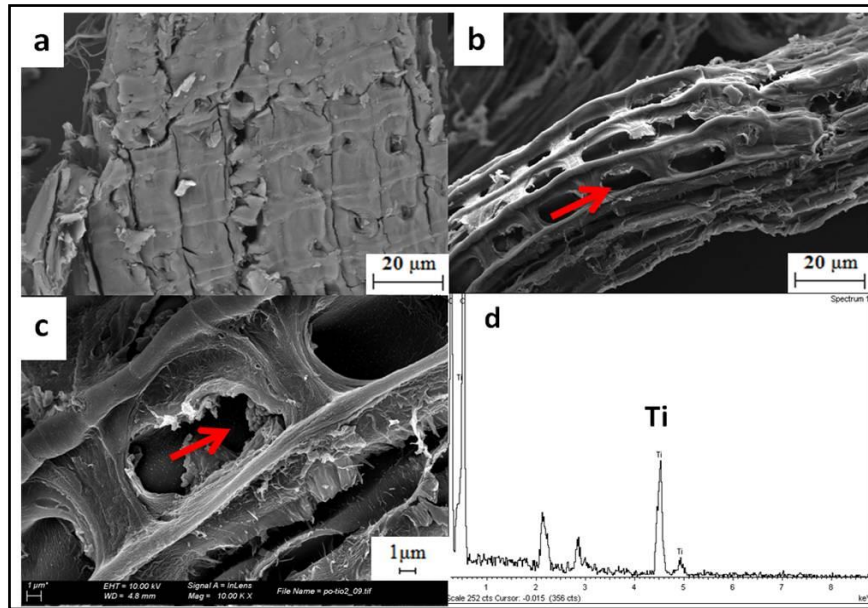


Figure 3.23 SEM images of (a) Pine and (b) and (c) Pine/TiO₂ at different magnifications. Finally, (d) EDS mapping of Pine/TiO₂ surface.

From different SEM images, the diameter of TiO₂ nanoparticles is able to be checked and it is found to be in the range of 25 and 70 nm, as we mentioned before. The spectra of EDS, corresponding to a semi-quantitative analysis, is shown on Figure 3.26 panel (d), where a strong peak for Ti confirms the presence of TiO₂ onto the pyrolyzed Pine surface, as in the previous cases (Figure 3.22).

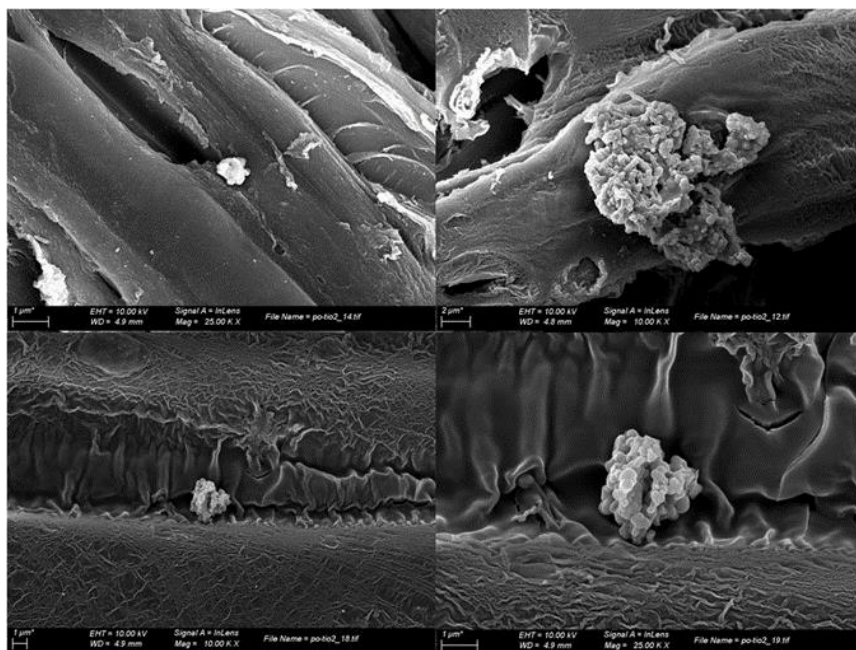


Figure 3.24 SEM images of Pine/TiO₂ at different magnifications.

3.3.1.2 ATR-FTIR characterization

As we mentioned before, COOH and OH are main functional groups involve in heavy metal removal. ATR-FTIR spectroscopy is conducted to identify them as shown in Figure 3.25 and Table 3.11. The results confirmed the existence of carboxylic acid (-COOH) and carbonyl (C=O) groups in both pine and TiO₂ loaded on pine.

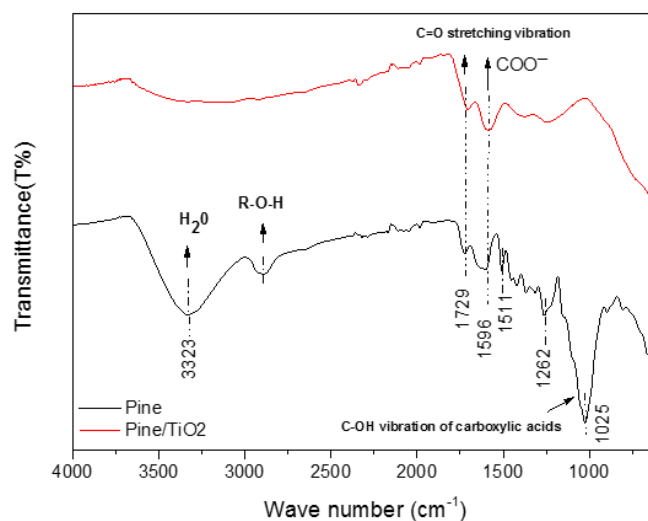


Figure 3.25 ATR-FTIR spectra of Pine and Pine/TiO₂.

Table 3.11. ATR-FTIR wavenumbers groups from te spectra of Pine and Pine/TiO₂

Wave Number (cm ⁻¹)	Assignments	Compounds	Band positions (cm ⁻¹)	
			Pine	Pine/TiO ₂
3200-3700	O-H stretching	Acid, methanol	3323	-
2700-3000	C-H _n stretching	Alkyl, aliphatic	2886	-
1700-1730	C=O stretching	Carboxyl, carbonyl	1729	1729
1450-1600	COO ⁻ stretching	Ketone, carbonyl	1684	1684
1000-1200	C=O stretching C-O-C stretching/bending C-N,R-O-C/R-O-CH ₃	Ketone, ether, phenol, chain anhydride	1025	-
730-3500	Native cellulose		893,1025,115, 1263,1425,1638 2909,3323	-

XRD analysis

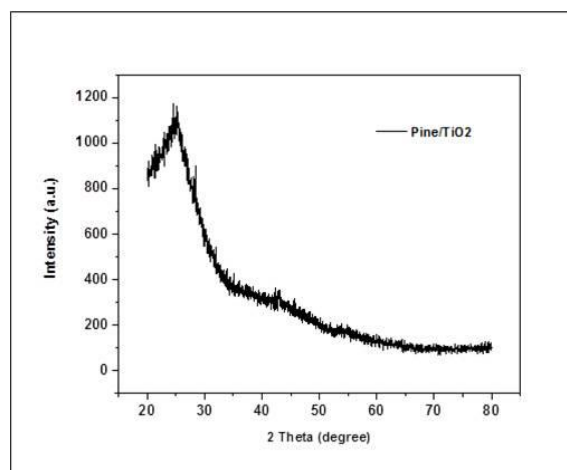


Figure 3.26 XRD spectra of Pine/TiO₂

XRD analysis is performed to study the crystallinity of the TiO₂ particles loaded inside biomass. Figure 3.26 shows the X-ray powder diffraction pattern collected on Pine/TiO₂. No appreciable diffraction peaks from TiO₂ particles are detected over the background given by the amorphous porous biomass structure. This may be due to the small loading of the TiO₂ to the amorphous character of the particles.

Influence of the aqueous solution pH

The pH of the solution affects the surface functional groups speciation (ionization), the charge of the adsorbent surface, and also the speciation of the metal adsorbates. In order to determine the effect of pH in the removal of Pb(II), Cd(II), Cu(II) and Cr(III) from aqueous solutions by Pine and Pine/TiO₂, biosorption experiments at different pHs within the range going from 2 to 6 are performed. The concentration of solution is 0.18mmol/L for each element in the multiple system. All the samples are stirred for 24 hour to reach adsorption equilibrium for Pine and Pine/TiO₂.

Figure 3.27 shows that the biosorption percentage increases with the pH for Pine and Pine/TiO₂. All the elements follow a similar trend. The biosorption reaches its maximum value at pH 4.0 for Pine/TiO₂, whereas it monotonically increases for Pine within the considered range. According to literature, as the solution pH increases, the biosorption removal of cationic metals increases⁴¹. At lower pH, the H⁺ ions compete effectively with the metal cations causing a decrease in the heavy metal biosorption capacity. When pH values increase, a decrease in competition with protons ions (H⁺) favors the metal ions uptake due to electrostatic interaction. From pH 6, due to a change on the metal speciation by hydroxide formation, lower concentration of metal

ion is found on the final solution which probably is not related with biosorption, but related with hydroxides metal precipitation ³⁶.

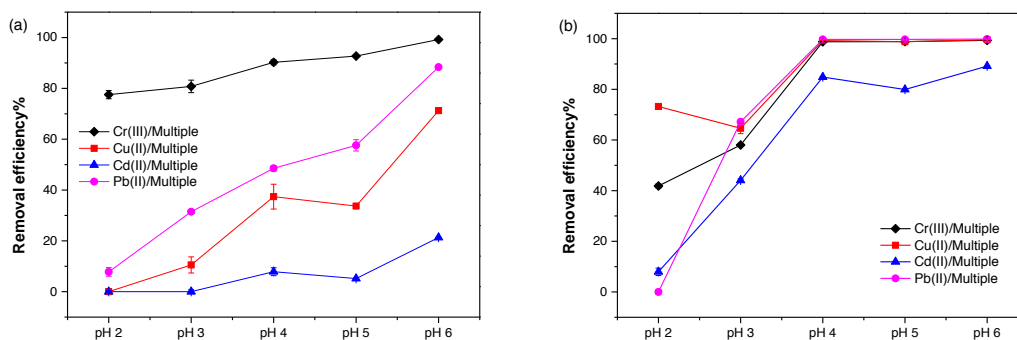


Figure 3.27 Effect of pH on biosorption of multi-element system (a)Pine and (b)Pine/TiO₂. Biosorption conditions: 10 mL of metal solution with a concentration of 0.18 mmol/L, 10 mg of material, T = 25.0°C, and stirring for 24 h.

In the present work the removal percentage of Pb(II), Cu(II), Cr(II) and Cd(III) by Pine/TiO₂ at pH 4.0 (100%,100%,100% and 80%, respectively) are notable higher than those of Pine (57%, 33%, 92% and 5.1%, respectively). These values are higher than those reported previously for Cu(II) adsorption on *Oil palm shell* ⁴². To avoid any possible precipitation by hydrolysis in multi-element system, also considering that the higher biosorption is found at pH 4.0, which is not far away from many real pH of wastewaters, this was chosen as the optimal pH value for further biosorption experiments, in order to determine the influence of other parameters (i.e. time and initial concentration, mainly).

Influence of the time of the biosorption process

The required equilibration time and the optimal contact time for a biosorption process has been checked. The time range is established from 5 to 1440 minutes. In Figure 3.28 the range from 5 min to 480 min is shown, because the biosorption of Pine and Pine/TiO₂ have reached the equilibrium at this last time. Similar to some results found in the literature, the biosorption of Cr(III), Cu(II), Cd(II) and Pb(II) exhibited an initial rapid stage during the first 10 min, which can be related to the good affinity between heavy metal ions and the adsorption sites of the adsorbents ⁴³. When the amount of available sites on the biosorbent surface is reduced (by pyrolysis process) a reduction in the biosorption rate is followed.

So, Figure 3.28 shows the influence of the contact time between biosorbent (Pine and Pine/TiO₂) and the adsorbate solution in single-element and multi-element systems.

The biosorption performance of Pine/TiO₂ toward all heavy metals is higher than that of the Pine in both systems, especially, for Cu(II) and Cd(II) that are three and four times higher than the others (Cr(III) and Pb(II), respectively).

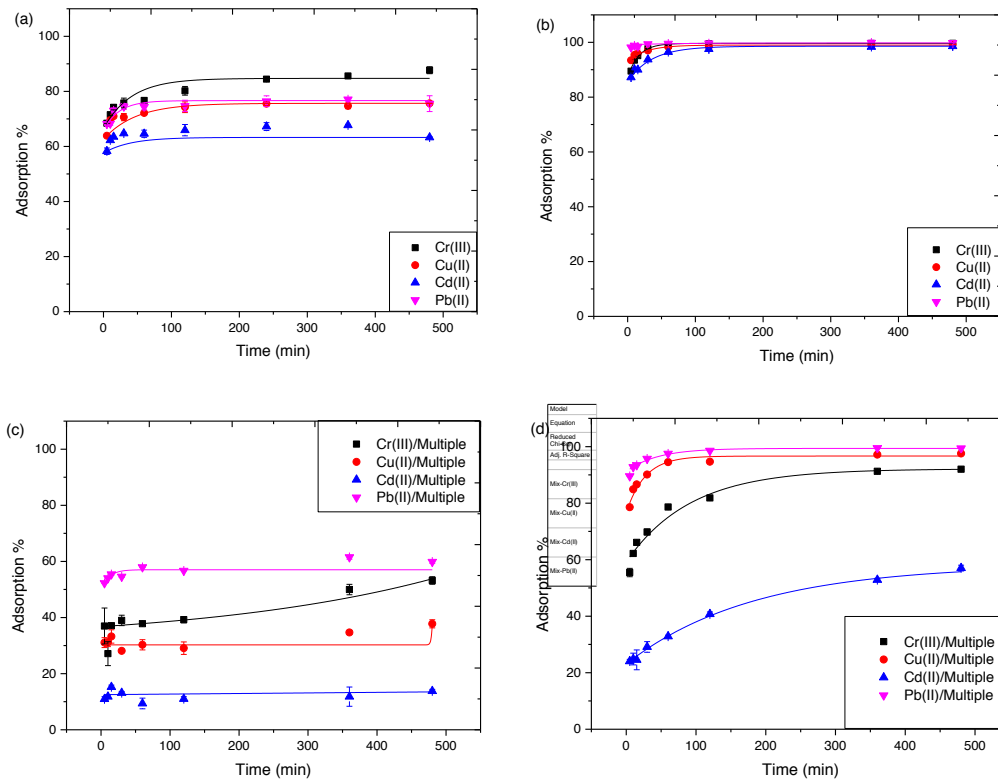


Figure 3.28 Biosorption kinetics for Cr(III), Cu(II), Cd(II) and Pb(II) on single (a,b) and multiple (c,d) systems by Pine (a,c) and Pine/TiO₂ (b,d). Initial 1.0 mL of aqueous solutions concentration are 0.18 mmol/L for each element, pH =4.0, same amount of 10 mg of biosorbents used, at T=25.0°C, and stirring for different times.

The removal percentages of Pine/TiO₂ in single-element system reach around 100% in the first 10 min, except for Cd(II) in multi-element system. However, the biosorption in this latter case need longer time to reach the equilibrium that is probably due to the competition between metals for occupying the adsorption sites. In the case of pine biomass, the heavy metal ion biosorption efficiency in both single and multi-element systems ranked as: Cr(III) > Pb(II) > Cu(II) > Cd(II), and as: Pb(II) > Cr(III) > Cu(II) > Cd(II), respectively. Pb(II) and Cr(III) have priority in occupying adsorption sites compared to Cu(II) and Cd(II). After 24 hours of biosorption experiments, Pine and Pine/TiO₂ reached the equilibrium in both single and multiple systems. Thus 24 hours is chosen for the optimal contact time value for further biosorption experiments.

Biosorption kinetics modeling

To further understand the biosorption interaction for Cr(III), Cu(II), Cd(II) and Pb(II) with pine and Pine/TiO₂, collected biosorption data is adjusted to two different models: pseudo-first-order and pseudo-second-order, which have been intensively applied to simulate the biosorption process⁴⁴.

As show in Table 3.12, Pine and Pine/TiO₂ experimental data are in well agreement with the PSO model, which suggests that the rate-controlling step for the biosorption of heavy metals is a chemisorption process. The adsorption constant rate (k_2) related with adsorption sites on Pine and Pine/TiO₂, also depends on the initial ions concentration.

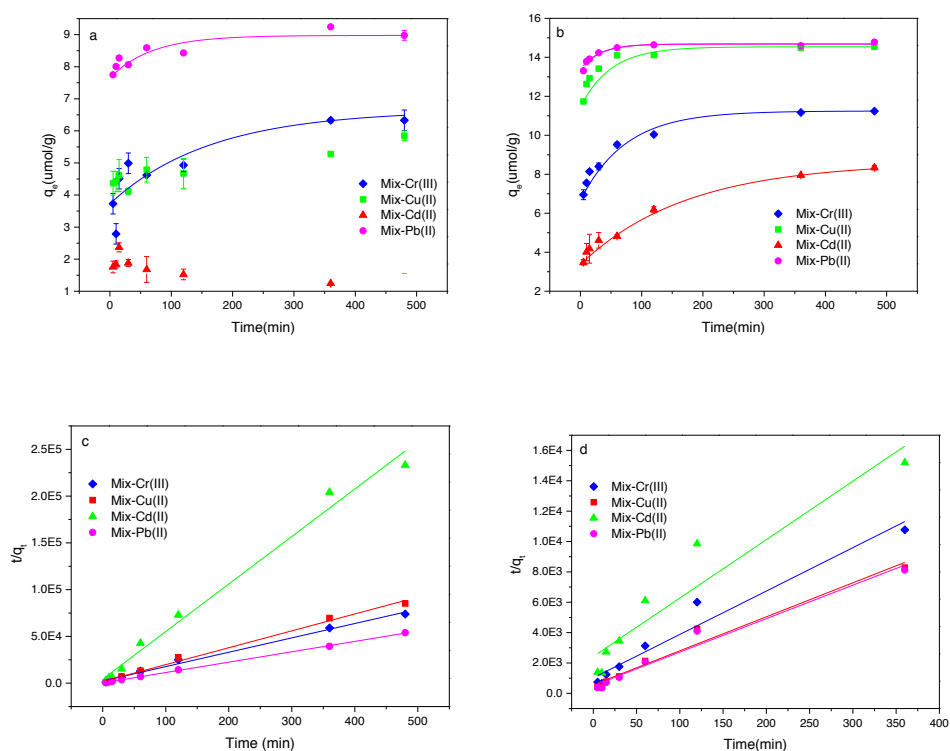


Figure 3.29 Kinetics modelling of the biosorption of heavy metals (Pb, Cd, Cu, Cr) in multiple system by (a,c) Pine and by (b,d) Pine/TiO₂. (a,b) shows the capacity vs time; and (c,d) are the fitting curves of the pseudo-second-order model. Initial 1.0 mL of aqueous solutions concentration are 0.18 mmol/L for each element, pH =4.0, same amount of 10 mg of biosorbents used, at T=25.0°C.

Table 3.12 Pseudo-second-order model. Kinetics Parameters of biosorption of Pb(II), Cd(II), Cr(II), and Cu(II) in single and multi-element systems by Pine and Pine/TiO₂ on the. Initial 1.0 mL of aqueous solutions concentration are 0.18 mmol/L for each element, pH =4.0, same amount of 10 mg of biosorbents used, at T=25.0°C.

M ⁿ⁺	C ₀	q _{e,exp} *	Pine			q _{e,exp}	Pine/TiO ₂		
	× 10 ³ mmol/L	× 10 ³ (mmol/g)	k ₂	q ₂ × 10 ³ (mmol/g)	R ²	× 10 ³ (mmol/g)	k ₂	q ₂ × 10 ³ (mmol/g)	R ²
Cr(III)	5.77	11.1	14.4	11.1	0.999	12.5	9.69	26.0	0.996
Cu(II)	7.23	11.3	47.8	11.3	0.999	14.8	9.33	30.5	0.997
Cd(II)	10.9	9.67	58.7	9.31	0.998	14.2	7.86	29.2	0.997
Pb(II)	21.6	10.4	127	9.58	0.999	12.6	12.3	25.9	0.997
Mix-Cr(III)	6.34	6.49	9.97	6.51	0.993	11.2	0.800	18.5	0.957
Mix-Cu(II)	9.54	5.63	18.2	5.54	0.994	14.5	0.890	23.7	0.971
Mix-Cd(II)	16.7	2.27	58.7	1.96	0.988	8.52	0.611	14.3	0.907
Mix-Pb(II)	30.8	8.89	45.2	9.01	0.999	14.8	0.949	24.0	0.973

*q_{e,exp}: experimental value of the equilibrium biosorption capacity. k₂: g mol⁻¹min⁻¹.

Influence of the initial metal concentration

The initial concentration of Cr(III), Cu(II), Cd(II) and Pb(II) is involved in biosorption process of Pine and Pine/TiO₂, as it provides a significant understanding of the competitive process of the four heavy metals. As seen in Figure 3.30, although the removal capacity of Cr(III), Cu(II), Cd(II) and Pb(II) increased with concentration levels, the biosorption capacity reaches saturation in Pine/TiO₂, and decreased for Cd(II) and Cu(II) in Pine biomass when working at high concentration levels of metals. For multi-element system the Pine/TiO₂ shows a higher capacity compared to the Pine, regarding the increase of metal concentration. Specially in the case of Cu(II), the removal capacity is higher in comparison with the other three metals.

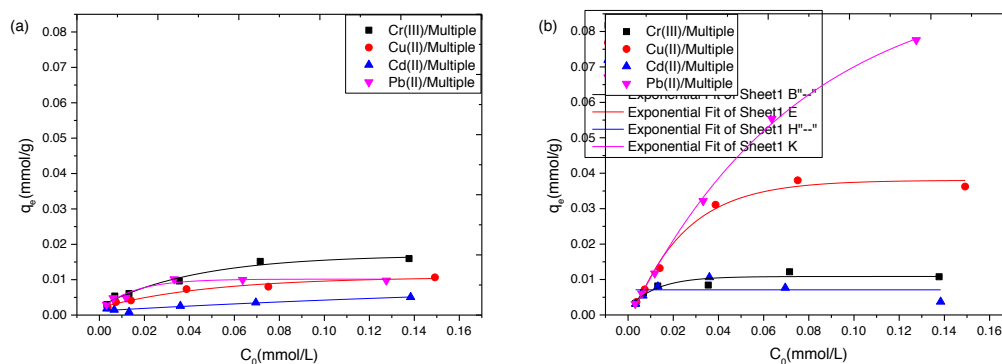


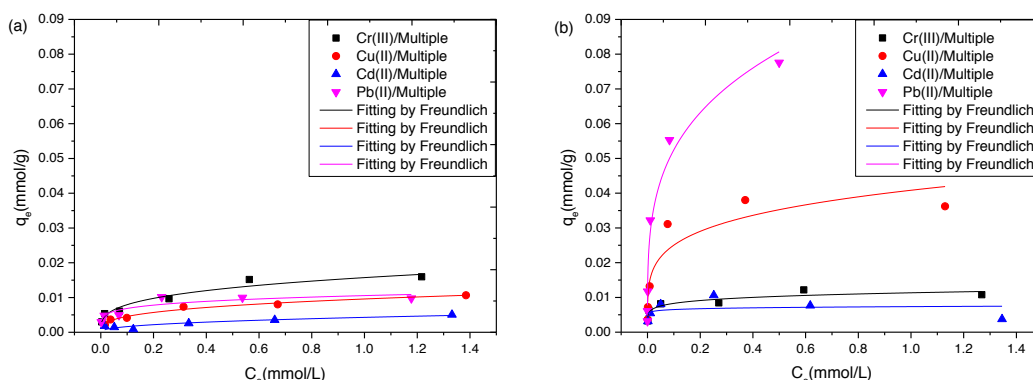
Figure 3.30 Influence of initial concentration on the biosorption of Cr(III), Cu(II), Cd(II) and Pb(II) by (a) Pine and (b) Pine/TiO₂. Biosorption conditions are at T=25.0°C, pH 4.0, stirring for 24 hours. Line fitting by Exponential function.

Biosorption isotherm modeling

Langmuir and Freundlich isotherm models are used to study the adsorption mechanism for the interaction of heavy metal ions on the adsorbent surface as previous studies.

As shown in Table 3.13 and Figure 3.31, the biosorption capacity of Cu(II) and Pb(II) in multi-element system by Pine/TiO₂ notable increased than those of Pine. However, Pine can be hardly described by both isotherms models except for Cr(III) and Cu(II) (data is showed in Table 3.13), probably due to the low adsorption capacity by such biomass for this two elements under competition conditions (multiple system). This could illustrate that the modification of the Pine using TiO₂ results in an increase of sites interactions on the material surface. The Pine/TiO₂ biosorption capacity of heavy metals in multi-element system follows as: Pb(II) > Cu(II) > Cr(III) > Cd(II). Pine/TiO₂ presents high capacities for Cu(II) and Pb(II) ions with 34.0 and 77.5 μmol/g, respectively. While capacity of Cr(III) and Cd(II) is 10.5 and 4.94 μmol/g, respectively.

Futhermore, the biosorption by Pine/TiO₂ of Cu(II) is better fitted with Langmuir than with Freundlich, with correlation coefficients of 0.97 and 0.84, respectively. However, biosorption of Cu(II) from a single system is the opposite way that shows better fit with Freundlich than Langmuir. Comparing both models in single and multiple heavy metal solution systems, as listed in Table 3.13, the experimental data of Pb(II) is fitted well with both models by Pine/TiO₂, which could be confirmed by correlation coefficients (R²). Pb(II) shows higher affinity to the surface of Pine/TiO₂, whereas Cu(II), Cr(III) and Cd(II) are hard to bind to the surface due to the competition with Pb(II)⁴⁷.



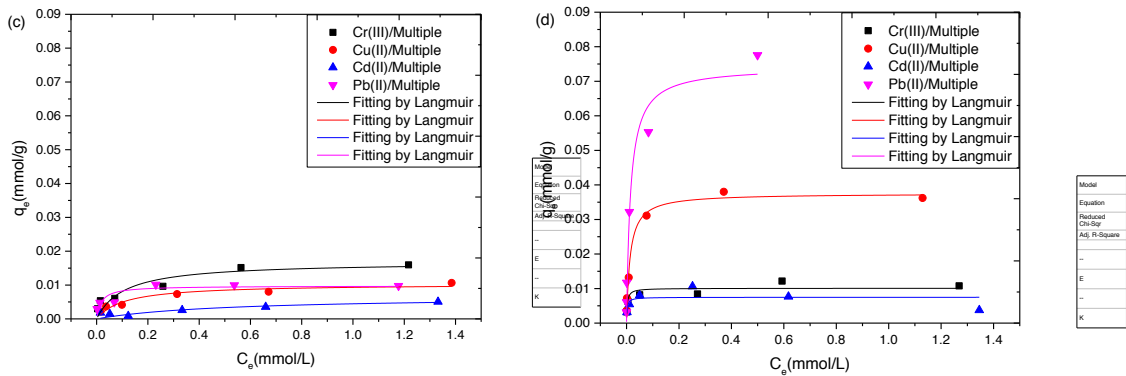


Figure 3.31 Biosorption isotherm modelling of heavy metals in multi-element system by Pine (a) (c) and Pine/TiO₂ (b) (d). (a) and (b) Freundlich and (c) and (d) Langmuir model adjustment. Biosorption conditions were at T=25.0°C, pH 4.0 and stirring for 24 hours.

Table 3.13 Langmuir and Freundlich isotherm parameters of biosorption of Pb(II), Cd(II), Cr(III), and Cu(II) ions in multiple system onto Pine and Pine/TiO₂. Biosorption conditions were at T=25.0°C, pH 4 and stirring for 24 h.

	M ⁿ⁺	$q_{e,exp} \times 10^3$ (mmol/g)	Langmuir			Freundlich		
			$q_{max} \times 10^3$ (mmol/g)	$b(\times 10^3)$ (L/mol)	R ²	$K_f \times 10^3$ (mmol/g)	n ($\times 10^3$)	R ²
Pine	Pb	28.6	32.7	5.02	0.916	26.5	0.295	0.965
	Mix-Cr(III)	12.4	16.8	9.26	0.793	15.7	0.297	0.940
	Mix-Cu(II)	5.28	10.3	9.20	0.892	9.58	0.322	0.972
	Mix-Cd(II)	2.84	6.72	1.98	0.609	4.29	0.420	0.771
	Mix-Pb(II)	12.5	9.75	55.1	0.673	10.6	0.187	0.798
Pine/TiO ₂	Pb	151	38.2	0.00263	1.00	1.00	1.00	1.00
	Mix-Cr(III)	10.5	10.1	360	0.756	11.3	0.136	0.827
	Mix-Cu(II)	34.3	37.5	75.2	0.980	40.8	0.212	0.841
	Mix-Cd(II)	4.94	7.49	435	0.217	7.35	0.0530	NA
	Mix-Pb(II)	77.5	74.2	66.8	0.949	97.1	0.267	0.975

3.3.2 Summary

In this part, TiO₂ is successfully synthesized on the surface of SO, ZO and Pine followed by sol-gel method. ATR-FTIR and SEM are have confirmed the presence of TiO₂.

Furthermore, pine and pine/TiO₂ are chosen to further experiment. A single-element system and multi-element system are used to removal heavy metals. The multi-element system composed by a mixture of Cr(III), Cd(II), Cu(II) and Pb(II) ions is used to simulate a realistic case of waste water polluted with heavy metals case for adsorption. Different parameters of adsorption processes are optimized in batch systems (pH of the solution, the initial concentration and the contact time). Surface morphology of the adsorbents were analyzed using scanning electron microscopy (SEM) and Fourier transform infrared spectroscopy (FT-IR).

The biosorption capacity in multiple system for Cr(III), Cu(II), Cd(II) and Pb(II) removal is greatly enhanced after loaded TiO₂ on Pine, especially to Cu(II) and Pb(II) with 130 and 98.4 μmol/g, respectively. The biosorption percentage in multi-element system of all heavy metal increase, follow as: Pb(II)>Cr(III)>Cu(II)> Cd(II). This biosorption process of Pb(II) and Cu(II) are better fit by Freundlich isotherm models by using Pine/TiO₂.

3.4 Biosorption mechanism of heavy metals by XAS

3.4.1 Chromium speciation: biosorption mechanism elucidation by XAS

Chromium is a common contaminant in surface and groundwaters that comes mainly from electroplating, leather tanning, and textile industries processes. Trivalent, Cr(III), and hexavalent, Cr(VI), oxidation states are the two main valence states found in polluted water^{48,49}. Cr(VI) is five hundred times more poisonous than Cr(III) and may cause carcinogenesis, mutation or teratogenesis to living creatures^{50,51}. Thus, Cr(VI) has been identified as a top-priority hazardous pollutant⁵². Therefore, it is of great significance to develop a cost-effective and eco-friendly technique to remove chromium from industrial wastewaters, before being disposed into aqueous systems.

For that purpose, biomass/biochar is here proposed to remove chromium from water systems. Pine biomass, Pine biochar (PG) and TiO₂ loaded onto biomass (Pine/TiO₂) are used to adsorb Cr(III) and Cr(VI) ions from aqueous solutions. These adsorbents have different selectivity behaviour for chromium, which is characterized by the measurement of the pH of the materials, attenuated total reflectance Fourier transform infrared spectroscopy (ATR-FTIR), scanning electron microscopy (SEM), Brunauer-Emmett-Teller technique (BET) analysis, zeta potential analysis and mineral components analysis. The objective is to determine the functional groups, the morphological structure and the mineral composition of the adsorbents. Furthermore, different parameters of the chromium biosorption process are optimized in batch systems (i.e. pH of the aqueous solution, the initial chromium concentration and the contact time are checked).

X-ray absorption spectroscopy (XAS), is unique sensitivity to the local structure, which can be exploited to elucidate the biosorption mechanism with those biomass/biochar systems of heavy metal in molecular level (for chromium particularly)^{53,54}. Some works in the literature have been found using this technique to study the biosorption mechanisms^{55,56}.

Comparison of biosorbent properties (Pine, Pine/TiO₂ and PG)

As indicated in the previous section, three biosorbents (Pine, Pine/TiO₂ and PG) are used to remove Cr(III) and Cr(VI) ions in single-metal systems. These three adsorbents show different biosorption capacities for the chromium metal ions, as shown in Figure 3.32. In general, Pine and Pine/TiO₂ have better biosorption capacity for Cr(VI) than PG, especially the case of Pine/TiO₂. In contrast, PG shows a different behaviour, while PG has a high adsorption for Cr(III) but neglected adsorption for Cr(VI). Pine original

biomass has shown low biosorption rates for both chromium species.

As can be found in the literature, the changes of mineral content (K, Ca, Mg and P), functional groups (carboxyl and hydroxyl groups), pH and large specific surface areas can influence the metal ions biosorption⁵⁷. In this sense, when treating biomass by a pyrolysis procedure working at high temperatures, it leads to an increment in porosity, concentration of minerals, pH and surface area compared with the original biomass. In the present case of pine biomass/biochar systems, the change in mineral content and the surface morphology can explain the higher capacity of Cr(III) by Pine/TiO₂ and PG than Pine biomass. SEM images to show corresponding morphology are shown in Figure 3.33. As mentioned above, Pine/TiO₂ has been shown to have a higher heavy metal removal efficiency than Pine (see Figure 3.32), which can be explained by the high porosity and the large pore size of Pine/TiO₂ (Figure 3.33 and Table 3.15). Thus, the results presented here demonstrate that pore structure is a key factor that can influence the sorption of heavy metals onto biomass.

The mineral concentration level in PG is higher than in Pine, especially for Ca. The respective values are 9.4 and 0.68 mg/kg for K⁺, 21 and 0.67 mg/kg for Ca²⁺, 2.1 and 0.15 mg/kg for Mg²⁺, and 1.3 and 0.070 mg/kg for phosphate species, for PG and Pine, respectively.²² The increase of minerals can be attributed to the pyrolysis process since minerals from biomass are pre-concentrated on the surface of adsorbents. Especially K⁺, Ca²⁺ and Mg²⁺ on the surface can be exchanged with Cr(III), which can explain such selectivity behaviour by PG⁵⁸.

It is well known that Cr(VI) is present in waters as chromate anion which can compete with OH⁻ at high water solution pH levels. In the case of positively charged sites, these will be the responsible to the possible interaction of anions onto biomaterials. Chromate anions will not interact with carboxyl neither with hydroxyl site groups from biomass, on the contrary they will suffer repulsion interaction⁵⁹. On the contrary, increased adsorption for Cr(VI) by Pine/TiO₂ is found probably due to their photocatalysis. Cr(VI) first interact with TiO₂ and later reduce to Cr(III). The opposite adsorption behaviour of PG is probably due to the increased pH of adsorbent (with pH 6 for Pine and Pine/TiO₂, and pH 9 for PG) which increases the competition with OH⁻ and decreases the Cr(VI) adsorption.

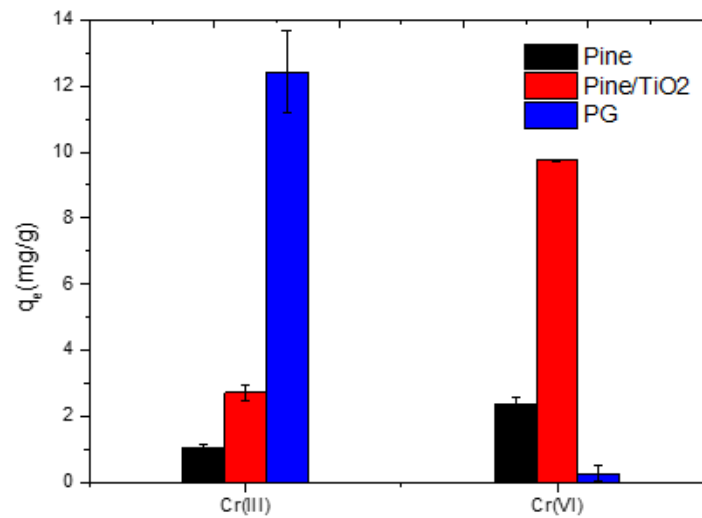


Figure 3.32 Biosorption capacity of Cr by using Pine, Pine/TiO₂ and PG. Initial metal ions concentration of 120 ppm of metal, pH 4.0, and 25 mg of adsorbent.

SEM characterization

SEM is used to study the morphological structure of the biosorbents. As shown in Figure 3.33, Pine/TiO₂ shows more pore structures than Pine. TiO₂ aggregates can be found at different sizes, as it has been mentioned in previous section. Later this morphology of all pine biomass/biochar systems will be related to the biosorption efficiency of them for chromium species.

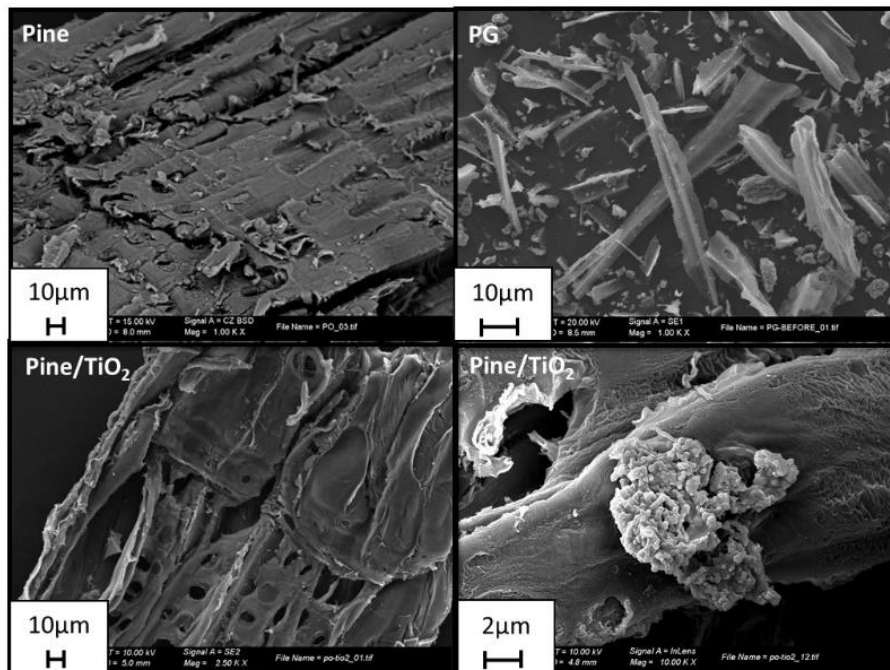


Figure 3.33 SEM images of a) Pine, b) PG, c) Pine/TiO₂, all at similar magnification; and d) Pine/TiO₂ at higher magnification.

ATR-FTIR characterization analysis

ATR-FTIR spectra of Pine, Pine/TiO₂ and PG are shown in Figure 3.34 and approximate assignments of the vibrational modes are listed in Table 3.14. Similarly as in previous cases and with similar relations with expected functional groups in the pine systems.

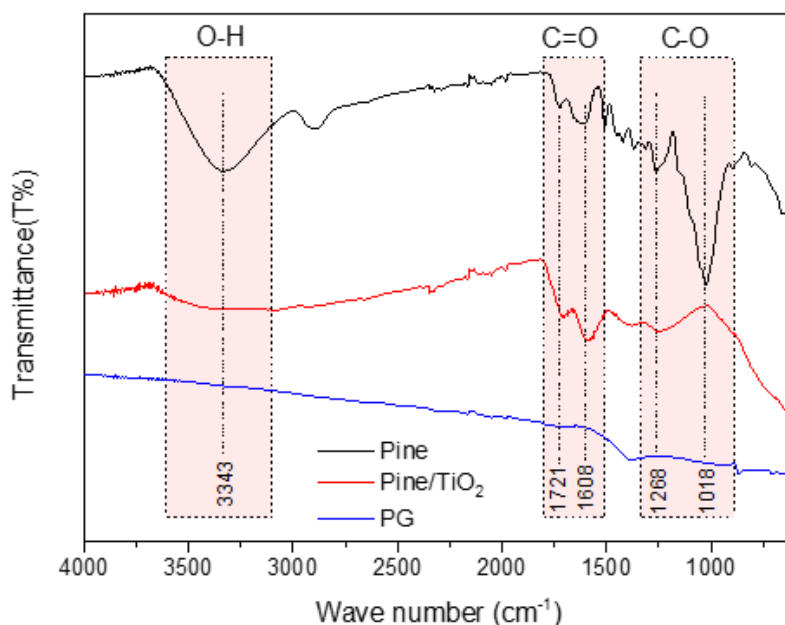


Figure 3.34 ATR-FTIR spectra of Pine, Pine/TiO₂ and PG.

Table 3.14 ATR-FTIR spectral bands assignments for Pine, Pine/TiO₂ and PG before use.

Wave numbers (cm ⁻¹)	Assignments	Biosorbents		
		Pine	Pine/TiO ₂	PG
3200-3700	O-H stretching	3343	3343	
2700-3000	C-H stretching	2903		
1780-1710	Carboxylic Acid C=O stretching	1721	1721	
1750-1630	Ketone, Ester, Amide C=O Stretching	1608	1608	
1000-1200	C=O/C-O-C C-N/R-O-C/R-O-CH ₃ stretching	1018	1018	1388
		1268	1268	

Comparing the three materials, a decrease in the intensity of the peaks corresponding to carboxyl (-COOH) and hydroxyl (-OH) groups is observed in the ATR-FTIR spectra of Pine/TiO₂ and PG after pyrolysis, especially for PG where a higher loss of functional groups can be due to the high temperature pyrolysis procedure. *Yuan et.al* has similar result that showed functional group (COOH) decompose under the high temperature

used for pyrolysis process, completely lost above 700 °C, being near to the PG case⁶⁰. On the other hand, a reduction in the amount of negative surface charges (related to groups such as -COOH, -COH and -OH) increases the pH of the biochar material since such groups are decomposed, which is corresponding to pH result of PG (pH around 9)²⁵.

Zeta potential and BET analysis

In this part, zeta potential and BET analysis are used to determine the surface charge of the biosorbent and surface area. They can be used to explain the different biosorption process (shown in Figure 3.35 and Table 3.15). In general, all adsorbents show negative charge at pH 4. PG and Pine/TiO₂ have a similar negative charge but higher than pine biomass. Therefore, PG and Pine/TiO₂ show higher electrostatic interactions with cation ions (Cr³⁺) but lower ability to attract anion ions (HCrO₄⁻). Furthermore, the zeta potential of PG and Pine/TiO₂ are similar, but PG shows higher biosorption capacity of Cr(III) than Pine/TiO₂. This means that electrostatic attraction is not the main biosorption process for PG. However, the surface area, pore volume and size all highly increased compared with pine, which is corresponding with their biosorption capacities (shown in Figure 3.32). Therefore, surface area and pore structure are key points to influence heavy metal removal. As we mentioned before, mineral components of PG can ion exchange with cation ions. In conclusion, the biosorption of Cr(III) by PG are mainly due to the large surface area and mineral ion exchange, which the former plays a more important role in this process. For the biosorption of Cr(VI) by Pine/TiO₂, it is possible that the reduction of Cr(VI) appears after adsorbing on the surface of TiO₂. The higher biosorption capacity of Cr(III) by Pine/TiO₂ can be explained by large surface and mineral ion exchange after the reduction process.

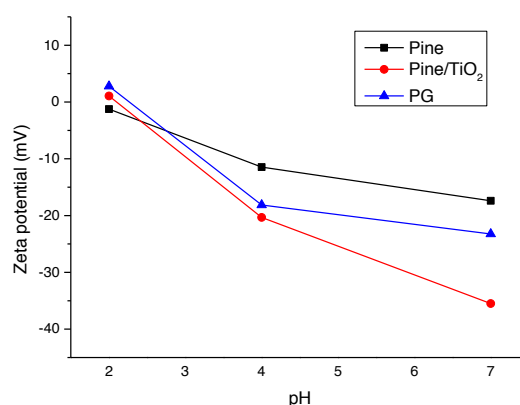


Figure 3.35 Zeta potential values of Pine, Pine/TiO₂ and PG. For each situation, triplicate measurements are performed and each sample is measured 3 times to determine the zeta potential values.

Table 3.15 BET analysis of Pine, Pine/TiO₂ and PG.

	Pine	Pine/TiO ₂	PG
Surface Area (m ² /g)	1.52	36.1	128
Pore Volume (cm ³ /g)	0.0177	0.0454	0.257
Pore Size (nm)	44.2	4.71	7.99
Zeta potential (mV) pH 4.0	-11.5	-20.3	-18.1

Influence of contact time

The influence of the contact time between sorbents (Pine, Pine/TiO₂ and PG) and Cr(III) and Cr(VI) aqueous solutions are studied. For that purpose, biosorption experiments are performed for different times (from 5 to 120 minutes) for each adsorbent (shown in Figure 3.36), as usual. In general, Pine/TiO₂ and PG are more effective than Pine biomass for total chromium removal. Biosorption equilibrium is reached in 30 minutes for each adsorbent for Cr(III) in single system, whereas adsorption equilibrium is reached in 1 hour for Cr(VI) also in single system, either by Pine and Pine/TiO₂. In the case of PG, the biosorption of Cr(VI) is negligible due to the electrostatic repulse on the surface and the competitive with OH⁻ from solution, so its efficiency is related to its better interaction with Cr(III).

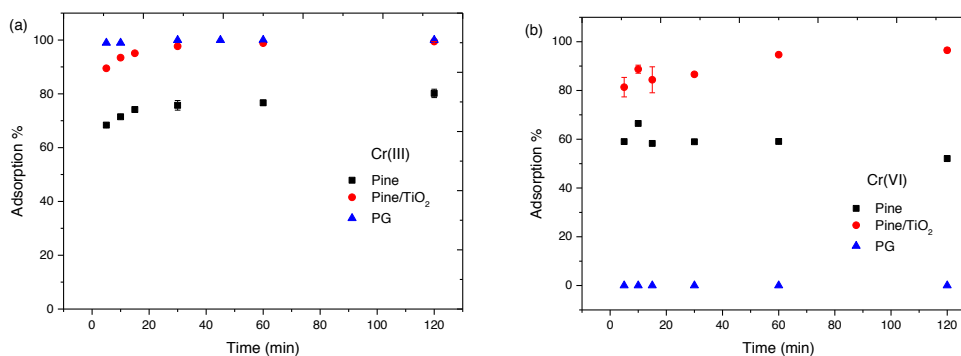
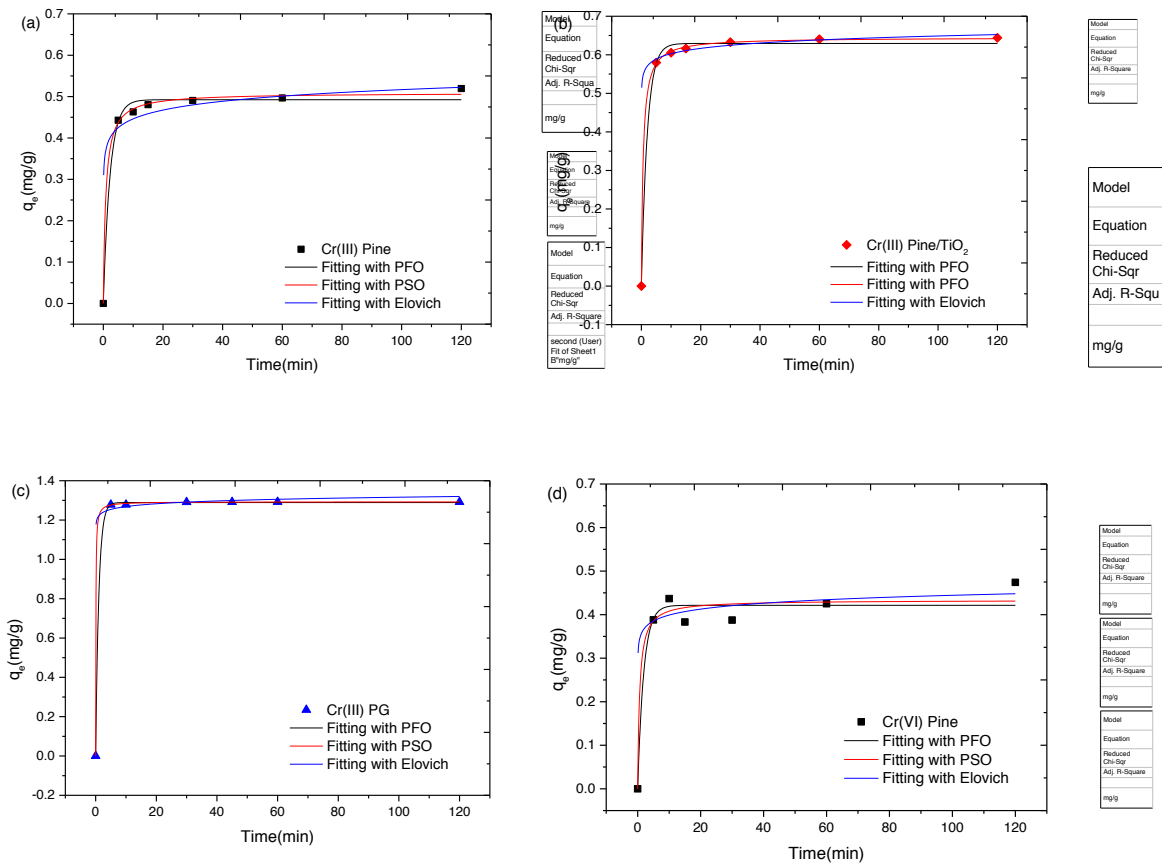


Figure 3.36 Biosorption percentage of Cr by Pine, Pine/TiO₂ and PG at different contact times. (a) Biosorption of Cr(III), and (b) Biosorption of Cr(VI). Initial metal ions concentration of 9 ppm of metal, pH 4.0, and 25 mg of adsorbent.

To understand the different adsorption behaviours in single element systems, kinetic modelling analysis is performed to find which model system can explain the obtained experimental results and to get information about the mechanisms of the heavy metal adsorption onto all the biomass/biochar systems.

Kinetic modelling

Kinetics modelling of Pine, Pine/TiO₂ and PG systems by PFO, PSO and Elovich analysis show that the adsorption process fit well with all the models for all the adsorbents and both chromium species, except the case of PG in Cr(VI) single system, while Intra-particle Diffusion does not fit well for any case. The relative constants found by applying the models are listed in Table 3.16. So, all those results mean that the adsorption of heavy metals on the surface of the adsorbents is due to a combination of the physisorption and chemisorption processes, such as valence forces sharing or exchanging electrons between the adsorbent and adsorbate, except for PG and Cr(VI). In this case, none of the selected model could successfully reproduce the trend of PG to fit the adsorption process of Cr(VI), probably related to have a negligible biosorption for this chromium specie.



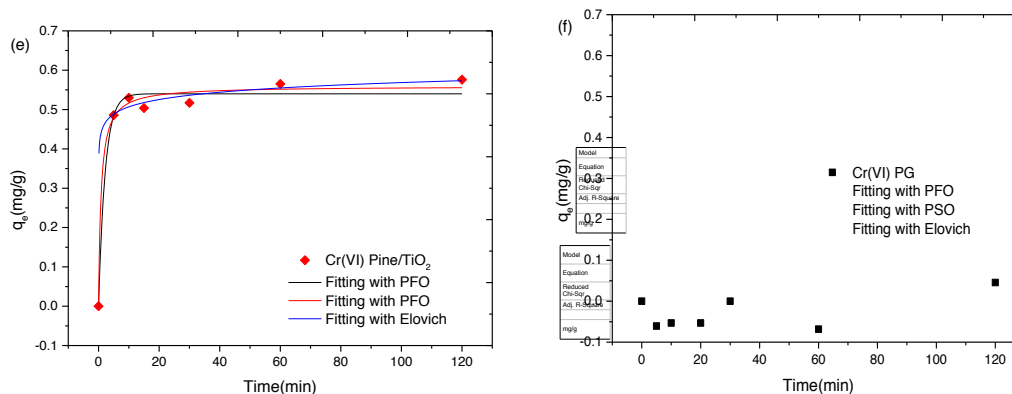


Figure 3.37 Different of fitting curves of Pine, Pine/TiO₂ and PG in Cr(III) (a, b and c) and Cr(VI) (d, e, and f) single systems.

Table 3.16 Biosorption kinetic constants for the biosorption of Cr(III) and Cr(VI) by Pine, Pine/TiO₂ and PG.

		PFO			PSO			Elovich		
		k ₁	q ₁	R ²	k ₂	q ₂	R ²	α	β	R ²
		(g/mg/min)	(mg/g)		(g/mg/min)	(mg/g)				
Cr(III)	Pine	0.438	0.492	0.991	2.39	0.509	0.998	32.6	6260	0.727
	Pine/TiO ₂	0.494	0.629	0.999	2.61	0.644	0.998	50.1	2.61	0.996
	PG	0.955	1.29	0.999	11.8	1.29	0.999	48.3	9.42	0.998
Cr(VI)	Pine	0.518	0.421	0.956	3.72	0.433	0.960	50.7	1.19	0.970
	Pine/TiO ₂	0.452	0.540	0.982	2.15	0.559	0.989	37.4	4465	0.994
	PG	NA	NA	NA	NA	NA	NA	NA	NA	NA

Influence of initial concentration

Six single-metal solutions at different concentration level (5 ppm, 10 ppm, 25 ppm, 50 ppm, 75 ppm, 120 ppm and 240 ppm) are prepared from 1,000 ppm stock solutions of each chromium specie. The study of the initial concentration range provides a significant understanding of both Cr metal ion species during the biosorption process. As shown in Figure 3.38 (b), it is confirmed in all the concentration range that the biosorption capacity of Cr(VI) is higher by Pine against PG, whereas the Pine/TiO₂ increased the adsorption of Cr(VI) probably due to TiO₂ particles (which have photocatalytic properties that are well known)^{61,62}. Many researches have been using TiO₂ or modified TiO₂ under UV or visible light irradiation for Cr(VI) reduction in wastewater^{63,64}. So here this possibility will be checked by XAS measurements. In addition, PG highly selective capacity for Cr(III) probably is due to the high mineral

content and large surface area, as mentioned above. They can provide more possibilities for the exchange of heavy metals cations from the solution, which could increase the adsorption capacity of positive Cr(III).

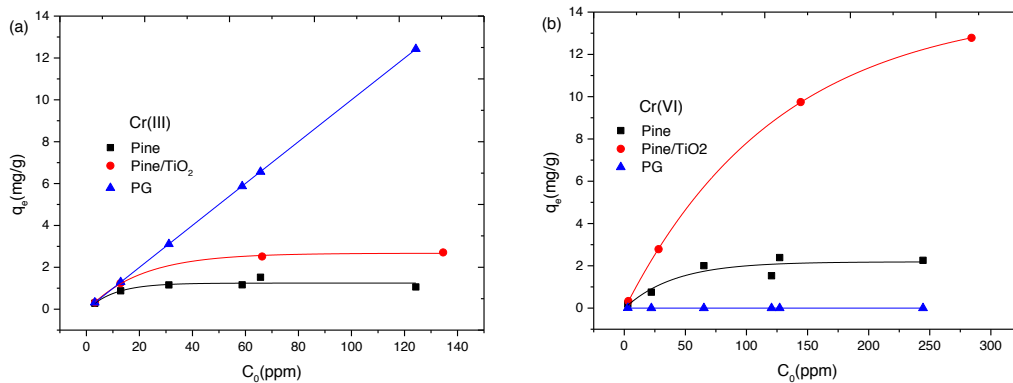


Figure 3.38 Effect of the initial concentration of heavy metals on their biosorption by Pine, Pine/TiO₂ and PG in Cr(III) single system (a), in Cr(VI) single system (b). Experimental conditions were $T=25\pm 1^\circ\text{C}$, pH 4.0, 25 mg of adsorbent, 2.5 mL of metals solution and stirring for 24 hours. Lines are a guide for the eyes.

Biosorption isotherm modelling

Langmuir and Freundlich isotherm models are used to study the adsorption mechanism for the interaction of heavy metal ions on the adsorbent surface as indicated previously. Langmuir model assumes that the uptake of metal ions occurs on an homogeneous surface by a monolayer deposition⁶⁵. The Freundlich isotherm model follows an empirical equation and is employed to describe the equilibrium process on an heterogeneous surface⁶⁶.

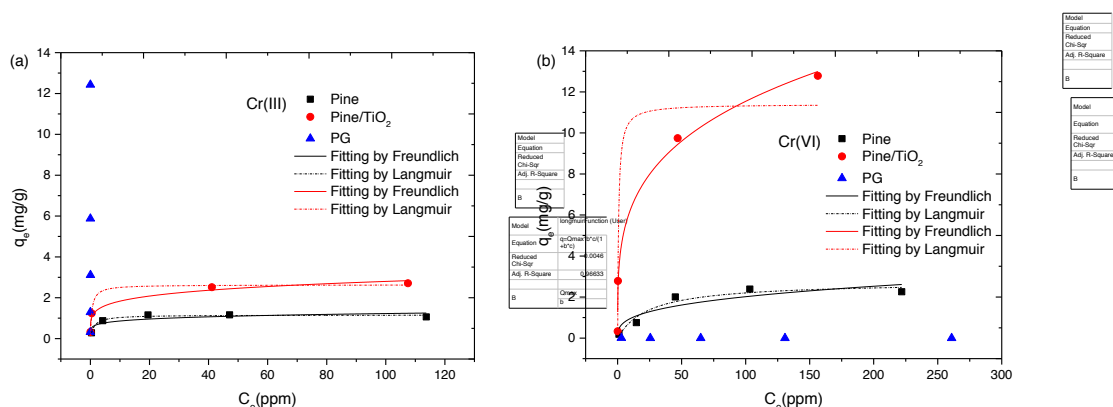


Figure 3.39 Biosorption isotherms modelling of heavy metal in single system by Pine, Pine/TiO₂ and PG. (a) in Cr(III) single system; (b) in Cr(VI) single system. Biosorption conditions were at $T=25\pm 1^\circ\text{C}$, pH 4.0 and stirring for 24 hours.

The biosorption of Cr(III) and Cr(VI) by Pine and Pine/TiO₂ are fitted well with Freundlich (correlation coefficients are listed in Table 3.17 and graphs are shown in Figure 3.39). The biosorption capacity of Cr(III) by PG notable increased than those of Pine. However, PG can be hardly described by both isotherm models probably due to high efficiency adsorption of metal ions by such biomass, and also not find the maximum Cr(III) capacity at the concentration range checked. This could illustrate that the modification of the Pine using TiO₂ and by gasification pyrolysis results in an increase of sites interactions on the material surface, either for Cr(VI) or Cr(III) interaction, respectively. Pine/TiO₂ presents different maximum capacities for Cr(III) and Cr(VI) ions with 1.23 and 12.8 mg/g, respectively, being quite high for Cr(VI). While Pine presents capacities for Cr(III) and Cr(VI) being 1.16 and 2.26 mg/g, respectively, lower than Pine/TiO₂ for Cr(VI) (show in Table 3.17). PG shows high maximum capacity for Cr(III) with 12.4 mg/g, and no adsorption for Cr(VI), showing a clear selectivity for Cr(III). Comparing these models listed in Table 3.17, the experimental data of Cr(III) and Cr(VI) ions are fitted well with both models by Pine/TiO₂, which could be confirmed by correlation coefficient (R²). Pine fits well Langmuir for both species of chromium (even with low maximum capacity), however, PG does not fit any of them. These results show biosorption of Cr by Pine/TiO₂ is monolayer on heterogeneous surface, and biosorption process of pine is monolayer. For the case of PG need further study. Therefore, XAS is discussed in the latter chapter.

Table 3.17 Langmuir and Freundlich isotherm parameters of Cr(III) and Cr(VI) ions onto Pine, Pine/TiO₂ and PG. Biosorption conditions are at T=25±1°C, pH 4.0.

		q _{e,max}	Freundlich			Langmuir		
		(mg/g)	K _f (mg/g)	n	R ²	q _{max} (mg/g)	B (L/mol)	R ²
Cr(III)	Pine	1.16	0.605	0.154	0.616	1.16	0.833	0.966
	Pine/TiO ₂	1.23	1.20	0.184	0.941	2.63	1.97	0.976
	PG	12.4	NA	NA	NA	NA	NA	NA
Cr(VI)	Pine	2.26	0.454	0.324	0.784	2.75	0.0407	0.930
	Pine/TiO ₂	12.8	3.40	0.266	0.982	11.4	1.29	0.938
	PG	0.005	NA	NA	NA	NA	NA	NA

NA means not data

3.4.2 Mechanism study for Cr(III) and Pb(II) by XAS

X-ray absorption spectroscopy (XAS), is unique sensitivity to the local structure, which can be exploited the adsorption mechanism of heavy metal in molecular level^{53,54}. Using this technique, several studies have performed to study the adsorption of biomass/biochar^{55,56}. However, few studies focus on the biosorption of heavy metals from multiple system by biomass/biochar or modified adsorbents at the same time. In this part, the X-ray absorption spectroscopy (XAS) is used to investigate the mechanism of the heavy metal binding to the Pine, Pine/TiO₂ and PG.

XAS is divided into two regimes: X-ray absorption near-edge spectroscopy (XANES) and extended X-ray absorption fine-structure spectroscopy (EXAFS). XANES is sensitive to formal oxidation state and coordination chemistry of absorption atom, while EXAFS is used to determine the distances, coordination number, and species of neighbours of the absorbing atom.

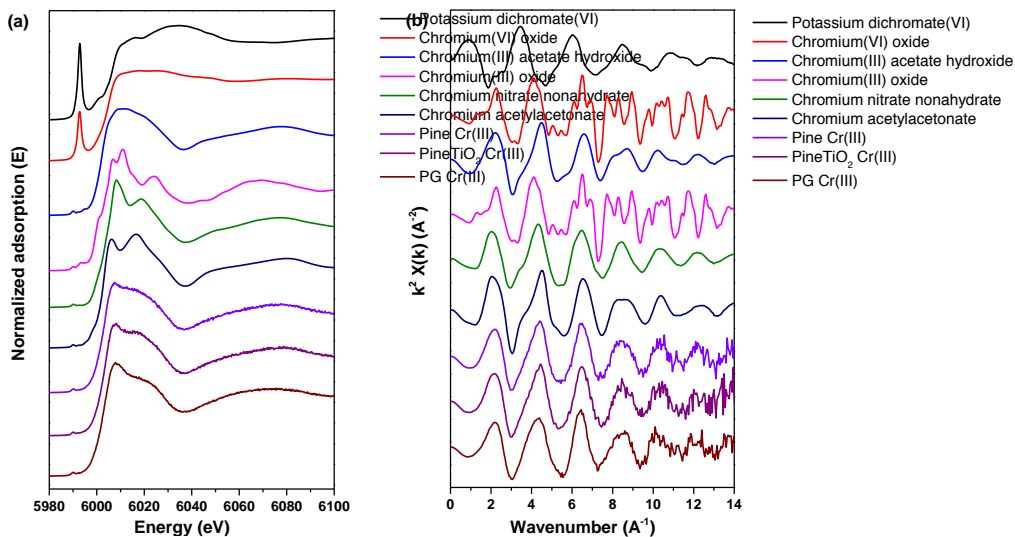
EXAFS can provide us the bond distance between heavy metals and biomass/biochar. This information is unique for each sample, therefore, we can get the useful information (such as function groups and specious) compared with references compounds (specially with XANES). In our case, it could explain which functional groups are responsible for the selective adsorption of the heavy metal species and the enhancement in adsorption capacity after loading pine biomass with TiO₂ particles and pyrolysing it with a gasification procedure.

Adsorption mechanism study of Cr

The XANES data are used to verify the species of heavy metal bound to the adsorbents. As show in Figure 3.40, the XANES spectra of six reference compounds are compared with Pine, PG and Pine/TiO₂ after biosorption from Cr(III) and Cr(VI) single systems. As we can see that Cr(VI) is getting reduced to Cr(III) after the adsorption for all case. Furthermore, the spectra of reduction state of Cr(III) are more similar to the spectra of Cr(III) acetate hydroxide (which includes the possible interaction with COOH functional group), and Cr(III) nitrate nonahydrate. COOH functional group has been identified present in the surface of pine and Pine/TiO₂ in previous ATR-FTIR results. Combined with ATR-FTIR and XANES, the biosorption of Cr by pine and Pine/TiO₂ could be explained by ion exchange with hydrogen ion from carboxylic functional group. The similar spectra to Cr(III) nitrate nonahydrate could be explained by the original aqueous salt solution, which can remain nearby to Cr(III).

Similarly, the biosorption of PG is mainly explained through both ion exchange with mineral components (present in the surface of PG), and also ion exchange with COOH functional groups. To obtain PG high pyrolysis temperatures are used, so there is also a loss of functional groups even not totally. In this sense, the increase of the surface can get a major environment of acetate groups around Cr(III) than the other possibilities.

However, the reduction of Cr(VI) by adsorbents are not clear in this study. Depth study related to this part is needed. From the literature, Cr(VI) is favorable interaction with catechol, a component of tannin present in wood biomass. Later, Cr(VI) can be reduced to Cr(III) after binding with catechol and can ion-exchange with hydrogen ion from carboxylic or hydrogen functional groups. Also, the active carbon of biochar can reduce Cr(VI) to Cr(III). This information helps us explain the reduction mechanism, but need to further study in the future.



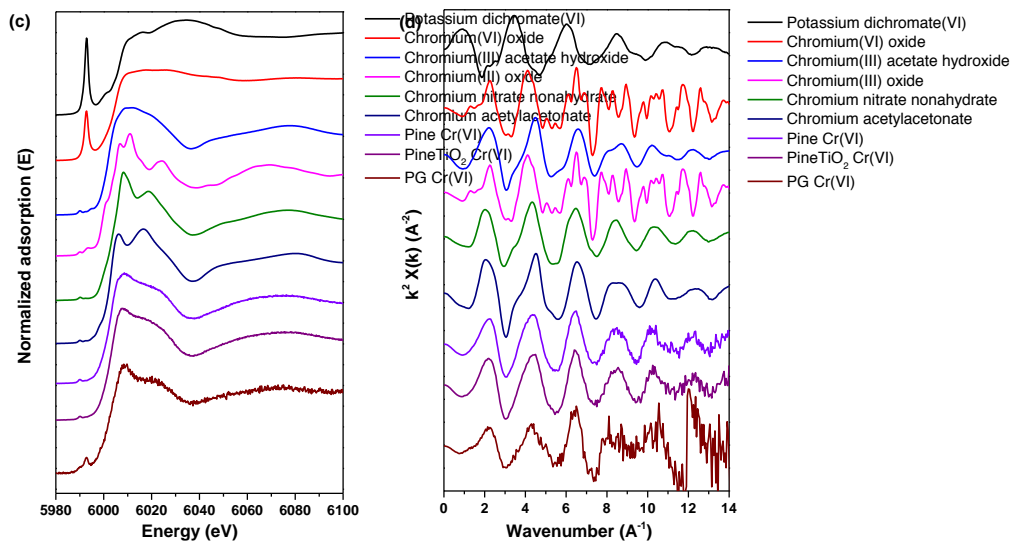


Figure 3.40 XAS spectra of references and Cr-loaded on Pine Pine/ TiO_2 and PG. (a) (b) are the normalized E-edge and k^2 -weighted spectra of XANES in Cr(III) system, (c) and (d) are normalized E-edge and k^2 -weighted of XANES in Cr(VI) systems.

Adsorption mechanism study of Pb(II)

The XANES data are used to verify the species of Pb bound to the biomass. As show in Figure 3.41, are the normalized L3-edge and the k-weighted spectra of XANES of Pine, Pine/ TiO_2 and other reference compounds in single and multi-element systems. Three Pb reference compounds include Lead(II) oxide, Lead(II) acetate trihydrate, Lead(II) nitrate.

Similar to the study of Cr methined above, the spectra of pine, Pine. TiO_2 and PG after biosorption of Pb (from single amd multiple systems) are more similar to the spectra of Pb(II) acetate trihydrate (which includes COOH functional group) for all case. COOH functional group has been identified present in the surface of pine and Pine/ TiO_2 in previous ATR-FTIR results. Combined with ATR-FTIR and XANES, the biosotption of Pb by pine and Pine/ TiO_2 could be explained by ion exchange with hydrogen ion from carboxylic functional group. PG also ion exchange with COOH functional groups even with few functional groups present on its surface.

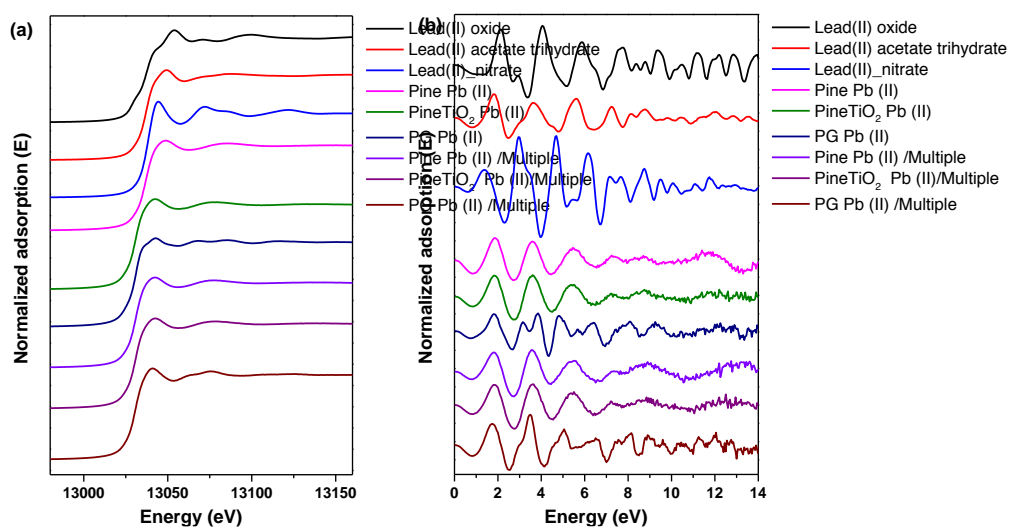


Figure 3.41 XAS spectra of references and Pb-loaded on Pine, Pine/TiO₂ and PG. (a) is the normalized L-edge spectra of XANES of Pb(II) in single and multiple systems, (b) K²-weighted of XANES of Pb(II) in single and multiple systems [composed by Cr(III), Cd(II), Cu(II), Pb(II)].

3.4.3 Summary

✓ Biosorption mechanism study of Cr in pine systems

Three adsorbents have been used successfully for the removal of Cr(III) and Cr(V) from aqueous systems. The biochars loaded with TiO₂ particles have increased the adsorption of Cr. This finding can be explained by an increase in porosity and a pre-concentration of mineral components during the pyrolysis process.

These adsorbents can be used to remove Cr from waste solution. Therefore, biomass could be an interesting alternative to synthetic materials for heavy metal removal. Biochar can also be an alternative with requires biomass pretreatment to enhancement the adsorption capacity.

✓ Biosorption mechanism study of heavy metals in pine systems

The results of XAS show that the adsorption mechanism of both Cr and Pb is ion exchange based, thus Cr and Pb ions exchange with hydrogen ions of the carboxylic acid groups (COOH) of the biomass/biochars systems. For chromium speciation, here we propose a two-step biosorption process for Cr(VI), being first adsorbed and secondly reduced to Cr(III) (which remains by ion exchange interaction with COOH).

3.5 Future trends: Disposal of biosorbents-heavy metals mixture

All the biosorbents loaded with heavy metals can release the immobilized heavy metals as secondary pollutants, especially under acidic conditions²⁴. So, the recycling of such metals is really possible (this has not been the purpose of this PhD thesis).

On another hand, the disposal of waste materials (such as our biomass/biochars systems) containing heavy metals is an important and challenging task. Nowadays, utilization of biosorbent loaded with heavy metal as brick materials is a promising way to solve disposal problem^{67,68}. With this purpose, pine and PG are used as a component (from 12 to 20% v/v) to prepare bricks after heavy metal biosorption. The bricks are properly characterized, so some of their properties of bricks are also checked. This study has been followed in collaboration with Professor Adrian Cristobal from INTEMA (Mar del Plata, Argentina).

There kinds of bricks are produced by adding different biomass/biochar, namely, AAPb20 (Pb loaded on pine, at 20% v/v in the brick), AAM20 (multiple metal ions loaded on pine, at 20% v/v) and APGM12 (multiple metal ions loaded on PG, 12% v/v in brick). All the brick samples are shown in Figure 3.42. To load the biomass/biochar systems, initial aqueous solutions of 0.18 mmol/L of both Pb(II) in single system, and Cr(III), Cu(II), Cd(II) and Pb(II) in multiple metal system are used.

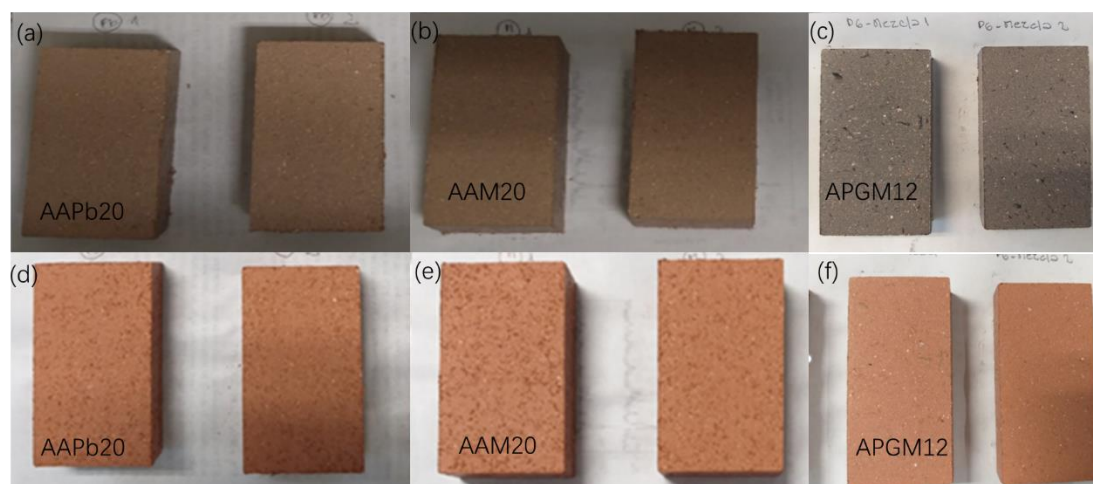


Figure 3.42 Bricks prepared with: (a), (d) AAPb20 pine loaded with Pb (20% v/v), (b), (e) AAM20 pine loaded with multiple metal ions (20% v/v), and (c), (f) APGM12 PG loaded with multiple metal ions (12% v/v). In all cases, the former is before and the latter is after sintered process, respectively.

The bricks are produced by a method as follows: 100 g of clay (from eastern quarry of

Buenos Aires), adding 20% volum of biomass loaded waste and 8 mL of water. While 12% volum of PG is added to bricks (due to the few amount of material). Later, the mixture is placed in a steel mold of 70 mm x 40 mm x 18 mm. Bricks are obtained under a pressure of 25 MPa and maintained for 10 seconds. Then brick samples are dried at room temperature for 24 hours. After drying process, the samples are thermally treated at 950 °C for another 3 hours with a heating rate of 1 °C / min (for sintering).



Figure 3.43 Mold and press machine used to make bricks.

DTA-TGA analysis

Differential thermal and thermal gravimetric analysis (DTA-TGA) are performed to characterize the bricks, in order to check the organic biomass related composition of bricks. Approximately 20 mg of biomass are analyzed by the Shimadzu TGA-50 and Shimadzu DTA-50 equipment, coupled with a TA-50 WSI analyzer, with the heating rate of 10 °C/min up to 1000 °C.

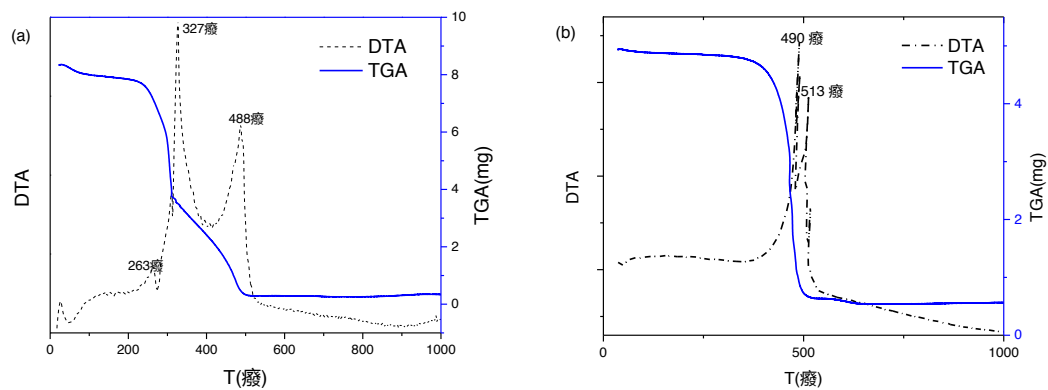


Figure 3.44 DTA-TGA analyses of (a) AAM20 and (b) APGM12.

The DTA results of pine (AAM20, Figure 3.46) show a small peak at 263°C that is assigned to the combustion of volatile components., a wide exothermic peak at 327°C that is attributed to the decomposition of hemicellulose, and then another wide peak with a maximum value at 488°C is corresponded to the co-firing reaction of cellulose and lignin. The TGA curve shows three stages of weight loss, one up to 230°C which corresponds to water and adsorbed gases, a second weight loss assigned to hemicellulose up to 315°C, and a final weight loss of up to 495°C corresponding to cellulose and lignin. It is estimated that there is a composition of 7.2% moisture and gases, 48.2% hemicellulose, 40.1% cellulose and lignin, and 4.5% of the remaining material as inorganic ash. These results indicate that the incorporated biomass burns in a wide range of temperature in the bricks, and not abruptly at a fixed temperature, which allows the slow diffusion of the gaseous products and avoid the cracking of the bricks.

In the case of PG bricks (Figure 3.42c), there are two exothermic peaks observed in DTA spectra. They appear at 490°C and 513°C, corresponding to the co-firing reaction of cellulose and lignin. The TGA curve shows that the weight loss happened around 500°C. Based on these results, it is estimated that 86.8% of cellulose and lignin are lost and only 13.2% of material is still left in the brick.

Compressive strength of bricks

The compression test is the most important test for assuring the engineering quality of a building material. The results of the compressive strength test on the bricks made from clay and from bricks prepared with biomass/biochar mixtures are shown in Table 3.18. The minimum compressive strength should be higher than 4 MPa.

Table 3.18 Compressive strength of bricks

Sample	Compressive strength σ_{rot} (MPa)	Compressive strength σ_{rot} average (MPa)
APGM12_1_	8.43	9.57
APGM12_2_	10.7	
AAPb20_1_	8.37	8.61
AAPb20_2_	8.84	
AAM20_1_	7.88	8.60
AAM20_2_	9.32	

As shown in Table 3.18, all bricks met the requirements of minimum compressive strength. It is concluded that biomass/biochar can be blended with clay to produce a good quality brick.

References

- (1) Wang, H.; Hijmans, R. J.; Res, E. Climate Change and Geographic Shifts in Rice Production in China. *Climate Change and Geographic Shifts in Rice Production in China*. **2019**.
- (2) Liang CHAI, Haojie LI, Benchuan ZHENG, Jinfang ZHANG, Cheng CUI, Jun JIANG, Bi ZHANG, liangcai JIANG, Lintao WU, J. K. Recent Advance, Problems and Outlooks in Rapeseed (Brassica Napus L.) Breeding in China. *Agric. Sci. Technol.* **2017**, *18* (12), 2612–2616.
- (3) Carvalho, J. L. N.; de Figueiredo, E. B.; de Oliveira, B. G.; La Scala, N.; Bordonal, R. de O.; Lal, R. Sustainability of Sugarcane Production in Brazil. A Review. *Agron. Sustain. Dev.* **2018**, *38* (2). <https://doi.org/10.1007/s13593-018-0490-x>.
- (4) Gain Report sees Brazil 2019/20 coffee crop at 59.3 million bags.
- (5) Vilaridi, G.; Palma, L. Di; Verdona, N. Heavy Metals Adsorption by Banana Peels Micro-Powder . Equilibrium Modeling by Non-Linear Models Chinese Journal of Chemical Engineering Heavy Metals Adsorption by Banana Peels Micro-Powder : Equilibrium Modeling by Non-Linear Models. *Chinese J. Chem. Eng.* **2017**, *26* (3), 455–464. <https://doi.org/10.1016/j.cjche.2017.06.026>.
- (6) Colombia: Banana production grew by 4.7% in 2017 <https://www.freshplaza.com/article/2190036/colombia-banana-production-grew-by-4-7-in-2017/>.
- (7) Langan, P.; Naskar, A. K.; Chen, F.; Bidy, M. J.; Wyman, C. E.; Gilna, P.; Davison, B. H.; Saddler, J. N.; Dixon, R. A.; Tschaplinski, T. J.; et al. Lignin Valorization: Improving Lignin Processing in the Biorefinery. *Science (80-)*. **2014**, *344* (6185), 1246843–1246843. <https://doi.org/10.1126/science.1246843>.
- (8) Ge, Y.; Li, Z. Application of Lignin and Its Derivatives in Adsorption of Heavy Metal Ions in Water: A Review. *ACS Sustain. Chem. Eng.* **2018**, *6* (5), 7181–7192. <https://doi.org/10.1021/acssuschemeng.8b01345>.
- (9) Tsang, D. C. W.; Knijnenburg, J. T. N.; Hunt, A. J.; Supanchaiyamat, N.; Jetsrisuparb, K. Lignin Materials for Adsorption: Current Trend, Perspectives and Opportunities. *Bioresour. Technol.* **2018**, *272* (June 2018), 570–581. <https://doi.org/10.1016/j.biortech.2018.09.139>.
- (10) Zou, J.; Dai, Y.; Wang, X.; Ren, Z.; Tian, C.; Pan, K.; Li, S.; Abuobaidah, M.; Fu, H. Structure and Adsorption Properties of Sewage Sludge-Derived Carbon with Removal of Inorganic Impurities and High Porosity. *Bioresour. Technol.* **2013**, *142*, 209–217. <https://doi.org/10.1016/j.biortech.2013.04.064>.
- (11) Smith, K. M.; Fowler, G. D.; Pullket, S.; Graham, N. J. D. Sewage Sludge-Based Adsorbents: A Review of Their Production, Properties and Use in Water Treatment Applications. *Water Res.* **2009**, *43* (10), 2569–2594. <https://doi.org/10.1016/j.watres.2009.02.038>.
- (12) Bagreev, A.; Badosz, T. J.; Locke, D. C. Pore Structure and Surface Chemistry of Adsorbents Obtained by Pyrolysis of Sewage Sludge-Derived Fertilizer. *Carbon N. Y.* **2001**, *39* (13), 1971–

1979. [https://doi.org/10.1016/S0008-6223\(01\)00026-4](https://doi.org/10.1016/S0008-6223(01)00026-4).
- (13) Rozada, F.; Otero, M.; Morán, A.; García, A. I. Adsorption of Heavy Metals onto Sewage Sludge-Derived Materials. *Bioresour. Technol.* **2008**, *99* (14), 6332–6338. <https://doi.org/10.1016/j.biortech.2007.12.015>.
- (14) Ghaffar, S. H.; Fan, M. Lignin in Straw and Its Applications as an Adhesive. *Int. J. Adhes. Adhes.* **2014**, *48*, 92–101. <https://doi.org/10.1016/j.ijadhadh.2013.09.001>.
- (15) Zhang, Y.; Yang, Y.; Tang, K. Physicochemical Characterization and Antioxidant Activity of Quercetin-Loaded Chitosan Nanoparticles Yuying. *Polym. Polym. Compos.* **2007**, *21* (7), 449–456. <https://doi.org/10.1002/app>.
- (16) Gabriel Blázquez, M. A. Martín-Lara, Guadalupe Tenorio, M. C. Batch Biosorption of Lead(II) from Aqueous Solutions by Olive Tree Pruning Waste: Equilibrium, Kinetics and Thermodynamic Study. *Chem. Eng. J.* **2011**, *168* (1), 170–177.
- (17) Yuvaraja, G.; Krishnaiah, N.; Subbaiah, M. V.; Krishnaiah, A. Biosorption of Pb(II) from Aqueous Solution by Solanum Melongena Leaf Powder as a Low-Cost Biosorbent Prepared from Agricultural Waste. *Colloids Surfaces B Biointerfaces* **2014**, *114*, 75–81. <https://doi.org/10.1016/j.colsurfb.2013.09.039>.
- (18) Zulkali, M. M. D.; Ahmad, A. L.; Norulakmal, N. H. Oryza Sativa L. Husk as Heavy Metal Adsorbent: Optimization with Lead as Model Solution. *Bioresour. Technol.* **2006**, *97* (1), 21–25. <https://doi.org/10.1016/j.biortech.2005.02.007>.
- (19) Yu, F.; Sun, L.; Zhou, Y.; Gao, B.; Gao, W.; Bao, C.; Feng, C.; Li, Y. Biosorbents Based on Agricultural Wastes for Ionic Liquid Removal: An Approach to Agricultural Wastes Management. *Chemosphere* **2016**, *165*, 94–99. <https://doi.org/10.1016/j.chemosphere.2016.08.133>.
- (20) Charles F. Baes, R. E. M. *The Hydrolysis of Cations*; 1976.
- (21) Feizi, M.; Jalali, M. Removal of Heavy Metals from Aqueous Solutions Using Sunflower, Potato, Canola and Walnut Shell Residues. *J. Taiwan Inst. Chem. Eng.* **2015**, *54*, 125–136. <https://doi.org/10.1016/j.jtice.2015.03.027>.
- (22) Kar, P.; Misra, M. Use of Keratin Fiber for Separation of Heavy Metals from Water. *J. Chem. Technol. Biotechnol.* **2004**, *79* (11), 1313–1319. <https://doi.org/10.1002/jctb.1132>.
- (23) Wan, S. W. N.; Megat, A. K. M. . Removal of Heavy Metal Ions from Wastewater by Chemically Modified Plant Wastes as Adsorbents: A Review. *Bioresour. Technol.* **2008**, *99* (10), 3935–3948. <https://doi.org/10.1016/j.biortech.2007.06.011>.
- (24) Wang, L.; Wang, Y.; Ma, F.; Tankpa, V.; Bai, S.; Guo, X.; Wang, X. Mechanisms and Reutilization of Modified Biochar Used for Removal of Heavy Metals from Wastewater: A Review. *Sci. Total Environ.* **2019**, *668*, 1298–1309. <https://doi.org/10.1016/j.scitotenv.2019.03.011>.
- (25) Li, H.; Dong, X.; da Silva, E. B.; de Oliveira, L. M.; Chen, Y.; Ma, L. Q. Mechanisms of Metal Sorption by Biochars: Biochar Characteristics and Modifications. *Chemosphere* **2017**, *178*,

- 466–478. <https://doi.org/10.1016/j.chemosphere.2017.03.072>.
- (26) Ding, Z.; Hu, X.; Wan, Y.; Wang, S.; Gao, B. Journal of Industrial and Engineering Chemistry Removal of Lead , Copper , Cadmium , Zinc , and Nickel from Aqueous Solutions by Alkali-Modified Biochar : Batch and Column Tests. *J. Ind. Eng. Chem.* **2016**, *33*, 239–245. <https://doi.org/10.1103/PhysRevB.86.155311>.
- (27) Chen, T.; Zhang, Y.; Wang, H.; Lu, W.; Zhou, Z.; Zhang, Y.; Ren, L. Influence of Pyrolysis Temperature on Characteristics and Heavy Metal Adsorptive Performance of Biochar Derived from Municipal Sewage Sludge. *Bioresour. Technol.* **2014**, *164*, 47–54. <https://doi.org/10.1016/j.biortech.2014.04.048>.
- (28) Hossain, M. K.; Strezov, V.; Chan, K. .; Ziolkowski, A.; Nelson, P. F. Influence of Pyrolysis Temperature on Production and Nutrient Properties of Wastewater Sludge Biochar. *J. Environ. Manage.* **2011**, *92* (1), 223–228. <https://doi.org/10.1016/j.jenvman.2010.09.008>.
- (29) Subedi, R.; Taupe, N.; Pelissetti, S.; Petruzzelli, L.; Bertora, C.; Leahy, J. J.; Grignani, C. Greenhouse Gas Emissions and Soil Properties Following Amendment with Manure-Derived Biochars: Influence of Pyrolysis Temperature and Feedstock Type. *J. Environ. Manage.* **2016**, *166*, 73–83. <https://doi.org/10.1016/j.jenvman.2015.10.007>.
- (30) Shen, Z.; Hou, D.; Jin, F.; Shi, J.; Fan, X.; Tsang, D. C. W.; Alessi, D. S. Effect of Production Temperature on Lead Removal Mechanisms by Rice Straw Biochars. *Sci. Total Environ.* **2019**, *655*, 751–758. <https://doi.org/10.1016/j.scitotenv.2018.11.282>.
- (31) Tan, X.; Liu, Y.; Zeng, G.; Wang, X.; Hu, X.; Gu, Y.; Yang, Z. Application of Biochar for the Removal of Pollutants from Aqueous Solutions. *Chemosphere* **2015**, *125*, 70–85. <https://doi.org/10.1016/j.chemosphere.2014.12.058>.
- (32) Agrafioti, E.; Kalderis, D.; Diamadopoulos, E. Arsenic and Chromium Removal from Water Using Biochars Derived from Rice Husk, Organic Solid Wastes and Sewage Sludge. *J. Environ. Manage.* **2014**, *133*, 309–314. <https://doi.org/10.1016/j.jenvman.2013.12.007>.
- (33) Son, E. B.; Poo, K. M.; Chang, J. S.; Chae, K. J. Heavy Metal Removal from Aqueous Solutions Using Engineered Magnetic Biochars Derived from Waste Marine Macro-Algal Biomass. *Sci. Total Environ.* **2018**, *615*, 161–168. <https://doi.org/10.1016/j.scitotenv.2017.09.171>.
- (34) Kizito, S.; Wu, S.; Kipkemoi Kirui, W.; Lei, M.; Lu, Q.; Bah, H.; Dong, R. Evaluation of Slow Pyrolyzed Wood and Rice Husks Biochar for Adsorption of Ammonium Nitrogen from Piggery Manure Anaerobic Digestate Slurry. *Sci. Total Environ.* **2015**, *505*, 102–112. <https://doi.org/10.1016/j.scitotenv.2014.09.096>.
- (35) Huff, M. D.; Lee, J. W. Biochar-Surface Oxygenation with Hydrogen Peroxide. *J. Environ. Manage.* **2016**, *165*, 17–21. <https://doi.org/10.1016/j.jenvman.2015.08.046>.
- (36) Nguyen, H.; You, S.; Hosseini-bandegharai, A. Mistakes and Inconsistencies Regarding Adsorption of Contaminants from Aqueous Solutions : A Critical Review. *Water Res.* **2017**, *120*, 88–116. <https://doi.org/10.1016/j.watres.2017.04.014>.

- (37) Argun, M. E.; Dursun, S.; Karatas, M.; Gürü, M. Activation of Pine Cone Using Fenton Oxidation for Cd(II) and Pb(II) Removal. *Bioresour. Technol.* **2008**, *99* (18), 8691–8698. <https://doi.org/10.1016/j.biortech.2008.04.014>.
- (38) Ofomaja, A. E.; Naidoo, E. B.; Modise, S. J. Biosorption of Copper(II) and Lead(II) onto Potassium Hydroxide Treated Pine Cone Powder. *J. Environ. Manage.* **2010**, *91* (8), 1674–1685. <https://doi.org/10.1016/j.jenvman.2010.03.005>.
- (39) Wang, H.; Gao, B.; Wang, S.; Fang, J.; Xue, Y.; Yang, K. Removal of Pb(II), Cu(II), and Cd(II) from Aqueous Solutions by Biochar Derived from KMnO₄ Treated Hickory Wood. *Bioresour. Technol.* **2015**, *197*, 356–362. <https://doi.org/10.1016/j.biortech.2015.08.132>.
- (40) Klapiszewski, Ł.; Siwińska-Stefańska, K.; Kołodziejka, D. Preparation and Characterization of Novel TiO₂/Lignin and TiO₂-SiO₂/Lignin Hybrids and Their Use as Functional Biosorbents for Pb(II). *Chem. Eng. J.* **2017**, *314*, 169–181. <https://doi.org/10.1016/j.cej.2016.12.114>.
- (41) Tao, Y.; Xue, B.; Zhong, J.; Yao, S.; Wu, Q. Influences of PH , Heavy Metals and Phosphate and Their Co-Influences on the Sorption of Pentachlorophenol on Cyanobacterial Biomass. *Water Res.* **2012**, *46* (11), 3585–3594. <https://doi.org/10.1016/j.watres.2012.04.003>.
- (42) Chong, H. L. H.; Chia, P. S.; Ahmad, M. N. The Adsorption of Heavy Metal by Bornean Oil Palm Shell and Its Potential Application as Constructed Wetland Media. *Bioresour. Technol.* **2013**, *130*, 181–186. <https://doi.org/10.1016/j.biortech.2012.11.136>.
- (43) Chakravarty, R.; Khan, M. M. R.; Das, A. R.; Guha, A. K. Biosorptive Removal of Chromium by Husk of Lathyrus Sativus: Evaluation of the Binding Mechanism, Kinetic and Equilibrium Study. *Eng. Life Sci.* **2013**, *13* (3), 312–322. <https://doi.org/10.1002/elsc.201200044>.
- (44) Basso, M. C.; Cerrella, E. G.; Cukierman, A. L. Lignocellulosic Materials as Potential Biosorbents of Trace Toxic Metals from Wastewater. *Ind. Eng. Chem. Res.* **2002**, *41* (15), 3580–3585. <https://doi.org/10.1021/ie020023h>.
- (45) Lagergren, S. About the Theory of So-Called Adsorption of Soluble Substances, Kungliga Svenska Vetenskapsakademiens. *Band 1898*, *24* (4), 39.
- (46) Blanchard, G.; Maunaye, M.; Martin, G. Removal of Heavy Metals from Waters by Means of Natural Zeolites. *Water Res.* **1984**, *18* (12), 1501–1507. [https://doi.org/http://dx.doi.org/10.1016/0043-1354\(84\)90124-6](https://doi.org/http://dx.doi.org/10.1016/0043-1354(84)90124-6).
- (47) Lee, S. Y.; Choi, H. J. Persimmon Leaf Bio-Waste for Adsorptive Removal of Heavy Metals from Aqueous Solution. *J. Environ. Manage.* **2018**, *209*, 382–392. <https://doi.org/10.1016/j.jenvman.2017.12.080>.
- (48) Vikrant, S.; Tony, Sarvinder, S.; K.K.Pant. Thermodynamic and Breakthrough Column Studies for the Selective Sorption of Chromium from Industrial Effluent on Activated Eucalyptus Bark. *Bioresour. Technol.* **2006**, *97* (16), 1986–1993. <https://doi.org/10.1016/j.biortech.2005.10.001>.
- (49) Miretzky, P.; A. Fernandez Cirelli. Cr(VI) and Cr(III) Removal from Aqueous Solution by Raw

- and Modified Lignocellulosic Materials: A Review. *J. Hazard. Mater.* **2010**, *180* (1–3), 1–19. <https://doi.org/10.1016/j.jhazmat.2010.04.060>.
- (50) Robert M. Sterritt; John N. Lester. Significance and Behaviour of Heavy Metals in Waste Water Treatment Processes III. Speciation in Waste Waters and Related Complex Matrices. *Sci. Total Environ.* **1984**, *34* (1–2), 117–141.
- (51) Nath, K.; Nishith, K. Hexavalent Chromium: Toxicity and Its Impact on Certain Aspects of Carbohydrate Metabolism of the Freshwater Teleost, *Colisa Fasciatus*. *Sci. Total environment* **1988**, *72*, 175–181.
- (52) Pellerin, C.; Booker, S. Reflections on Hexavalent Chromium: Health Hazards of an Industrial Heavyweight. *Env. Heal. Perspect* **2000**, *108* (9), A402-7.
- (53) Cui, L.; Noerpel, M. R.; Scheckel, K. G.; Ippolito, J. A. Wheat Straw Biochar Reduces Environmental Cadmium Bioavailability. *Environ. Int.* **2019**, *126* (January), 69–75. <https://doi.org/10.1016/j.envint.2019.02.022>.
- (54) Whaley-Martin, K. J.; Koch, I.; Reimer, K. J. Determination of Arsenic Species in Edible Periwinkles (*Littorina Littorea*) by HPLC-ICPMS and XAS along a Contamination Gradient. *Sci. Total Environ.* **2013**, *456–457*, 148–153. <https://doi.org/10.1016/j.scitotenv.2013.03.066>.
- (55) Rajapaksha, A. U.; Alam, M. S.; Chen, N.; Alessi, D. S.; Igalavithana, A. D.; Tsang, D. C. W.; Ok, Y. S. Removal of Hexavalent Chromium in Aqueous Solutions Using Biochar: Chemical and Spectroscopic Investigations. *Sci. Total Environ.* **2018**, *625*, 1567–1573. <https://doi.org/10.1016/j.scitotenv.2017.12.195>.
- (56) Jiang, W.; Cai, Q.; Xu, W.; Yang, M.; Cai, Y.; Dionysiou, D. D.; O’Shea, K. E. Cr(VI) Adsorption and Reduction by Humic Acid Coated on Magnetite. *Environ. Sci. Technol.* **2014**, *48* (14), 8078–8085. <https://doi.org/10.1021/es405804m>.
- (57) Mohammad, A.-W.; Abdulrasoul, A.; Ahmed H., E.-N.; Mahmoud E.A., N.; Adel R. A., U. Pyrolysis Temperature Induced Changes in Characteristics and Chemical Composition of Biochar Produced from *Conocarpus* Wastes. *Bioresour. Technol.* **2013**, *131*, 374–379. <https://doi.org/10.1016/j.biortech.2012.12.165>.
- (58) Marks, E. A. N.; Mattana, S.; Alcañiz, J. M.; Domene, X. Biochars Provoke Diverse Soil Mesofauna Reproductive Responses Inlaboratory Bioassays. *Eur. J. Soil Biol.* **2014**, *60*, 104–111. <https://doi.org/10.1016/j.ejsobi.2013.12.002>.
- (59) Chen, Y.; Wang, B.; Xin, J.; Sun, P.; Wu, D. Adsorption Behavior and Mechanism of Cr(VI) by Modified Biochar Derived from *Enteromorpha Prolifera*. *Ecotoxicol. Environ. Saf.* **2018**, *164* (August), 440–447. <https://doi.org/10.1016/j.ecoenv.2018.08.024>.
- (60) Yuan, J. H.; Xu, R. K.; Zhang, H. The Forms of Alkalis in the Biochar Produced from Crop Residues at Different Temperatures. *Bioresour. Technol.* **2011**, *102* (3), 3488–3497. <https://doi.org/10.1016/j.biortech.2010.11.018>.
- (61) Sun, B.; Reddy, E. P.; Smirniotis, P. G. Visible Light Cr(VI) Reduction and Organic Chemical

- Oxidation by TiO₂ Photocatalysis. *Environ. Sci. Technol.* **2005**, *39* (16), 6251–6259.
<https://doi.org/10.1021/es0480872>.
- (62) Liu, W.; Ni, J.; Yin, X. Synergy of Photocatalysis and Adsorption for Simultaneous Removal of Cr(VI) and Cr(III) with TiO₂ and Titanate Nanotubes. *Water Res.* **2014**, *53* (lii), 12–25.
<https://doi.org/10.1016/j.watres.2013.12.043>.
- (63) Wang, Q.; Shi, X.; Xu, J.; Crittenden, J. C.; Liu, E.; Zhang, Y.; Cong, Y. Highly Enhanced Photocatalytic Reduction of Cr(VI) on AgI/TiO₂ under Visible Light Irradiation: Influence of Calcination Temperature. *J. Hazard. Mater.* **2016**, *307*, 213–220.
<https://doi.org/10.1016/j.jhazmat.2015.12.050>.
- (64) Joshi, K. M.; Shrivastava, V. S. Photocatalytic Degradation of Chromium (VI) from Wastewater Using Nanomaterials like TiO₂, ZnO, and CdS. *Appl. Nanosci.* **2011**, *1* (3), 147–155.
<https://doi.org/10.1007/s13204-011-0023-2>.
- (65) Rahman, M. S.; Islam, M. R. Effects of PH on Isotherms Modeling for Cu(II) Ions Adsorption Using Maple Wood Sawdust. *Chem. Eng. J.* **2009**, *149* (1–3), 273–280.
<https://doi.org/10.1016/j.cej.2008.11.029>.
- (66) Baseri, H.; Tizro, S. Treatment of Nickel Ions from Contaminated Water by Magnetite Based Nanocomposite Adsorbents: Effects of Thermodynamic and Kinetic Parameters and Modeling with Langmuir and Freundlich Isotherms. *Process Saf. Environ. Prot.* **2017**, *109*, 465–477.
<https://doi.org/10.1016/j.psep.2017.04.022>.
- (67) Benlalla, A.; Elmoussaouiti, M.; Dahhou, M.; Assafi, M. Utilization of Water Treatment Plant Sludge in Structural Ceramics Bricks. *Appl. Clay Sci.* **2015**, *118*, 171–177.
<https://doi.org/10.1016/j.clay.2015.09.012>.
- (68) Muñoz V., P.; Morales O., M. P.; Letelier G., V.; Mendivil G., M. A. Fired Clay Bricks Made by Adding Wastes: Assessment of the Impact on Physical, Mechanical and Thermal Properties. *Constr. Build. Mater.* **2016**, *125*, 241–252.
<https://doi.org/10.1016/j.conbuildmat.2016.08.024>.

Chapter 4

Conclusions

Conclusions

In this study, biosorbents from biomasses and modified biomasses have been used to remove Cr(III), Cd(II), Cu(II) and Pb(II) ions from single and multiple systems. Cr mainly Cr(III) and Cr(VI) are specially studied. Characterization of the biosorbents including SEM and ATR-FTIR were performed for all biomasses to study their morphology and metal binding groups. BET and zeta potential were performed for part of the biosorbents to study the surface area and charge. Different parameters of biosorption processes are optimized in batch systems, including the pH of solution, the initial concentration, the contact time and the temperature. Kinetics modelling is performed to better understand the biosorption process, including the pseudo-first order, the pseudo-second order, the Elovich model and intraparticle diffusion models to fit the experimental data. Isotherm modeling, including Langmuir and Freundlich models, is also checked to study the biosorption process. Furthermore, XAS was used to explain the adsorption mechanism of heavy metal in molecular level for biosorbents from pine systems. The main conclusions are presented here in the following.

1. Characteration of biosorbents by SEM, ATR-FTIR, XRD, BET and zeta potential.

The morphological structures are different depending on the groups of biomass residues from SEM results. The ATR-FTIR results show that carboxyl group present in all biomasses which is assigned to be the main responsible for heavy metals biosorption, as reported elsewhere. In addition, the concentration of metals loaded onto biomasses does not affect the ATR-FTIR spectra of the functional groups for the biomass of poplar (CO). The same behaviour is expected for the rest of biomasses. XRD analysis is performed to study the crystallinity of the TiO₂ particles loaded inside biomass. XRD result shows that an amorphous porous biomass structure for Pine/TiO₂. This may be due to the small loading of the TiO₂ to the amorphous character of the particles. BET analysis show that the surface area, pore volume and size of Pine/TiO₂ and PG all highly increased compared with pine, which is corresponding with their biosorption capacities. Therefore, surface area and pore structure are key points to influence heavy metal removal. Zeta potential values show that all biosorbents are negative charge on the surface at pH 4.0. While biochar and modified biomass show higher negative than raw biomass, so they can better interact with the cationic species of heavy metals in solution at this pH 4.0. The pH of the materials and the mineral content are two factors also characterized here that

give important information, i.e. to confirm the ionic exchange biosorption process of heavy metals by functional groups of the biomass (as carboxylic acid).

2. Comparison of biosorption from different biosorbent systems.

Different types of feedstocks (poplar, corn, sludge waste) and their biochars are used to study the biosorption capacity from a mixture of multiple heavy metals. The results show that the adsorption capacity is dependent on the type of feedstock and on the pyrolysis conditions. The adsorption capacity of the biomass types is ranked as follows: FO (from industry sludge waste) > ZO (from agriculture corn biomass waste) >> CO (from wood poplar biomass waste). Biochars, which are the product of the pyrolysis of feedstocks, clearly improve the adsorption efficiency in the case of those derived from wood and agricultural biomasses. The mineral composition in biochars was higher than from the corresponding biomasses, due to a preconcentration of them under the pyrolysis process. These minerals can also be ion exchanged with the heavy metals in the solution. Furthermore, also the presence of some compound from tannins and lignin (especially in biomass systems) can facilitate the biosorption by complexation process. In summary, complexation and cation exchange have been found to be the two main adsorption mechanisms in systems containing multiple heavy metals, with cation exchange being the most significant, as seen when characterising the materials by SEM and ATR-FTIR. All the waste biomasses presented here are good alternatives for heavy metal removal from wastewaters.

Furthermore, pine and Pine/TiO₂, have been used as sorbents for the removal of heavy metals. Pine show better adsorption capacity for all the elements in single-element system (as expected due to adsorption competition in the multi-element system). On the other hand, Pine/TiO₂ has higher adsorption capacity in both systems, in single and multi-element one, even under heavy metal competition system. This can be explained due to the increase on surface area, pore volume and size of Pine/TiO₂, as seen from BET results, which is mentioned before. Moreover, as in the preparation of Pine/TiO₂ there is pyrolysis step, also the relative increase on mineral content can participate in the increase of the heavy metals biosorption in this material.

Moreover, pine, Pine/TiO₂ and PG are used to remove Cr(III) and Cr(VI) ions from aqueous solution. As a summary, results show that the adsorption of Cr(III) is mainly

through ion exchange with either carboxylic groups mainly with pine, and either with the mineral components present on the other biomaterials surfaces (Pine/TiO₂ and PG) . Pyrolysis process can increase the concentration of such minerals to increase the adsorption capacity. For Pine/TiO₂, together with the ion exchange as main responsible of the biosorption of chromium, also complexation with catechol can help Cr(VI) adsorption.

3. Mechanism study for Cr(III) and Pb(II) by XAS

The results of XAS can confirm that the adsorption mechanism of both Cr and Pb is ion exchange based mainly, thus Cr and Pb ions exchange with hydrogen ions of the carboxylic acid groups (COOH) of the biomass/biochars systems. For chromium speciation, also from XAS results we can propose a two-step biosorption process for Cr(VI), being first adsorbed and secondly reduced to Cr(III) (which remains by ion exchange interaction with COOH).

4. Utilization of biosorbent loaded with heavy metal as brick component

Pine and PG are used as a component (from 12 to 20% v/v) to prepare bricks after heavy metal biosorption. Both bricks met the requirements standards and can be blended with clay to produce a good quality brick, which is a favorable future application.

In conclusion, these biosorbents are shown to be a promising material, and they are also expected to be applied in large scale to deal with the polluted water all over the world.

Annex

Annex I

Article submitted to *Scientific Reports*. Under Revision process.

Comparison of biochars derived from different types of feedstock and their potential for heavy metal removal in multiple-metal solutions

Jing-Jing Zhao^{1,2,#}, Xin-Jie Shen^{1,#}, Xavier-Domene^{3,4}, Josep-Maria Alcañiz^{3,4}, Xing Liao^{1*}, Cristina Palet^{2*}

¹Oil Crops Research Institute of Chinese Academy of Agricultural Sciences/Key Laboratory of Biology and Genetic Improvement of Oil Crops of the Ministry of Agriculture, Wuhan 430062, China

²GTS-UAB Research Group, Department of Chemistry, Facultat de Ciències, Universitat Autònoma de Barcelona, 08193 Cerdanyola del Vallès, Catalunya, Spain

³Centre for Research on Ecology and Forestry Applications (CREAF) and ⁴Universitat Autònoma Barcelona, 08193 Cerdanyola del Vallès, Spain

These authors contributed equally to this work.

*Correspondence to:

Cristina Palet, Professor, PhD., GTS-UAB Research Group, Department of Chemistry, Facultat de Ciències, Universitat Autònoma de Barcelona, 08193 Cerdanyola del Vallès, Catalunya, Spain, cristina.palet@uab.cat

Xing Liao, Professor., Oil Crops Research Institute of Chinese Academy of Agricultural Sciences/Key Laboratory of Biology and Genetic Improvement of Oil Crops of the Ministry of Agriculture, Wuhan 430062, China, liao@oilcrops.cn

Abstract

Three different types of feedstocks and their biochars were used to remove Cr(III), Cd(II), Cu(II) and Pb(II) ions from a mixture of multiple heavy metals. The effect of the initial concentration of heavy metals in solution has been analysed, and kinetics modelling and a comparison of the adsorption capacity of such materials have been performed to elucidate the possible adsorption mechanisms. The results show that the adsorption capacity is dependent on the type of feedstock and on the pyrolysis conditions. The adsorption capacity of the biomass types is ranked as follows: FO (from sewage sludge) >> LO > ZO (both from agriculture biomass waste) >> CO (from wood biomass waste). Biochars, which are the product of the pyrolysis of feedstocks, clearly improve the adsorption efficiency in the case of those derived from wood and agricultural biomasses. Complexation and cation exchange have been found to be the two main adsorption mechanisms in systems containing multiple heavy metals, with cation exchange being the most significant. The pore structure of biomass/biochar cannot be neglected when investigating the adsorption mechanism of each material. All the disposal biomasses presented here are good alternatives for heavy metal removal from wastewaters.

Introduction

Chromium, copper, cadmium and lead are the main heavy metal species in the wastewater industry^{1,2}. Relatively modest concentrations of Cr(III), Cd(II) and Pb(II) have toxic effects on the environment and humans. Cu(II) is also a potential toxicant at high doses³. According to the World Health Organization (WHO), maximum concentration limits of Cr(III), Cu(II), Cd(II) and Pb(II) (<0.55 mg/L for Cr(III), <0.017 mg/L for Cu(II), <0.01 mg/L for Cd(II), and <0.065 mg/L for Pb) have been established for irrigation water⁴⁻⁷. To address heavy metal contamination, biosorption is a promising technique for the removal of contaminants from wastewaters due to its low cost and eco-friendly nature compared with other methods^{8,9}. Biosorption processes are based on the use of feedstocks or biomasses, which are usually wastes from agriculture, wood from forests, and sewage industrial sludge¹⁰⁻¹².

On the other hand, biochar is a porous carbonaceous material obtained during the oxygen-limited pyrolysis of biomass derived from a variety of feedstocks¹³. Biochar has proven to be effective in the removal of heavy metal contaminants from wastewaters due to its specific properties, such as a large surface area, a porous structure, surface-enriched functional groups and the presence of some mineral components^{14,15}. The heavy metal adsorption efficiency of biochars can vary widely depending on the types of feedstocks and the pyrolysis temperature^{16,17}. The most commonly used feedstock to produce biochar is agricultural waste, such as corn, rice, fruit peels, and wood from forests. In addition, biochar derived from original materials, such as daily manure, wastewater sludges and micro algae, has also been studied in the last decade¹⁸⁻²⁰. Therefore, a large body of literature focuses on the use of biochar to remove heavy metals, such as Pb(II), Cu(II), Cr(III), Cd(II), Ni(II) and Zn(II), which are the most studied metals from wastewaters^{21,22}. Biochar has good removal efficiencies in single-metal systems but lower capacities in multiple-metal systems due to the competition between the heavy metals present in wastewaters. Based on the literature, five sorption mechanisms have been proposed to explain biochar adsorption systems, which vary considerably with biochar properties and the target metals. These mechanisms include electrostatic interactions, cation exchange, complexation with functional groups, metal precipitation and reduction of metal species^{9,14}. However, few studies have compared the sorption capacities of biochar derived from different types of feedstocks via different sorption mechanisms in multiple-heavy-metal systems. Therefore, it is necessary to study the sorption mechanisms of heavy metals on biochar to improve the metal removal efficiency and guide the application of biochar in the future. Most importantly, biochar application can help solve the large worldwide problem of biomass disposal.

In this study, three types of feedstock from wood, agriculture and industrial sewage sludge wastes were used to remove Cr(III), Cd(II), Cu(II) and Pb(II) ions from

multiple-metal systems. Additionally, three biochars were produced from poplar, corn and sewage sludge to determine the influence of the pyrolysis process on the adsorption systems. The objectives of this study are (1) to compare the adsorption capacities of the three different types of feedstocks and derived biochars and (2) to evaluate the possible adsorption mechanisms of biochar in multiple-heavy-metal systems.

Materials and Methods

Biomass and biochars

Biomass obtained from different sources, namely, poplar biomass (CO, from wood), sewage sludge (PO, from industry sewage sludge wastes), corn (ZO) and *Brassica napus* (LO) biomasses (both from agriculture wastes), were chosen to evaluate their adsorption capacities, and were all used to remove Cr(III), Cd(II), Cu(II) and Pb(II) ions in multiple-metal systems. Additionally, three biochars (CL, ZL and FL) were produced from poplar, corn and sewage sludge, respectively. These biochars were thermally dried and pyrolysed at the Prat del Llobregat wastewater treatment plant (WWTP) (Barcelona, Spain), and all were produced by slow pyrolysis processes. The temperature conditions and duration of the pyrolysis processes, together with a description of the original biomasses, are listed in Table 1. While poplar, corn, sewage sludge and their biochars were kindly provided by the Centre for Research on Ecology and Forestry Applications (CREAF, Barcelona, Spain), *Brassica napus* is produced in China and was kindly provided by the Oil Crops Research Institute, Chinese Academy of Agricultural Sciences, Wuhan.

Chemical and reagents

All the chemicals were analytical grade. A 1,000 mg/L stock solution of a multiple-element system was prepared by dissolving the required amounts of Cr(NO₃)₃·9H₂O, Cu(NO₃)₂·3H₂O, Cd(NO₃)₂·4H₂O and Pb(NO₃)₂ (all 99% from Panreac, Barcelona, Spain).

Characterization of adsorbents

The physicochemical properties of biochar, including pH, surface area, porosity, surface charge, functional groups, and mineral contents, play an important role in explaining the process of sorption of metals. The morphologies of biomasses and their biochars were analysed by scanning electron microscopy (SEM) at the Electron Microscopy Facilities of the *Universitat Autònoma de Barcelona* (UAB, Catalunya, Spain). Attenuated total reflectance Fourier transform infrared spectroscopy (ATR-FTIR, Tensor 27, Bruker, USA) was performed to identify the chemical functional groups present on the adsorbents. FTIR data were obtained in the wavenumber

range of 600 to 4000 cm^{-1} with an average of 16 or 64 scans at 4.0 cm^{-1} resolution at *Servei d'Anàlisi de Química* (UAB, Catalunya, Spain). A Flash 2000 C.E. Elemental Analyzer (Thermo Fisher Scientific, USA) was used to analyse the C and H components of the biochars. A Flash EA 1112 Elemental Analyzer (Thermo Fisher Scientific, USA) was used to analyse N. Inductively coupled plasma optical emission spectrometry (ICP-OES) using a Varian 725-ES Radial ICP Optical Emission Spectrometer (Varian Inc., USA) was used to analyse K, Ca, Mg and P. The O/C, H/C and N/C ratios were calculated from the molar concentrations of the elements of interest, and each ratio was calculated by dividing the total weight of the element by its molecular weight²³. The pH was measured as follows: biochars were prepared in triplicate by adding water at a ratio of 1:10 (biochar/g:deionized water/mL) and vertically agitating for 24 h at a speed of 60 rpm. Then, the suspensions were vacuum filtered with Whatman 42 filter paper, and the pH was measured immediately²³. The components of the biochars and the pH were analysed at CREAM, and the measurement equipment was all from *Servei d'Anàlisi de Química* (UAB, Catalunya, Spain).

Batch adsorption experiments

Adsorption experiments were carried out at room temperature ($25 \pm 1^\circ\text{C}$). Multiple-metal solutions (containing Cr(III), Cu(II), Cd(II) and Pb(II)) were prepared from 1,000 ppm initial stock solutions of each metal, and the concentration ranged from 5 to 100 ppm. Batch experiments were performed by adding 25 mg of adsorbent in 5 mL tubes and then adding 2.5 mL of heavy metal aqueous solutions. The tubes were then placed on a rotary mixer (CE 2000 ABT-4, SBS Instruments SA, Barcelona, Spain) and shaken at 25 rpm for 24 h. The two phases were separated by decantation and filtered through 0.22 μm Millipore filters (Millex-GS, Millipore). The concentrations of heavy metals in the supernatant phase were analysed by ICP-mass spectrometry (MS) (XSERIES 2 ICP-MS, Thermo Scientific, USA). The adsorption of the selected heavy metals by the adsorbents was expressed as the adsorption percentage calculated by using Equation (1). Furthermore, the capacity of the adsorbent was calculated by using Equation (2):

$$\% \text{ Adsorption} = \frac{(C_0 - C_e)}{C_0} \times 100 \quad (1)$$

$$q_e = \frac{(C_0 - C_e) \times V}{m} \quad (2)$$

where q_e (mg/g) is the capacity of the adsorbent, expressed as the amount of heavy metal per adsorbent mass unit at equilibrium; V (L) is the volume of the heavy metal solution; C_0 and C_e are the initial and equilibrium heavy metal concentrations in solution (both in mg/L), respectively; and m (g) is the dry weight of the adsorbent. To study the adsorption mechanism, it is more convenient to convert q_e into mmol/g. All

the results are expressed as the mean value of duplicate measurements.

Results and Discussion

Comparison of biosorbent adsorption properties

As indicated in the previous section, four feedstocks and three biochars were used to remove Cr(III), Cd(II), Cu(II) and Pb(II) ions in multiple-metal systems: biomass PO (poplar from wood), FO (sewage sludge from solid industrial waste), ZO (corn from agriculture waste), and LO (*Brassica napus* from agriculture waste). Additionally, biochars obtained by the pyrolysis of PO, FO and ZO (PL, FL and ZL, respectively) were evaluated as heavy metal adsorbents. These seven sorbents show different biosorption capacities for the different metal ions, as shown in Figure 1. In general, for all metals, biochars have better sorption capacity than the original biomass, which can be explained by surface changes during the pyrolysis process, such as changes in porosity, functional groups and mineral content. Based on the literature, high pyrolysis temperatures lead to increased porosity and surface area compared with the original biomaterial (as shown in Figure 2). High porosity and large surface areas can increase the adsorption of metals²⁴. High temperature also increases the concentration of minerals (K, Ca, Mg and P) on the surface of sorbents that can be used for ion exchange with heavy metals^{24–26}. Minerals from biomass are not burned, so the pyrolysis process acts as a mineral pre-concentration step. The adsorption percentages according to the type of feedstock were ranked as follows: sewage sludge (FO) >> agriculture waste biomass (LO) > (ZO) >> wood biomass (CO). This ranking can be explained by the different mineral compositions and functional groups present, which is confirmed by the measured adsorption capacity (see Table 2, Figure 3 and part of the effect of the initial concentration).

SEM characterization

SEM was used to study the morphological structure of the biomass and biochar. As shown in Figure 2, biochars CL and ZL show more pore structures than CO and ZO, respectively. Furthermore, FL did not have much change in porosity compared with the original biomass FO (see Figure 2). Additionally, LO has been shown to have a higher heavy metal removal efficiency than CO and ZO (see Figure 1), which can be explained by the high porosity and the large pore size of LO. This behaviour clearly shows that LO has a pore structure similar to that of CL and ZL, even before pyrolysis (see Figure 2). Thus, the results presented here demonstrate that pore structure is a key factor that can influence the sorption of heavy metals onto biomass, and Bagreev et al reported similar results^{27–29}.

ATR-FTIR characterization analysis

ATR-FTIR analysis was carried out to identify the functional groups present in the different adsorbents that might be involved in the sorption process. FTIR spectra of

biomass and their biochars are shown in Figure 3 (a)–(d). The wavenumbers and approximate assignments of the vibrational modes for the FTIR spectra are listed in Table 3. The peaks at 3200–3270 cm^{-1} and 1780–1710 cm^{-1} correspond to the O–H and C=O stretching vibrations, respectively, which confirms the presence of carboxyl groups on the adsorbents³⁰. Carboxyl acid groups are very useful for the adsorption of heavy metal ions and can be found in most of the adsorbents studied here (ZO, ZL, CO, CL, LO), except for FO (sewage sludge) and the corresponding biochar FL (see Figure 3c). These differences can be explained by the compositions of ZO, CO, and LO, which are cellulose and lignin-based biomasses that contain carboxyl groups. However, FO and FL are from industry sewage sludge, and their main components are carbon, hydrogen, oxygen and nitrogen, which are suitable for the production of activated carbon³¹.

Furthermore, a decrease in the intensity of the peaks corresponding to carboxyl (–COOH) and hydroxyl (–OH) groups is observed in the FTIR spectra after pyrolysis, probably due to the loss of functional groups in the lignocellulosic materials with increasing temperature. The decrease in the H/C and O/C atomic ratios for biochars (Table 2) confirms this hypothesis. On the other hand, a reduction in the amounts of negative surface charges (related to functional groups such as –COOH, –COH and –OH) will increase the pH of the biochar and, thus, the metal adsorption efficiency of such materials³². In this sense, ZL (pH 10.3) has been found to have higher adsorption of heavy metals than CL (pH 8.21). The adsorption results for these biochars were as follows: LO > ZL > CL (see Figure 1). The finding that LO has a higher adsorption efficiency than ZL and CL can be explained by the higher amount of carboxyl functional groups on the surface of LO that are available to react with heavy metals (see Figure 3d).

Mineral composition analysis

Based on the literature, mineral composition, including potassium (K), calcium (Ca), magnesium (Mg) and phosphorus (P) in biomass and biochar, is also responsible for metal adsorption from aqueous solutions^{14,33}. As seen from the results of the mineral composition analysis of all adsorbents under study (collected in Table 2), the mineral concentrations of FO and FL (from sewage sludge) are much higher than those of agriculture waste (ZO, LO) and wood biomass (CO). Furthermore, the concentrations of mineral components (K, Ca, Mg, P) increased after pyrolysis (see Table 2). The pre-concentration of minerals on biochar is mainly due to the formation of biomass ash during pyrolysis. FO and FL have higher mineral concentrations that can provide more opportunities to adsorb heavy metals from water, which can explain the adsorption results (FO > LO > ZO > CO), as shown in Figure 1. Therefore, this behaviour illustrates the importance of mineral composition in the adsorption process.

The LO biomass yielded promising adsorption results without any modification or

pyrolysis process, probably as a result of both its higher porosity level and the important amount of functional groups on its surface, such as carboxyl and hydroxyl groups. Therefore, the authors believe that this material should be studied in more depth in the future.

Next, the kinetic modelling was performed and the influence of the initial heavy metal concentrations in solution were investigated for the three groups of materials, namely, sewage sludge (FO), wood waste (CO), and agricultural waste (ZO), together with their biochar materials (FL, ZL and CL). From the group of agricultural waste, LO and ZO, we chose the latter.

Effect of contact time

The effect of the contact time between sorbents (CO, CL, ZO, ZL, FO, FL) and heavy metals in multiple-metal systems (Cr(III), Cu(II), Cd(II), Pb(II)) was studied. For that purpose, adsorption experiments were performed (as indicated in the experimental section) for different times (5, 15, 30, 45, 60, 120, 240, 360, 540, 1440 and 2880 minutes) for each adsorbent (Figure 4). In general, biochars from ZO (from agriculture) wastes were more effective than those from sewage sludge and wood biomass. Adsorption equilibrium was reached at different times for each biomass or biochar. ZO and ZL were both effective at adsorption of all metal ions and reached equilibrium in 5 minutes. In the case of CO, the equilibrium time differed as a function of the heavy metal, so adsorption equilibrium was reached in 5 minutes for Pb(II) and Cd(II), in 1 h for Cu(II), and in 24 h for Cr(III). Additionally, CL reached equilibrium slowly compared with CO, requiring approximately 8 h for Cr(III), Cu(II) and Pb(II) and 24 h for Cd(II). In contrast, biochar from sewage sludge (FL) was less effective than FO (especially for Cd(II)). FL also needed a longer time than FO to reach adsorption equilibrium (approximately 6 h), while FO adsorption of all metals took only 5 minutes. Thus, 24 h was chosen as the optimal contact time for further adsorption experiments.

To understand the different adsorption behaviours in multiple-heavy-metal systems, kinetic analysis was performed to find a model that explains the obtained results and to obtain information about the mechanisms of heavy metal adsorption onto biomass and biochar systems.

Kinetic modelling

Two different kinetic models, the pseudo-first-order (PFO) and pseudo-second-order (PSO) models, have been widely used to describe adsorption. The PFO and PSO models assume that the rate of metals adsorbed on the surface of sorbents is proportional to the number of unoccupied sites; PFO kinetics is controlled by the physical process, and PSO kinetics is controlled by chemical processes, including

valence forces sharing or exchanging electrons between the adsorbent and adsorbate. The PFO and PSO mathematic model expressions are given in Equation (3) and Equation (4):

$$\log(q_e - q_t) = \log(q_e) - \frac{k_1}{2.303} t \quad (3)$$

$$\frac{1}{q_t} = \left(\frac{1}{k_2 q_e^2} \right) \times \frac{1}{t} + \frac{1}{q_e} \quad (4)$$

where q_t and q_e are the capacity at time t and at equilibrium, respectively (and expressed as mmol/g), and k_1 and k_2 are the rate constants. In most cases, the PFO equation is linear only over approximately the first 30 minutes; therefore, it is appropriate for the initial contact time but not for the whole range³⁴. Kinetics modelling analysis showed that the adsorption process did not fit well with the PFO model but fit well with the PSO model for all the adsorbents. This result means that the adsorption of heavy metals on the surface of the adsorbents is a chemical adsorption process, such as valence forces sharing or exchanging electrons between the adsorbent and adsorbate. The relative constants found by applying the model are listed in Table 4 only for Pb in the multiple-metal system. Higher capacities of Pb(II) have been found except in the case of CO.

Effect of initial concentration

Five multiple-metal solutions (5 ppm, 25 ppm, 50 ppm, 75 ppm and 100 ppm) were prepared from 1,000 ppm stock solutions of each heavy metal. The initial concentration study provides a significant understanding of the competition between the four heavy metals during the adsorption process. The adsorption capacity of all the adsorbents for the four metals is shown in Figure 5, and the adsorption capacity for Pb(II) in multiple-metal systems is listed in Table 5. As shown in Figure 5, the adsorption capacity of heavy metals (Cr(III), Cu(II), Cd(II), Pb(II)) from different types of feedstocks is ranked as follows: FO (from sewage sludge) > CO (from wood) and ZO (from agriculture). All adsorbents have the same priority for heavy metals, such as Cr(III), Cu(II) and Pb(II) metal ions, and the adsorption of Cd(II) was much lower than that of the other metals, probably due to the competition between the heavy metals. The ranking of the adsorption of biochars from different types of feedstocks was ZL (from agriculture) > FL (from sewage sludge) > CL (from wood), which could be explained by the different mineral compositions of the adsorbents. High mineral amounts provide more possibilities for the exchange of heavy metals from the solution (because the concentration of minerals is increased after pyrolysis), which could increase the adsorption capacity. As shown in Table 2, the concentrations of some mineral components of FL (Ca 89.1 g/kg, P 51.2 g/kg) are much higher than those of ZL (Ca 2.55 g/kg, P 1.83 g/kg) and CL (Ca 9.6 g/kg, P 2.0 g/kg), but potassium contents are the exception (FL (K 9.1 g/kg), ZL (K 23.4 g/kg), and CL (K 6.6 g/kg)). This

behaviour can be related to the adsorption capacity values of these biochars (see Table 5).

FL has a higher mineral content than FO; however, a slight decrease in the adsorption capacity for Cr(III) and Pb(II) and a much higher decrease in the adsorption capacity for Cd(II) were observed for FL. The slight decrease in FL capacity could be explained by the loss of functional groups on the surface of the biomass. As shown in Figure 3, most of the functional groups of FL were lost during the pyrolysis process, which was confirmed by the decrease in the H/C and C/H ratios (Table 2).

Possible adsorption mechanism

In previous studies reported in the literature, five mechanisms have been proposed to govern metal sorption by biochar from aqueous solutions, namely, complexation, cation exchange, precipitation, electrostatic interactions, and chemical reduction^{9,14}. However, the role that each mechanism plays for each metal varies considerably depending on the target metals and adsorbents. Fei et al described the molecular-level adsorption of Pb(II) and Cu(II) to peat biomass mainly through carboxyl groups ($-\text{COOH}$)³⁵. Whereas both electrostatic interactions and complexation with biochar surfaces are responsible for Cr adsorption and reduction^{36,37}.

Until now, few studies have focused on the comparison of different types of feedstocks for the removal of heavy metals from multiple-metal aqueous systems (more similar to real water situations). According to the results of Lu et al., the adsorption of Pb(II) by sewage sludge-derived biochar mainly occurred through proton-active carboxyl ($-\text{COOH}$) and hydroxyl ($-\text{OH}$) functional groups on the biochar surface, as well as coprecipitation or complexation on the mineral surfaces³⁸. After comparison of the characterization and evaluation of the adsorption capacity of different types of feedstocks, a new perspective has been found to explain the adsorption mechanisms onto biomass and biochar adsorbents. We demonstrate that complexation and cation exchange are the two main adsorption mechanisms, with the influence of cation exchange being larger than that of complexation in the present cases.

Furthermore, an increase in mineral concentrations was found in biochars after the pyrolysis of the corresponding biomasses, which could explain the increase in the adsorption capacity to heavy metals of the biochars (CL and ZL, respectively)³⁸. FO and FL (which have higher mineral concentrations than the other adsorbents presented here and lack carboxyl groups on their surfaces) have higher adsorption capacities than CO and ZO (which have lower mineral concentrations and more carboxyl groups). The adsorption capacities of FO and FL are similar, which may be due to the similar porosity of both materials before and after pyrolysis. Although there is an increase in the mineral concentrations on the surface of FL (which will

increase its adsorption capacity), the loss of carboxyl groups as a function of temperature during pyrolysis can globally reduce the adsorption capacity of FL for heavy metals¹⁴. Therefore, FO and FL have similar adsorption capacities.

In summary, heavy metals are adsorbed on the surface of biomass/biochar via exchange mainly with Ca, K, and Mg but also with protons from carboxyl and hydroxyl groups. In addition, if these latter functional groups are present at high amounts on the bioadsorbent surface, they can also complex heavy metals from the aqueous solutions (see Figure 6). Finally, it is important to note that the amount of either mineral or carboxyl groups can differ depending on the composition of the original biomass and, in the case of biochars, as a function of the pyrolysis conditions employed^{39,40}.

Conclusions

Seven biosorbents have been used successfully for the removal of Cr(III), Cu(II), Cd(II) and Pb(II) from multiple-metal aqueous systems. The biochars produced from wood and agriculture waste have higher adsorption capacities than the initial biomasses do. This finding can be explained by an increase in porosity and a pre-concentration of mineral components during the pyrolysis process. Complexation and cation exchange are the two main adsorption mechanisms in multiple-heavy-metal systems, and these mechanisms are influenced by the kind of feedstock and its mineral composition and by the pyrolysis treatment, being more effective for agriculture waste than for wood biomass. The sludge can be used directly to remove heavy metals without pyrolysis pretreatment.

In summary, these disposal biomasses can be used to remove heavy metals from multiple-metal aqueous systems because of their low cost, eco-friendliness and availability. Therefore, biomass could be an interesting alternative to synthetic materials for heavy metal removal. Biochar can also be an alternative, even though it requires biomass pretreatment.

Acknowledgements

This research was supported by grants from the National Key Research and Development Program of China (No. 2018YFD0200904), the Agricultural Science and Technology Innovation Program of China (No. CAAS-ASTIP-2013-OCRI), and Spanish research projects (Nos. CTM2015-65414-C2-1-R and AGL2015-70393-R). Also, China Scholarship Council (No. 201509110114). All the authors are grateful to the UAB Microscopy Service (*Servei de Microscòpia Electrònica* from UAB, Catalunya, Spain) for the SEM analysis; to M. Resina who helped perform the analysis of heavy metals by ICP-MS.

Author Contributions

J.J. Zhao and X.J. Shen carried out most of the experiments and wrote the main manuscript text. X. Domene and J.M. Alcañiz provided the biomass/biochar and participated in data collection. X. Liao and C. Palet contributed valuable discussions and helped revise the manuscript. All authors reviewed and approved the final manuscript for publication.

Additional Information

Publisher's note: Springer Nature remains neutral with regard to jurisdictional claims in published maps and institutional affiliations.

Competing Interests

The author(s) declares no competing interests.

References

1. Dursun, A. Y. A comparative study on determination of the equilibrium, kinetic and thermodynamic parameters of biosorption of copper(II) and lead(II) ions onto pretreated *Aspergillus niger*. *Biochem. Eng. J.* **28**, 187–195 (2006).
2. Kurniawan, T. A., Chan, G. Y. S., Lo, W. hung & Babel, S. Comparisons of low-cost adsorbents for treating wastewaters laden with heavy metals. *Sci. Total Environ.* **366**, 409–426 (2006).
3. Tchounwou, P. B., Yedjou, C. G., Patlolla, A. K. & Sutton, D. J. *Volume 3: Environmental Toxicology. Molecular, Clinical and Environmental Toxicology* **101**, (2012).
4. Chiroma, T. M. & Ebebele, R. O. Comparative Assessment Of Heavy Metal Levels In Soil, Vegetables And Urban Grey Waste Water Used For Irrigation In Yola And Kano. *Int. Ref. J. Eng. Sci. ISSN* **3**, 2319–183 (2014).
5. Florio, M. The economic rate of return of infrastructures and regional policy in the European Union. *Ann. Public Coop. Econ.* **68**, 39–64 (1997).
6. Priori, S. G., Napolitano, C. & Schwartz, P. J. Electrophysiologic mechanisms involved in the development of torsades de pointes. *Cardiovasc. Drugs Ther.* **5**, 203–212 (1991).
7. Fawell, J. K. Cadmium in drinking water. 2 (2011). doi:10.1016/j.kjms.2011.05.002
8. Inyang, M. *et al.* Removal of heavy metals from aqueous solution by biochars derived from anaerobically digested biomass. *Bioresour. Technol.* **110**, 50–56 (2012).
9. Tan, X. *et al.* Application of biochar for the removal of pollutants from aqueous solutions. *Chemosphere* **125**, 70–85 (2015).
10. Njoku, V. O., Islam, M. A., Asif, M. & Hameed, B. H. Utilization of sky fruit husk agricultural waste to produce high quality activated carbon for the herbicide bentazon adsorption.

- Chem. Eng. J.* **251**, 183–191 (2014).
11. Rahman, M. S. & Islam, M. R. Effects of pH on isotherms modeling for Cu(II) ions adsorption using maple wood sawdust. *Chem. Eng. J.* **149**, 273–280 (2009).
 12. Rozada, F., Otero, M., Parra, J. B., Morán, A. & García, A. I. Producing adsorbents from sewage sludge and discarded tyres: Characterization and utilization for the removal of pollutants from water. *Chem. Eng. J.* **114**, 161–169 (2005).
 13. Lehmann, J., Gaunt, J. & Rondon, M. Bio-char sequestration in terrestrial ecosystems - A review. *Mitig. Adapt. Strateg. Glob. Chang.* **11**, 403–427 (2006).
 14. Li, H. *et al.* Mechanisms of metal sorption by biochars: Biochar characteristics and modifications. *Chemosphere* **178**, 466–478 (2017).
 15. Ding, Z., Hu, X., Wan, Y., Wang, S. & Gao, B. Journal of Industrial and Engineering Chemistry Removal of lead, copper, cadmium, zinc, and nickel from aqueous solutions by alkali-modified biochar: Batch and column tests. *J. Ind. Eng. Chem.* **33**, 239–245 (2016).
 16. Zhao, S. X., Ta, N. & Wang, X. D. Effect of temperature on the structural and physicochemical properties of biochar with apple tree branches as feedstock material. *Energies* **10**, (2017).
 17. Sun, Y. *et al.* Effects of feedstock type, production method, and pyrolysis temperature on biochar and hydrochar properties. *Chem. Eng. J.* **240**, 574–578 (2014).
 18. Agrafioti, E., Kalderis, D. & Diamadopoulos, E. Arsenic and chromium removal from water using biochars derived from rice husk, organic solid wastes and sewage sludge. *J. Environ. Manage.* **133**, 309–314 (2014).
 19. Son, E. B., Poo, K. M., Chang, J. S. & Chae, K. J. Heavy metal removal from aqueous solutions using engineered magnetic biochars derived from waste marine macro-algal biomass. *Sci. Total Environ.* **615**, 161–168 (2018).
 20. Kizito, S. *et al.* Evaluation of slow pyrolyzed wood and rice husks biochar for adsorption of ammonium nitrogen from piggery manure anaerobic digestate slurry. *Sci. Total Environ.* **505**, 102–112 (2015).
 21. Donat, R., Akdogan, A., Erdem, E. & Cetisli, H. Thermodynamics of Pb²⁺ and Ni²⁺ adsorption onto natural bentonite from aqueous solutions. *J. Colloid Interface Sci.* **286**, 43–52 (2005).
 22. Kenawy, I. M., Hafez, M. A. H., Ismail, M. A. & Hashem, M. A. Adsorption of Cu(II), Cd(II), Hg(II), Pb(II) and Zn(II) from aqueous single metal solutions by guanyl-modified cellulose. *Int. J. Biol. Macromol.* **107**, 1538–1549 (2018).
 23. Marks, E. A. N., Mattana, S., Alcañiz, J. M. & Domene, X. Biochars provoke diverse soil mesofauna reproductive responses in laboratory bioassays. *Eur. J. Soil Biol.* **60**, 104–111 (2014).

24. Chen, T. *et al.* Influence of pyrolysis temperature on characteristics and heavy metal adsorptive performance of biochar derived from municipal sewage sludge. *Bioresour. Technol.* **164**, 47–54 (2014).
25. Hossain, M. K., Strezov Vladimir, V., Chan, K. Y., Ziolkowski, A. & Nelson, P. F. Influence of pyrolysis temperature on production and nutrient properties of wastewater sludge biochar. *J. Environ. Manage.* **92**, 223–228 (2011).
26. Subedi, R. *et al.* Greenhouse gas emissions and soil properties following amendment with manure-derived biochars: Influence of pyrolysis temperature and feedstock type. *J. Environ. Manage.* **166**, 73–83 (2016).
27. Zou, J. *et al.* Structure and adsorption properties of sewage sludge-derived carbon with removal of inorganic impurities and high porosity. *Bioresour. Technol.* **142**, 209–217 (2013).
28. Smith, K. M., Fowler, G. D., Pullket, S. & Graham, N. J. D. Sewage sludge-based adsorbents: A review of their production, properties and use in water treatment applications. *Water Res.* **43**, 2569–2594 (2009).
29. Bagreev, A., Badosz, T. J. & Locke, D. C. Pore structure and surface chemistry of adsorbents obtained by pyrolysis of sewage sludge-derived fertilizer. *Carbon N. Y.* **39**, 1971–1979 (2001).
30. Huff, M. D. & Lee, J. W. Biochar-surface oxygenation with hydrogen peroxide. *J. Environ. Manage.* **165**, 17–21 (2016).
31. Rozada, F., Otero, M., Morán, A. & García, A. I. Adsorption of heavy metals onto sewage sludge-derived materials. *Bioresour. Technol.* **99**, 6332–6338 (2008).
32. Yuan, J. H., Xu, R. K. & Zhang, H. The forms of alkalis in the biochar produced from crop residues at different temperatures. *Bioresour. Technol.* **102**, 3488–3497 (2011).
33. Zhang, H., Voroney, R. P. & Price, G. W. Effects of temperature and processing conditions on biochar chemical properties and their influence on soil C and N transformations. *Soil Biol. Biochem.* **83**, 19–28 (2015).
34. Nguyen, H., You, S. & Hosseini-bandegharai, A. Mistakes and inconsistencies regarding adsorption of contaminants from aqueous solutions : A critical review. *Water Res.* **120**, 88–116 (2017).
35. Qin, F. *et al.* Mechanisms of competitive adsorption of Pb, Cu, and Cd on peat. *Environ. Pollut.* **144**, 669–680 (2006).
36. Zhou, L. *et al.* Investigation of the adsorption-reduction mechanisms of hexavalent chromium by ramie biochars of different pyrolytic temperatures. *Bioresour. Technol.* **218**, 351–359 (2016).
37. Xu, X., Huang, H., Zhang, Y., Xu, Z. & Cao, X. Biochar as both electron donor and electron shuttle for the reduction transformation of Cr(VI) during its sorption. *Environ. Pollut.* **244**,

- 423–430 (2019).
38. Qambrani, N. A., Rahman, M. M., Won, S., Shim, S. & Ra, C. Biochar properties and eco-friendly applications for climate change mitigation, waste management, and wastewater treatment: A review. *Renew. Sustain. Energy Rev.* **79**, 255–273 (2017).
 39. Rajapaksha, A. U. *et al.* Dissolved organic matter characterization of biochars produced from different feedstock materials. *J. Environ. Manage.* **233**, 393–399 (2019).
 40. Shen, Z. *et al.* Effect of production temperature on lead removal mechanisms by rice straw biochars. *Sci. Total Environ.* **655**, 751–758 (2019).

Figure legends:

Figure 1 Adsorption of Cr(III), Cd(II), Cu(II), and Pb(II) ions by CO, CL, ZO, ZL, FO, FL and LO in the multiple-metal aqueous system. Initial metal concentration of 0.18 mmol of each metal, contact time of 24 h, initial pH of 4.0, and 25 mg of adsorbent in 2.5 ml of initial solution.

Figure 1

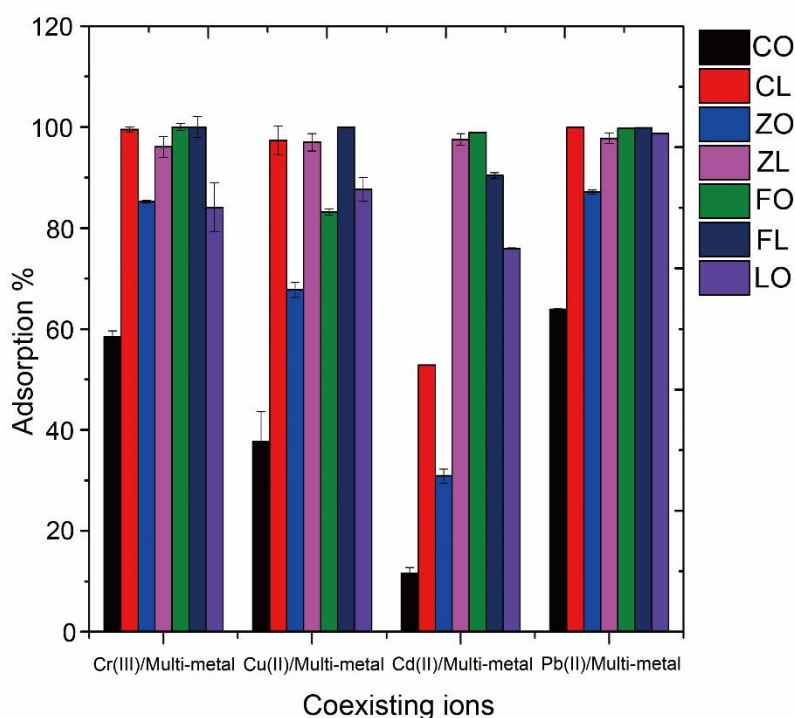
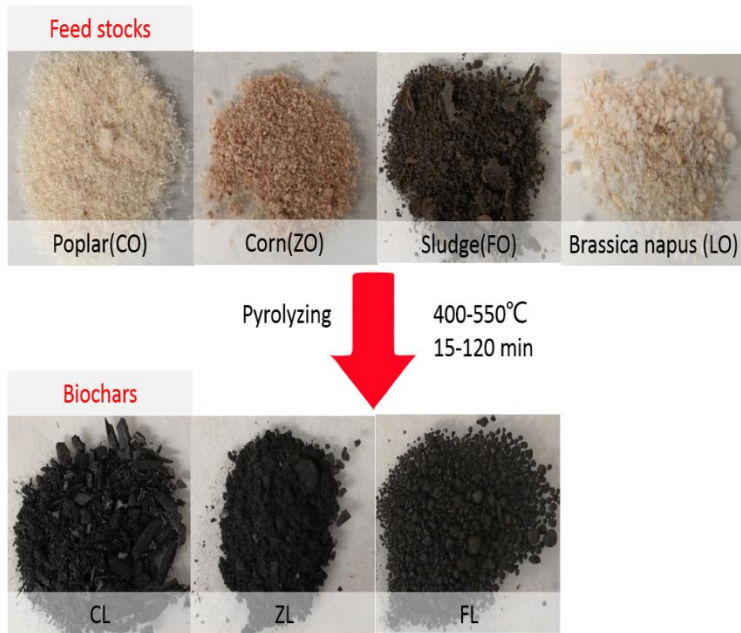


Figure 2 Images of biomasses and biochars. (a) Images of raw CO, CL, ZO, ZL, FO, FL and LO. (b) SEM images of CO, CL, ZO, ZL, FO, FL and LO.

Figure 2

(a)



(b)

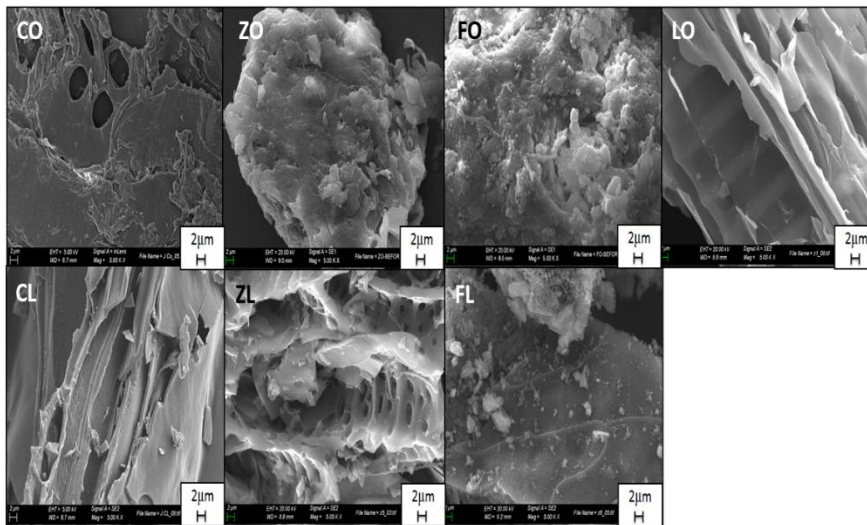


Figure 3 ATR-FTIR spectra of CO and CL (a), ZO and ZL (b), FO and FL (c), and LO (d).

Figure 3

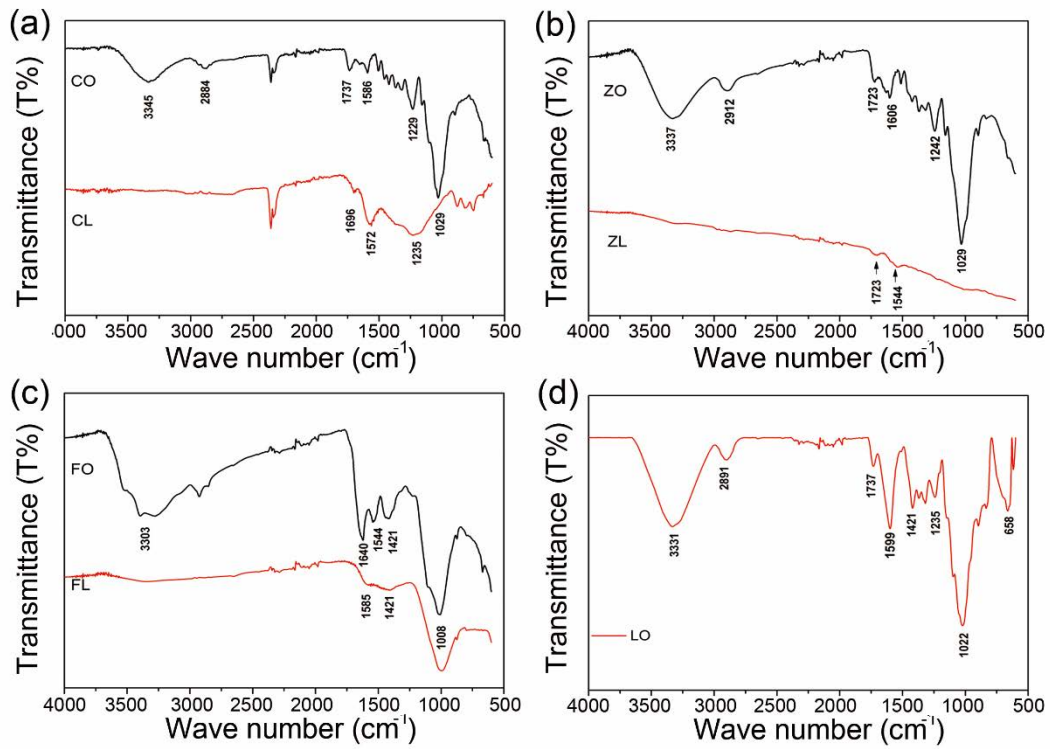


Figure 4 Adsorption percentage of Cr(III), Cu(II), Cd(II), and Pb(II) by CO (a), CL (b), ZO (c), ZL (d), FO (e) and FL (f) from the multiple-metal system at different contact times. Initial metal ions concentration of 0.18 mmol/L of metal, pH 4.0, and 25 mg of adsorbent.

Figure 4

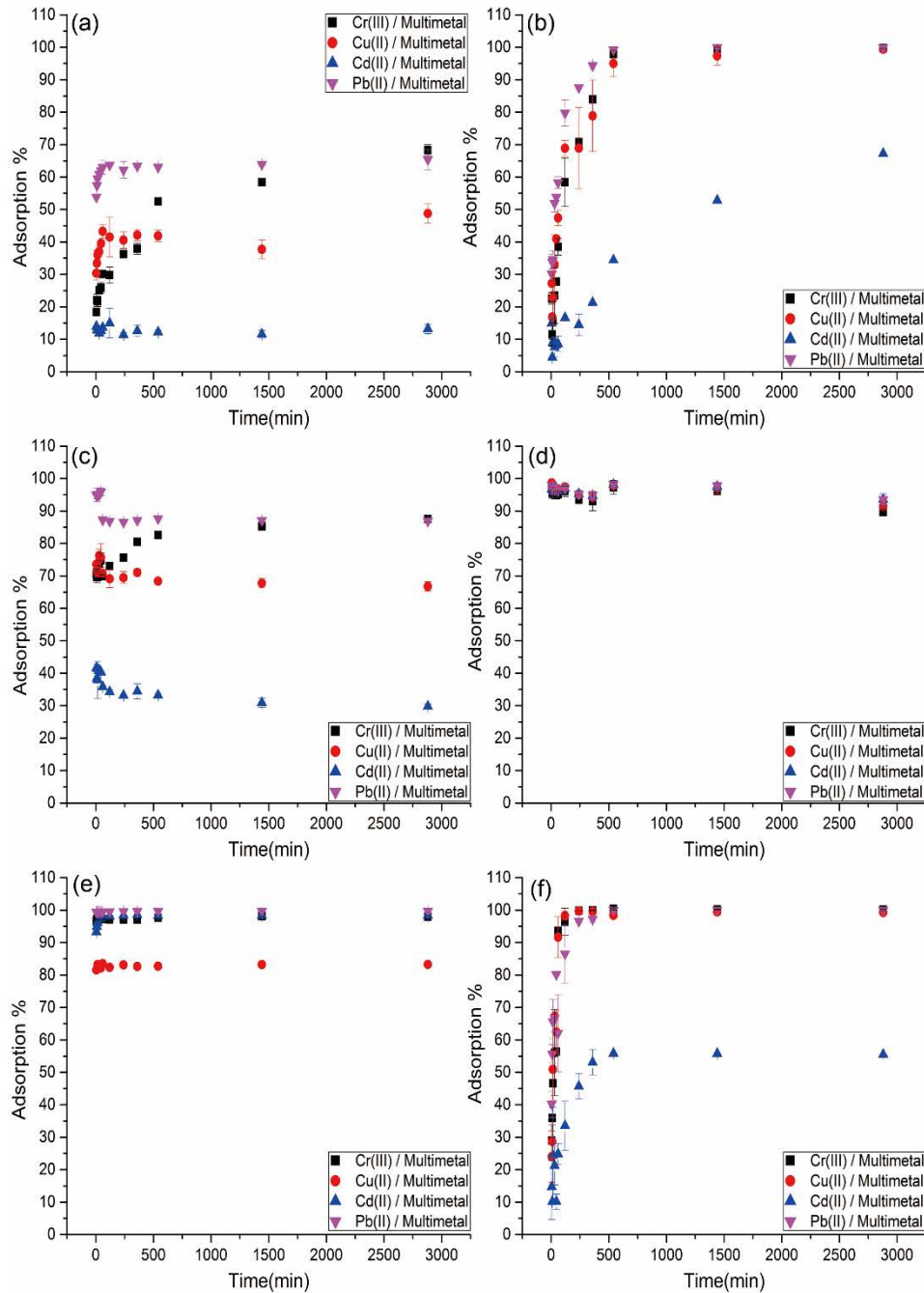


Figure 5 Effect of the initial concentration of heavy metals on their adsorption by CO (a), CL (b), ZO (c), ZL (d), FO (e) and FL (f) in multiple-metal systems. Experimental conditions were $T=25\pm 1^\circ\text{C}$, pH 4.0, 25 mg of adsorbent, 2.5 mL of metals solution and stirring for 24 hours.

Figure 5

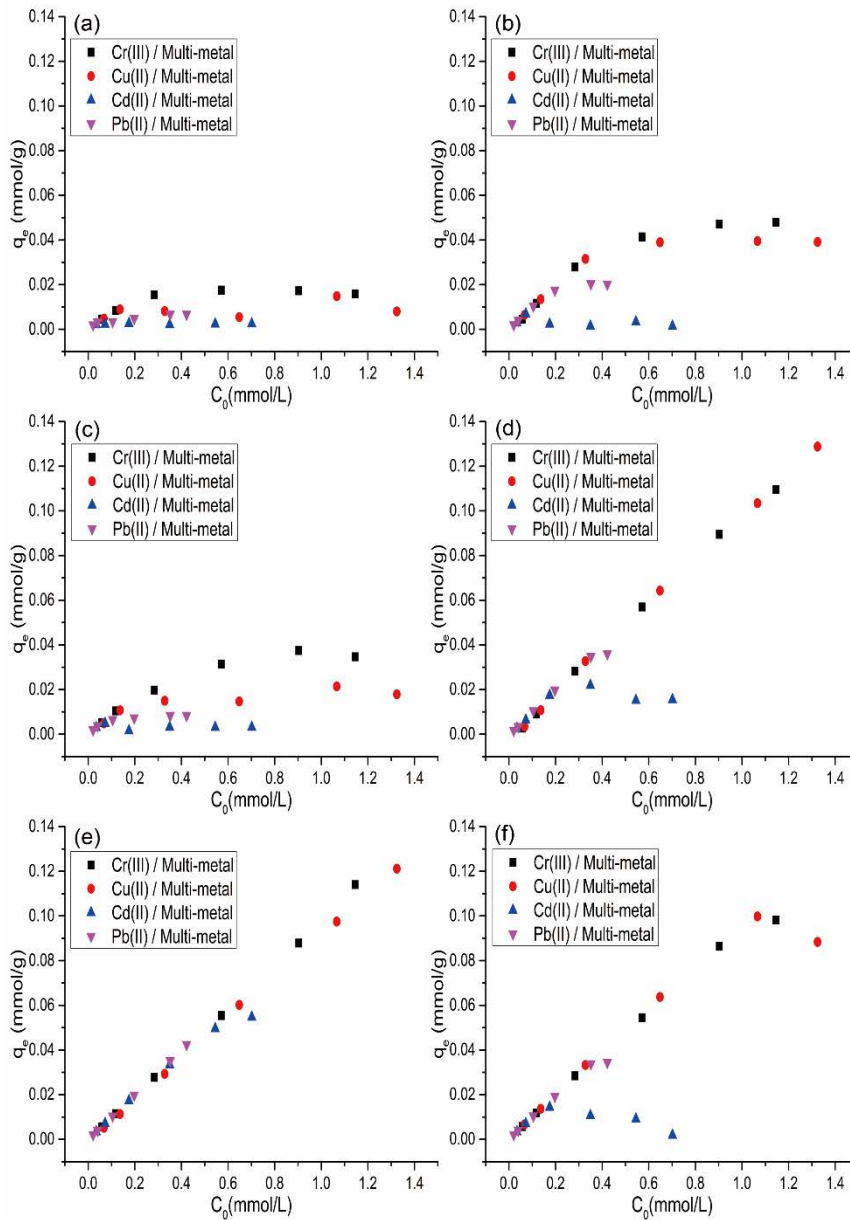


Figure 6 Schematic diagram illustrating the mechanism of heavy metal removal by biomass and/or biochar.

Figure 6

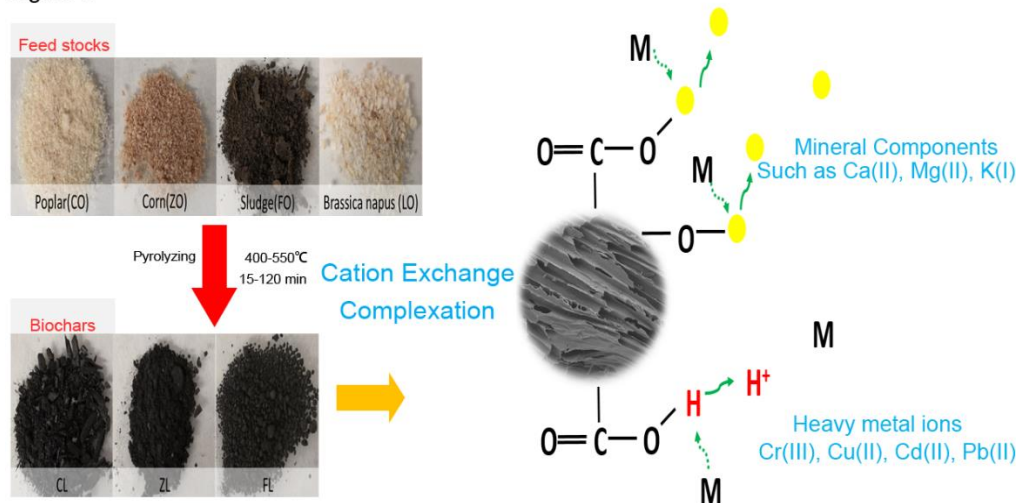


Table 1 Feedstock biomasses and biochar preparation procedure description.

Materials	Description	Pyrolysis (temperature)	Time
CO	Populus nigra (Poplar) wood		
CL	Biochar of populus	Slow pyrolysis 500-550 °C	15
ZO	Carozo Zea mays		
ZL	Biochar of Carozo	slow pyrolysis 400-500 °C	120
FO	Sewage sludge		
FL	Biochar of Sewage sludge	slow pyrolysis 500-550 °C	15
LO	Brassica napus		

Table 2 Physicochemical properties of CL, ZL and FL.

	CL wood	ZL corn	FL sewage sludge
Components	Cellulose (50%), Hemicellulose (25-35%) Lignin (15-25%),	Cellulose/glucan (37%), Xylan (21%) Lignin (18%)	Carbon (50-70 %), Hydrogen (6-7.3 %), Oxygen (21-24 %), Nitrogen (15-18 %),
Temperature	500-550 °C	400-500 °C	500-550 °C
pH	8.21	10.3	8.70 (FO 7.95)
H/C	0.026	0.29 (ZO 1.7)	0.054 (FO 0.17)
O/C	0.15	0.090 (ZO 0.74)	0.22 (FO 2.5)
K g/kg	6.6	23 (ZO 9.4)	9.1 (FO 4.1)
Ca g/kg	9.6	2.6 (ZO 0.22)	89 (FO 41)
Mg g/kg	1.3	1.2 (ZO 0.15)	12 (FO 5.5)
P g/kg	2.0	1.8 (ZO 0.20)	51 (FO 24)

H/C and O/C values are the molar ratio

Table 3 FTIR spectral band assignments for CO, CL, ZO, ZL, FO, FL and LO before use.

Wave numbers (cm ⁻¹)	Assignments	Sorbents						
		CO	CL	ZO	ZL	FO	FL	LO
3200-3700	O-H stretching	3346		3337		3303		3331
2700-3000	C-H _n stretching	2884		2912				2912
1780-1710	Carboxylic Acid C=O stretching	1737	1698	1723	1723			1737
1750-1630	Ketone, Ester, Amide C=O Stretching	1688	1672	1606	1644	1640	1686	1599
1000-1200	C=O/C-O-C C-N/R-O-C/R-O-CH ₃ stretching	1229	1236	1242				1236
750-870	aromatic C-H					1008	1008	1022
								868

Table 4 Adsorption kinetic constants for the adsorption of Pb(II) by CO, CL, ZO, ZL, FO and FL in the multiple-metal system.

Pb(II)/Multi-metal	Pseudo-second-order model		
	k ₂ (g/mmol/min)	q ₂ (μmol/g)	R ²
CO	0.98	9.20	1.000
CL	0.26	14.7	0.998
ZO	12.0	12.7	1.000
ZL	0.26	16.7	0.999
FO	5.68	16.7	0.999
FL	0.66	16.5	0.999

Table 5 Adsorption capacity of biomass and biochar in multiple-heavy-metal systems.

q _e (μmol/g)	CO	CL	ZO	ZL	FO	FL
Cr(III)	15.9	27.9	35.7	109	114	98.2
Cu(II)	9.10	31.7	13.4	128	88.3	99.7
Cd(II)	2.32	2.39	3.02	15.5	54.7	14.3
Pb(II)	6.75	17.5	8.39	35.9	35.1	33.7

Annex II

Article under preparation for *Environmental Science & Technology*. To be submitted on June 2019.

XAS study of adsorption mechanisms of hexavalent and trivalent chromium by different Pine biomass systems

Jingjing Zhao¹, Giannantonio Cibin², Roberto Boada¹, Cristina Palet^{1*}

¹GTS-UAB Research Group, Department of Chemistry, Facultat de Ciències, Universitat Autònoma de Barcelona, 08193 Cerdanyola del Vallès, Catalunya, Spain

²Diamond Light Source, HSC Oxfordshire, OX11 0DE, United Kingdom

*Corresponding Authors: cristina.palet@uab.cat;

Abstract

Pine biomass, Pine biochar (PG) and TiO₂ loaded on biomass (Pine/TiO₂) were used to remove Cr(III) and Cr(VI) ions from aqueous solution. The adsorption results of Pine/TiO₂ showed a better adsorption capacity for Cr(VI) than Cr(III), while PG shows high selectivity for Cr(III) and negligible adsorption for Cr(VI). To explain the selectivity behaviour of Cr by these adsorbents, the pH, Fourier transform infrared spectroscopy (FT-IR), scanning electron microscopy (SEM) and mineral components analysis were performed to characterise the functional groups, morphological structure and mineral composition of the adsorbents. Furthermore, different parameters of adsorption processes were optimized in batch systems (the pH of the solution, the initial concentration and the contact time). Results show that the adsorption of Cr(III) is mainly through ion exchange with mineral components. Pyrolysis process can increase the concentration of mineral components to increase the adsorption capacity. From X-ray absorption spectroscopy (XAS) results it can be confirmed that carboxyl and hydroxyl groups are involved in the adsorption process for Cr(III).

Introduction

Chromium is a common contaminant in surface water and ground waters that comes mainly from electroplating, leather tanning, and textile industries processes. Trivalent, Cr(III), and hexavalent, Cr(VI), oxidation states are the two main valence states found in polluted water.^{1,2} Cr(VI) is five hundred times more poisonous than Cr(III) and may cause carcinogenesis, mutation or teratogenesis to living creatures.^{3,4} Thus, Cr(VI) has been identified as a top-priority hazardous pollutant.⁵ Therefore, it is

of great significance to develop a cost-effective and eco-friendly technique to remove Cr from industrial wastewater before being disposed into aqueous systems.

Numerous physical and chemical separation techniques are being used to remove heavy metals, such as solvent extraction, ion-exchange, adsorption, membrane filtration, electrochemical treatment technologies.⁶⁻⁸ Among the conventional techniques for removing pollutants from water, adsorption methods are considered to be the most advantageous due to their high efficiency, low cost and ease handling.^{9,10} Particularly, lignocellulosic residues (including wood and agricultural residues) have proved to be efficient and low-cost adsorbents for the Cr removal.^{2,11} In addition, biochar, a pyrolysis product obtained from biomass, highly increases the adsorption of heavy metals mainly due to its large surface and pore structure. As a function of the pyrolysis temperature, biochar can also have abundant chemical functional groups and high concentration of minerals compared with the original biomass.¹²⁻¹⁵ Currently, there is a large amount of wood biomass that has no market value and that it often causes an environmental problem if they are not disposed properly. Within this framework, pine wood biomass and biochar have emerged as ideal adsorbents.

Furthermore, in the literature TiO₂ nanoparticles are used as reagent materials due to their large surface/volume ratio and their photocatalytic behaviour under UV/visible light, which have been applied for Cr reduction. Wang *et.al* performed Cr(VI) adsorption under UV by using TiO₂ as photocatalyst, and 94% of Cr(VI) was photoreduced within 1h at pH 3.¹⁶ However, particles are easily to aggregate in this process which largely hindering their efficiency. Moreover, TiO₂ can be supported on biomass in adsorption systems. Hence, synthesis TiO₂ on the biomass could help to solve such aggregation problems. Additional, using low-cost biomass as a support is a potential and eco-friendly way to removal heavy metals.

X-ray absorption spectroscopy (XAS), is unique sensitivity to the local structure, which can be exploited the adsorption mechanism of heavy metal in molecular level.^{17,18} Using this technique, several studies have performed to study the adsorption of biomass/biochar^{19,20}.

In this study, three kinds of adsorbents, namely, pine biomass (PO, from wood), pine gasification (PG, biochar from gasification of pine) and TiO₂ modified pine (Pine/TiO₂, TiO₂ loaded on pine) were used to study the chromium selectivity species from aqueous solution. The objectives of this study are (1) to compare the adsorption capacities of the three different types adsorbents and (2) to evaluate the possible selectivity mechanisms of chromium by XAS.

Materials and Methods

Biomass/biochar and biochar loaded with TiO₂

PO, Pine/TiO₂ and PG were chosen to evaluate their adsorption capacities, and were all used to remove Cr(III) and Cr(VI) ions in single-metal systems. PG biochar was thermally dried and pyrolysed at the plant of *Centro de Investigación* (Júndiz, Spain), and was produced by gasification pyrolysis processes. The temperature conditions and duration of the pyrolysis processes are between 600-900 °C for 75 minutes. While PO and PG were kindly provided by the Centre for Research on Ecology and Forestry Applications (CREAF, Barcelona, Spain).

Pine/TiO₂ was prepared by the method reported by Wang²¹. First stage was pre-treatment of Pine. The sample of Pine was washed with deionized water and dried in an oven at 75°C for 24 h. 5 g of acid treated pine were suspended in nitric acid at pH 3.0 for 4 days as a conditioning procedure. After a step of filtration from the acidic media, the treated Pine was washed with deionized water multiple times until neutral pH (pH of the washing water). Then the material was dried in an oven at 75°C for 24 h. The second stage was syntheses TiO₂ on the surface of pine by sol-gel method²². 5 g acid treated Pine was dispersed in 120 mL ethanol followed by addition of 40 mL Titanium (IV) butoxide (97%) (which is the TiO₂ precursor). The mixture was stirred at ambient temperature for 1 hour before adding a solution containing 16 mL of HCl 37% (v/v) and 40 mL alcohol (97%) with constant stirring for 1 hour more. The solution was filtered, and then washed with alcohol (97%) before drying at 70°C for 24 hours. The dried sample was milled and pyrolyzed at 25 °C for 1 hour in a muffle to yield the Pine/TiO₂.

Chemical and reagents

All the chemicals were analytical grade. A 1,000 mg/L concentration of stock aqueous solution was prepared for Cr(III) and Cr(VI) species by dissolving the appropriated amounts of Chromium nitrate nonahydrate (Cr(NO₃)₃·9H₂O) and Potassium dichromate (VI) (K₂Cr₂O₇), respectively. Both reagents had a purity of 99% and were obtained from Panreac. The ethanol (C₂H₆O, 97%), nitric acid (HNO₃) and hydrochloric acid (HCl, 37% v/v) all were purchased from Panreac (*Catalunya*, Spain). Titanium (IV) butoxide (C₁₆H₃₆O₄Ti, 97% v/v) was from Sigma-Aldrich (Missouri, USA).

Characterization of materials

The morphology was analyzed by scanning electron microscopy (SEM) coupled with energy dispersive X-ray (EDX), from the Electron Microscopy Facilities of UAB

(Barcelona, Spain). Attenuated total reflectance Fourier transform infrared spectroscopy (ATR-FTIR, Tensor 27, Bruker, USA) was performed to identify the chemical functional groups present on the adsorbents. FTIR data were obtained in the wavenumber range of 600 to 4000 cm^{-1} with an average of 16 scans at 4.0 cm^{-1} resolution at *Servei d'Anàlisi de Química* (UAB, Catalunya, Spain). The pH of adsorbents were measured as follows: biochars were prepared in triplicate by adding water at a ratio of 20:1 (biochar/mg:deionized water/mL) and vertically agitating for 24 h at a speed of 25 rpm. Then, the pH was measured immediately²³.

Batch adsorption experiments

Adsorption experiments were carried out at room temperature ($25 \pm 1^\circ\text{C}$). Cr(III) and Cr(VI) were prepared from 1,000 ppm initial stock solutions of each metal, and the concentration ranged from 0 to 300 ppm. Batch experiments were performed by adding 25 mg of adsorbent in 5 mL tubes and then adding 2.5 mL of heavy metal aqueous solutions. The tubes were then placed on a rotary mixer (CE 2000 ABT-4, SBS Instruments SA, Barcelona, Spain) and shaken at 25 rpm for 24 h. The two phases were separated by decantation and filtered through 0.22 μm Millipore filters (Millex-GS, Millipore). The concentrations of heavy metals in the supernatant phase were analysed by ICP-mass spectrometry (MS) (XSERIES 2 ICP-MS, Thermo Scientific, USA). The adsorption of the selected heavy metals by the adsorbents was expressed as the adsorption percentage calculated by using Equation (1). Furthermore, the capacity of the adsorbent was calculated by using Equation (2):

$$\% \text{ Adsorption} = \frac{(C_0 - C_e)}{C_0} \times 100 \quad (1)$$

$$q_e = \frac{(C_0 - C_e) \times V}{m} \quad (2)$$

where q_e (mg/g) is the capacity of the adsorbent, expressed as the amount of heavy metal per adsorbent mass unit at equilibrium; V (L) is the volume of the heavy metal solution; C_0 and C_e are the initial and equilibrium heavy metal concentrations in solution (both in mg/L), respectively; and m (g) is the dry weight of the adsorbent. All the results are expressed as the mean value of duplicate measurements.

X-ray absorption spectroscopy study

For the XAS experiments, PO, Pine/TiO₂ and PG samples were exposed to 2 mM Cr(III) and Cr(VI) single-element solutions during 24 h in a rotatory sacker. Subsequently, the solids were detected from the solution and washed with milliQ water at room temperature ($25 \pm 1^\circ\text{C}$) for 3 times to eliminate the Cr solution and left only the Cr adsorbed. Finally, the samples were dried in oven at 70 $^\circ\text{C}$ for 1 day. XAS

measurements were performed at the B18 beamline of the Diamond Light Source synchrotron facility (Didcot, United Kingdom)²⁴. EXAFS was collected at Cr K-edge using QEXAFS scanning mode and the Si(111) monochromator crystals. The measurements were performed at liquid nitrogen temperature to minimize radiation damage. Due to the low concentration of Cr in the samples, the measurements were performed in fluorescence mode using the 4-element Si-Drift detector available at the beamline. Reference samples were measured in transmission mode using gas ionization chambers filled with the appropriate amount of nitrogen and argon to absorb 15% (I_0) and 70% (I_t and I_{ref}) of the beam. XAS data analysis (i.e., spectra averaging, background subtraction, and spectra normalization) was performed according to standard procedures using the ATHENA program included in the Demeter package²⁵.

Results and Discussion

Comparison of biosorbent adsorption properties

As indicated in the previous section, three adsorbents (Pine, Pine/TiO₂ and PG) were used to remove Cr(III) and Cr(VI) ions in single-metal systems. These three sorbents show different biosorption capacities for the Cr metal ions, as shown in Figure 1. In general, Pine and Pine/TiO₂ have better sorption capacity of Cr(VI) than PG, especially the case of Pine/TiO₂. In contrast, PG showed a different behaviour, while PG have an drastically increased adsorption of Cr(III) but neglected adsorption of Cr(VI). From previous results from the literature, the changes of mineral content (K, Ca, Mg and P), functional groups (carboxyl and hydroxyl groups), pH and large specific surface area influence the metal ions sorption²⁶. Furthermore, high pyrolysis temperatures lead to an increment in porosity, concentration of minerals, pH and surface area compared with the original biomaterial²⁷.

In the present case, the change in mineral content and surface morphology can explain the higher capacity of Cr(III) by Pine/TiO₂ and PG than Pine biomass, as shown in Figure 1. The mineral concentration level in PG is higher than in Pine, especially for Ca. The respective values were 9.36 and 0.68 mg/kg for K⁺, 20.5 and 0.67 mg/kg for Ca²⁺, 2.1 and 0.15 mg/kg for Mg²⁺, and 1.3 and 0.07 mg/kg for total phosphorus content for PG and Pine, respectively²³. The increase of minerals can be attributed to the pyrolysis process since minerals from biomass are pre-concentrated on the surface of adsorbents. Especially K⁺, Ca²⁺ and Mg²⁺ on the surface can be exchanged with Cr(III), which can explain such selectivity behaviour by PG.²⁸

It is well known that Cr(VI) is present in waters as chromate anion which can compete with OH⁻ at high water solution pH levels, in the case of positively charged

sites (such as amino groups), and will not interact with carboxyl neither with hydroxyl site groups from biomass²⁹. Hence, increased adsorption Cr(VI) by Pine/TiO₂ was found probably due to electrostatic attraction since carboxyl and hydroxyl functional groups are lost after the pyrolysis process, leading to a positively charge surface which can interact with chromate ion. The opposite adsorption behaviour of PG was probably due to the increased pH of adsorbent (with pH 6 for Pine and Pine/TiO₂, and pH 9 for PG) which increases the competition with OH⁻ and decreases the Cr(VI) adsorption.

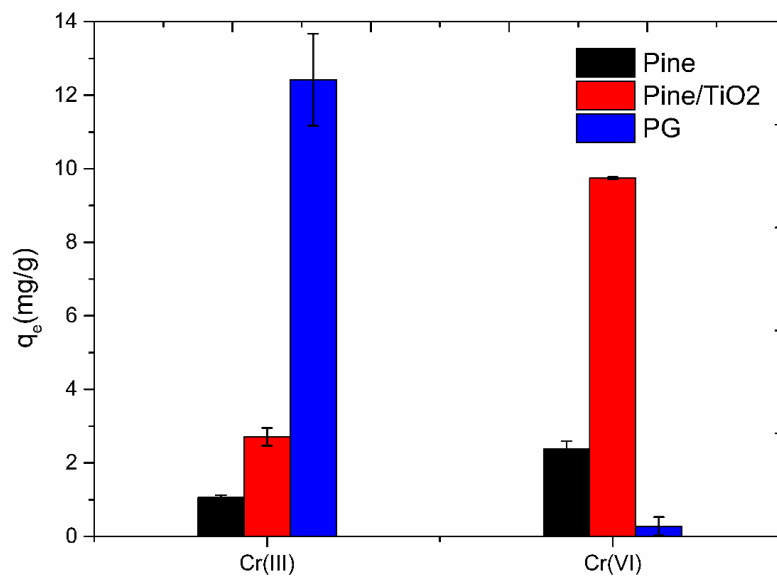


Figure 1 Adsorption capacity of Cr by using Pine, Pine/TiO₂ and PG. Initial metal ions concentration of 120 ppm of metal, pH 4.0, and 25 mg of adsorbent.

SEM characterization

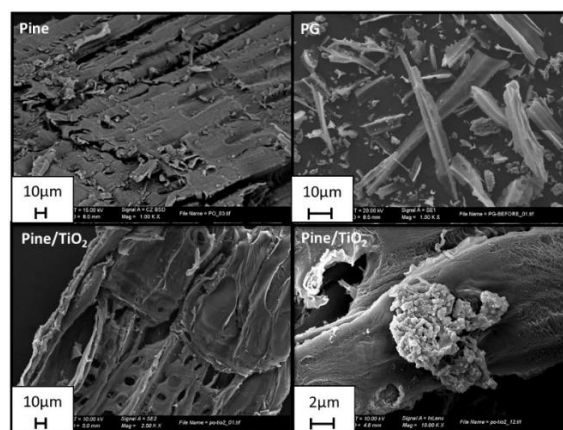


Figure.2 SEM images of a) Pine, b) PG, c) Pine/TiO₂, all at similar magnification; and d) Pine/TiO₂ at higher magnification.

SEM was used to study the morphological structure of the adsorbents. As shown in Figure 2, Pine/TiO₂ shows more pore structures than Pine. TiO₂ aggregate can be found in different sizes, and most of the aggregate size are less than 10 μm (see Figure 2). Furthermore, PG (porosity 81%) did not have much change in porosity compared with the Pine (porosity 72%) which has been published in previous study²³. As mentioned above, Pine/TiO₂ has been shown to have a higher heavy metal removal efficiency than Pine (see Figure 1), which can be explained by the high porosity and the large pore size of Pine/TiO₂. Thus, the results presented here demonstrate that pore structure is a key factor that can influence the sorption of heavy metals onto biomass, as Al-Wabel *et al* that reported similar results²⁶.

ATR-FTIR characterization analysis

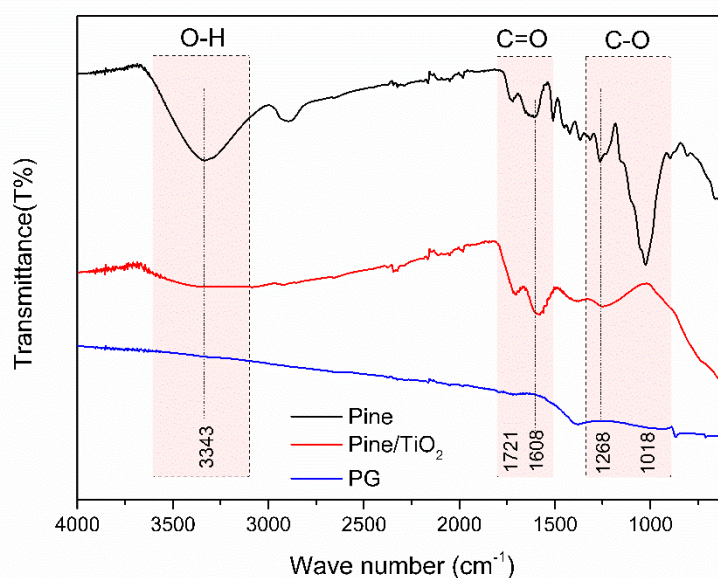


Figure 3 ATR-FTIR spectra of Pine, Pine/TiO₂ and PG.

Table 1 FTIR spectral bands assignments for Pine, Pine/TiO₂ and PG before use.

Wave numbers (cm ⁻¹)	Assignments	Biosorbents		
		Pine	Pine/TiO ₂	PG
3200-3700	O-H stretching	3343	3343	
2700-3000	C-H stretching	2903		
1780-1710	Carboxylic Acid	1721	1721	
	C=O stretching			
1750-1630	Ketone, Ester, Amide	1608	1608	
	C=O Stretching			
1000-1200	C=O/C-O-C	1018	1018	1388
	C-N/R-O-C/R-O-CH ₃ stretching	1268	1268	

ATR-FTIR analysis was carried out to identify the functional groups present in the different adsorbents that might be involved in the sorption process. FTIR spectra of Pine, Pine/TiO₂ and PG are shown in Figure 3. The wavenumbers and approximate assignments of the vibrational modes for the FTIR spectra are listed in Table 1. The peaks at 3200-3270 cm⁻¹ and 1780-1710 cm⁻¹ correspond to the O-H and C=O stretching vibrations, respectively, which confirms the presence of carboxyl groups (-COOH) on the adsorbents, which are very useful for the adsorption of heavy metal ions.

Additionally, a decrease in the intensity of the peaks corresponding to carboxyl (-COOH) and hydroxyl (-OH) groups is observed in the FTIR spectra of Pine/TiO₂ and PG after pyrolysis, especially for PG lost most of functional groups due to the pyrolysis of lignocellulosic materials at high temperature. The decrease in the H/C and O/C atomic ratios for biochars confirms this hypothesis²³. *Yuan et.al* has similar result that showed functional group (COOH) decompose under the high temperature used for pyrolysis process, completely lost above 700°C³⁰. On the other hand, a reduction in the amount of negative surface charges (related to groups such as -COOH, -COH and -OH) increases the pH of the biochar, since such groups were decomposed³¹, as mentioned. FTIR of PG (pH=9) shown in Figure 3, it does not show any feature and provided more positivity surface density, so OH⁻ ions in solution surround the surface and repulse the adsorption of Cr(VI) anion. FTIR results are in agreement with the discussion in previous section.

Effect of contact time

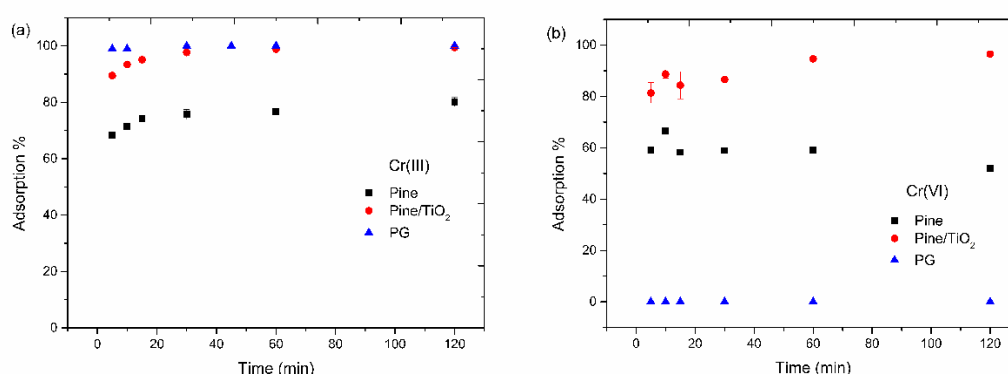


Figure 4 Adsorption percentage of Cr by Pine, Pine/TiO₂ and PG at different contact times. (a) Adsorption of Cr(III), and (b) Adsorption of Cr(VI). Initial metal ions concentration of 9 ppm of metal, pH 4.0, and 25 mg of adsorbent.

The effect of the contact time between sorbents (Pine, Pine/TiO₂ and PG) with Cr(III) and Cr(VI) were studied. For that purpose, adsorption experiments were performed for different times (from 5 to 120 minutes) for each adsorbent (shown in Figure 4). In general, Pine/TiO₂ and PG were more effective than Pine biomass. Adsorption equilibrium was reached in 30 minutes for each adsorbents in Cr(III) single system, whereas adsorption equilibrium was reached 1 hour in Cr(VI) single system by Pine and Pine/TiO₂. In the case of PG, the adsorption of Cr(VI) was negligible due to the electrostatic repulse on the surface.

To understand the different adsorption behaviours in single element systems, kinetic analysis was performed to find which model system can explain the obtained experimental results and to get information about the mechanisms of the heavy metal adsorption onto all the biomass/biochar systems.

Kinetic modelling

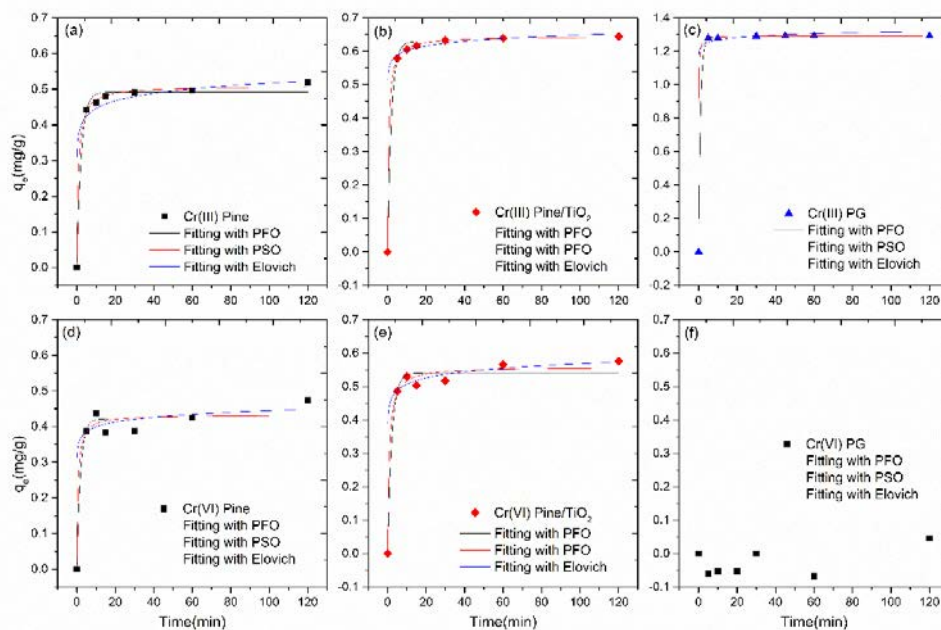


Figure 5 Different of fitting curves of Pine, Pine/TiO₂ and PG in Cr(III) (a, b and c) and Cr(VI) (d, e, and f) single systems.

Table 2 Adsorption kinetic constants for the adsorption of Cr(III) and Cr(VI) by Pine, Pine/TiO₂ and PG.

		PFO			PSO			Elovich		
		k ₁	q ₁	R ²	k ₂	q ₂	R ²	α	β	R ²
		(g/mg/min)	(mg/g)		(g/mg/min)	(mg/g)				
Cr(III)	Pine	0.438	0.492	0.991	2.38	0.509	0.998	32.6	6260	0.727
	Pine/TiO ₂	0.494	0.629	0.999	2.61	0.644	0.998	50.1	2.6139	0.996
	PG	0.955	1.289	0.999	11.8	1.292	0.999	48.3	9.42	0.998
Cr(VI)	Pine	0.518	0.421	0.956	3.72	0.433	0.960	50.7	1.19	0.970
	Pine/TiO ₂	0.452	0.540	0.982	2.15	0.559	0.989	37.4	4465	0.994
	PG	NA	NA	NA	NA	NA	NA	NA	NA	NA

NA means not data

Four different kinetic models, the pseudo-first-order (PFO), pseudo-second-order (PSO), Elovich models and Intra-particle Diffusion, have been widely used to describe adsorption onto different biomass systems. The PFO and PSO models assume that the rate of metals adsorbed on the surface of sorbents is proportional to the number of unoccupied sites; PFO kinetics is controlled by the physical adsorption process, and PSO kinetics is controlled by chemical processes, including valence forces sharing or exchanging electrons between the adsorbent and adsorbate. Elovich equation is often used to describe the kinetics of chemisorption on highly heterogeneous adsorbents, which means a multilayer adsorption if adsorption sites are increase exponentially with adsorption. The Intra-particle Diffusion modelling suggested that if the sorption mechanism is via intraparticle diffusion then a plot of q_t versus $t^{1/2}$ will be linear. The PFO and PSO, Elovich and Intra-particle Diffusion mathematic model expressions are given in Equation (3), Equation (4), Equation (5) and Equation (6), respectively:

$$q_t = q_1[1 - \exp(-k_1 t)] \quad (3)$$

$$q_t = \frac{k_2 q_2^2 t}{1 + k_2 q_2 t} \quad (4)$$

$$q_t = \frac{\ln(\alpha\beta)}{\beta} + \frac{\ln t}{\beta} \quad (5)$$

$$q_t = k_i(t_{1/2}) + C \quad (6)$$

where q_t , q_1 and q_2 are the capacity at time t and at equilibrium, respectively (and expressed as mg/g), and k_1 , k_2 , α , β , k_i and C are the kinetics rate constants. Kinetics modelling of PFO, PSO and Elovich analysis showed that the adsorption process fitted well with all the models for all the adsorbents and both chromium species, except the case of PG in Cr(VI) single system. While Intra-particle Diffusion does not fit well for any case. So, all those results mean that the adsorption of heavy

metals on the surface of the adsorbents is due to a combination of the physics and chemical adsorption process, such as valence forces sharing or exchanging electrons between the adsorbent and adsorbate, except for PG and Cr(VI). In this case, none of the selected model could successfully reproduce the trend of PG to fit the adsorption process of Cr(VI). Probably due to a special adsorption mechanism which will be discussed at the molecular level by XAS (shown in XAS section). The relative constants found by applying the models are listed in Table 2. Highest capacities of Cr(III) in all biomass cases and lowest capacities of Cr(VI) by PG have been found.

Effect of initial concentration

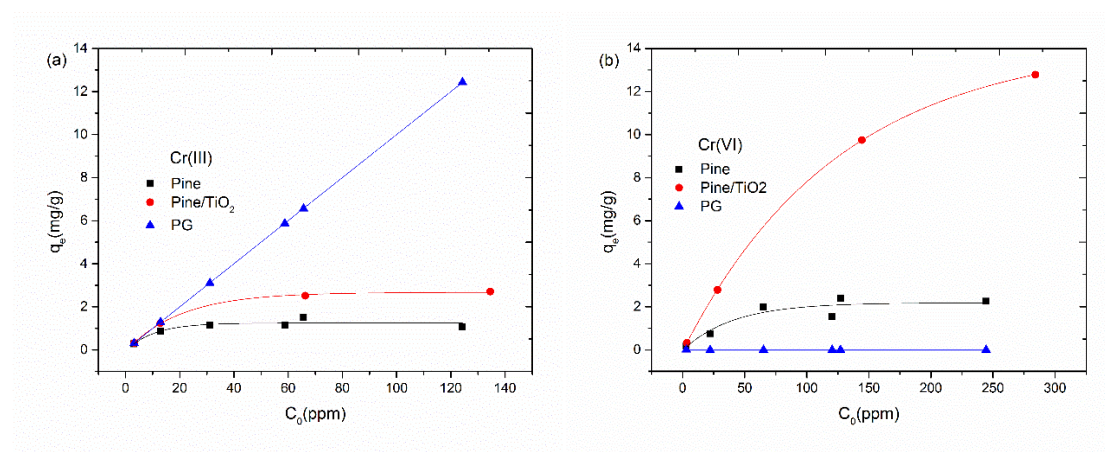


Figure 6 Effect of the initial concentration of heavy metals on their adsorption by Pine, Pine/TiO₂ and PG in Cr(III) single system (a), in Cr(VI) single system (b). Experimental conditions were $T=25\pm 1^\circ\text{C}$, pH 4.0, 25 mg of adsorbent, 2.5 mL of metals solution and stirring for 24 hours. Lines are a guide for the eyes.

Six single-metal solutions (5 ppm, 10 ppm, 25 ppm, 50 ppm, 75 ppm, 120 ppm and 240 ppm) were prepared from 1,000 ppm stock solutions of each heavy metal. The study of the initial concentration range provides a significant understanding of both Cr metal ion species during the adsorption process. As shown in Figure 6 (b), the adsorption capacity of Cr(VI) is higher by Pine against PG, whereas the Pine/TiO₂ increased the adsorption of Cr(VI) probably due to TiO₂ photocatalysis that has been considered as promising Cr(VI) reduction technology. Many researches have been using TiO₂ or modified TiO₂ under UV or visible light irradiation for Cr(VI) reduction in wastewater^{32,33}. In addition, PG highly selective capacity for Cr(III) probably due to the high mineral amounts as mentioned above. They can provide more possibilities for the exchange of heavy metals cations from the solution, which could increase the adsorption capacity of positive Cr(III).

Biosorption isotherm modelling

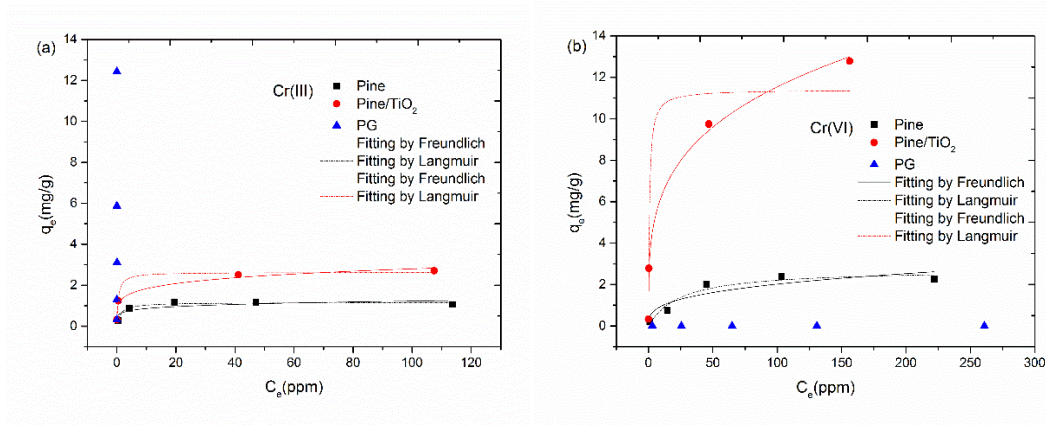


Figure 7 Adsorption isotherms modelling of heavy metal in single system by Pine, Pine/TiO₂ and PG. (a) in Cr(III) single system; (b) in Cr(VI) single system. Biosorption conditions were at T=25±1°C, pH 4.0 and stirring for 24 hours.

Table 3 Langmuir and Freundlich isotherm parameters of Cr(III) and Cr(VI) ions onto Pine, Pine/TiO₂ and PG. Biosorption conditions were at T=25±1 °C, pH 4.0.

		$q_{e,max}$	Freundlich			Langmuir		
		(mg/g)	K_f	n	R^2	q_{max}	B	R^2
			(mg/g)			(mg/g)	(L/mol)	
Cr(III)	Pine	1.16	0.605	0.154	0.616	1.16	0.833	0.966
	Pine/TiO ₂	1.23	1.20	0.184	0.941	2.63	1.97	0.976
	PG	12.4	NA	NA	NA	NA	NA	NA
Cr(VI)	Pine	2.26	0.454	0.324	0.784	2.75	0.0407	0.930
	Pine/TiO ₂	12.8	3.40	0.266	0.982	11.4	1.29	0.938
	PG	0.005	NA	NA	NA	NA	NA	NA

NA means not data

Langmuir and Freundlich isotherm models are widely used to study the adsorption mechanism for the interaction of heavy metal ions on the adsorbent surface. Langmuir model assumes that the uptake of metal ions occurs on homogeneous surface by a monolayer deposition. The generalized Langmuir isotherm can be represented by equation:

$$q_e = \frac{Q_{max}K_L C_e}{1 + K_L C_e} \quad (7)$$

where C_e is the equilibrium concentration of metal ions in the solution ($\mu\text{mol/L}$), q_{max} is the amount of metal ion required to form a monolayer (in this case in $\mu\text{mol/g}$) and K_L ($\text{L}/\mu\text{mol}$) is the equilibrium constant related to the energy of adsorption.

The Freundlich isotherm model follows an empirical equation and was employed to describe the equilibrium process on heterogeneous surface. The adsorption equilibrium constant is determined by the surface of non-homogeneous of the

adsorbent, which can be expressed as:

$$q_e = K_f C_e^n \quad (8)$$

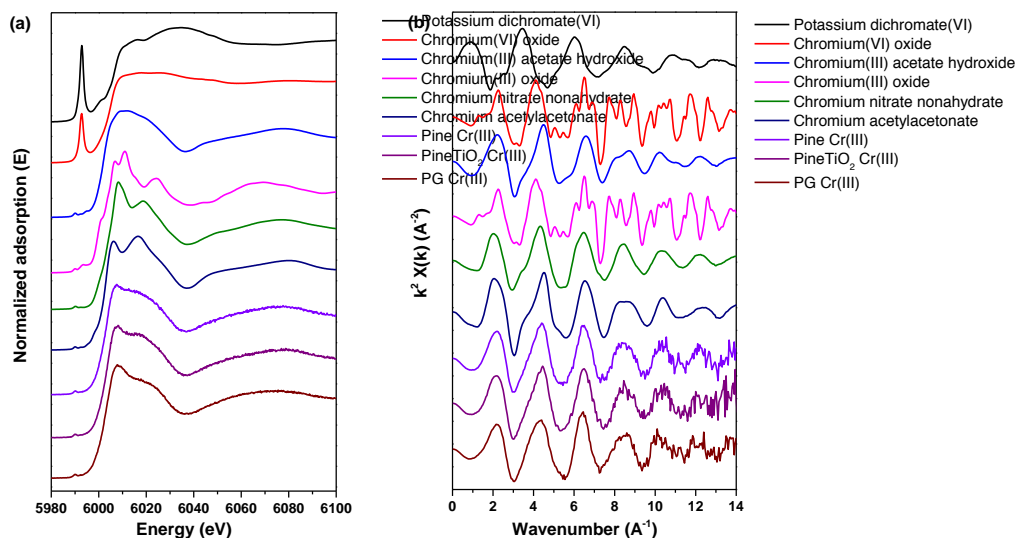
where K_f ($\mu\text{mol/g}$) and n (dimensionless) are the Freundlich isotherm constants, which indicate the biosorption capacity and the heterogeneity factor, respectively. The biosorption of Cr(III) and Cr(VI) by Pine and Pine/TiO₂ were fitted well with Freundlich (correlation coefficients were listed in Table 3 and graphs are shown in Figure 7). The biosorption capacity of Cr(III) by PG notable increased than those of Pine. However, PG can be hardly described by both isotherm models probably due to high efficiency adsorption of metal ions by such biomass. This could illustrate that the modification of the Pine using TiO₂ and by gasification pyrolysis results in an increase of sites interactions on the material surface. Pine/TiO₂ presents different capacities for Cr(III) and Cr(VI) ions with 1.23 and 12.78 mg/g, respectively, being quite high for Cr(VI). While Pine presents capacities of Cr(III) and Cr(VI) being 1.16 and 2.26 mg/g, respectively, lower than Pine/TiO₂ for Cr(VI) (show in Figure 1). PG shows highest capacity of Cr(III) with 12.42 mg/g, and no adsorption for Cr(VI), which shows a clear selectivity of Cr(III). Comparing these models listed in Table 3, the experimental data of Cr(III) and Cr(VI) ions were fitted well with both models by Pine/TiO₂, which could be confirmed by correlation coefficient (R^2). Pine fitted well Langmuir in both cases, however, PG doesn't fit any of them. To explicit the adsorption mechanism of PG, XAS was discussed in the latter chapter.

Adsorption mechanism study of Cr

The XANES data were used to verify the species of heavy metal bound to the adsorbents. As show in Figure 3.41, the XANES spectra of six reference compounds are compared with Pine, PG and Pine/TiO₂ after biosorption from Cr(III) and Cr(VI) single systems. As we can see that Cr(VI) is getting reduced to Cr(III) after the adsorption for all case. Furthermore, the spectra of reduction state of Cr(III) are more similar to the spectra of Cr(III) acetate hydroxide (which includes the possible interaction with COOH functional group), and Cr(III) nitrate nonahydrate. COOH functional group has been identified present in the surface of pine and Pine/TiO₂ in previous ATR-FTIR results. Combined with ATR-FTIR and XANES, the biosorption of Cr by pine and Pine/TiO₂ could be explained by ion exchange with hydrogen ion from carboxylic functional group. The similar spectra to Cr(III) nitrate nonahydrate could be explained by the original aqueous salt solution, which can remain nearby to Cr(III).

Similarly, the biosorption of PG is mainly explained through both ion exchange with mineral components (present in the surface of PG), and also ion exchange with COOH functional groups. To obtain PG high pyrolysis temperatures are used, so there is also a loss of functional groups even not totally. In this sense, the increase also of the surface can get a major environment of acetate groups around Cr(III) than the other possibilities.

However, the reduction of Cr(VI) by adsorbents are not clear in this study. Depth study related to this part is needed. From the literature, Cr(VI) is favorable interaction with catechol, a component of tannin present in wood biomass. Later, Cr(VI) can be reduced to Cr(III) after binding with catechol and can ion-exchange with hydrogen ion from carboxylic or hydrogen functional groups. Also, the active carbon of biochar can reduce Cr(VI) to Cr(III). This information helps us explain the reduction mechanism, but need to further study in the future.



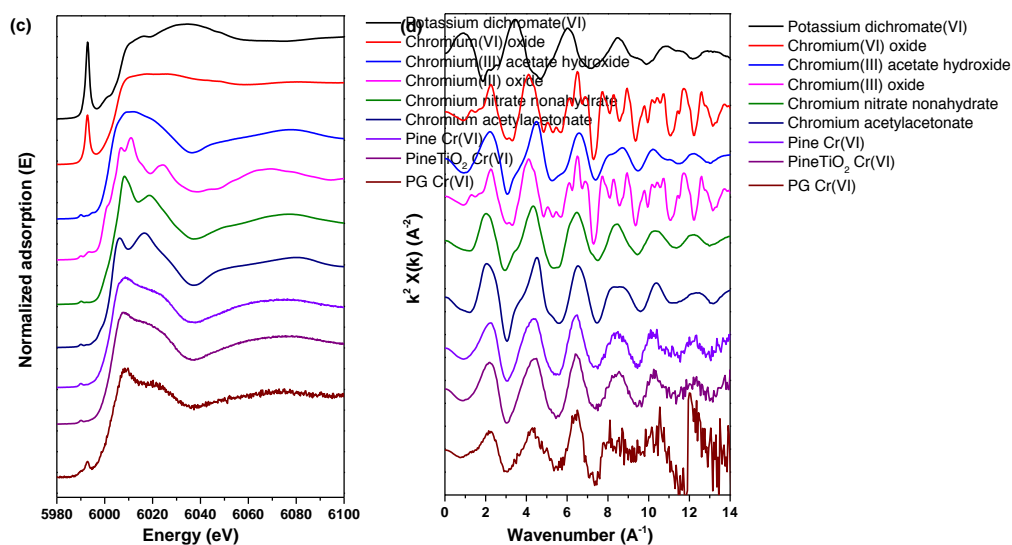


Figure 3.41 XAS spectra of references and Cr-loaded on Pine Pine/TiO₂ and PG. (a) (b) are the normalized E-edge and k^2 -weighted spectra of XANES in Cr(III) system, (c) and (d) are normalized E-edge and k^2 -weighted of XANES in Cr(VI) systems.

Conclusions

Three adsorbents have been used successfully for the removal of Cr(III) and Cr(V) from aqueous systems. The biochars loaded with TiO₂ particles have increased the adsorption of Cr. This finding can be explained by an increase in porosity and a pre-concentration of mineral components during the pyrolysis process.

In this study, combined the techniques of EXAFS along with FT-IR analyses, we describe the molecular level adsorption of Cr(III) and Cr(VI) by Pine, PG and Pine/TiO₂ for the first time to study the adsorption mechanism.

In summary, these adsorbents can be used to remove Cr from waste solution. Therefore, biomass could be an interesting alternative to synthetic materials for heavy metal removal. Biochar can also be an alternative with requires biomass pretreatment to enhancement the adsorption capacity.

Acknowledgements

This research was supported by grants from Spanish research projects (Nos. CTM2015-65414-C2-1-R and AGL2015-70393-R) and China Scholarship Council (No. 201509110114). We acknowledge Diamond Light Source facility for beamtime no. SP18561 at B18 beamline. All the authors are grateful to the UAB Microscopy Service (*Servei de Microscòpia Electrònica* from UAB, Catalunya, Spain) for the SEM analysis and to M. Resina who helped perform the analysis of heavy metals by ICP-MS. R.B. acknowledges funding support from the European Union's Horizon 2020 research and innovation program under the Marie Skłodowska-Curie grant agreement No. 665919.

References

- [1] S. Vikrant, S. Tony, Sarvinder, K.K.Pant, Thermodynamic and breakthrough column studies for the selective sorption of chromium from industrial effluent on activated eucalyptus bark, *Bioresour. Technol.* **97** (2006) 1986–1993. doi:10.1016/j.biortech.2005.10.001.
- [2] P. Miretzky, A. Fernandez Cirelli, Cr(VI) and Cr(III) removal from aqueous solution by raw and modified lignocellulosic materials: a review., *J. Hazard. Mater.* **180** (2010) 1–19. doi:10.1016/j.jhazmat.2010.04.060.
- [3] Robert M. Sterritt, John N. Lester, Significance and behaviour of heavy metals in waste water treatment processes III. Speciation in waste waters and related complex matrices, *Sci. Total Environ.* **34** (1984) 117–141.
- [4] K. Nath, K. Nishith, Hexavalent chromium: Toxicity and its impact on certain aspects of carbohydrate metabolism of the freshwater teleost, *Colisa fasciatus*, *Sci. Total Environment.* **72** (1988) 175–181.
- [5] C. Pellerin, S. Booker, Reflections on hexavalent chromium: health hazards of an industrial heavyweight., *Env. Heal. Perspect.* **108** (2000) A402-7.
- [6] S.W.N. Wan, A.K.M.. Megat, Removal of heavy metal ions from wastewater by chemically modified plant wastes as adsorbents: A review, *Bioresour. Technol.* **99** (2008) 3935–3948. doi:10.1016/j.biortech.2007.06.011.
- [7] A. Demirbas, Heavy metal adsorption onto agro-based waste materials: A review, *J. Hazard. Mater.* **157** (2008) 220–229. doi:10.1016/j.jhazmat.2008.01.024.
- [8] D. Pradhan, L.B. Sukla, M. Sawyer, P.K.S.M. Rahman, Recent bioreduction of hexavalent chromium in wastewater treatment: A review, *J. Ind. Eng. Chem.* **55** (2017) 1–20. doi:10.1016/j.jiec.2017.06.040.
- [9] X. Tan, Y. Liu, G. Zeng, X. Wang, X. Hu, Y. Gu, Z. Yang, Application of biochar for the removal of pollutants from aqueous solutions, *Chemosphere.* **125** (2015) 70–85. doi:10.1016/j.chemosphere.2014.12.058.
- [10] M. Inyang, B. Gao, Y. Yao, Y. Xue, A.R. Zimmerman, P. Pullammanappallil, X. Cao, Removal of heavy metals from aqueous solution by biochars derived from anaerobically digested biomass, *Bioresour. Technol.* **110** (2012) 50–56. doi:10.1016/j.biortech.2012.01.072.
- [11] F. Gode, E.D. Atalay, E. Pehlivan, Removal of Cr(VI) from aqueous solutions using modified red pine sawdust, *J. Hazard. Mater.* **152** (2008) 1201–1207. doi:10.1016/j.jhazmat.2007.07.104.
- [12] S.X. Zhao, N. Ta, X.D. Wang, Effect of temperature on the structural and physicochemical properties of biochar with apple tree branches as feedstock material, *Energies.* **10** (2017). doi:10.3390/en10091293.
- [13] Y. Sun, B. Gao, Y. Yao, J. Fang, M. Zhang, Y. Zhou, H. Chen, L. Yang, Effects of feedstock

type, production method, and pyrolysis temperature on biochar and hydrochar properties, *Chem. Eng. J.* **240** (2014) 574–578. doi:10.1016/j.cej.2013.10.081.

[14] A. Bagreev, T.J. Bandosz, D.C. Locke, Pore structure and surface chemistry of adsorbents obtained by pyrolysis of sewage sludge-derived fertilizer, *Carbon N. Y.* **39** (2001) 1971–1979. doi:10.1016/S0008-6223(01)00026-4.

[15] M.K. Hossain, V. Strezov, K. Chan, A. Ziolkowski, P.F. Nelson, Influence of pyrolysis temperature on production and nutrient properties of wastewater sludge biochar, *J. Environ. Manage.* **92** (2011) 223–228. doi:10.1016/j.jenvman.2010.09.008.

[16] X. Wang, S.O. Pehkonen, A.K. Ray, Removal of Aqueous Cr(VI) by a Combination of Photocatalytic Reduction and Coprecipitation, *Ind. Eng. Chem. Res.* **43** (2007) 1665–1672. doi:10.1021/ie030580j.

[17] L. Cui, M.R. Noerpel, K.G. Scheckel, J.A. Ippolito, Wheat straw biochar reduces environmental cadmium bioavailability, *Environ. Int.* **126** (2019) 69–75. doi:10.1016/j.envint.2019.02.022.

[18] K.J. Whaley-Martin, I. Koch, K.J. Reimer, Determination of arsenic species in edible periwinkles (*Littorina littorea*) by HPLC-ICPMS and XAS along a contamination gradient, *Sci. Total Environ.* **456–457** (2013) 148–153. doi:10.1016/j.scitotenv.2013.03.066.

[19] A.U. Rajapaksha, M.S. Alam, N. Chen, D.S. Alessi, A.D. Igalavithana, D.C.W. Tsang, Y.S. Ok, Removal of hexavalent chromium in aqueous solutions using biochar: Chemical and spectroscopic investigations, *Sci. Total Environ.* **625** (2018) 1567–1573. doi:10.1016/j.scitotenv.2017.12.195.

[20] W. Jiang, Q. Cai, W. Xu, M. Yang, Y. Cai, D.D. Dionysiou, K.E. O’Shea, Cr(VI) adsorption and reduction by humic acid coated on magnetite, *Environ. Sci. Technol.* **48** (2014) 8078–8085. doi:10.1021/es405804m.

[21] W. Liu, J. Ni, X. Yin, Synergy of photocatalysis and adsorption for simultaneous removal of Cr(VI) and Cr(III) with TiO₂ and titanate nanotubes, *Water Res.* **53** (2014) 12–25. doi:10.1016/j.watres.2013.12.043.

[22] J.R. Kim, E. Kan, Heterogeneous photocatalytic degradation of sulfamethoxazole in water using a biochar-supported TiO₂ photocatalyst, *J. Environ. Manage.* **180** (2016) 94–101. doi:10.1016/j.jenvman.2016.05.016.

[23] E.A.N. Marks, S. Mattana, J.M. Alcañiz, X. Domene, Biochars provoke diverse soil mesofauna reproductive responses in laboratory bioassays, *Eur. J. Soil Biol.* **60** (2014) 104–111. doi:10.1016/j.ejsobi.2013.12.002.

[24] A.J. Dent, G. Cibir, S. Ramos, A.D. Smith, S.M. Scott, L. Varandas, M.R. Pearson, N.A. Krumpa, C.P. Jones, P.E. Robbins, B18: A core XAS spectroscopy beamline for Diamond, *J. Phys. Conf. Ser.* **190** (2009). doi:10.1088/1742-6596/190/1/012039.

[25] B.R. and M. Newville, ATHENA, ARTEMIS, HEPHAESTUS: data analysis for X-ray absorption spectroscopy using IFFFIT, *J. Synchrotron Radiat.* **12** (2005) 537–541.

- [26] A.-W. Mohammad, A. Abdulrasoul, E.-N. Ahmed H., N. Mahmoud E.A., U. Adel R. A., Pyrolysis temperature induced changes in characteristics and chemical composition of biochar produced from conocarpus wastes, *Bioresour. Technol.* **131** (2013) 374–379. doi:10.1016/j.biortech.2012.12.165.
- [27] Y. Chen, L.M. de Oliveira, E.B. da Silva, X. Dong, L.Q. Ma, H. Li, Mechanisms of metal sorption by biochars: Biochar characteristics and modifications, *Chemosphere.* **178** (2017) 466–478. doi:10.1016/j.chemosphere.2017.03.072.
- [28] Renata Wnetrzak, J.J. Leahy, Katarzyna W. Chojnacka, Agnieszka Saeid, Etelvino Novotny, Lars Stoumann Jensen, Witold Kwapinski, Influence of pig manure biochar mineral content on Cr(III) sorption capacity, *J. Chem. Technol. Biotechnol.* **89** (2014) 569–578. doi:10.1002/jctb.4159.
- [29] Y. Chen, B. Wang, J. Xin, P. Sun, D. Wu, Adsorption behavior and mechanism of Cr(VI) by modified biochar derived from *Enteromorpha prolifera*, *Ecotoxicol. Environ. Saf.* **164** (2018) 440–447. doi:10.1016/j.ecoenv.2018.08.024.
- [30] J.H. Yuan, R.K. Xu, H. Zhang, The forms of alkalis in the biochar produced from crop residues at different temperatures, *Bioresour. Technol.* **102** (2011) 3488–3497. doi:10.1016/j.biortech.2010.11.018.
- [31] H. Li, X. Dong, E.B. da Silva, L.M. de Oliveira, Y. Chen, L.Q. Ma, Mechanisms of metal sorption by biochars: Biochar characteristics and modifications, *Chemosphere.* **178** (2017) 466–478. doi:10.1016/j.chemosphere.2017.03.072.
- [32] Q. Wang, X. Shi, J. Xu, J.C. Crittenden, E. Liu, Y. Zhang, Y. Cong, Highly enhanced photocatalytic reduction of Cr(VI) on AgI/TiO₂ under visible light irradiation: Influence of calcination temperature, *J. Hazard. Mater.* **307** (2016) 213–220. doi:10.1016/j.jhazmat.2015.12.050.
- [33] K.M. Joshi, V.S. Shrivastava, Photocatalytic degradation of Chromium (VI) from wastewater using nanomaterials like TiO₂, ZnO, and CdS, *Appl. Nanosci.* **1** (2011) 147–155. doi:10.1007/s13204-011-0023-2.
- [34] D. Mohan, C.U. Pittman, Activated carbons and low cost adsorbents for remediation of tri- and hexavalent chromium from water, *J. Hazard. Mater.* **137** (2006) 762–811. doi:10.1016/j.jhazmat.2006.06.060.
- [35] D. Park, Y.S. Yun, J.M. Park, XAS and XPS studies on chromium-binding groups of biomaterial during Cr(VI) biosorption, *J. Colloid Interface Sci.* **317** (2008) 54–61. doi:10.1016/j.jcis.2007.09.049.

Annex III

Article under preparation. In collaboration with Eliane C de Resende from Federal Institute of Minas Gerais, Brazil.

The mechanism and adsorption heavy metal study of Pine biomass and pyrolyzed Pine loaded with TiO₂ in aqueous solution

Jingjing Zhao¹, Eliane Cristina de Resende², Roberto Boada Romero¹, Julio Bastos-Arrieta³, Cristina Palet Ballús¹

¹Group of Separation Techniques in Chemistry, Department of Chemistry, Universitat Autònoma de Barcelona, 08193 Bellaterra, Catalunya, Spain;

²Department of Science and Language, Federal Institute of Minas Gerais, 38900-000, Bambuí, Minas Gerais, Brazil

³Physical Chemistry, Zellescher Weg 19, TU Dresden, 01069 Dresden, Germany

* Corresponding Author: cristina.palet@uab.cat

Abstract:

Pine biomass and pyrolyzed pine loaded with TiO₂ (Pine/TiO₂) have been used as sorbent for the removal of heavy metal ions from aqueous solution. A single-element system and multi-element system were used to removal heavy metals. The multi-element system composed by a mixture of Cr(III), Cd(II), Cu(II) and Pb(II) ions was used to simulate a realistic case of waste water polluted with heavy metals case for adsorption. Different parameters of adsorption processes were optimized in batch systems (pH of the solution, the initial concentration and the contact time). Surface morphology of the adsorbents were analyzed using scanning electron microscopy (SEM) and Fourier transform infrared spectroscopy (FT-IR). Pine showed better adsorption capacity for all heavy metals in single-element system, on the other hand Pine/TiO₂ increased the adsorption in multi-element system, especially to Cu(II) and Pb(II) with 34 and 77 μmol/g, respectively. The results of X-ray absorption spectroscopy (XAS) shows that the adsorption mechanism of Pb is ion exchange, while Pb ions exchange hydrogen ions in carboxylic acids in solution.

Key words: biomass, pyrolysis, heavy metal, TiO₂, XAS

Introduction

The development of low-cost techniques for removing toxic heavy metals from the environment is one of the most important goals in environmental science. Heavy

metals present a major concern for the environment due to its high toxicity to living organisms. Numerous physical and chemical separation techniques are being used to remove heavy metals, such as solvent extraction, ion-exchange, adsorption, membrane filtration and electrochemical treatment technologies (Huang et al., 2018; Hussain et al., 2014; Lin and Juang, 2002; Maren et al., 2017; Zhang et al., 2015). Among the conventional techniques for removing pollutants from water, adsorption methods are considered to be the most advantageous due to their high efficiency, low cost and ease handling. Within this framework, biomass has emerged as an ideal option for developing economic and eco-friendly wastewater treatments.

Previous research articles have reported the successful use of different kinds of wood biomass for removal of metal ions from aqueous solution, such as *pine cone* for Cd(II) and Pb(II) with the maximum biosorption capacity were 285.7 and 140.1 $\mu\text{mol/g}$, respectively (Argun et al., 2008). *Pine cone powder* for the removal of Cu(II) and Pb(II) with maximum capacity of 411.1 and 155.8 $\mu\text{mol/g}$, respectively (Ofomaja et al., 2010). Pb(II), Cu(II), and Cd(II) with maximum sorption capacities of 739.6, 534.4, and 250.9 $\mu\text{mol/g}$ by *hickory wood*, respectively (Wang et al., 2015). Although all of these biomass show strong biosorption capacity, they are applied in single-element system. It is known that biosorption in multi-element system is decreased due to the competition of heavy metals. Therefore, it is necessary to find an effective approach for heavy metal removal in multi-element system. Pine wood could be highlighted as a potential material, once among the wood biomass, pine is abundantly grown in the world and the waste is of no market value. Also in the literature, biosorption capacity can be increased by using pyrolyzed biomass comparing with original biomass (Qian et al., 2016).

TiO₂ nanoparticles is also a good adsorbent for removing heavy metals, but TiO₂ nanoparticles easily aggregate which limited the application. However, once Pine as a holder, it could be avoided the aggregate of TiO₂. In this study, combined wood biomass and TiO₂, a new pretreatment of pine was carried out, by adding Titanium dioxide (TiO₂) before the pyrolysis procedure, we were able to get TiO₂ nanoparticles on the Pine surface.

The aim of this study was to effectively remove Pb(II), Cd(II), Cu(II) and Cr(III) in a multi-element system and study the adsorption mechanism of Pine and Pine/TiO₂, as simulation of real wastewater, proving the suitability of Pine and their waste, for wastewater remediation methodologies.

Materials and methods

Chemical and reagents

The Pine is sawdust from pine bark to make wood, which was grinded and dried before using. It was kindly supplied by CREAM Institute (at Autonomous University of Barcelona, UAB, Barcelona, Spain). All the chemicals used were of analytical grade. The ethanol (C_2H_6O , 97%), nitric acid (HNO_3) and hydrochloric acid (HCl , 37% v/v) were purchased from Panreac (Barcelona, Spain). Titanium (IV) butoxide ($C_{16}H_{36}O_4Ti$, 97% v/v) was from Sigma-Aldrich (MO, USA). A 1000 mg/L stock solution of single and multiple element systems were prepared by dissolving the required amounts of $Pb(NO_3)_2$, $Cd(NO_3)_2 \cdot 4H_2O$, $Cu(NO_3)_2 \cdot 3H_2O$ and $Cr(NO_3)_3 \cdot 9H_2O$ (all 99% from Panreac, Barcelona, Spain).

Pretreatment of Pine

The sample of Pine was washed with deionized water and dried in an oven at $75^\circ C$ for 24 h. The acid-treated Pine was prepared by the methods reported by Kan (Kim et al., 2009). 5 g of Biomass were suspended in nitric acid at pH 3.0 for 4 days as a conditioning procedure. After a step of filtration from the acidic media, the treated Pine was washed with deionized water multiple times until neutral pH (pH of the washing water). Then the material was dried in an oven at $75^\circ C$ for 24 h and stored in a desiccator.

Pine pyrolysed with TiO_2

The Pine/ TiO_2 was prepared using the sol-gel method reported by Wang. 5 g acid treated Pine was dispersed in 120 mL ethanol followed by addition of 40 mL Titanium (IV) butoxide (97%) (which is the TiO_2 precursor). The mixture was stirred at ambient temperature for 1 hour before adding a solution containing 16 mL of HCl 37% (v/v) and 40 mL alcohol (97%) with constant stirring (for 1 hour more). The solution was filtered, and then washed with alcohol (97%) before drying at $70^\circ C$ for 24 hours. The dried sample was milled and pyrolyzed at $325^\circ C$ for 1 hour in a muffle to yield the Pine/ TiO_2 .

Characterization of materials

The morphology was analyzed by scanning electron microscopy (SEM) coupled with energy dispersive X-ray (EDX), from the Electron Microscopy Facilities of UAB (Barcelona, Spain). The X-ray diffraction (XRD) patterns were collected to identify any crystallographic structures for the samples by using a powder X-ray Diffractometer with $Cu\ K\alpha$ radiation (XRD, D8 ADVANCE, Bruker). Fourier transform infrared spectroscopy (ATR-FTIR) spectra were recorded on a Nicolet IS10 spectrometer with a spectral range from 600 to $4000\ cm^{-1}$, from Servei d'Anàlisi de Química (UAB,

Barcelona, Spain).

Batch biosorption experiments

Biosorption experiments were carried out at room temperature ($25\pm 1^\circ\text{C}$) and evaluated for the metals in individual solution (single-element system) and for all metals together from the same initial stock solution (multi-element system). Metal concentration, for both different systems, was ranged from 0.05 to 4 mmol/L. Batch experiments were done by adding 10 mg of biomass in a 5 mL tubes, then filled with 1 mL of heavy metal aqueous solutions. The tubes were then placed on a rotary mixer (CE 2000 ABT-4, SBS Instruments SA, Barcelona, Spain) properly shaken at 25 rpm for 24 hours. After the biosorption, the two phases were separated by decantation and filtered through 0.22 μm Millipore filters (Millex-GS, Millipore). The concentrations of heavy metals in the supernatant phase were determined by an inductively coupled plasma mass spectrometry, ICP-MS (XSERIES 2 ICP-MS, Thermo Scientific). The uptake of the heavy metal by the Pine and Pine/TiO₂ is expressed as the percentage of removal Pine and Pine/TiO₂ calculated following Equation (1). Moreover, it was expressed as the amount of adsorbent at the equilibrium following Equation (2):

$$\% \text{ Removal} = \frac{(C_0 - C_e)}{C_0} \times 100 \quad (1)$$

$$q_e = \frac{(C_0 - C_e) \times V}{m} \quad (2)$$

Where q_e (mg/g) is the amount of heavy metal adsorbed at equilibrium; V (L) is the volume of solution; C_0 (mg/L) and C_e (mg/L) are the initial and equilibrium heavy metal concentrations in solution, respectively; and m (g) is the dried mass of adsorbent. In order to study the functional groups and metal-binding mechanisms, it is more convenient to express q_e as ($\mu\text{mol/g}$). All results were expressed as the mean value of the replicates.

X-ray absorption spectroscopy analysis

After adsorption in multi-element systems, Pine and Pine/TiO₂ were dried on oven at 70°C for 1 day. XAS data include X-ray absorption near-edge structures (XANES) and extended X-ray absorption fine structure (EXAFS) spectroscopy were performed at Diamond Synchrotron (London, England). EXAFS collected at Pb L3-edge using QEXAFS scanning mode of the monochromators. Measurements performed at liquid nitrogen temperature. The concentration of the heavy metals in the samples were mM. Fluorescence yield measure using the recently implemented multi-element Si drift detector with Xpress3 electronics. Transmission measurements performed using ionization chambers. References samples measured in transmission mode at room temperature.

Results and discussion

Characterization of biosorbents.

In order to study the morphological structure and surface elemental composition, Pine and Pine/TiO₂ were characterized by SEM-EDX. The SEM images show differences in the morphology of both materials. As it can be seen in Figure 1 panels (a) and (b), Pine/TiO₂ shows more developed pore structure than bare Pine. The images Figure 1 panel (c) exhibited TiO₂ were synthesized on the surface of Pine. From different SEM images, the diameter of TiO₂ nanoparticles was able to be checked and found to be in the range of 25 and 70 nm. TiO₂ aggregate can be found in different sizes, but most of the aggregate size are less than 1 μm. The spectra of EDX, corresponding to a semi-quantitative analysis, shows on Figure 1 panel (d) a strong peak for Ti and nearby is O, which confirms the presence of TiO₂ onto the pyrolyzed Pine surface.

According to literature, the results of FTIR shows that carboxyl (R-COOH) and alcoholic or phenolic hydroxyl groups (R-OH) are main functional groups contributing to coordination between heavy metals and the sorbent surfaces (Costa et al., 2010). To identify the existence of expected functional groups, ATR-FTIR spectroscopy was conducted. Figure 2 shows the FTIR spectra for Pine and Pine/TiO₂. It is reported that hemicellulose, cellulose and lignin are the three main components in bare wood biomass, confirmed by a group of complex infrared absorbance in the finger print region (1830-730 cm⁻¹) of Pine (McKendry, 2002). A broad band in the region of 3100-3600 cm⁻¹ corresponding to the hydroxyl from the adsorbed water. The peaks at 1729 cm⁻¹ and 1596 cm⁻¹ could be attributed to C=O stretching and COO⁻, respectively (Roberto M. Silverstein, 2015). The peak at 1025 cm⁻¹ probably corresponds to the carboxylic C-O stretching and C-O deformation. The obtained FTIR spectra confirmed the existence of carboxylic acid (-COOH) and carbonyl (C=O) groups in both Pine and Pine/TiO₂ (See in Table 1).

XRD was performed to study the crystallinity of the TiO₂ particles loaded inside biomass. Figure S2 of the supplementary information shows the X-ray powder diffraction pattern collected on Pine/TiO₂. No appreciable diffraction peaks from TiO₂ particles were detected over the background given by the amorphous porous biomass structure. This may be due to the small loading of the TiO₂ to the amorphous character of the particles.

The effect of pH.

Among all parameters, pH plays a significant role in controlling the biosorption of heavy metals. The pH of the solution affects the surface functional groups, charge of

the adsorbent and the degree of ionization and speciation of adsorbate. In order to determine the effect of pH in the removal of Pb(II), Cd(II), Cu(II) and Cr(III) from aqueous solutions by Pine and Pine/TiO₂, adsorption experiments at different pHs within the range going from 2 to 6 were performed. The concentration of solution is 0.18mmol/L in single and multi-element systems. All the samples were stirred for 24 hour to reach adsorption equilibrium for Pine and Pine/TiO₂.

Figure 3 shows that the biosorption percentage increases with the pH for Pine and Pine/TiO₂. All the elements follow a similar trend. The biosorption reaches its maximum value at pH 4 for Pine/TiO₂, whereas it monotonically increases for Pine within the range considered. According to literature, as solution pH increases, the biosorption removal of cationic metals increases, whereas that of anionic metals decreases (Tao et al., 2012). At lower pH, the H⁺ ions compete effectively with the metal cations causing a decrease in biosorption capacity. When pH values increase, a decrease in competition with protons ions (H⁺) favors the metal ions uptake due to electrostatic interaction. From pH 6, due to a change on the metal speciation by hydroxide formation, lower concentration of metal ion is found on the final solution which probably is not related with biosorption, but related with hydroxides metal precipitation.

In the present work the removal percentage of Pb(II), Cu(II), Cr(II) and Cd(III) by Pine/TiO₂ at pH 4 (100%,100%,100% and 80%, respectively) were notable higher than those of Pine (57%, 33%, 92% and 5.1%, respectively). These values are higher than those reported previously for Cu(II) adsorption on *Oil palm shell* (Chong et al., 2013). To avoid any possible precipitation by hydrolysis in multi-element system, also considering that the higher biosorption is found at pH 4, which is near the real pH of wastewater, this was chosen as the optimal pH value for further biosorption experiments, in order to determine the influence of other parameters (i.e. time and initial concentration, mainly).

Effect of the initial metal concentration

The initial concentration of Cr(III), Cu(II), Cd(II) and Pb(II) were involved in biosorption process of Pine and Pine/TiO₂, as it provides a significant understanding of the competitive process of the four heavy metals. See Figure 4, although the removal capacity of Cr(III), Cu(II), Cd(II) and Pb(II) increased with concentration levels, the biosorption capacity reaches saturation to Pine/TiO₂ and decreased for Cd(II) and Cu(II) to Pine when working at high concentration levels of metal. For multi-element system the Pine/TiO₂ shows a high capacity compared to the Pine, as it is higher regarding the increase of metals concentration. Specially in the case of Cu(II), the removal capacity was higher considering the other three metals.

Biosorption isotherm modeling

Langmuir and Freundlich isotherm models are widely used to study the adsorption mechanism for the interaction of heavy metal ions on the adsorbent surface. Langmuir model assumes that the uptake of metal ions occurs on homogeneous surface by a monolayer deposition. The generalized Langmuir isotherm can be represented by equation:

$$q_e = \frac{Q_{max}K_L C_e}{1 + K_L C_e} \quad (3)$$

Where C_e is the equilibrium concentration of metal ions in the solution ($\mu\text{mol/L}$), Q_{max} is the amount of metal ion required to form a monolayer (in this case is $\mu\text{mol/g}$) and $K_L(\text{L}/\mu\text{mol})$ is the equilibrium constant related to the energy of adsorption.

The Freundlich isotherm model follows an empirical equation and was employed to describe the equilibrium process on heterogeneous surface. The adsorption equilibrium constant is determined by the surface of non-homogeneous of the adsorbent, which can be expressed as:

$$q_e = K_f C_e^n \quad (4)$$

Where K_f ($\mu\text{mol/g}/(\mu\text{mol/L})^n$) and n (dimensionless) are the Freundlich isotherm constants, which indicate the biosorption capacity and the heterogeneity factor, respectively (Nguyen et al., 2017). The biosorption of Cu(II) and Pb(II) by Pine/TiO₂ were fitted well with Freundlich (correlation coefficients were listed in Table 2 and graphs are shown in Figure 5). The biosorption capacity of Cu(II) and Pb(II) in multi-element system by Pine/TiO₂ notable increased than those of Pine. However, Pine can be hardly described by both isotherms models except for Cr(III) and Cu(II) (data is showed in Table 2), probably due to the low adsorption capacity by such biomass. This could illustrate that the modification of the Pine using TiO₂ results in an increase of sites interactions on the material surface. The biosorption capacity of heavy metal in multi-element system follows as: Pb(II) > Cu(II) > Cr(III) > Cd(II). Pine/TiO₂ presents high capacities for Cu(II) and Pb(II) ions with 34 and 77 $\mu\text{mol/g}$, respectively. While capacity of Cr(III) and Cd(II) is 10.5 and 4.95 $\mu\text{mol/g}$, respectively.

Comparing both models listed in Table 2, the experimental data of Pb(II) were fitted well with both models, which could be confirmed by correlation coefficient (R^2). The biosorption of Cu(II) was better fitted with Langmuir and Freundlich, with correlation coefficient were 0.98 and 0.84, respectively. We assume that Pb(II) is priority binding to the surface of Pine/TiO₂, whereas the adsorption of Cu(II), Cr(III) and Cd(II) were hard to bind to the surface due to the competition of those heavy metals.

Effect of the time

The biosorption kinetics also participate in identifying the required equilibration time

and the optimal contact time for a biosorption process. The time range was established from 5 min to 1440 min, here we only show the range from 5 min to 480 min because the adsorption of Pine and Pine/TiO₂ have reached the equilibrium at 480 min (shown in Figure 6). Similar to the results of literatures, the biosorption of Cr(III), Cu(II), Cd(II) and Pb(II) exhibited an initial rapid stage during the first 10 min, this is could be due to the absorption sites and affinity between heavy metal ions and adsorbents (Chakravarty et al., 2013). Followed by a reduction in the adsorption rate due to the reduction of available sites for biosorption.

Figure 6 shows the effect of contact time on removal percentage of Pine and Pine/TiO₂ in single-element and multi-element systems. The biosorption performance of Pine/TiO₂ toward all heavy metals was higher than that of the Pine in both systems, especially, the biosorption efficiencies of Cu(II) and Cd(II) were three and four times higher respectively.

The removal percentage of Pine/TiO₂ in single-element system reach 100% in the first 10 min. However, the adsorption in multi-element system need longer time to reach the adsorption equilibrium. It's probably due to the competition of occupying the adsorption sites in multi-element system. The heavy metal ion biosorption percentage of Pine in single-element system ranked as: Cr(III)>Pb(II)>Cu(II)>Cd(II), while in multi-element system ranked as: Pb(II)>Cr(III)>Cu(II)>Cd(II)>Pb(II) has priority in occupying adsorption sites and Cr(III) second to Pb(II) compared with other metals. After 24 hours adsorption, Pine and Pine/TiO₂ reached the adsorption equilibrium in both systems. Thus 24 hours was chosen for the optimal contact time value for further biosorption experiments to determine the optimal values of the other parameters.

Biosorption kinetics modeling

To further understand the competitive biosorption behavior of Cr(III), Cu(II), Cd(II) and Pb(II), the biosorption kinetics curves were analyzed using two different models: pseudo-first-order and pseudo-second-order, which have been intensively applied to simulate the biosorption process.

The pseudo-first-order model (PFO) for solid/liquid systems of adsorption states that the rate is proportional to the number of unoccupied sites, is controlled by physic process (Lagergren, 1898). The expression is given as:

$$\log(q_e - q_t) = \log(q_e) - \frac{k_1}{2.303} t \quad (5)$$

A pseudo-second-order model (PSO) assumes that the rate of adsorption is proportional to the square of the number of unoccupied sites(Blanchard et al., 1984), a chemical process sorption process controls the rate, including valence forces

sharing or exchange of electrons between adsorbent and adsorbate.

$$\frac{1}{q_t} = \left(\frac{1}{k_2 q_e^2} \right) \times \frac{1}{t} + \frac{1}{q_e} \quad (6)$$

Here, the following abbreviations apply: q_t and q_e are the biosorption amount at time t and at equilibrium, respectively; k_1 , k_2 represents the rate constant.

According to literature (Nguyen et al., 2017), in most cases, the PFO equation is linear only over approximately the first 30 min, so it is appropriate for the initial contact time, not for the whole range. The PSO model was applied up to 480 min of experiment.

As show in Table 4, Pine and Pine/TiO₂ are well agreement with the PSO model, which suggests that the adsorption rate of the heavy metals was controlled by chemistry process. The adsorption rate constant (k_2) related with adsorption sites on Pine and Pine/TiO₂, also depends on the initial ions concentration. As we can see in Table 4, Pb(II) shows higher adsorption rate compared with other heavy metals, which means Pb(II) priority occupied the adsorption sites. It could be explained by the higher atomic weight, greater electro-negativity and ionic radius of Pb(II). The data of PFO model was also checked, however, Pine and Pine/TiO₂ can not be well explained by this model. Its means that the adsorption of Pine and Pine/TiO₂ were not depend on the physic process or the physic process wasn't the main controlling step.

Adsorption mechanism study using XAS

In order to study the interaction of the heavy metal ions with the different site of adsorption present in Pine and Pine/TiO₂, The X-ray absorption spectrum (XAS) was used to investigate the mechanism of heavy metal binding to the Pine and Pine/TiO₂. XAS is divided into two regimes: X-ray absorption near-edge spectroscopy (XANES) and extended X-ray absorption fine-structure spectroscopy (EXAFS). XANES is sensitive to formal oxidation state and coordination chemistry of absorption atom, while EXAFS is used to determine the distances, coordination number, and species of neighbors of the absorbing atom. EXAFS can provide us the bond distance between heavy metals and biomass. All this information is unique for each sample, so we can get the useful information (such as function groups and specious) compared with references compounds. In our case, it could explain which function groups are responsible for selective adsorption of heavy metals and the enhancement in adsorption capacity when including TiO₂ nanoparticles.

As show in Figure 7, are the normalized L3-edge and the k-weighted spectra of XANES of Pine, Pine/TiO₂ and other reference compounds in single and multi-element systems. Three Pb reference compounds include Lead(II) oxide, Lead(II)

acetate trihydrate, Lead(II) nitrate. The spectra of pine and Pine/TiO₂ after biosorption of Pb (from single and multiple systems) are more similar to the spectra of Pb(II) acetate trihydrate (which includes COOH functional group) for all cases. COOH functional group has been identified present in the surface of pine and Pine/TiO₂ in previous ATR-FTIR results. Combined with ATR-FTIR and XANES, the biosorption of Pb by pine and Pine/TiO₂ could be explained by ion exchange with hydrogen ion from carboxylic functional group.

Conclusions

The biosorption capacity in multi-element system for Cr(III), Cu(II), Cd(II) and Pb(II) removal was greatly enhanced after loading TiO₂ on Pine. The biosorption percentage in multi-element system of all heavy metals increased, following the order: Pb(II) > Cr(III) > Cu(II) > Cd(II), especially Cu(II) and Pb(II) by the Pine/TiO₂ get higher capacity than Pine. This biosorption process of Pb(II) was better fit by Freundlich isotherm models by using Pine/TiO₂. XAS Results show that the adsorption mechanism of Lead(II) is ion exchange, which is mainly through proton-active carboxyl (-COOH) functional groups on the sorbent surface. Results from the present research indicated that Pine/TiO₂ is a suitable material for the removal of metals from wastewaters. The application of Pine/TiO₂ as a biosorbent gives a contribution to solve a pressing problem of heavy metal aqueous contamination, at the same time gives a useful purpose for the Pine waste from wood industry.

Acknowledgments

This work was supported by Spanish research project [CTM2015-65414-C2-1-R], China Scholarship Council [No.201509110114] and Brazil Pos-doc scholarship. The authors are grateful to the UAB Microscopy Service (Servicio de Electrónica Microscópica from UAB) for the SEM and EDS analysis. Also, thanks to the Diamond Synchrotron Facilities for the XAS analysis.

References

- Ahmad, M., Usman, A.R.A., Soo, S., Kim, S., Joo, J., Yang, J.E., Sik, Y., 2012. Journal of Industrial and Engineering Chemistry Eggshell and coral wastes as low cost sorbents for the removal of Pb²⁺, Cd²⁺ and Cu²⁺ from aqueous solutions. *J. Ind. Eng. Chem.* 18, 198–204. <https://doi.org/10.1016/j.jiec.2011.11.013>
- Argun, M.E., Dursun, S., Karatas, M., Gürü, M., 2008. Activation of pine cone using Fenton oxidation for Cd(II) and Pb(II) removal. *Bioresour. Technol.* 99, 8691–8698. <https://doi.org/10.1016/j.biortech.2008.04.014>
- Blanchard, G., Maunay, M., Martin, G., 1984. Removal of heavy metals from waters by means of

- natural zeolites. *Water Res.* 18, 1501–1507. [https://doi.org/http://dx.doi.org/10.1016/0043-1354\(84\)90124-6](https://doi.org/http://dx.doi.org/10.1016/0043-1354(84)90124-6)
- Chakravarty, R., Khan, M.M.R., Das, A.R., Guha, A.K., 2013. Biosorptive removal of chromium by husk of *Lathyrus sativus*: Evaluation of the binding mechanism, kinetic and equilibrium study. *Eng. Life Sci.* 13, 312–322. <https://doi.org/10.1002/elsc.201200044>
- Chong, H.L.H., Chia, P.S., Ahmad, M.N., 2013. The adsorption of heavy metal by Bornean oil palm shell and its potential application as constructed wetland media. *Bioresour. Technol.* 130, 181–186. <https://doi.org/10.1016/j.biortech.2012.11.136>
- Chung, T., Loganathan, P., Vinh, T., Vigneswaran, S., 2015. Simultaneous adsorption of Cd, Cr, Cu, Pb, and Zn by an iron-coated Australian zeolite in batch and fixed-bed column studies. *Chem. Eng. J.* 270, 393–404. <https://doi.org/10.1016/j.cej.2015.02.047>
- Costa, J.F. de S.S., Vilar, V.J.P., Botelho, C.M.S., da Silva, E.A.B., Boaventura, R.A.R., 2010. Application of the Nernst-Planck approach to lead ion exchange in Ca-loaded *Pelvetia canaliculata*. *Water Res.* 44, 3946–3958. <https://doi.org/10.1016/j.watres.2010.04.033>
- Huang, C., Liu, W., Li, Z., Zhang, S., Chen, F., Yu, H., Shao, S., Nan, J., Wang, A., 2018. High recycling efficiency and elemental sulfur purity achieved in a biofilm formed membrane filtration reactor. *Water Res.* 130, 1–12. <https://doi.org/10.1016/j.watres.2017.10.043>
- Hussain, S.N., Heras, N. De, Asghar, H.M.A., Brown, N.W., Roberts, E.P.L., 2014. ScienceDirect Disinfection of water by adsorption combined with electrochemical treatment. *Water Res.* 54, 170–178. <https://doi.org/10.1016/j.watres.2014.01.043>
- Kim, I., Yamashita, N., Tanaka, H., 2009. Photodegradation of pharmaceuticals and personal care products during UV and UV/H₂O₂ treatments. *Chemosphere* 77, 518–525. <https://doi.org/10.1016/j.chemosphere.2009.07.041>
- Kim, J.R., Kan, E., 2016. Heterogeneous photocatalytic degradation of sulfamethoxazole in water using a biochar-supported TiO₂ photocatalyst. *J. Environ. Manage.* 180, 94–101. <https://doi.org/10.1016/j.jenvman.2016.05.016>
- Lagergren, S., 1898. About the theory of so-called adsorption of soluble substances, *Kungliga Svenska Vetenskapsakademiens. Band 24*, 39.
- Lin, S., Juang, R., 2002. Removal of free and chelated Cu (II) ions from water by a nondispersive solvent extraction process. *Water Res.* 36, 3611–3619.
- Maren, K., Menard, D., Barbeau, B., 2017. The influence of iron oxide nanoparticles upon the adsorption of organic matter on magnetic powdered activated carbon. *Water Res.* 123, 30–39. <https://doi.org/10.1016/j.watres.2017.06.045>
- McKendry, P., 2002. Energy production from biomass (part 1): overview of biomass. *Bioresour. Technol.* 83, 37–46. [https://doi.org/10.1016/S0960-8524\(01\)00118-3](https://doi.org/10.1016/S0960-8524(01)00118-3)
- Nguyen, H., You, S., Hosseini-bandegharai, A., 2017. Mistakes and inconsistencies regarding adsorption of contaminants from aqueous solutions: A critical review. *Water Res.* 120, 88–116.

<https://doi.org/10.1016/j.watres.2017.04.014>

Ofomaja, A.E., Naidoo, E.B., Modise, S.J., 2010. Biosorption of copper(II) and lead(II) onto potassium hydroxide treated pine cone powder. *J. Environ. Manage.* 91, 1674–1685.

<https://doi.org/10.1016/j.jenvman.2010.03.005>

Qian, L., Zhang, W., Yan, J., Han, L., Gao, W., Liu, R., Chen, M., 2016. Bioresource Technology Effective removal of heavy metal by biochar colloids under different pyrolysis temperatures. *Bioresour. Technol.* 206, 217–224.

<https://doi.org/10.1016/j.biortech.2016.01.065>

Tao, Y., Xue, B., Zhong, J., Yao, S., Wu, Q., 2012. Influences of pH, heavy metals and phosphate and their co-influences on the sorption of pentachlorophenol on cyanobacterial biomass. *Water Res.* 46, 3585–3594.

<https://doi.org/10.1016/j.watres.2012.04.003>

Wang, H., Gao, B., Wang, S., Fang, J., Xue, Y., Yang, K., 2015. Removal of Pb(II), Cu(II), and Cd(II) from aqueous solutions by biochar derived from KMnO₄ treated hickory wood. *Bioresour. Technol.* 197, 356–362.

<https://doi.org/10.1016/j.biortech.2015.08.132>

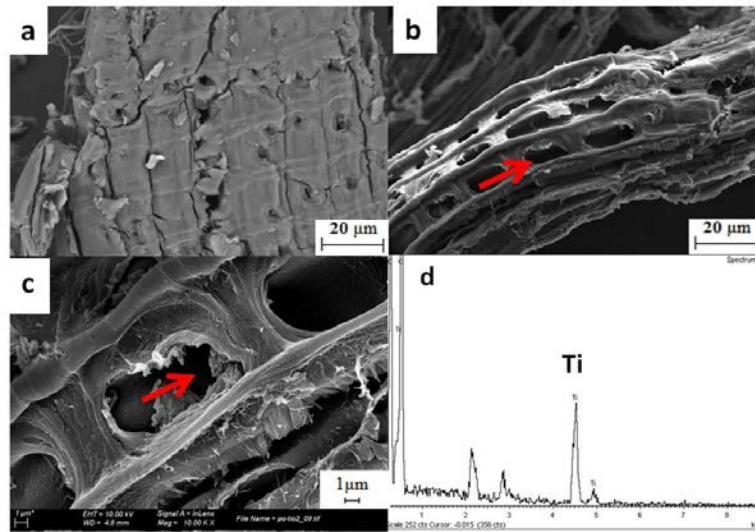
Wang, S., Ji, L.J., Wu, B., Gong, Q., Zhu, Y., Liang, J., 2008. Influence of surface treatment on preparing nanosized TiO₂ supported on carbon nanotubes. *Appl. Surf. Sci.* 255, 3263–3266.

<https://doi.org/10.1016/j.apsusc.2008.09.031>

Zhang, J., Amini, A., Neal, J.A.O., Boyer, T.H., Zhang, Q., 2015. Development and validation of a novel modeling framework integrating ion exchange and resin regeneration for water treatment. *Water Res.* 84, 255–265.

<https://doi.org/10.1016/j.watres.2015.07.027>

Figure 1



SEM images of Pine and Pine/TiO₂, SEM image of Pine (a), SEM images of Pine/TiO₂ at different magnifications (b) and (c), and EDS mapping of Pine/TiO₂ surface (d).

Figure 2

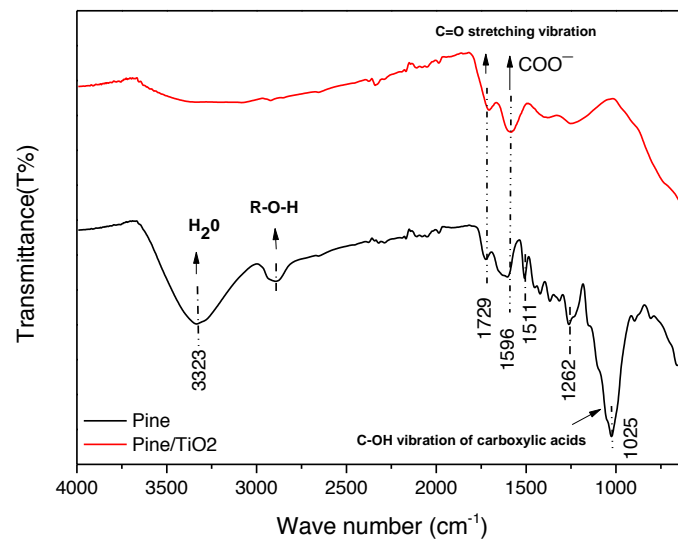
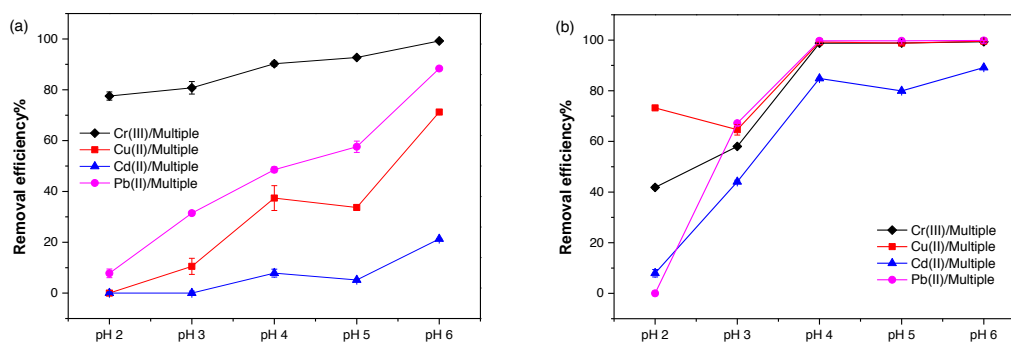


Figure 2 FTIR spectra of Pine and Pine/TiO₂.

Table 1. FT-IR spectral of Pine and Pine/TiO₂

Wave Number (cm ⁻¹)	Assignments	Compounds	Band positions (cm ⁻¹)	
			Pine	Pine/TiO ₂
3200-3700	O-H stretching	Acid, methanol	3323	-
2700-3000	C-H _n stretching	Alkyl, aliphatic	2886	-
1700-1730	C=O stretching	Carboxyl, carbonyl	1729	1729
1450-1600	COO ⁻ stretching	Ketone, carbonyl	1684	1684
1000-1200	C=O stretching C-O-C stretching/bending C-N,R-O-C/R-O-CH ₃	Ketone, ether, phenol, chain anhydride	1025	-
730-3500	Native cellulose		893,1025,1150, 1263,1425,163 8 2909,3323	-

Figure 3



Effect of pH on biosorption of multi-element system (a)Pine, (b)Pine/TiO₂. Condition: 10 mL of solution in pH 2 to pH 6, concentration 0.18 mmol/L, 10 mg of material, T = 25±1°C to 24 h.

Figure 4.

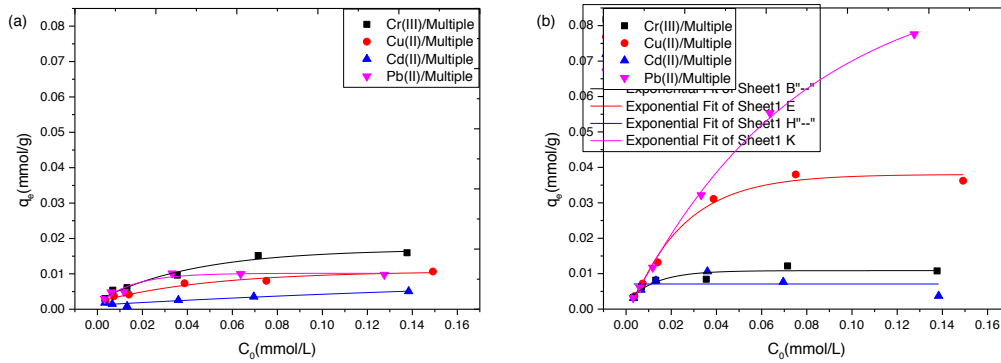


Figure 4. Effect of initial concentration on the biosorption of Cr(III), Cu(II), Cd(II) and Pb(II) by Pine (a) and Pine/TiO₂ (b). Biosorption conditions were at T=25±1°C, pH 4, stirring for 24 hours. Line fitting by Exponential.

Figure 5

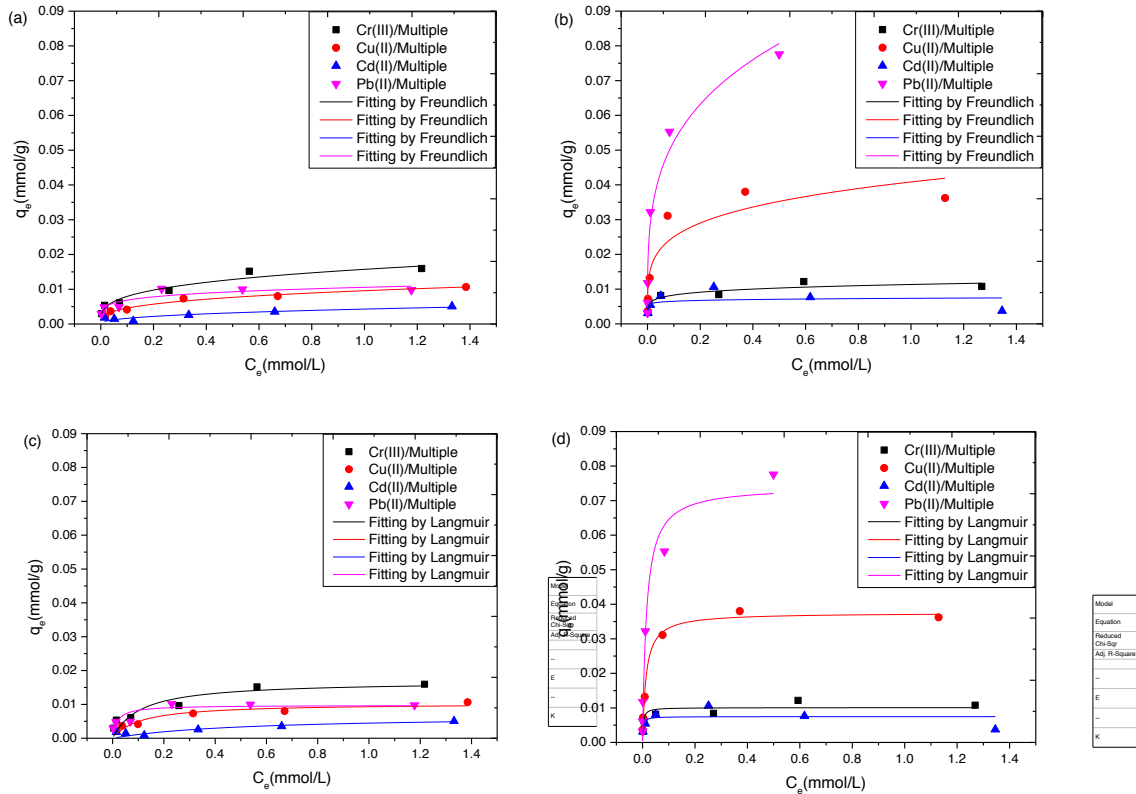


Figure 5. Adsorption isotherms of heavy metals in multi-element system by Pine (a)(c) and Pine/TiO₂ (b)(d). Biosorption conditions were at T=25±1 °C, pH 4 and stirring for 24 hours.

Table 2 Langmuir and Freundlich isotherm parameters of competitive biosorption of Pb(II), Cd(II), Cr(III), and Cu(II) ions onto pine/TiO₂. Biosorption conditions were at T=25±1 °C, pH 4

M^{n+}	$Q_{e,exp}$ ($\mu\text{mol/g}$)	Langmuir			Freundlich		
		Q_{max} ($\mu\text{mol/g}$)	b (L/mol) ($\times 10^3$)	R^2	K_f ($\mu\text{mol/g}$)	n ($\times 10^3$)	R^2
Pine							
Mix-Cr(III)	12.4	16.8	9.26	0.793	15.7	0.296	0.940
Mix-Cu(II)	5.28	10.3	9.20	0.892	9.58	0.322	0.972
Mix-Cd(II)	2.84	6.72	1.97	0.609	4.29	0.420	0.771
Mix-Pb(II)	12.5	9.75	55.1	0.672	10.6	0.187	0.800
Pine/TiO ₂							
Mix-Cr(III)	10.5	10.1	359	0.756	11.3	0.136	0.827
Mix-Cu(II)	34.3	37.5	75.2	0.980	40.8	0.212	0.841
Mix-Cd(II)	4.94	7.49	434	0.217	7.35	0.0531	NA
Mix-Pb(II)	77.5	74.2	66.8	0.949	97.1	0.267	0.975

Figure 6

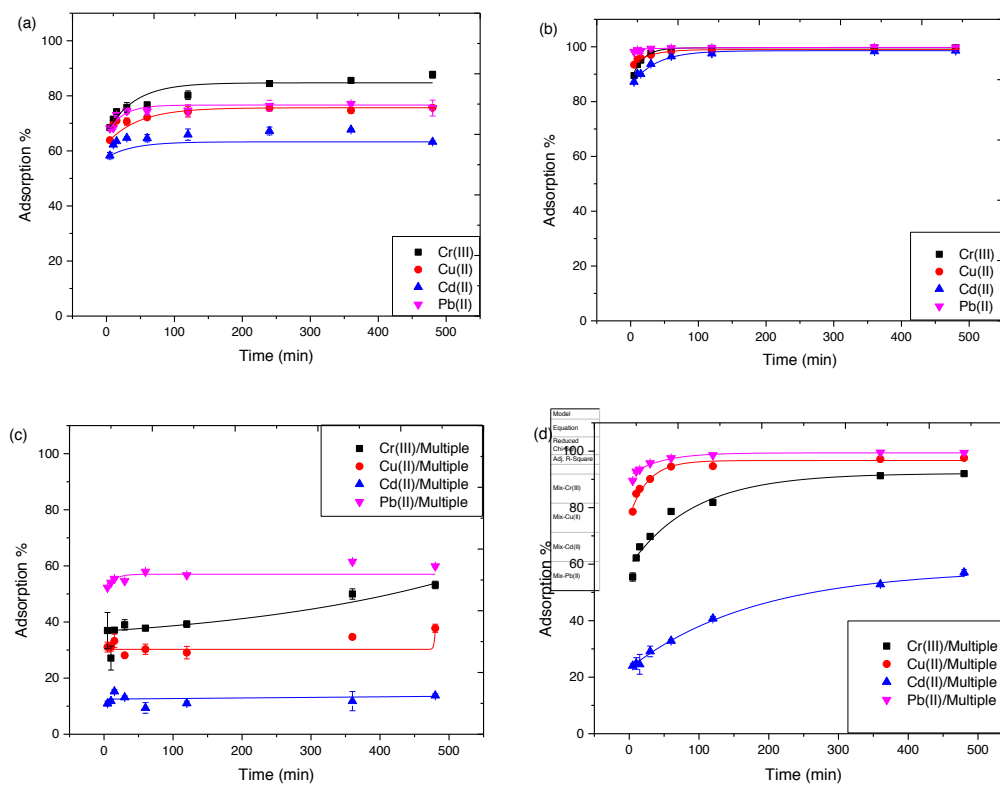


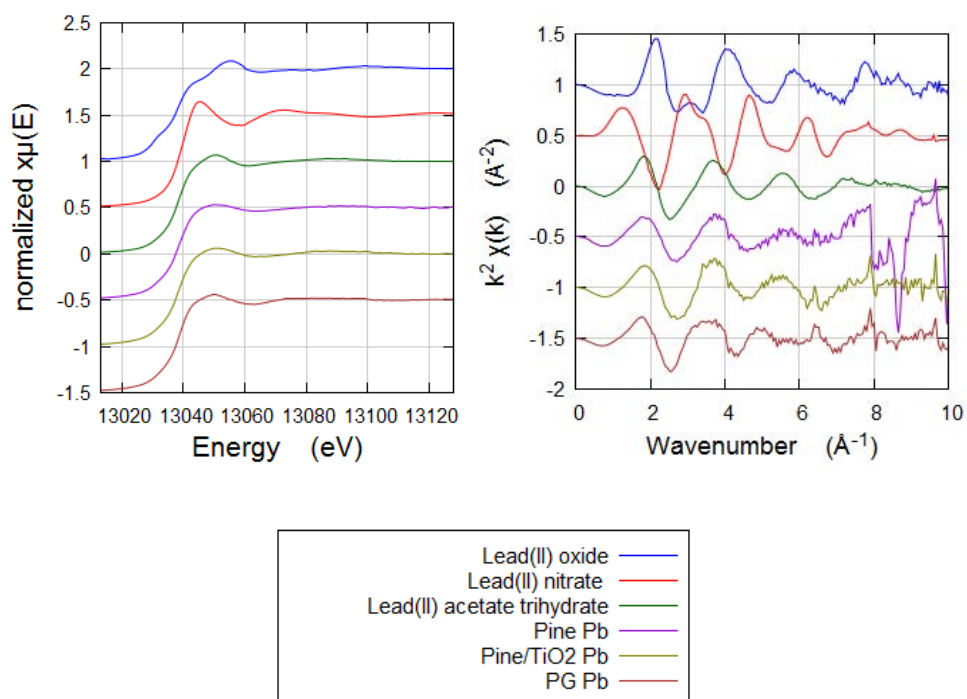
Figure 6. Biosorption kinetics for Cr(III), Cu(II), Cd(II) and Pb(II) on Pine and Pine/TiO₂ in single and multi-element system. Biosorption conditions were at $T=25\pm 1^\circ\text{C}$, pH 4 and heavy metal concentration is 0.18 mmol/L, and stirring for different times.

Table 3. Kinetics Parameters of single and multi-element systems of Pb(II), Cd(II), Cr (II), and Cu(II) ions onto Pine and Pine/TiO₂ on the Pseudo-second-order Model. Biosorption conditions were at T=25±1°C, pH 4 and heavy metal concentration is 0.18 mmol/L.

M ⁿ⁺	Pine					Pine/TiO ₂			
	C ₀	Q _{e,exp}	Pseudo-second-order model			Q _{e,exp}	Pseudo-second-order model		
	mg/L	(μmol/g)	k ₂	Q ₂ (μmol/g)	R ²	(μmol/g)	k ₂	Q ₂ (μmol/g)	R ²
Cr(III)	5.77	11.1	14.4	11.1	0.999	12.5	9.69	26.0	0.996
Cu(II)	7.23	11.3	47.8	11.3	0.999	14.8	9.33	30.5	0.997
Cd(II)	10.9	9.67	58.7	9.31	0.998	14.2	7.86	29.2	0.997
Pb(II)	21.6	10.4	127	9.58	0.999	12.6	12.3	25.9	0.997
Mix-Cr(III)	6.34	6.49	9.97	6.51	0.993	11.2	0.800	18.5	0.957
Mix-Cu(II)	9.54	5.63	18.2	5.54	0.994	14.5	0.890	23.7	0.971
Mix-Cd(II)	16.7	2.27	58.7	1.96	0.988	8.52	0.611	14.3	0.907
Mix-Pb(II)	30.8	8.89	45.2	9.01	0.999	14.8	0.949	24.0	0.973

Q_{e,exp}: experimental value of the equilibrium biosorption capacity. k₂: g mol⁻¹min⁻¹.

a)



b)

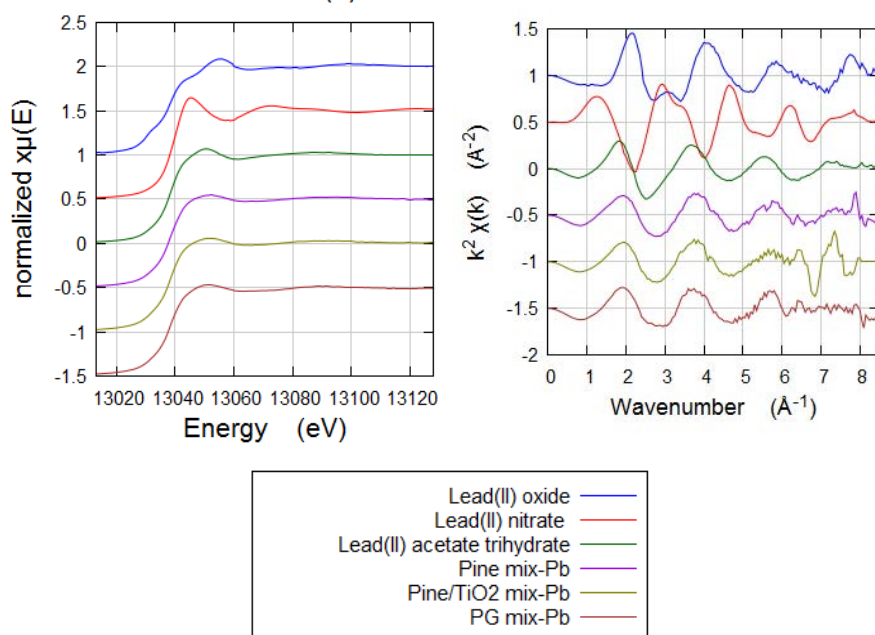


Figure 7. XAS spectra of references and Pb-loaded on Pine and Pine/TiO₂. (a) is the normalized K-edge and k-weighted spectra of XANES in single-element Pb(II) system, (b) normalized K-edge and k-weighted of XANES in multi-element [Cr(III), Cd(II), Cu(II), Pb(II)] system.

Annex IV

Article under preparation. In collaboration with Institut of Oil Crops Research Institute of Chinese Academy of Agricultural Sciences, Wuhan, China.

Recycling disposal of agriculture waste to remove Cr(III), Cd(II), Cu(II) and Pb(II) from aqueous solution

Xinjie Shen^{1,+}, Jingjing Zhao^{2,+}, Xing Liao^{1*}, Cristina Palet^{2*}

¹Oil Crops Research Institute of Chinese Academy of Agricultural Sciences/Key Laboratory of Biology and Genetic Improvement of Oil Crops of the Ministry of Agriculture, Wuhan 430062, China

²GTS-UAB Research Group, Department of Chemistry, Facultat de Ciències, Universitat Autònoma de Barcelona, 08193 Cerdanyola del Vallès, Catalunya, Spain

+These authors contributed equally to this work.

*Corresponding Authors: cristina.palet@uab.cat; liao@oilcrops.cn

Abstract

1. Introduction

Polluted water contaminated by heavy metals has received increasing attention due to its high toxicity, persistence in sediment, and biological accumulation of the heavy metals, which lead to potential threat to animals and human beings. The polluted resource is mainly from fertilizer leaching, sewage discharge, industrial wastewater, and urban construction over the last two decades¹. Therefore, using low-cost techniques for removing toxic heavy metals from the wastewater is one of the most important goals in environmental science. Conventional techniques for removing heavy metals include solvent extraction, ion-exchange, adsorption, membrane filtration and electrochemical treatment technologies. While adsorption method is considered to be the most advantageous due to its high efficiency, low cost and ease handling.

China is the one of the most producers and consumers of Rice (*Oryza sativa L*) and Canola (*Brassica napus L.*) in the world. Meanwhile Canola is suitable rotational crop with rice, while canola grown in winter and rice in summer². Mass cultivation of rice and canola were grown on a large scale in China, and harvested area reached 30 million ha in 2010 and 6.5 ha in 2014 for rice and canola, respectively^{3,4}. The field burning of agriculture straw residue is a common method to dispose waste after harvesting seasons in China. However, this way to burn the straw residues in open

field is forbidden now due to the emission of CO₂ that leads to global warming⁵. Therefore, millions of tons of canola and rice straw residues were considered as a significant agriculture waste disposal problem.

Rice and canola have been proved to be good adsorbents to remove heavy metals in the past studies, such as . However, most of the studies are focus on the single heavy metal system, and the adsorption of capacity is decreased when come refer to the real multiple heavy metals system. Thus, it's necessary to study the adsorption capacity in the multiple system to solve heavy metals wastewater problem. While Chromium (Pb), copper (Cu), cadmium (Cd) and lead (Pb) are the major heavy metals specious in polluted water. Such as Taihu Lake, is one of the largest freshwater lake in China, has been reported as a heavily contaminated area by Pb, Cd, Cr, and Cu^{6,7}. Therefore, we prepare a multiple system composed by Pb(II), Cd(II), Cr(II), and Cu(III) to simulate a real water system for adsorption study by rice and canola straw residues.

Therefore, rice straw residue (RO) and canola straw residue (LO) as natural adsorbents could solve two serious environmental problems: the disposal of agriculture wastes and as adsorbents to remove heavy metals from wastewater. Although LO and RO as adsorbents to removal heavy metals have been reported, no works combined these two kinds of biomasses to removal heavy metals in multiple system. The objective of this work is: (1) to investigate for the first time the potential of LO and RO in the removal of heavy metals from multiple system; (2) to optimize adsorption conditions including pH, initial concentration and contact time of adsorption; (3) to better understand the results, adsorption isotherms models (Langmuir, Freundlich and Redlich-Peterson) were used to adjust the experimental data; and kinetics models of pseudo first order, pseudo second order and Elovich also were tested.

Materials and Methods

Materials

Canola (LO, *Brassica napus*) and Rice (RO, *Oryza sativa L*) were provided by Oil Crops Research Institute of Chinese Academy of Agricultura (Wuhan, China). They were grinded and dried for further use in metal uptake experiments. Wuhan, China. All biomasses were grinded and dried before use. While all the chemicals were analytical grade. 1,000 mg/L stock solutions of single and a multiple-element system were prepared by dissolving the required amounts of Cr(NO₃)₃·9H₂O, Cu(NO₃)₂·3H₂O, Cd(NO₃)₂·4H₂O and Pb(NO₃)₂, respectively (all 99% from Panreac, Barcelona, Spain).

Characterization of adsorbents

The physicochemical properties of biomass, including pH, surface area, porosity,

surface charge, and functional groups play an important role in explaining the process of sorption of metals. The morphologies of biomasses were analysed by scanning electron microscopy (SEM) at the Electron Microscopy Facilities of the *Universitat Autònoma de Barcelona* (UAB, Catalunya, Spain). Mineral components of materials were analysed by ICP-mass spectrometry (MS) (XSERIES 2 ICP-MS, Thermo Scientific, USA) after a complete digestion procedure⁸. Grinded materials (50 mg) was weighed in duplicate into digestion tubes. 10 mL of concentrated nitric acid and 10 mL of hydrogen peroxide were added into the tubes. The tubes were then heated between 90-120°C in microwave for further digestion. Fourier transform infrared spectroscopy (ATR-FTIR, Tensor 27, Bruker, USA) was performed to identify the chemical functional groups present on the adsorbents. FTIR data were obtained in the wavenumber range of 600 to 4000 cm⁻¹ with an average of 64 scans at 4.0 cm⁻¹ resolution at *Servei d'Anàlisi de Química* (UAB, Catalunya, Spain). The pH measure of materials followed Sakala's etc. method. 25 mL distilled water was added to 2.5 g of materials and the mixture were shaken for 16h, then the suspensions were filtered and was measured by pH meter⁹.

Batch adsorption experiments

Batch adsorption experiments were carried out at room temperature (25±1°C). A multi-element solution composed by a mixture of 0.18 mM solutions of Cr(III), Cd(II), Cu(II) and Pb(II) was prepared from 1,000 ppm initial stock solutions of each metal. The concentrations of isotherm solutions include single and multiple systems, which were ranged from 0.05 to 6 mM. Batch experiments were performed by following steps: 25 mg of adsorbent were placed in 5 mL tubes and then 2.5 mL of heavy metal aqueous solutions were added into the tube. Later samples were placed on a rotary mixer (CE 2000 ABT-4, SBS Instruments SA, Barcelona, Spain) and shaken at 25 rpm for 24 h. The two phases were separated by decantation and later filtered through 0.22 µm Millipore filters (Millex-GS, Millipore). Furthermore, using ICP-mass spectrometry (MS) (XSERIES 2 ICP-MS, Thermo Scientific, USA) to analyse the concentrations of heavy metals in the supernatant phase.

Kinetics

25 mg of biomass was added to 2.5 mL solutions of 0.18 mM multiple system (pH = 4.0) and was shaken at 25 rpm for 5, 10, 20, 30, 45, 60, 120, 240, 480, 1440 min. it is reported that the equilibrium adsorption time for all biomasses was no longer than 5 min, and longer adsorption time does not affect the equilibrium. Thus, a reaction time of 24 h was used in the following adsorption studies, which is corresponding to previous study¹⁰.

Influence of pH

25 mg of biomass was added to 2.5 mL solutions of 0.18 mM multiple system (pH = 4). The initial pH of each solution was adjusted to 2, 3, 4, 5 and 6 with HCl and NaOH

before adding biomass. The mixture was shaken at 25 rpm for 24 h to reach equilibrium.

Equilibrium study

25 mg of biomass was added to 2.5 mL solutions (pH = 4) containing different heavy metals concentrations range from 0.05-2 mM for multiple system (Cr,Cu,Cd and Pb), and 0.1-4 mM for single systems (Cr, Cu and Pb). The mixture was shaken at 25 rpm for 24 h to reach equilibrium.

Calculation

The adsorption of the selected heavy metals by the adsorbents was expressed as the adsorption percentage calculated according to Equation (1). Furthermore, the capacity of the adsorbent was calculated following Equation (2):

$$\% \text{ Adsorption} = \frac{(C_0 - C_e)}{C_0} \times 100 \quad (1)$$

$$q_e = \frac{(C_0 - C_e) \times V}{m} \quad (2)$$

where q_e (mg/g) is the adsorption capacity of heavy metals; V (L) is the volume of the heavy metal solution; C_0 and C_e are the initial and equilibrium heavy metal concentrations in solution (both in mg/L), respectively; and m (g) is the dry weight of the adsorbent. To study the adsorption competition, the unit form of q_e is mmol/g.

For the equilibrium study, the experimental data were fitted by Langmuir and Freundlich isotherm models, which are typically used to describe the adsorption mechanism for the interaction of heavy metal ions on the adsorbent surface. Langmuir model assumes that the uptake of metal ions occurs on homogeneous surface by a monolayer deposition, but heterogeneous surface described by Freundlich model. Both are expressed as Equations (3) and Equation (4);

$$q_e = \frac{q_{max} K_L C_e}{1 + K_L C_e} \quad (3)$$

$$q_e = K_f C_e^n \quad (4)$$

Where, C_e is the equilibrium concentration of metal ions in the solution ($\mu\text{mol/L}$), q_{max} is the amount of metal ion required to form a monolayer (in this case is $\mu\text{mol/g}$) and K_L ($\text{L}/\mu\text{mol}$), K_f ($\mu\text{mol/g}$) and n (dimensionless) are the equilibrium constants. n ranges between 0 and 1 and is a measure of adsorption intensity or surface heterogeneity. A lower n value indicates a greater degree of heterogeneity on the biochar surface.

For the kinetics study, the experimental data were fitted by the pseudo-first-order (PFO), pseudo-second-order (PSO), Elovich models, which are typically used to describe the adsorption process. The PFO and PSO models assume that the rate of metals adsorbed on the surface of sorbents is proportional to the number of

unoccupied sites and is the physical process controlled by PFO, whereas chemical processes controlled by PSO. The Elovich is often used to describe the kinetics of chemisorption on highly heterogeneous adsorbents, and assuming that the adsorption sites are increase exponentially with adsorption. It means a multilayer adsorption. The PFO, PSO and Elovich mathematic model expressions are given in Equation (5), (6) and (7):

$$q_t = q_e [1 - \exp(-k_1 t)] \quad (5)$$

$$q_t = \frac{k_2 q_e^2 t}{1 + k_2 q_e t} \quad (6)$$

$$q_t = \frac{\ln(\alpha\beta)}{\beta} + \frac{\ln t}{\beta} \quad (7)$$

where q_t and q_e are the capacity at time t and at equilibrium, respectively (and expressed as mmol/g), α is the initial adsorption rate (mmol/g min), β is the desorption constant related to the extent of the surface coverage and activation energy for chemisorption, and k_1 , and k_2 are the rate constants of PFO and PSO.

All the results are expressed as the mean value of duplicate measurements. Standard Deviation function (SD) was used to analyse the data errors and described in Equation (8):

$$SD = \sqrt{\frac{\sum(x-\bar{x})^2}{(n-1)}} \quad (8)$$

Where x takes on each value in the set; \bar{x} is the average (statistical mean) of the set of values and n is the number of values. The parameters of the kinetics and isotherm models studied in this work were obtained by nonlinear equation. While squares regression analysis using OriginPro 9.6 program.

Results and Discussion

Characterization

Table 2 Total concentration of minerals and heavy metals in LO and RO residues.

mg/kg	pH	Fe	Mn	Ni	Cu	As	Pb	Mg	P	K
Canola		6410	208.1	40.5	229	15.5	568.7	554	24280	37900
Rice		6291.	2348	70.5	747	15.2	1691	2051.6	25108	28700

Concentration of minerals and heavy metals of LO and RO residues are given in Table 2. LO and RO adsorbents have similar concentration of ions metals except Cu, Mg and Pb, the latter are higher than the former probably due to the varies of biomass residues.

SEM and ATR-FTIR were carried out to analysis the morphology structure and function groups of LO and RO. The metals ions analysis of LO and RO illustrate the differences of physicochemical properties of adsorbents, which beneficial to understand the adsorption process.

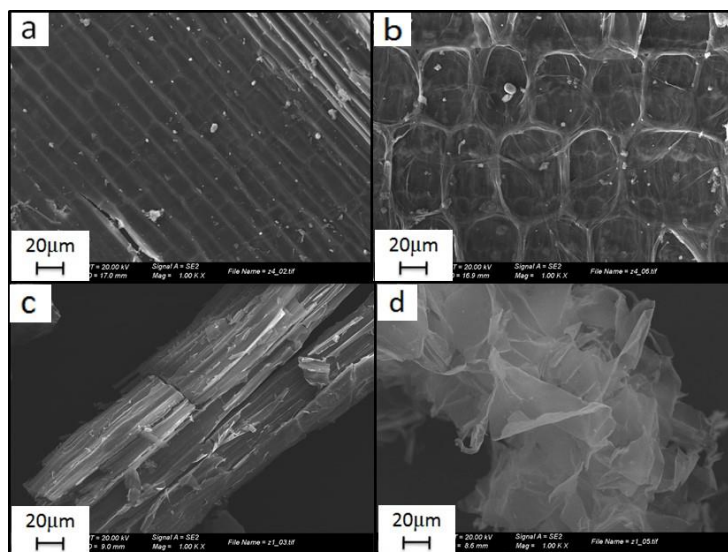


Figure 1 SEM images of RO (a),(b), and LO (c),(d) in different magnifications.

The SEM images of RO are shown in Figure 1 (a),(b), RO presents a typical structure of lignin. LO straw also includes lignin structure shown in Figure 1 (c), and its stem part is shown in Figure 1(d). It is well known that lignin provides structural rigidity to the cell walls of many plant species and accounts for a 15–40% of the dried wood and agricultural residues, together with cellulose and hemicelluloses¹¹. Furthermore, it has been proved a potential adsorbent to remove heavy metals due to its unique polyphenol structure, physicochemical properties^{12,13}.

ATR-FTIR characterization analysis

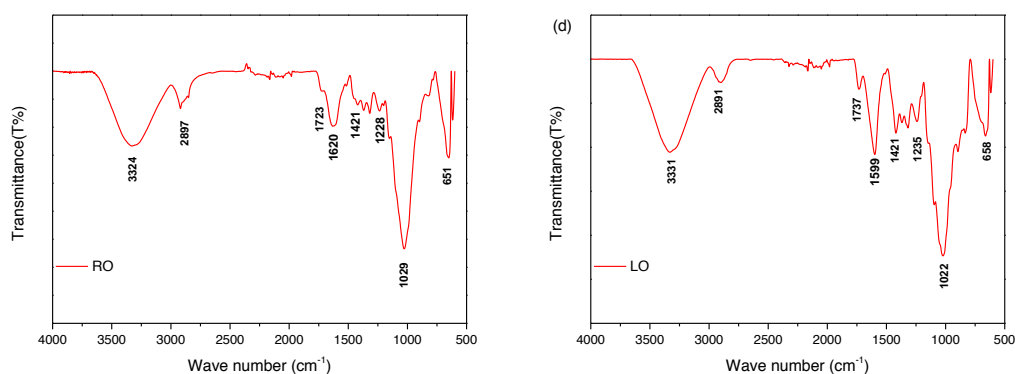


Figure 2 FTIR spectra of LO and RO

ATR-FTIR analysis was carried out to identify the functional groups present in the adsorbents that might be involved in the biosorption process. In Figure 2, the FTIR spectra display several absorption peaks, indicating the complex nature of the examined adsorbents. Cellulose, hemicellulose and lignin are the main components of straw of agriculture biomass¹⁴ and their function groups can be found in studied adsorbents. It can be observed that there are strong broad peak at around 3400 cm^{-1}

which is assigned to different O-H stretching and another peak at around 2920 cm^{-1} related to asymmetric and symmetric methyl and methylene stretching groups present in the spectra of cellulose¹⁵. While within the range of $800\text{-}1800\text{ cm}^{-1}$ are the “fingerprint” region, which are assigned to stretching vibrations of different groups of cellulose and lignin components. In the “fingerprint” region, the peaks at 1620 , 1599 , 1421 , 1236 and 1228 cm^{-1} are correspond to C=C, C-O stretching or bending vibrations of different groups present in lignin (such as aromatic rings). The peaks at 1723 and 1737 cm^{-1} are due to C=O, C-H, C-O-C, C-O deformation or stretching vibrations of different groups in carbohydrates. According to the literatures, the peaks at $3200\text{-}3270\text{ cm}^{-1}$ and $1780\text{-}1710\text{ cm}^{-1}$ correspond to the O-H and C=O stretching vibrations, respectively, which confirms the presence of carboxyl groups (-COOH) on the adsorbents. The additional peaks at 1029 and 1022 cm^{-1} are characteristic of C-H, C-O deformation, bending, or sfdtretching vibrations of many groups in lignin and carbohydrates. Furthermore, carboxyl groups are responsible for the heavy metals adsorption and can be found in LO and RO, which are responsible for heavy metals adsorption in multiple system. In addition, the peak of RO around 1620 cm^{-1} related to C=C structure of aromatic rings is stronger than LO, indicates RO has more lignin component than LO. This is corresponding with the SEM result mentioned above.

Effect of solution pH

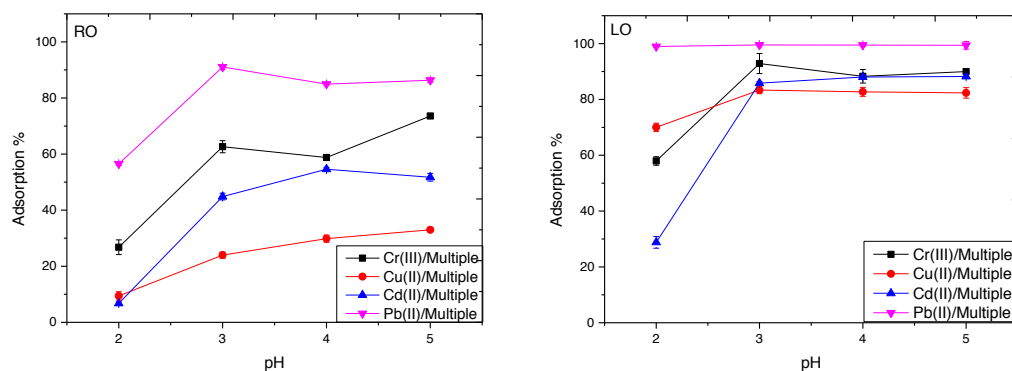


Figure 3 The effluence of solution pH onto RO and LO. Biosorption conditions were at $T=25\pm 1^\circ\text{C}$, 25 mg of adsorbent, initial concentration of solution is 0.18 mmol/L , contact time is 24 h.

As shown in Figure 3, is the effluence of pH onto LO and RO, while LO has better adsorption capacity compared with RO. The adsorption percentage of both materials are increased with increased pH and the lowest adsorption are found at pH 2. At lower pH, hydronium ions (H_3O^+) on surface ligands limit cations sorption due to their repulsive force¹⁶. The adsorption competition of heavy metals were also found at

both case, as show in Figure 3(a), the adsorption sequence by RO are ranked as: Pb(II)> Cr(III)> Cd(II)> Cu(II). Similar to RO, LO has similar adsorption sequence except the case of Cu(II) at pH 2. It's worth noting that both materials show better selective of Cd, which implies both are potential adsorbents to remove heavy metals in multiple system. Considering pH value in real system is near to 4, while at high pH, the strong alkalinity of adsorbents which will cause heavy metals precipitation ¹⁷. Therefore, pH 4 was chosen as the optimized value in the following studies.

Kinetics and isotherm

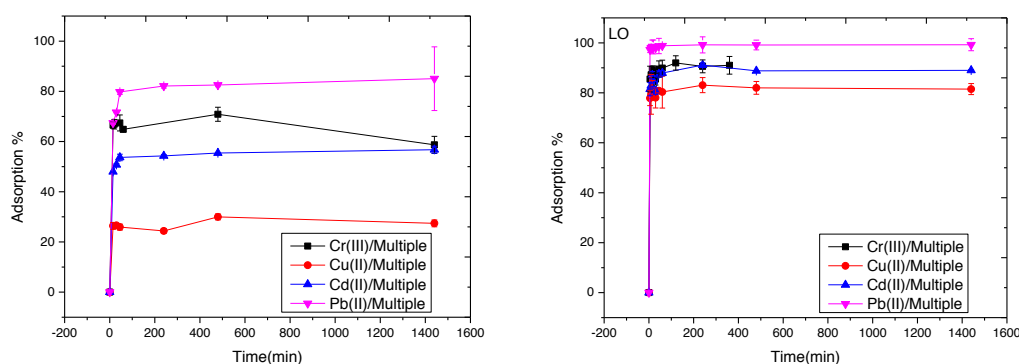


Figure 3 The effect of time on adsorption of heavy metals in multiple system.

Adsorption is a surface phenomenon that occurs due to physical forces or chemical interactions. Adsorption isotherms and kinetics are the most important characteristics that govern the adsorbate uptake rate; they represent the adsorption efficiency of the adsorbent and determine the adsorption parameters.

The adsorption of heavy metals by LO and RO were initially rapid and reached equilibrium time in 5 minutes for all heavy metals in multiple system (Figure 3). LO has higher adsorption in multiple system than RO, with percentage range of 80-100 for all heavy metals. RO shows selectivity of these four heavy metals and adsorption sequence followed as: Pb(II)> Cr(III) >Cd(II) Cu(II). In order to check the adsorption ability, another different biomasses were used to compare the adsorption ability under the same condition (Table 1). As show in Table 1, RO and LO have better adsorption than other biomasses. It's worth noting that LO and RO adsorbents show higher adsorption capacity of Cd, with 10.5 $\mu\text{mol/g}$ and 6.7 $\mu\text{mol/g}$, respectively. Previous studies show lower removal percentage in most residues, which limited the application of these materials in multiple wastewater system. The better selective of Cd in our study indicate that both residues are potential adsorbents for heavy metals removal in multiple system.

Table 1 Comparison of adsorption capacity of metal ions with other adsorbents

	Cr(III)	Cu(II)	Cd(II)	Pb(II)
adsorbents	q($\mu\text{mol/g}$)	q($\mu\text{mol/g}$)	q($\mu\text{mol/g}$)	q($\mu\text{mol/g}$)
Brassica napus	9.81	9.75	10.53	8.92
Oryza sativa L	7.24	3.78	6.76	8.92
Pine	7.35	4.02	1.48	9.09
Poplar	9.41	7.04	1.93	7.04
Corn	11.78	10.1	4.87	1.78
Coffee shell	2.48	4.61	0.75	20.1
Sugar cane	2.46	3.41	0.515	9.59
cork	7.98	5.92	2.53	11.53
Coffee grounds	3.48	7.10	0.143	10.8

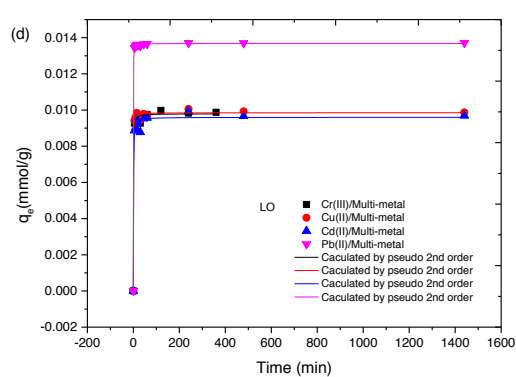
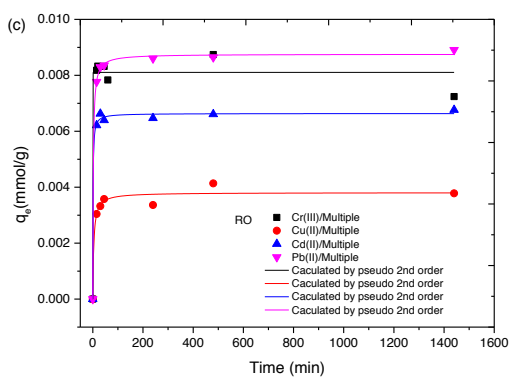
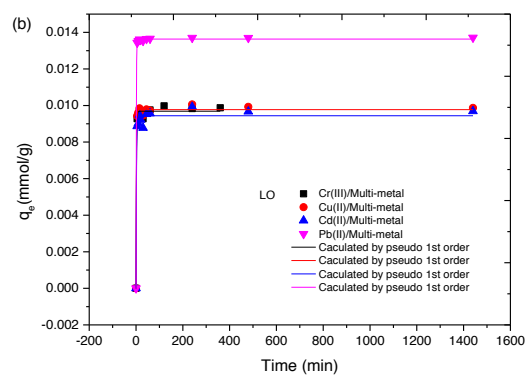
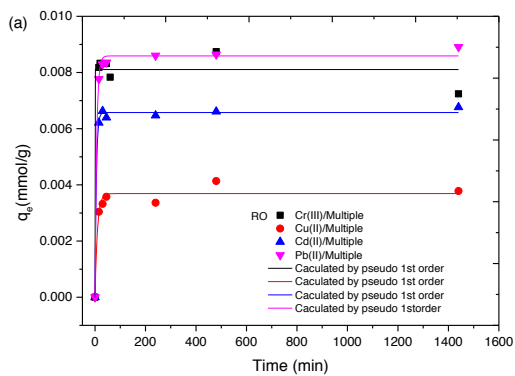
Kinetics model

Here, for rice (RO) and canola (LO) biomass, also the same three kinetic models are followed to describe the mechanism of the heavy metals biosorption process. Experimental data for RO and LO are adjusted to the models as it is shown in Figure 3.7, The RO and LO constants values from the kinetic models, such as k_i , q_i , α and the calculated q_e , (experimental adsorption capacity) are listed in Table 3.3, together with the correlation fits of each model (R^2).

The results of RO and LO indicate that PFO, PSO and Elovich equations all fitted well with experimental data for all metal ions with high correlation coefficients ($R^2 > 0.960$). The equilibrium biosorption capacities for Cr(III), Cu(II), Cd(II) and Pb(II) in multiple system are 8.70, 3.80, 6.70 and 8.90 $\mu\text{mol/g}$ for RO, and 9.90, 9.90, 9.70 and 14.0 $\mu\text{mol/g}$ for LO.

Table 3.3. Biosorption kinetic constant values for Cr(III), Cu(II), Cd(II) and Pb(II) by LO and RO in multiple system.

	Experim ental	PFO				PSO			Elovich		
		$q_{exp} \times 10^3$ (mmol/g)	k_1 (min^{-1})	$q_1 \times 10^3$ (mmol/g)	R^2	k_2 (g/mmol min)	$q_2 \times 10^3$ (mmol/g)	R^2	a	b	R^2
Cr(III)	LO	9.90	0.624	9.70	0.995	322	9.80	0.997	7152	3.1×10^{24}	0.998
	RO	8.70	160	8.10	0.972	67.6	3.80	0.972	6063	2787	0.965
Cu(II)	LO	9.90	0.662	9.70	0.997	418	9.80	0.998	11970	7.0×10^{44}	0.998
	RO	3.80	0.107	3.70	0.961	67.6	3.80	0.971	6063	2787	0.968
Cd(II)	LO	9.70	0.543	9.40	0.986	206	9.60	0.991	6306	1.4×10^{20}	0.992
	RO	6.70	0.194	6.60	0.997	168	6.60	0.997	12110	1.2×10^{28}	0.997
Pb(II)	LO	14.0	0.845	14.0	0.999	746	14.0	0.999	8526	5.6×10^{44}	0.999
	RO	8.90	0.153	8.60	0.996	60.2	8.80	0.999	4870	1.1×10^{12}	0.998



Model	Equation	Reduced Chi-Square	Adj. R-Square
mix cr			
mix cu			
mix cd			
mix pb			

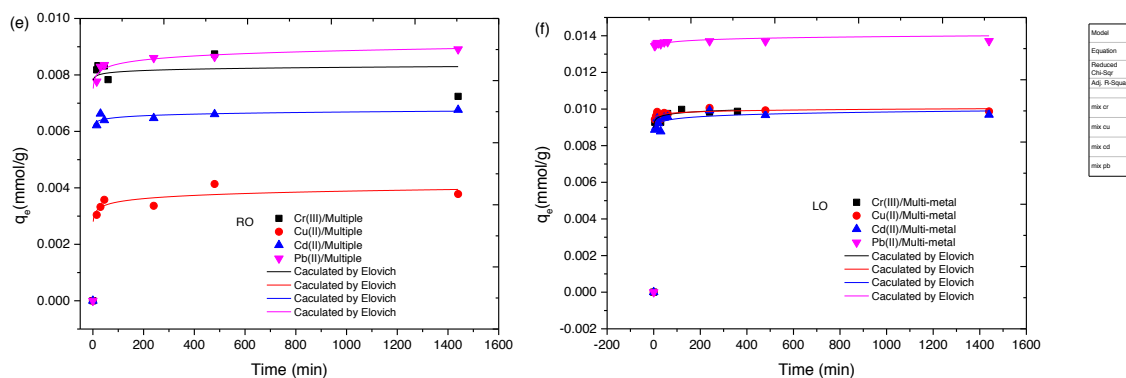


Figure 4 Kinetics modeling for Cr(III), Cu(II), Cd(II) and Pb(II) in multiple system by using (a), (c) and (e) RO and (b), (d) and (f) LO, both fitted by PFO, PSO, and Elovich, respectively. Initial 2.5 mL of aqueous solutions concentration are 0.18 mmol/L for each element, pH =4.0, same amount of 25 mg of biosorbents used, at T=25.0°C.

In summary, biosorption process of rice (RO) and canola (LO) are rate-controlled by physisorption and chemisorption, and they follow a multilayer biosorption process. In addition, a mention should be done to the intraparticle diffusion model that does not fit well for any case. So, all those results mean that the biosorption of heavy metals on the surface of the biosorbent is mainly due to a combination of the physics and chemical interaction between both. Furthermore, it is a multilayer biosorption process.

The effect of the amount of initial concentration onto RO and LO for heavy metals removal in single and multiple systems are checked by varying initial concentration from 0.05 up to 3 mmol/L of each metal ion. From the results shown in Figure 5, it can be seen that the adsorption capacity of RO and LO for the heavy metals under study (Pb, Cd, Cu and Cr) increases with the increase of the metal ion initial concentration until reaching a maximum level in both, individual and multiple systems (except for Pb in single system that the maximum capacity of the materials have not been achieved). In multiple systems in general, RO and LO both reach the adsorption maximum capacity for all heavy metals probably due to the competition between them caused by limited adsorption sites on surface of adsorbents. In single systems, LO show potential adsorption ability for Cr, Cu and Pb, and RO only for Pb. Cu and Cr adsorption by RO reaches a maximum adsorption rate, probably related to their lower affinity to the RO site groups. Basically, this result can be explained by the availability of the adsorption sites on the surface of RO and LO. At low initial concentration, the ratio of surface adsorption sites and heavy metal ion amount is high, hence the metal ions could interact with the adsorbent to occupy the

adsorption sites, so they can be removed from the solution. But with the increase in adsorbate concentration of all the heavy metals in the multiple system, there is a competition of occupying adsorption sites, and the number of adsorption sites is not enough to adsorb all heavy metals, which is in agreement with previous works found in the literature^{18,19}.

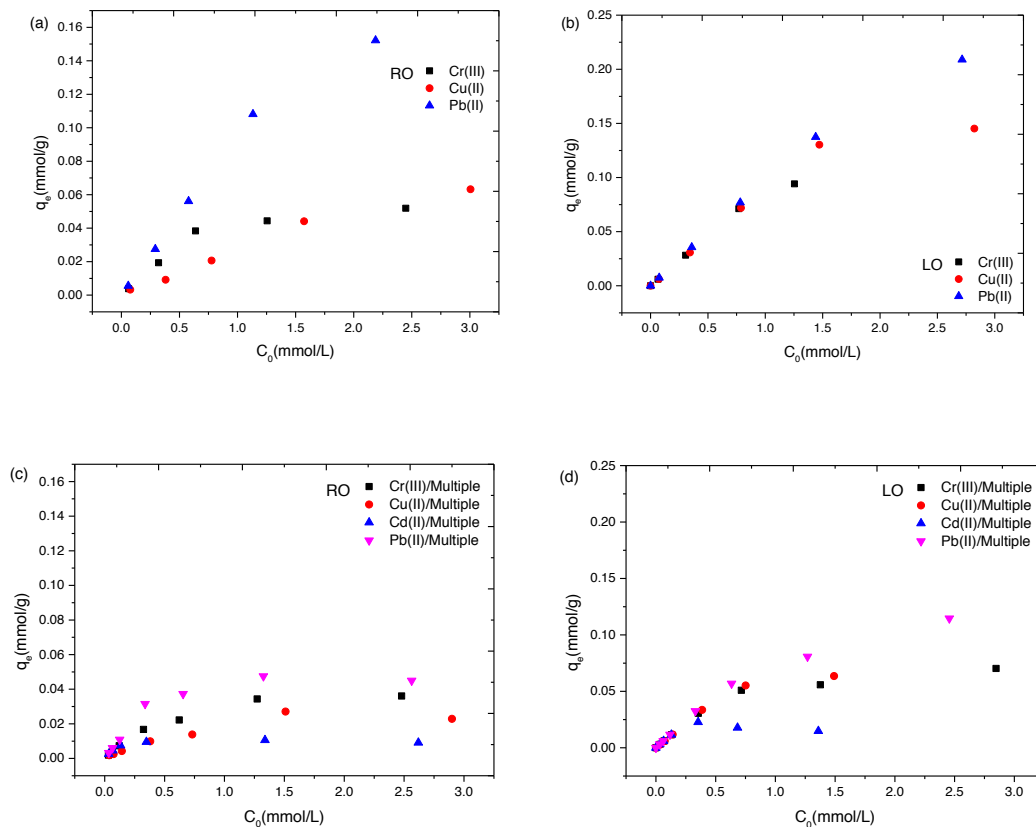


Figure 5 Influence of the initial concentration of heavy metals on their adsorption by (a) CO, (b) CL, (c) ZO, (d) ZL, (e) FO and (f) FL in multiple-metal systems. Experimental conditions were $T=25\pm 1^\circ\text{C}$, $\text{pH } 4.0$, 25 mg of adsorbent, 2.5 mL of metals solution and stirring for 24 hours.

Biosorption isotherm modeling for rice (RO) and canola (LO)

To evaluate the maximum biosorption capacity of biosorbents RO and LO, Langmuir and Freundlich isotherm models are here used. While the Freundlich is used for modeling the biosorption of metal ions on heterogeneous surfaces and Langmuir is used for modelling the monolayer biosorption process in homogeneous cases.

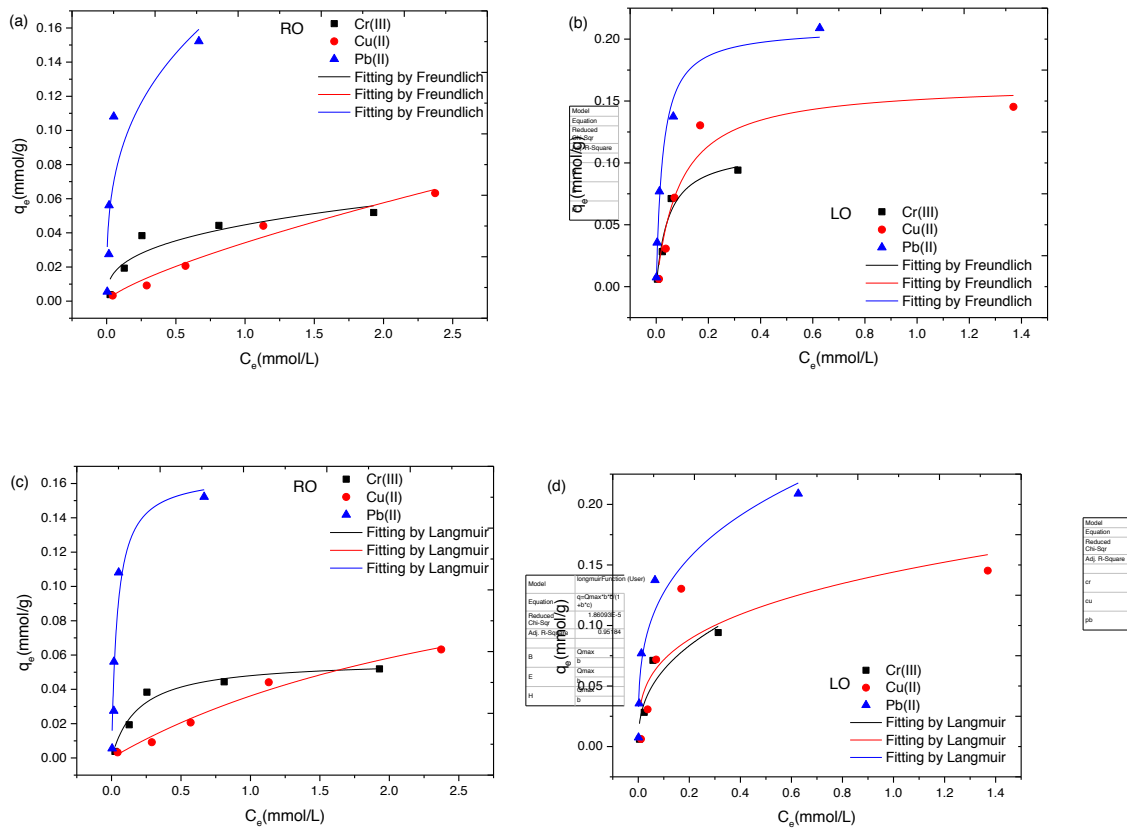


Figure 6 Biosorption isotherms of heavy metals in individual-element systems by RO (a) (c) and LO (b) (d) by Freundlich and Langmuir models, respectively. Biosorption conditions are: initial 2.5 mL of aqueous solutions, pH 4.0, and same amount of 25 mg of biosorbents used, at $T=25.0^{\circ}\text{C}$ and stirring for 24h.

The plots of q_t (adsorption capacity) versus C_e (concentration at the equilibrium state) of each metal in individual systems are shown in Figure 3.9, and in the multiple system are presented in Figure 3.10. The corresponding constant values are shown in Table 3.3. The correlation coefficients (R^2) values are very low suggesting that the biosorption does not follow the modeling. R_L is calculated by the Langmuir constant (b) that suggesting a biosorption is favorable or unfavorable. It must lie within 0–1, where $R_L > 1$, $R_L = 1$ and $R_L < 0$ indicate the unfavorable, linear and irreversible biosorption, respectively.

In this study, the Langmuir equation fits the experimental data better than the Freundlich equation in both biosorbent systems (RO and LO). The Freundlich model cannot fit all the experimental data properly, as R^2 values are generally lower than Langmuir (shown in Table 3.4 and as represented in Figures 3.9 and 3.10). Moreover, Langmuir does not fit well for Cd in multiple system by LO probably due to the

competition between all the metal ions (Cd was together with Pb, Cu and Cr), as can be seen in Figure 3.10. In addition, the R_L values are between 0 and 1 for all metal ions in all systems indicates that the biosorption of all the metal ions onto LO and RO are favorable (either in single and multiple systems by LO and RO).

Furthermore, the maximum biosorption capacities for Cr(III), Cu(II) and Pb(II) in single systems by LO are 112, 165 and 210 $\mu\text{mol/g}$, respectively, while by RO are 57.2, 150 and 166 $\mu\text{mol/g}$, respectively. In the case of the multiple system for Cr(III), Cu(II), Cd(II) and Pb(II) those values by LO are 67.2, 72.3, 15.7 and 102 $\mu\text{mol/g}$, respectively, while by RO are 40.9, 30.9, 10.5 and 45.5 $\mu\text{mol/g}$, respectively. All these data is properly collected in Table 3.4. So, as expected from the previous results, RO shows less adsorption maximum capacities than LO for all heavy metals either in single and multiple systems.

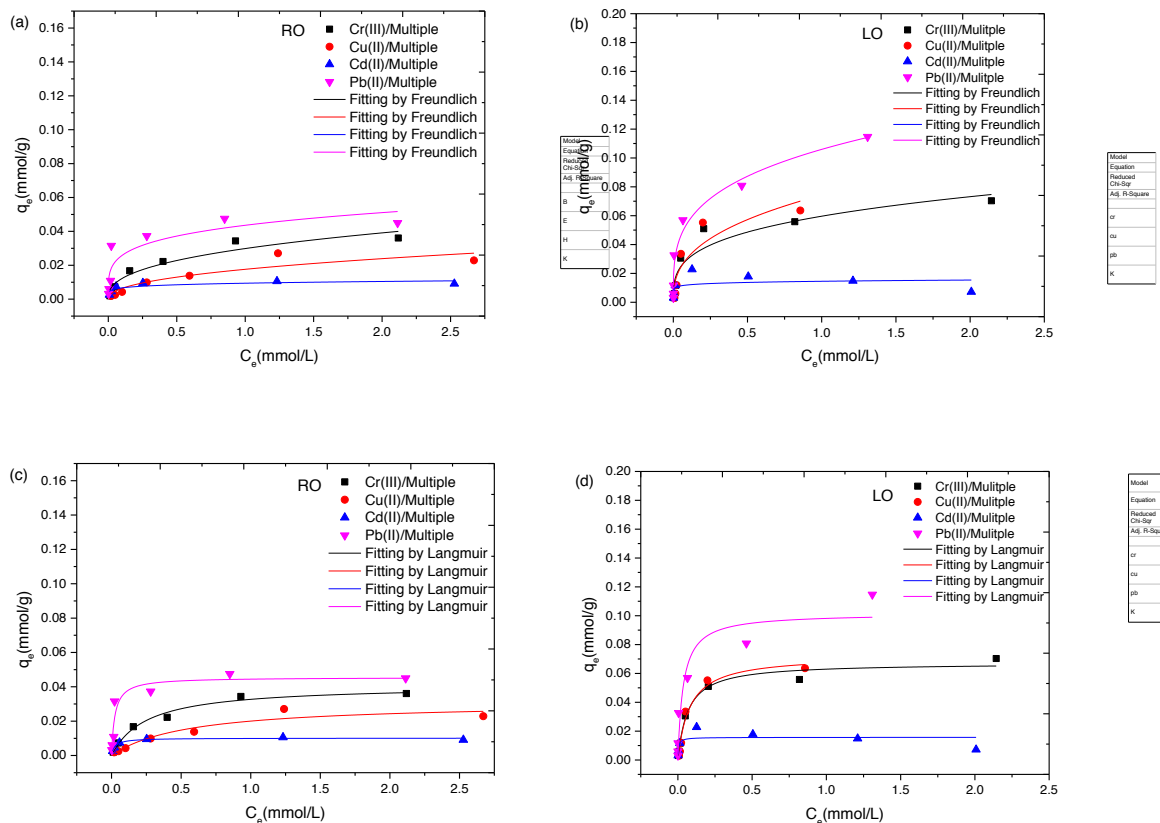


Figure 7 Biosorption isotherms of heavy metals in multiple system by RO (a) (c) and LO (b) (d) by Freundlich and Langmuir models, respectively. Biosorption conditions are 25 mg of biosorbent in each case at $T=25.0^{\circ}\text{C}$ and aqueous solution at $\text{pH } 4.0$ and stirring for 24 hours.

Table 3.4 Langmuir and Freundlich isotherm parameters for the biosorption onto LO and RO of Pb, Cu and Cr ions in both individual and multiple systems, and Cd only in multiple system.

		Freundlich		R ²	Langmuir			R _L
		K _f (mmol/g)	n		q _{max} (mmol/g)	b (L/mol)	R ²	
Cr(III)	LO	0.157	0.392	0.796	0.112	21	0.939	0.04
	RO	0.0447	0.339	0.813	0.0572	5.1	0.950	0.07
Cu(II)	LO	0.144	0.303	0.657	0.165	11	0.907	0.03
	RO	0.0342	0.751	0.963	0.150	0.31	0.979	0.5
Pb(II)	LO	0.249	0.292	0.921	0.210	40	0.979	0.02
	RO	0.181	0.321	0.752	0.166	24	0.924	0.02
Cr(III)/Multiple	LO	0.0596	0.295	0.888	0.0672	14	0.963	0.02
	RO	0.0298	0.389	0.923	0.0409	3.9	0.985	0.09
Cu(II)/Multiple	LO	0.0743	0.375	0.801	0.0723	12	0.963	0.2
	RO	0.0176	0.440	0.824	0.0309	1.8	0.909	0.2
Cd(II)/Multiple	LO	0.0145	0.082	0.040	0.0157	202	0.441	0.002
	RO	0.00940	0.150	0.651	0.0105	42	0.960	0.009
Pb(II)/Multiple	LO	0.106	0.280	0.968	0.102	28	0.886	0.001
	RO	0.0436	0.228	0.764	0.0455	42	0.894	0.01

Thermodynamic parameters

The Gibbs free energy is used to describe the degree of spontaneity of the biosorption process. It is assumed that a more energetically favorable biosorption deals with a higher negative Gibbs free energy value. It can be evaluated using Langmuir constants calculated by Equation (9).

$$\Delta G^0 = -RT \ln b \quad (9)$$

The standard Gibb's free energy (G_0) values for RO and LO of each heavy metal in the multiple metal system are listed in Table 3.5. The negative values ΔG^0 suggested that the biosorption of these metal ions onto RO and LO are spontaneous processes and thermodynamically favorable under the experimental conditions.

Table 3.5 the Gibbs free energy of LO and RO in multiple system.

Biosorbent	Metal ion	b	ΔG^0 J/mol
LO	Cr(III)/Multiple	14.9	-6695
	Cu(II)/Multiple	12.6	-6279
	Cd(II)/Multiple	202	-13160
	Pb(II)/Multiple	28.0	-8254
RO	Cr(III)/Multiple	3.97	-3414
	Cu(II)/Multiple	1.80	-1493
	Cd(II)/Multiple	42.3	-9279
	Pb(II)/Multiple	42.1	-9264

4. Conclusions

This study sets out to apply waste biomass as biosorbent for heavy metal removal from single and multiple systems. Characterization of the biosorbents including SEM and ATR-FTIR were performed for all biomasses to study their morphology and metal binding groups. The morphological structures are different depending on the groups of biomass residues. RO present a typical structure of lignin. It is also clearly shown that LO has a bigger mesoporous diameter, which probably is a key factor that can influence its high sorption capacity for the heavy metals onto this biomass. It is worth noting that RO and LO adsorbents show higher adsorption capacity for Cd. Rice and canola biomass wastes are potential biosorbents for heavy metals removal in multiple systems.

Acknowledgements

This research was supported by grants from the National Key Research and Development Program of China (No. 2018YFD0200904), the Agricultural Science and Technology Innovation Program of China (No. CAAS-ASTIP-2013-OCRI), and Spanish research projects (Nos. CTM2015-65414-C2-1-R and AGL2015-70393-R). Also, China Scholarship Council (No. 201509110114). All the authors are grateful to the UAB Microscopy Service (Servei de Microscòpia Electrònica from UAB, Catalunya, Spain) for the SEM analysis; to M. Resina who helped perform the analysis of heavy metals by ICP-MS.

Author Contributions

J.J. Zhao and X.J. Shen carried out most of the experiments and wrote the main manuscript text. X. Liao and C. Palet contributed valuable discussions and helped revise the manuscript. All authors reviewed and approved the final manuscript for publication.

Additional Information

Publisher's note: Springer Nature remains neutral with regard to jurisdictional claims in published maps and institutional affiliations.

Competing Interests

The author(s) declares no competing interests.

References

1. Dai, L. *et al.* Multivariate geostatistical analysis and source identification of heavy metals in the sediment of Poyang Lake in China. *Sci. Total Environ.* **621**, 1433–1444 (2017).
2. OECD. *China in the Global Economy Environment, Water Resources and Agricultural Policies Lessons from China and OECD Countries.* (2006).

3. Wang, H., Hijmans, R. J. & Res, E. Climate change and geographic shifts in rice production in China Climate change and geographic shifts in rice production in China. (2019).
4. Liang CHAI, Haojie LI, Benchuan ZHENG, Jinfang ZHANG, Cheng CUI, Jun JIANG, Bi ZHANG, liangcai JIANG, Lintao WU, J. K. Recent Advance, Problems and Outlooks in Rapeseed (*Brassica napus* L.) Breeding in China. *Agric. Sci. Technol.* **18**, 2612–2616 (2017).
5. Sun, J. *et al.* An estimation of CO₂ emission via agricultural crop residue open field burning in China from 1996 to 2013. *J. Clean. Prod.* **112**, 2625–2631 (2016).
6. Rajeshkumar, S. *et al.* Studies on seasonal pollution of heavy metals in water, sediment, fish and oyster from the Meiliang Bay of Taihu Lake in China. *Chemosphere* **191**, 626–638 (2018).
7. WANG Hai, WANG Chun-xia, W. Z. SPECIATIONS OF HEAVY METALS IN SURFACE SEDIMENT OF TAIHU LAKE. *Environ. Chem.* **21**, 430–435 (2002).
8. Jackson, H. F. L. J. F. Analysis of Plant Waste Materials. in *Analysis of Plant Waste Materials* **20**, 25 (1999).
9. Sakala, G. M., Rowell, D. L. & Pilbeam, C. J. Acid-base reactions between an acidic soil and plant residues. *Geoderma* **123**, 219–232 (2004).
10. Zulkali, M. M. D., Ahmad, A. L. & Norulakmal, N. H. *Oryza sativa* L. husk as heavy metal adsorbent: Optimization with lead as model solution. *Bioresour. Technol.* **97**, 21–25 (2006).
11. Langan, P. *et al.* Lignin Valorization: Improving Lignin Processing in the Biorefinery. *Science (80-.)*. **344**, 1246843–1246843 (2014).
12. Ge, Y. & Li, Z. Application of Lignin and Its Derivatives in Adsorption of Heavy Metal Ions in Water: A Review. *ACS Sustain. Chem. Eng.* **6**, 7181–7192 (2018).
13. Tsang, D. C. W., Knijnenburg, J. T. N., Hunt, A. J., Supanchaiyamat, N. & Jetsrisuparb, K. Lignin materials for adsorption: Current trend, perspectives and opportunities. *Bioresour. Technol.* **272**, 570–581 (2018).
14. Ghaffar, S. H. & Fan, M. Lignin in straw and its applications as an adhesive. *Int. J. Adhes. Adhes.* **48**, 92–101 (2014).
15. Zhang, Y., Yang, Y. & Tang, K. Physicochemical Characterization and Antioxidant Activity of Quercetin-Loaded Chitosan Nanoparticles Yuying. *Polym. Polym. Compos.* **21**, 449–456 (2007).
16. Feizi, M. & Jalali, M. Removal of heavy metals from aqueous solutions using sunflower, potato, canola and walnut shell residues. *J. Taiwan Inst. Chem. Eng.* **54**, 125–136 (2015).
17. Shen, Z., Zhang, Y., McMillan, O., Jin, F. & Al-Tabbaa, A. Characteristics and mechanisms of nickel adsorption on biochars produced from wheat straw pellets and rice husk. *Environ. Sci. Pollut. Res.* **24**, 12809–12819 (2017).